Development of a novel soil erosion risk map for arable land in Switzerland

Inauguraldissertation
der Philosophisch-naturwissenschaftlichen Fakultät
der Universität Bern

vorgelegt von
Pascal, Bircher
von Stansstad

LeiterInnen der Arbeit:
Prof. Dr. Chinwe Ifejika Speranza
Prof. em. Dr. Hans Hurni
Dr. Hanspeter Liniger
Geographisches Institut / Centre for Development and Environment
Universität Bern
Dr. Volker Prasuhn
Agroscope

Development of a novel soil erosion risk map for arable land in Switzerland

Inauguraldissertation
der Philosophisch-naturwissenschaftlichen Fakultät
der Universität Bern

vorgelegt von
Pascal, Bircher
von Stansstad

LeiterInnen der Arbeit:
Prof. Dr. Chinwe Ifejika Speranza
Prof. em. Dr. Hans Hurni
Dr. Hanspeter Liniger
Geographisches Institut / Centre for Development and Environment
Universität Bern
Dr. Volker Prasuhn
Agroscope

Von der Philosophisch-naturwissenschaftlichen Fakultät angenommen.

Bern, 25.03.2025

Der Dekan
Prof. Dr. Jean-Louis Reymond

Summary

Soil erosion is a global problem and has a negative impact on food security. Long-term mapping helps to determine the extent of soil loss and to take appropriate mitigation measures. Estimating soil loss is a critical scientific challenge due to limitations in data availability to quantify actual soil loss from erosion. To address this limitation, models have been employed to quantify potential soil erosion risk. The most widespread models are the Universal Soil Loss Equation / Revised Universal Soil Loss Equation -USLE/RUSLE. The USLE/RUSLE models have been expressed in literature as an equation: A = R * K * L*S * C * P, with A representing the estimated average long term soil loss (actual erosion risk) in tons per hectare per year, R the rainfall-runoff erosivity factor, K the soil erodibility factor, L the slope length factor, S the slope steepness factor, C the cover- and management factor and with P the support practice factor.

However, not all factors in the USLE/RUSLE models have been tested internationally or adapted for Switzerland. The LS- and C-factor are the most sensitive factors in the (R)USLE-model and require testing of the LS-factor with different flow algorithms and at different spatial resolutions. In particular, the topographical LS-factor in the (R)USLE calculation including different multiple flow algorithms and different resolutions are internationally less known and have also not been tested for Switzerland. Further, problems persist with calibrating and validating erosion models. Often the standard (R)USLE approach without any adaptation to regional conditions is applied in literature. In addition, for cover- and management and support practice factors (CP) only standard values are used in literature and software tools (like a CP-Tool) for calculation of actual soil erosion risk at field levels are rare. Software tools for calculating the CP-factors at field size level are not available, thus the calculation of actual soil erosion risk was not possible for Switzerland. Further, the 2010 developed potential erosion risk map of Switzerland (ERM2 2010) with a resolution of 2 m was available only for agriculturally used area (covering crop- and permanent grassland) of Switzerland, as data on cropland areas was not available to create an erosion risk map only for croplands. The ERM2 2010 was also not calibrated with measured soil loss data and was not corrected for factors specific to Swiss arable landscapes. Consequently, only the standard version of the (R)USLE was applied for Switzerland thus making the ERM2 2010 inadequate as a decision basis for land management and governance in Switzerland.

This thesis thus aims to improve the knowledge basis for managing soil erosion in

Switzerland by creating a corrected nationwide potential erosion risk map as a tool for decision support and developing software tools for scenario calculations based on adapted CP-factor. To achieve these objectives and to fill the above-mentioned gaps, four sub-objectives were defined: (1) to compare suitable multiple flow algorithms for LS-factor calculation to improve soil loss prediction, and based on this, (2) to compare modelled and measured soil loss, (3) to develop software tools for calculating actual erosion risk, and (4) to subject arable land areas to a correction factor thereby replace the ERM2 2010 of Switzerland with an improved erosion risk map - ERM2 2019 for the arable land. These four sub-objectives resulted into four publications. The first three publications were peer-reviewed and the fourth was a final report to the Swiss Federal Office for Agriculture.

In Paper 1, I showed the importance of flow barriers such as roads, railway lines and forests for disturbing or interrupting the flow paths by comparing different multiple flow algorithms on different resolutions (2m vs 25 m). The identified water flow paths show patterns of possible soil loss areas and hints for mitigation measures against soil loss. The LS-factor calculated based on compared multiple flow algorithms was then incorporated into modelling soil loss (Paper 2), used as input for software tools to calculate actual erosion risk (Paper 3) and for developing a new erosion risk map for Switzerland (Paper 4).

In Paper 2, I compared modelled and long-term measured soil loss on five representative areas. These five areas located between the northern Prealps and the Jurassic Alps depict the agricultural areas in the Swiss Plateau. The mismatch of the modelled soil loss compared to the measured soil erosion was about the factor 8. This result showed the need to calibrate the modelled soil loss. For the comparison of different CP-Tools in paper 3 a correction factor was applied on the modelled soil loss in paper 4.

Thus, in Paper 3, I introduced two software tools to calculate the C-factor, which captures the influence of cropping and management practices and the P-factor on erosion. I then connected this CP-factor with the novel potential erosion risk map of Switzerland 2019 with a Geographical Information System-tool (GIS-tool) programmed in QGIS. The developed software tool for calculating the CP factor uses input data like crop sequences, tillage practices, inter-cropping period, and direction of tillage. Secondly, this tool was coupled with a GIS to obtain the actual erosion risk. The advantage of combining the CP-Tool with the GIS-tool (Paper 3) is that management scenarios can be calculated on selected fields and can provide an impression of different soil erosion mitigation measures. Both software tools (CP-Tool and GIS-tool) allow calculating the actual erosion risk on field block level and

comparing different scenarios. This enables the use of the tools for decision support in soil conservation for research and practice such as by the Federal Office of Environment and the Federal Office of Agriculture for regulatory purposes, extension advice and for training purposes.

In Paper 4, the potential erosion risk map (ERM2 2019) covers the relatively constant factors of the RUSLE comprising the topographical factor LS, the soil erodibility factor (K) and the rain erosivity factor (R). The sensitive cover- and management and support practice factors (CP) are not included in the ERM2 2019, because the CP-factor highly varies on field block level and within years. A modification on the LS-factor and a conservative reduction factor of 5 was applied on the modelled soil loss for the ERM2 2019. Through these adaptions the ERM2 2019 provides a more realistic assessment of soil erosion risk on arable land than the ERM2 2010, where the standard RUSLE-approach was applied.

The results from this research and the development of the software have filled the research gaps relating to application of the RUSLE on arable land. In addition, the study fulfils the objectives to create an upgraded erosion risk map for Switzerland. Some limitations are that since the start of the study, the basic input data for calculating the RUSLE, such as soil maps for K-factor creation and improvements for distinguishing arable and permanent grassland (cadastral survey) have been significantly improved in 2021. This led to an update of the arable land layer in 2022 for the erosion risk map in Switzerland (Federal metadata catalogue) in a followed up project. In future studies, better soil maps may also be available to improve the soil erodibility factor map for Switzerland.

Abbreviations

C-factor (C): Cover- and management factor of (R)USLE

DEM: Digital Elevation Model

DEM2: Digital Elevation Model with 2 metres resolution

DEM25: Digital Elevation Model with 25 metres resolution

DINF: Deterministic Infinity

DZV: Direktzahlungsverordnung: Direct Payments Ordinance

ERM: Erosion risk map

ERM2 2010: Erosion risk map of Switzerland 2010

ERM2 2019: Erosion risk map of Switzerland 2019

FAO: Food and Agriculture Organization of the United Nations

FCover: Fraction of Vegetation Cover

FOAG: Federal Office For Agriculture

FOEN: Federal Office For Environment

GIS: Geographical Information System

ITPS: Intergovernmental Technical Panel on Soils

K-factor (K): Soil erodibility factor of (R)USLE

L-factor (L): Slope-length factor of (R)USLE

MFA: Multiple Flow Algorithm

MFD: Multiple Flow Direction

MTFD: Multiple Triangular Flow Direction

MODIS: Moderate Resolution Imaging Spectroradiometer

MUSLE87: Modified Universal Soil Loss Equation 87

ÖLN: Ökologischer Leistungsnachweis: proof of ecological performance

P-factor (P): Support practice factor of (R)USLE

PPP: Plant Protection Products

R-factor (R): Rain erosivity factor of (R)USLE

RUSLE: Revised Universal Soil Loss Equation

RUSLE2015: Revised Universal Soil Loss Equation 2015. The new assessment of soil loss by water erosion in Europe.

S-factor (S): Slope factor of (R)USLE

SDG: Sustainable Development Goals

TLM3D: Topographical Landscape Model 3D

USLE: Universal Soil Loss Equation

VBBo: Verordnung über die Belastungen des Bodens: Ordinance on the Pollution of Soil

WAT: Watershed

Acknowledgments

It would not have been possible to successfully complete this thesis without support of all kinds. I would like to thank the Centre for Development and Environment (CDE; Dr. Schwilch Gudrun, Heierle Emmanuel, Fries Matthias) and the Geographical Institute (GIUB) of the University of Bern for providing the workspace with the corresponding technical equipment and its use.

I would also like to express my gratitude to the supervisors and directors of the project, who were always willing to help and listen to me during the project. I would especially like to mention my competent supervisors Dr. Prasuhn Volker (Agroscope, Zurich) and Dr. Liniger Hanspeter (CDE, Bern), who always took the time to give me active support in the form of advice and, as co-authors of the publications, made a great contribution with their knowledge.

I would like to thank Prof. em. Dr. Hurni Hans (CDE, Bern), supervisor of the PhD thesis, for the successful start and the first steps as a PhD student. I would also like to thank Prof. Dr. Ifejika Speranza Chinwe (GIUB, Bern), who took over the PhD thesis as supervisor after the retirement of Prof. em. Dr. Hurni Hans and showed a lot of patience and provided a lot of helpful feedback for this thesis.

I would also like to thank my fellow students for productive discussions during the coffee breaks. I would like to thank Dr. Schmidt Simon (formerly Environmental Geosciences, University of Basel) for the successful cooperation and the opportunity to maintain a regular exchange between the two projects Erosion Risk Map Permanent Grassland (FOEN) and Erosion Risk Map Arable Land (FOAG). I would also like to thank other participants from the University of Basel (Prof. Dr. Alewell Christine and Dr. Meusburger Katrin; currently WSL).

I would like to thank the representatives of the FOAG (Ulrich Andrea and Zimmermann Michael) for the funding and the constructive discussions on the project.

Finally, I would like to thank my parents Bircher Denise and Bircher Anton, who always supported me. I would also like to thank my brother Bircher Yves and my friends for their support during my studies and for the distraction on non-working days and weekends.

Table of Contents

Part 1: Overview and background

1. Introduction

Soil can be regarded as a non-renewable resource because soil formation rates of about ~1 t ha^{-1} yr^{-1} have been reported for Europe (Verheijen et al. 2012). It is thus important to avoid soil loss by erosion thereby protecting soil functions, such as serving as the base for food production, as habitat and as carbon sink (Coulibaly et al. 2022, Derpsch et al 2024, Nazir et al. 2024).

To protect soil against erosion, it is thus necessary to have tools to identify where soil erosion happens and to establish measures to prevent/minimize soil erosion through sustainable land management practices.

Although there has been substantial scientific research and societal awareness dedicated to soil erosion, it remains a considerable threat in many parts of the world. According to the 2015 Status of the World's Soil Resources Report (Food and Agriculture Organization of the United Nations (FAO) and Intergovernmental Technical Panel on Soils (ITPS 2015), soil erosion was identified as the main threat to soil functions in five of the seven regions investigated (Africa, Asia, Latin America, Near East and North Africa, and North America), and in the first four regions, the trend for erosion was worsening. In contrast, erosion was found to be reducing only in Europe, North America, and the Southwest Pacific (FAO 2019: 1). Yet, Panagos et al. (2015: 438) reported: ”The mean soil loss rate in the European Union’s erosion-prone lands (agricultural, forests and semi-natural areas) was found to be 2.46 t ha^{-1} yr^{-1}, resulting in a total soil loss of 970 Mt annually.”

The need for stewardship in soil use is captured by the sustainable development goals (SDG) that target soil as a fundamental basis for global and local development:

- SDG 2: «End hunger, achieve food security and improved nutrition and promote sustainable agriculture» (United Nations 2016: 4,14)
- SDG 15: «Protect, restore and promote sustainable use of terrestrial ecosystems, sustainably manage forests, combat desertification, and halt and reverse land degradation and halt biodiversity loss» (United Nations 2016: 10,40)

These goals reflect the continued need for sustainable land management and for safeguarding soils. However, safeguarding soils requires relevant methods to guide decision-making regarding land management practices and policy instruments. Yet, knowledge on such methods and their applications are missing for Switzerland. Thus, in this thesis I discuss the

main drivers of soil loss and enhance the existing methodology for calculating soil erosion risk and soil loss for Switzerland.

In the simplified framework of this thesis (Figure 1), the factors precipitation, crop fields, slope length and slope steepness (topographic conditions) can be identified as drivers that influence soil erosion processes by water.

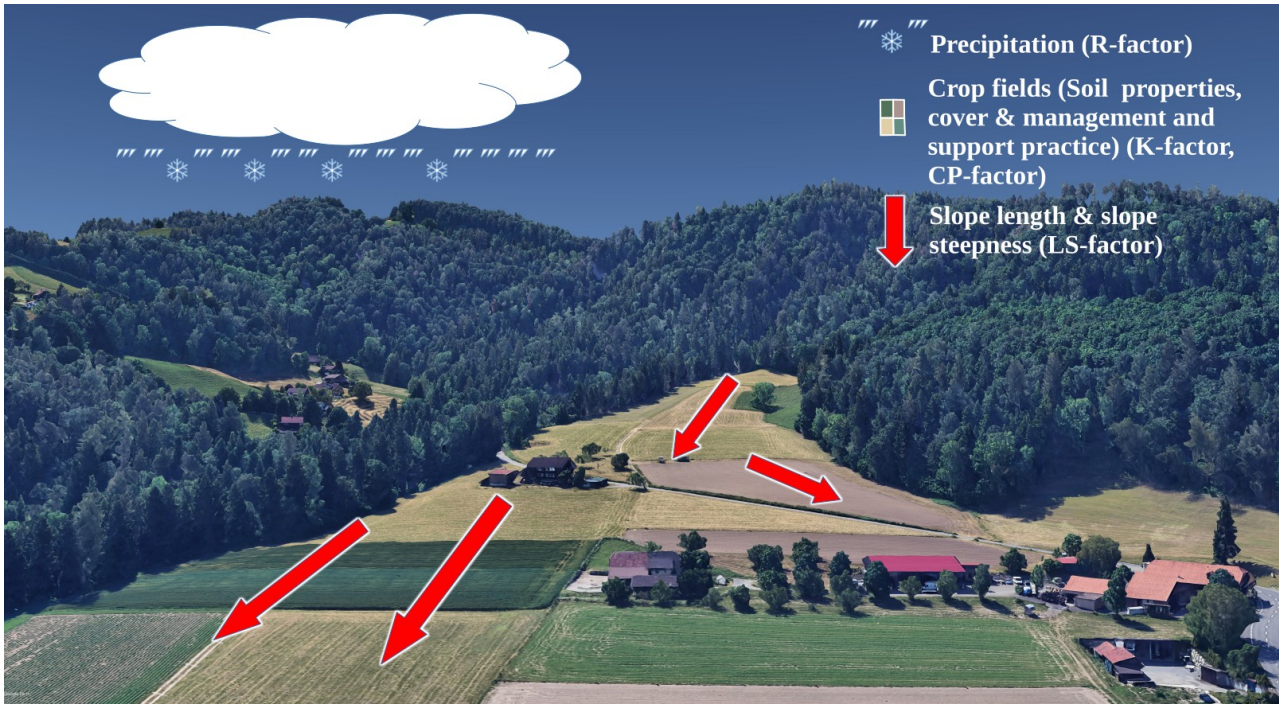

Figure 1: Simplified, general framework for representing factors that influence soil erosion processes and their (R)USLE (see Equation 1) components (created with Google Earth Pro).

In this chapter, I discuss the broad research context of this thesis, the research gaps it addresses, the objectives and the methods adopted to address them. I then present an overview of the research papers, and develop a synthesis of the research results and the conclusion.

Soil erosion research methods include measuring, mapping and modelling soil erosion. Digital soil loss models can be distinguished between physically based, stochastic and empirically based models (Morgan 2005). The empirical Universal Soil Loss Equation (USLE) is derived from a data basis of about 10,000 plot years (Wischmeier & Smith 1978). Its successor the Revised Universal Soil Loss Equation (RUSLE) allows combining basic data of different quality like Digital Elevation Models (DEMs), soil maps, precipitation with varying resolution to a nationwide erosion risk map (such as the ERM2 2019) available also for decision support.

The USLE/RUSLE models consist of six factors including topographical (LS with L = slope length, S = slope steepness), soil erodibility (K), soil erosivity (R), cover- and management

factor (C) and support practice (P) factor (Wischmeier and Smith 1978, Renard et al. 1997) also named as actual erosion risk (Equation 1). Whereas the potential erosion risk consists only of four of the six USLE/RUSLE factors representing mainly constant factors (Equation 2) excluding the cover- and management and support practice factors (C and P).

Equation 1: $A=R*K*L*S*C*P$

Equation 2: $A=R*K*L*S$

In Switzerland, the potential erosion risk map 2010 (ERM2 2010) was created on agricultural land (Gisler et al. 2010, Gisler et al. 2011, Prasuhn et al. 2013) with a resolution of two metres based on the USLE/RUSLE model. The legal basis in Switzerland is the Ordinance on Soil Pollution (Verordnung über Belastungen des Bodens (VBBo): Ordinance on the Pollution of Soil), which sets guideline values for tolerable soil loss rates for agriculturally used soils up to 70 cm and over 70 cm depth at 2 and 4 tonnes per hectare and year, respectively and aims to maintain soil fertility. The Ordinance on Direct Payments in Agriculture (Direktzahlungsverordnung (DZV): Direct Payments Ordinance) regulates the conditions and the procedure for direct payments and determines the amount of financial contributions to farmers. According to the appendix of DZV (Item 5.1.2): "There must be no relevant erosion and management-related soil loss on the arable land. Soil loss is considered relevant if it corresponds at least to the cases in the "2 to 4 tonnes/ha" section of the Agridea fact sheet "How much soil is lost?" from November 2007."

A subsequent research by Alder et al. (2013) describes a model for identifying the water connection of potentially erosion-prone agricultural land and mainly based on the ERM2 2010. Considering water connection is important in Switzerland because the input of substances into watercourses can be either directly, from areas adjacent to a watercourse, or indirectly, from areas that are farther away from a watercourse but are connected to it via inlet shafts and meteoric water drainage and meteoric water discharges. The potential watercourse connection map of erosion-prone areas shows areas in a form of "worst case scenario" (permanent fallow, no buffer strips or structural measures), areas where there is a considerable risk of substances entering water bodies if the land is not managed appropriately. The potential watercourse connection map thus forms an aid for targeted planning of measures in water protection, whether on the connected erosion-prone parcel itself or for the creation of

suitable buffer strips or other structural measures at the point of transition into the water body (Alder et al. 2013). The potential watercourse connection map also incorporates PPP (plant protection products) and organic as well as mineral fertilizer transport into water bodies (Koch & Prasuhn 2021).

To better manage soil quality in Switzerland, several software tools have been developed for research and for assessing soil properties, mitigation measures and to promote a sustainable use of the resource soil. Three examples (**soil compaction calculator**, **spraycalculator** and **humus balance calculator**) are highlighted here. For calculating soil compaction, the app named **Terranimo** requires information about the soil (texture, moisture) and the agricultural machine (wheel load, tyre pressure). Based on these inputs, **Terranimo** calculates the strength of the soil and the soil pressure. If the soil pressure exceeds the strength of the soil, there is a high risk of compaction damage in the subsoil and therefore damage to important soil functions. Terranimo can then be used to assess soil moisture conditions, machines, tyres or tyre pressure settings that can avoid the risk of damaging compaction in the subsoil, whereby the wheel load, tyres and tyre pressure are configured in such a way that the soil is no longer at risk of compaction. The **spraycalculator,** enables to obtain the recommended amount of pesticide to use, and consequently helps to save costs and protect the environment.

The humus content of a soil is of central importance for soil fertility and is significantly influenced by management. Agroscope provides farmers with a **humus balance calculator** for arable soils. This is freely available on the web and is smartphone-compatible. It can be used to assess whether the current management (ÖLN-Ökologischer Leistungsnachweis: proof of ecological performance) keeps the humus content stable, promotes it or whether there is a risk of humus loss. However these software tools do not capture the effects of soil cover on soil erosion.

To close these gaps, the Swiss Federal Office for the Evironment (**FOEN**) and the Swiss Federal Office for Agriculture (**FOAG**) initiated two research projects one focusing on permanent **grassland** (Schmidt S. 2018) and the other one focusing on **arable land**. This thesis is based on the project focusing on erosion risk mapping of arable land in Switzerland and was conducted in a framework to upgrade the ERM2 2010 to provide scientific evidence and software tools to support the FOAG in soil erosion mitigation measures and legal strategies. Regular meetings between the two projects and the responsible offices (**FOEN & FOAG**) allowed an optimal exchange of data and results.

1.1 Scientific gaps

While the above mentioned developments in erosion mitigation research have enhanced the consideration of erosion risk in agricultural land management, several gaps persist in the scientific understanding of erosion risk modelling and this thesis addresses the following gaps:

1. LS- and C-factors of the USLE/RUSLE model are the most sensitive factors in the USLE-model (Auerswald 1987, Panagos et al. 2015a). LS-factor calculation on different resolutions were so far not tested for Switzerland.

2. There are still challenges (mismatch of field mapped and modelled soil loss) with calibrating and validating soil erosion models (Favis-Mortlock 1998).

3. Often only standard approaches of the (R)USLE are applied in literature, without adaptation to regional conditions (Fiener et al. 2020).

4. Little is internationally known about LS-Factor-Calculations (including different algorithms and resolutions (Deumlich 2012 [1–25 m], Fu et al. 2015 [2–30 m], Yang 2015) and they have also not been systematically tested for Switzerland.

5. For CP-factor calculation only standard values are mostly used in literature (Chen et al. 2011, Panagos et al. 2015b). Calculation tools are rarely available on field block level, thus the calculation of the actual erosion risk was hitherto not possible for Switzerland. Very sensitive factors like C-factors are recently published by Auerswald et al. (2021) and Prasuhn (2022) and reflect the relevance of this variable in the USLE/RUSLE and is consequently also relevant for the ERM2 2019 developed in this thesis.

6. The ERM2 2010 does not differentiate erosion risk between arable land and permanent grassland (Gisler et al. 2010).

7. The ERM2 2010 was not calibrated with long-term measured soil loss data and the standard (R)USLE approach was used (Gisler et al. 2010).

1.2 Objectives

This thesis thus addresses the aforementioned scientific gaps and aims to improve the scientific evidence for erosion risk modelling, to create a nationwide potential erosion risk map for Switzerland as a tool for decision support and to develop software tools for scenario calculations based on adapted cover- and management and support practice factor (CP). The

sub-objectives are:

1. To map the LS factor as best as possible with a high-resolution digital terrain model and to define a suitable multiple flow algorithm to improve soil loss predictions (sub-objective 1, addresses scientific gaps 1 and 4)

2. To compare the soil loss from long-term field mapping with the modelled soil erosion in order to identify similarities or inconsistencies and, if necessary, calibrate the model (sub-objective 2, addresses scientific gaps 2 and 3).

3. To develop open source software tools for calculating the cover and management and support practice factor CP and actual erosion risk on field block level for mitigation measures. (sub-objective 3, addresses scientific gap 5).

4. To create an upgraded, optimized and corrected potential erosion risk map for arable land in Switzerland based on the comparison of mapped and modelled soil loss (sub-objective 4 addresses scientific gaps 6 and 7).

1.3 Study area

The study area can be described at three different scales represented in the publications. Scale one represents the field block area of Switzerland (Figure 2, a), which is the basis for the calculation of the LS-factor in the ERM2 2019 including also the extent of arable land. Scale two represents the 1:25,000 national map extent Lyss (Figure 2, b) which represents an extrapolation from the Frienisberg extent (Bircher P. 2019: 4). Scale three can be described by citing the second publication, where “the study site is located about 20 km north-west of Bern, in the Cantone of Bern, where five long-term assessed subareas of soil erosion mapping (Frienisberg (FRI), Suberg (SUB), Lobsigen (LOB), Seedorf (SEE), Schwanden (SCH)) provide a representative reflection of the agriculturally used area in the Swiss plateau between the northern Prealps and the Jurassic Alps. The area is situated between 475 m and 720 m a.s.l. The region is characterized by a moderate climate, with an annual average temperature of approximately 8.5 °C and annual precipitation of 1048 mm. Most soils are well drained Cambisols and Luvisols on ground moraines and tertiary molasses; they are mostly sandy loams. Farm size is relatively small, averaging 16.7 ha; the average field size is also small at 1.3 ha (a farm can comprise several fields). Crop rotations are versatile and usually include temporary grassland of about 22% in the summer half-year and 37% in the winter half-year. The five selected study sites consist of 203 fields with crop rotation and about 258 ha, or 645,242 pixels at a resolution of 2 × 2 m.” (Figure 2, c) (Bircher P. 2022: 2)

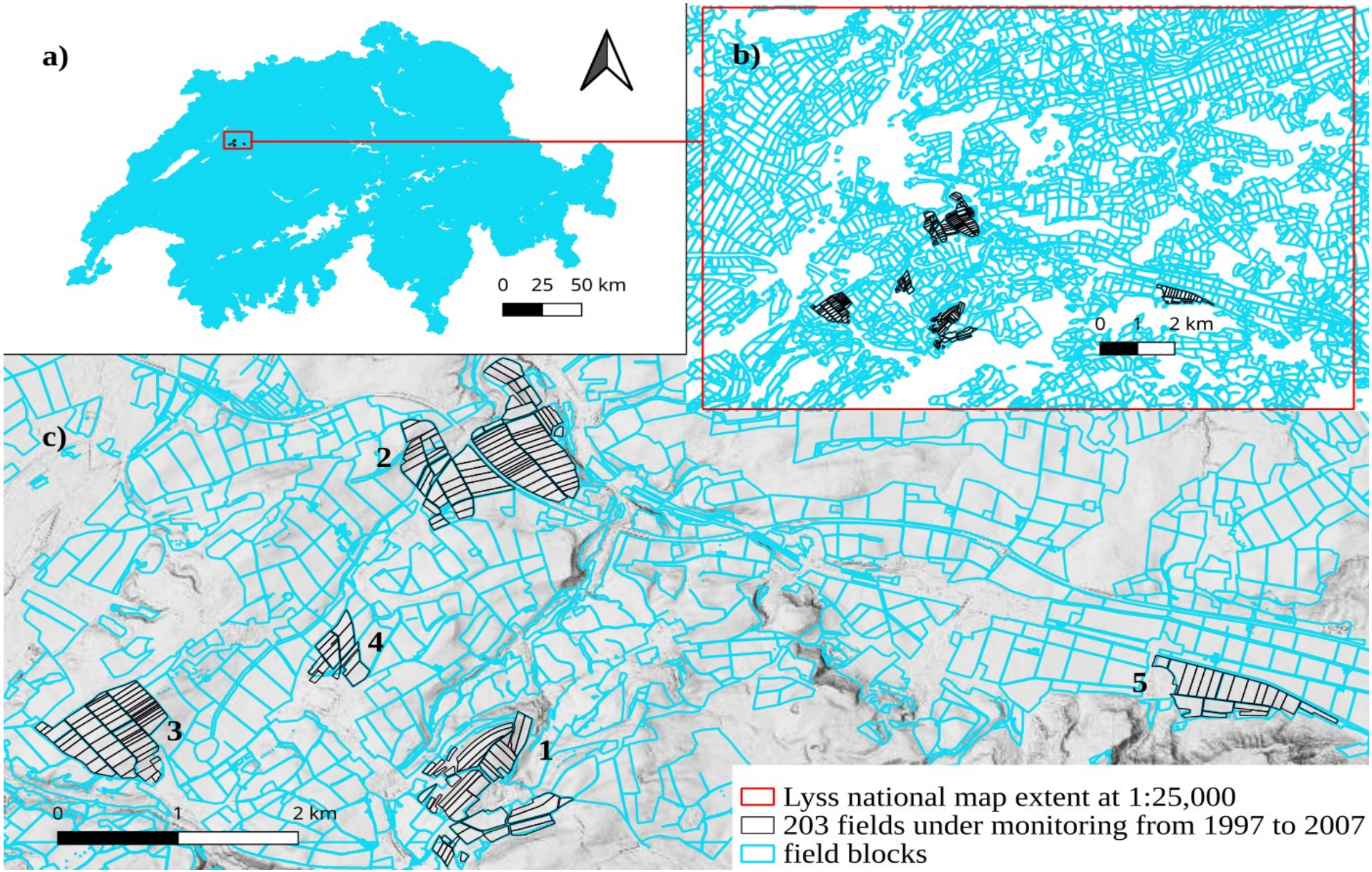

Figure 2: Study sites: a) Field block map Switzerland (ERM2 2019), b) Lyss national map extent at 1:25,000 (red), c) 203 fields under monitoring from 1997 to 2007 (black); 1 = Frienisberg (FRI), 2 = Suberg (SUB), 3 = Lobsigen (LOB), 4 = Seedorf (SEE), 5 = Schwanden (SCH). (Hillshade @swisstopo)

1.4 Methodological framework

The applied methodological framework is briefly described based on the publications and on the following sub chapters (Figure 3).

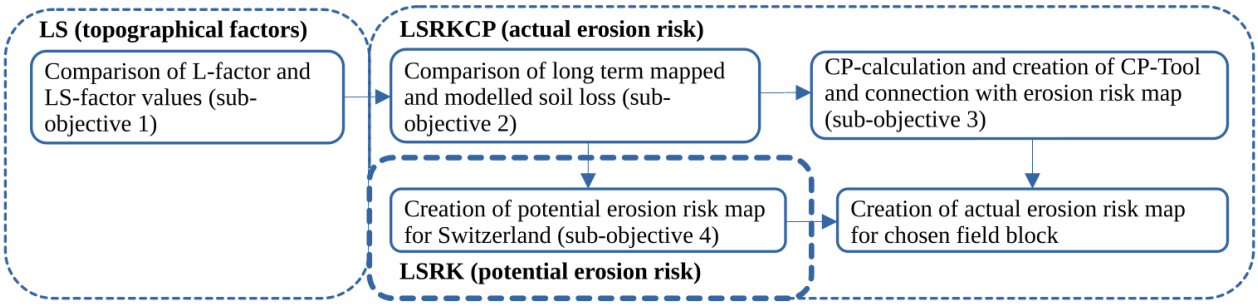

Figure 3: Methodological framework of approaches connecting publications (sub-objectives) and tools to resulting output of actual erosion risk.

1.4.1 Statistical comparison of slope length (L-factor) and combined slope length (L) and slope steepness factor (S) (LS-factor) values (Sub-objective 1)

Water flow is essential for modelling soil erosion and is represented in the L-factor, whereas the slope is represented in the S-factor. In the test area Frienisberg (Canton of Bern), and on map extent Lyss (1:25,000), 21 different existing multiple flow algorithms for LS-factor calculation were compared using a 2 m and 25 m resolution digital elevation model (Bircher et al. 2019a; Table 1, Paper 1). In addition, the influence of flow barriers like streets and railways were incorporated to calculate the LS-factor.

We tried to find out, which flow path algorithm suits best for our conditions. Thus, we compared results of LS-factor calculation based on different multiple flow algorithms and DEM resolutions of 2m and 25m using GIS and statistical methods in Frienisberg.

For this purpose, 21 different L-factor calculations were processed, whereas field blocks as micro-catchments are crucial for spatial confinement of the contributing area. Furthermore various multiple flow algorithms result in similar L-factor values and calculated mean LS factor values hardly differ in resolutions of 2 m - 25 m, but reality and spatial distribution are better represented by resolution of 2 m.

1.4.2 Statistical comparison of long-term mapped and modelled soil loss (Sub-objective 2)

The test area consisted of five sub-areas called Frienisberg, Suberg, Lobsigen, Seedorf and Schwanden (Bircher et al. 2022; Table 1, Paper 2). In these areas, long term mapped and modelled soil loss were compared to calibrate the modelled soil loss (Sub-objective 2). Field mapped data was collected during 10 years between 1997-2007 of event-related erosion

damage mapping by Prasuhn (2011; 2012).

The individual factors were determined as follows:
The erosivity factor (R) captures the erosivity of precipitation in [MJ mm ha^{-1} h^{-1} a^{-1} or N h^{-1} a^{-1}] based on a study by Schmidt et al. (2016). The precipitation factor was interpolated from various federal and cantonal meteorological data (86 stations; Meteoschweiz & cantons BE, LU, SG) with covariates (snow depths, CombiPrecip, DEM, etc.).

The K factor (erodibility factor) [t ha h ha^{-1} MJ^{-1} mm^{-1} or t h N^{-1} ha^{-1}] accounts for soil properties of granularity and organic matter based on soil maps of different scales. The scales range from 1:10,000 to 1:25,000. “For each of the 203 fields, grain size, skeletal content and humus content were additionally determined by an experienced soil expert using a feeling finger test in the field. Laboratory analyses were performed on 21 selected fields (texture, humus content), and the K-factor was determined based on the obtained texture distribution and organic matter content using the formula by Schwertmann et al. (1990)” (Bircher et al. 2022: 4)

The LS factor [unitless] is the slope length (L) and slope gradient factor (S) and is modelled based on the digital elevation model (SwissALTI3D 2015) with 2 m resolution and field block map of Switzerland. A multiple flow algorithm (Seibert & McGlynn 2007) was used to determine the L-factor and multiplied by the S-factor based on the approach of Desmet & Govers (1996).

The C-factor [unitless] is the cover and management factor and contains information regarding crop rotation and tillage methods such as plowing, mulching, and no-till. “Based on interviews with all farmers and observations during the field visits, the crop rotation and tillage methods (no-till and strip-till; mulch tillage that leaves >30% of crop residues on the soil surface; reduced tillage which leaves <30% of the soil surface covered with crop residues; mouldboard or disk plough with soil inversion) were detemined for each field for the years 1997 to 2006 in order to calculate the cover and management factor C. The C-factors were determined using a C-factor calculation tool (Mosimann and Rüttimann, 2006), adapted to Swiss conditions.” (Bircher et al. 2022: 4)

The P-factor [unitless] corresponds to the factor that considers erosion control measures, such as slope-parallel or slope-transverse tillage and terracing (e.g.: vines and hedges). In Bircher et al. (2022) the support practice factor (P) was established in the field by observing the direction of tillage. When the tillage direction oriented with the slope, the P-factor was set at

1.0 for the entire field or all containing pixels. If tillage was done perpendicular to the slope, known as cross-slope direction, the P-factor=1.0 was only applied when the slope length (SL) was above a critical value. The critical SL was derived by calculating $SLcrit = 170 * e^{-0.13 * Slope\ (\%)}$ using the field blocks and DEM data (Bircher et al. 2022). For pixels below the critical SL, the P-factor value was determined from the slope gradient based on the classification according to DIN 19708 (2017) and the formula of Schäuble (2005) with P = 0.4 + 0.02* Slope (%). For the Example 1 below, this means that below the 46.3 m of the slope the P-factor is 0.6, above the 46.3 m the P-factor is 1.

Example 1 with 10 % Slope: $Slcrit = 170 * e^{-0.13* 10\%} = 46.3$ m

$P = 0.4 + 0.02*$ Slope (10 %) = 0.6

The potential erosion risk [t ha^{-1} a^{-1}] differs from the actual erosion risk [t ha^{-1} a^{-1}] in that the C and P factors are missing. Therefore, the potential erosion risk is considerably higher (factor 10-100; depending on crop and tillage method) than the actual erosion risk (A) (Wischmeier & Smith 1978, Renard et al. 1997).

We compared modelled and measured soil loss using GIS and statistical methods (e.g.: mean, median) for the five sub-areas where soil loss was monitored for 10 years (1997-2007). Those five sub-areas represent the arable land of Switzerland under crop rotation well. We compared mapped soil loss from 203 fields over the 10 years with RUSLE-based modelled soil loss values. The mean mapped soil loss was 0.77 t/ha/yr, while the modelled was 6.20 t/ha/yr. The comparison of mapped and modelled soil loss shows a substantial overestimation by modelling in the order of a factor 8, leading to an adaptation of the LS-factor and a reduction of modelled soil loss by factor 5 in paper 4 (sub-objective 4) and used in paper 3 (sub-objective 4). Areas with high mapped soil loss rates >4 t/ha/yr were modelled quite accurately by the model. Areas with low mapped soil loss rates <4 t/ha/yr were drastically overpredicted by the model.

1.4.3 Cover and management factor (C) and support practice factor (P) - CP-calculation and creation of CP-Tool and connection with erosion risk map (Sub-objective 3)

The software-based CP-Tool was programmed in python. The creation of a CP-Tool is based on the comparison of different CP-Tools and crop sequences (Bircher et al. 2021, Table 1, Paper 3). With a QGIS-model, the CP-Tool and the potential erosion risk map can be combined to calculate the actual erosion risk on field block level. Mitigation measures based on different crop sequences are possible to calculate with the combination of the CP-Tool and

the QGIS-model (Bircher et al. 2021).

Programming methods for CP-factor calculations using python and a QGIS-model tool connects potential erosion risk (sub-objective 4) with the CP-factor by multiplication to get the actual erosion risk for a specific field block incorporating also results from paper 1 (sub-objective 1) and 2 (sub-objective 2). The following points could be realized with the CP-Tool:

- CP-factor tool adapted to Swiss agronomic and environmental conditions.
- Easy calculation of CP-factor for various crop rotations and management practices.
- USLE-CP-factor and actual erosion risk calculation on small scale field block level.
- Developed and programmed based on open source resources for further improvements.
- Both tools increase the knowledge of management practices for GIS- and non-GIS users.

1.4.4 Creation of potential erosion risk map for Switzerland (Sub-objective 4)

The potential erosion risk consists of only four of the six RUSLE-model factors. These four factors represent the more or less constant factors LS, R, K for the arable land of Switzerland (Bircher et al. 2019b; Table 1, Paper 4). The LS-factor was determined using the field block map as spatial basis. After multiplying all factors resulting in the map of potential erosion risk at field block level, this map was clipped with the mask of crop fields (arable land) only, excluding permanent grassland. The data for distinguishing between arable land and permanent grassland was derived from a **platform** collecting cantonal data and providing it. For the Swiss K-factor, more data based on different soil maps and scales from 1:1,000 to 1:200,000 are used than in the ERM2 2010.

We tried to implement a correction factor to balance the mismatch between field mapped and modelled soil loss (Bircher et al 2019b). A conservative correction factor of 5 was applied to the erosion risk map (ERM2 2019) to respect overlooked erosion events, errors of mapping, errors of digitization and not to over correct the ERM2019. Not only statistically based reasons such as descriptive comparisons (Mean, Median, Maximum, Minimum etc.) lead to the factor 5. The aim was to reflect high erosion events (>4 t /ha y) in a realistic manner.

1.5 Overview of research papers

This thesis consists of three peer reviewed publications and one final report that is non-peer

reviewed (Table 1). In publication 1 flow pattern comparisons were included to calculate the LS-factor, in publication 2 comparisons between mapped and modelled soil loss were made and in publication 3, a CP-Tool was developed and compared with other tools based on crop sequences. In the final report (publication 4) a correction approach referring to results in publication 1 & 2 for the national potential erosion risk map on arable land in Switzerland was applied.

Table 1: Overview of peer reviewed and not peer reviewed research publications

No	**Title**	**Authors**	**Peer-reviewed journal**	**Current state**
1	Comparing different multiple flow algorithms to calculate RUSLE factors of slope length (L) and slope steepness (S) in Switzerland	Bircher Pascal, Liniger Hanspeter, Prasuhn Volker	Geomorphology	Published (2019a)
2	Comparison of long-term field-measured and RUSLE-based modelled soil loss in Switzerland	Bircher Pascal, Liniger Hanspeter, Prasuhn Volker	Geoderma Regional	Published (2022)
3	Tools for USLE-CP-factor calculation and actual erosion risk on field block level for Switzerland	Bircher Pascal, Liniger Hanspeter, Prasuhn Volker, Kupferschmied Patrick	MethodsX	Published (2021)
4	Summary of Upgrade and optimization of the erosion risk map (ERM2). The new ERM2 (2019) for the arable land of Switzerland. Final report. 2019. In German.	Bircher Pascal, Liniger Hanspeter, Prasuhn Volker	Non-peer reviewed final report	Published (2019b)

Publication 1: Comparing different multiple flow algorithms to calculate RUSLE factors of slope length (L) and slope steepness (S) in Switzerland

The topographic LS-factor is one of the most difficult factors of the Revised Universal Soil Loss Equation (RUSLE) to define in a landscape with varying topography. For the application of the RUSLE not only at the plot but at catchment or landscape level, different multiple flow algorithms (MFA) have been developed and applied in various studies. However, these different MFAs in combination with various convergence values and applied at different resolutions of digital elevation models (DEM) have not been addressed so far. This publication focuses on filling this gap in the context of the agricultural area of Switzerland. To evaluate different factors of slope steepness (S-factor) and slope length (L-factor), we tested four different multiple flow algorithms (MFA) (Deterministic Infinity (DINF), Multiple Flow Direction (MFD), Multiple Triangular Flow Direction (MTFD), Watershed (WAT)) and compared them with the MFA approach (Flow 95 in MUSLE87) used in the existing erosion risk map of

Switzerland with a resolution of two metres. The MFAs we tested, used three different convergence settings and two digital terrain models (DEM) – one with a very fine two metre resolution (DEM2) and one with a coarser resolution of 25 m (DEM25) – enabling us to examine the influence of DEM resolution on the LS-factor. In total, we evaluated 21 L-factor variations to assess the significance for the prediction of the potential erosion risk. The calculations were applied at a local (test area Frienisberg, 88.7 ha) and at a regional scale (Lyss, 11,855 ha) in the agricultural Swiss Plateau. Both test areas were segmented into field blocks with an average size of 5 ha (14 field blocks in Frienisberg and 2305 field blocks in Lyss). A field block can contain several fields with different types of agricultural land use and is delineated by surrounding hydrological barriers. For these field blocks, the various L-factors were calculated automatically using Geographic Information Systems (GIS). Finally, the LS-factors were calculated for two selected MFAs. The L-factors calculated with the various MFAs and the high-resolution DEM2 differed negligibly in terms of statistical values (mean values, standard deviation) and in the spatial distribution of the pixels both among each other and in comparison to the L-factor of the existing erosion risk map. As expected, using the coarser DEM25 resulted in considerably lower S-factors but surprisingly in higher L-factors, so that there was little difference in the average LS values between the DEM25 and the DEM2. However, spatial distribution of the L-factor values and the soil erosion risk was much more differentiated in the DEM2 and better reflected the topography compared with the DEM25. Erosion risk hotspots such as slope depressions with concentrated runoff and thalweg erosion could be reliably identified. Moreover, the lower-resolution DEM25 was not well suited to the chosen approach with field blocks of a mean size of 5 ha, as the intersection of polygon and raster data produced edge errors depending on the clipping method. This study showed that a high-resolution DEM was more important for the calculation of the LS-factor and potential soil erosion risk than the choice of MFA, and that the calculation of LS-factors based on field blocks offered a number of advantages mainly in determining the channel network and maximum flow length.

Publication 2: Comparison of long-term field-measured and RUSLE-based modelled soil loss in Switzerland

Long-term field measurements to asses model-based soil erosion predictions by water are rare. We have compared field measurements based on erosion assessment surveys

from a 10-year monitoring process with spatial-explicit model predictions with the Revised Universal Soil Loss Equation (RUSLE). Robust input data were available for both the mapped and the modelled parameters for 203 arable fields covering an area of 258 ha in the Swiss Midlands. The 1639 mapped erosion forms were digitized and converted to raster format with a 2 m resolution. A digital terrain model using 2 m resolution and a multiple flow direction algorithm for the calculation of the topographic factors and the support practice factor was available for modelling with the RUSLE. The other input data for the RUSLE were determined for each field. The comparison of mapped and modelled soil loss values revealed a substantially higher estimation of soil loss values from modelling by a factor of 8, with a mean mapped soil loss of 0.77 t/ha/yr vs. modelled soil loss of 6.20 t/ha/yr. However, high mapped soil losses of >4 t/ha/yr were reproduced quite reliably by the model, while the model predicted drastically higher erosion values for mapped losses of <4 t/ha/yr. Our study shows the value of long-term field data based on erosion assessment surveys for model evaluation. RUSLE-type model results should be compared with erosion assessment surveys at the field to landscape scale in order to improve the calibration of the model. Further factors related to land management like headlands, traffic lanes and potato furrows need to be included before they may be used for policy advice.

Publication 3: Tools for USLE-CP-factor calculation and actual erosion risk on field block level for Switzerland

The calculation of the cover management factor (C-factor) and support practices factor (P-factor) is an important element in the Universal Soil Loss Equation (USLE). In Switzerland, a potential soil erosion risk map of arable land and a field block map that represents the basis of the agriculturally used areas in the country are available. A CP-factor tool was developed adapted to Swiss agronomic and environmental conditions, which allows to calculate CP-factors easily for various crop rotations and management practices. The calculated CP-factor values can be linked to any field block in the potential soil erosion risk map to determine the actual soil erosion risk for the field block. A plausibility check with other C-factor tools showed a sound match. This user-friendly calculation makes the CP-Tool and the actual erosion risk more accessible for authorities and GIS users. With Python and QGIS as open source resources, it is also possible to easily improve the tools. Linking the two tools provides substantial added

value for education and training, advising farmers and policy, as well as scientific research, and can serve as a reference for other countries.

Publication 4: Summary of upgrade and optimization of the erosion risk map (ERM2). The new ERM2 (2019) for the arable land of Switzerland. Final report. 2019

The new erosion risk map (ERM2 2019) of Switzerland is still based on the Revised Universal Soil Loss Equation (RUSLE), but with a new calculation algorithm and different software. The RUSLE is an empirical erosion model and shows the mean long-term erosion risk in tons per hectare per year. It allows to combine data of different quality with its modular structure of six factors. For this purpose, ERM2 2019 uses four of the six mentioned factors to represent the potential erosion risk without cover and management factor as well as erosion mitigation measures (C and P factor). The following features are new compared to the old erosion risk map (ERM2 2010): A) The new field block map is now based on the new topographic landscape model data (TLM3D 2015; version 1.3) from the Swisstopo. B) To calculate the L-factor (slope length or size of the catchment), different multiple flow algorithms based on the SwissALTI3D elevation model in a 2x2m grid were extensively tested and evaluated. The MTFD approach of Seibert & Glynn (2007) with convergence setting 1.1 was finally selected. C) The calculation of the S-factor (slope) remained largely unchanged. D) The new LS factor is not statistically substantially different from the previous ERM2 2010, but is now based on the open source software SagaGis. E) The K-factor (soil erodibility) was methodically implemented in the same way as in the previous ERM2 2010, but includes additional detailed cantonal soil data. F) The new R-factor map (erosivity of precipitation) achieves significantly higher average values than the R-factor of the previous ERM2 2010. This is due to a different methodology and better data.

The calculated potential erosion risk was offset with C and P factors to the actual erosion risk in the Frienisberg region and compared to the 10-year erosion damage mapping in the Frienisberg region. The erosion model resulted in a massive overestimation of soil erosion in the order of a factor of 5. Therefore, the potential erosion risk was corrected and reclassified accordingly. The new, corrected ERM2 2019 therefore differs significantly from the old ERM2 2010. Due to this correction, the new ERM2 2019 can be offset with C and P factors to the actual soil erosion and related to the legal guideline

values for tolerable soil erosion.

The distinction between arable and permanent grassland - and thus an erosion risk map (ERM) only for arable land (including artificial meadow) - could previously only be implemented for 19 cantons for which the corresponding parcel-specific digital data were available. Accordingly, a map of the potential erosion risk of arable land is now available for these 19 cantons. About 75 % of the arable land in Switzerland could thus be mapped on a parcel-by-parcel basis. The long-term mean potential soil erosion of these areas is about 17 t ha^{-1} a^{-1}. For the remaining seven cantons, the distinction between arable land and permanent grassland is based, among other things, on satellite data (Fraction of Vegetation Cover (FCover) 300m, Moderate Resolution Imaging Spectroradiometer (MODIS)). The data quality is significantly worse here. In addition to the erosion risk map, a map of flow paths for surface runoff on agricultural land based on the L-factor is now provided.

A C-factor tool that takes into account land management (crop rotation and tillage) has been newly developed. It is available as an alpha version on a virtual computer. A web application to link the new C-factor tool to the new ERM2 2019 is still under development.

2. Synthesis

2.1 Summary of most important results

Through this study, I have been able to fill the existing research gaps regarding the use of RUSLE and its application to arable lands in Switzerland through achieving my research objectives:

- Sub-objective 1: To map the LS factor as best as possible with a high-resolution digital terrain model and to define a suitable multiple flow algorithm to improve soil loss predictions (Publication 1).
- Sub-objective 2: To compare the soil loss from long-term field mapping with the modelled erosion in order to identify similarities or inconsistencies and, if necessary, calibrate the model (Publication 2).
- Sub-objective 3: To develop open source software tools for calculating the cover – and management and support practice factor CP and actual erosion risk on field block level for mitigation measures (Publication 3).
- Sub-objective 4: To create an upgraded, optimized and corrected potential erosion risk map for arable land in Switzerland based on the comparison of mapped and modelled soil loss (Publication 4).

Publication 1: Comparing different multiple flow algorithms to calculate RUSLE factors of slope length (L) and slope steepness (S) in Switzerland (Sub-objective 1)

This study showed that a high-resolution DEM was more important for the calculation of the LS-factor and potential soil erosion risk than the choice of MFA. Water flow patterns implemented in LS-factor including MFA-analysis cannot identify the flow of water including erosion. Indeed, flow patterns of water must be included in a more intensive way also to (R)USLE approaches. "We do not have experimental data to evaluate the results of the 21 L-factor variations. Therefore, we cannot say what is more convenient, but we can make a qualitative assessment and point out differences." (Bircher et al. 2019a:18) Experimental data would be needed to make the best decision, but such data would be very difficult to obtain.

For LS-factor calculations we used the MTFD-algorithm (Seibert & McGlynn 2007) with convergence value 1.1 in Paper 2, 3 and 4 due to comparable values based on the algorithms used in the ERM2 2010. However, spatial distribution of the L-factor values and the soil erosion risk was much more differentiated in the DEM2 and better reflected the topography

compared with the DEM25. Moreover, the lower-resolution DEM25 was not well suited to the chosen approach with field blocks.
The multiple flow algorithm used in the ERM2 2019 was also published as a flow path map (L-factor) on https://map.geo.admin.ch. The flow path map is helpful for consultation and mitigation measures, it shows thalweg and locations with possible offsite damage. It also can be used for other issues such as PPP (plant protection products) transport in water bodies.

Multiple flow algorithms can show flow patterns reflecting the topography in a more realistic manner than single flow algorithms. Flow barriers like streets, forests etc. have a big influence on flow paths. No big differences were identified in resolution of LS-factor between 2 m and 25 m.

Publication 2: Comparison of long-term field-measured and RUSLE-based modelled soil loss in Switzerland (Sub-objective 2)

There is a mismatch of modelled data compared to measured data of nearly factor 8. Separated in different mapped erosion classes the high soil loss rate values (> 4 t/ha) are represented well by the model (factors 0.8-3.3) but only represent a small area (8.7 ha) with 125.9 t/yr soil loss. In contrast, the classes with low mapped soil loss rates (< 4 t/ha) are not well captured within the applied model (factor 6.4-28.5) but represent a big area (249.4 ha) with a soil loss of 74.6 t/yr (Bircher et al. 2022). We corrected the modelled soil loss with factor 5 in publication 3 and 4, to mainly cover high soil loss rates (> 4 t / ha). In future projects, also mapped data from 2007-2017 can be used to calibrate the model (Prasuhn et al. 2020) and may lead to a wider accepted correction of the modelled soil loss.

A question remains whether the reported mismatch of modelled and measured soil loss of about factor 8 is based on an overestimation of the model or underestimation of the measured data? This question is difficult to answer. The USLE/RUSLE represents a long-term average modelled soil loss, which raises the questions if 10 years of measurement for calibration is sufficient? The USLE/RUSLE mainly incorporates the sheet erosion and rill erosion forms. In the field, however, it is mainly rill erosion and thalweg erosion that can be observed and measured adequately. The headland would have to be modelled separately. Tractor lanes and field margins would also have to be modelled separately. Is the influence of the many temporary ley grass in Switzerland sufficiently taken into account by the C factor represented by the carry-over effect? It can thus be concluded that the standard USLE does not model what we measure in the field.

Publication 3: Tools for USLE-CP-factor calculation and actual erosion risk on field block level for Switzerland (Sub-objective 3)

With the two newly developed tools (CP-factor-Tool and GIS-Tool), the actual erosion risk can be calculated at field block level and scenario analyses can be carried out on the effect of different crop sequences and tillage methods. By linking with ERM2 2019, this can be done separately for each arable field in Switzerland.

This increases the possible use of the ERM2 2019 and the tools for policies and management practices. For the enforcement of the DZV (Direktzahlungsverordnung: Direct Payments Ordinance), tools are needed to draw up suitable mitigation measures to reduce erosion. With the CP tool, such mitigation measures can be created and visualized. This helps the advisor to convince the farmer to take appropriate measures. Scenario calculations allow to distinguish between different field crops and land management practices (plough, direct seeding etc).

Publication 4: Summary of upgrade and optimization of the erosion risk map (ERM2). The new ERM2 (2019) for the arable land of Switzerland. Final report. 2019 (Sub-objective 4)

In this final report, an upgraded, optimized and corrected potential erosion risk map for arable land in Switzerland was created based on the comparison of mapped and modelled soil loss. Due to the mismatch between mapped and modelled erosion, a correction factor was introduced which reduces the erosion by a factor of 5. This factor was not only scientifically based, but with respect to the target users (farmers, scientists and federal offices) and without the correction factor, the tolerable soil erosion according to VBBo (Verordnung über die Belastungen der Bodens: Ordinance on the Pollution of Soil) guideline values would be exceeded almost everywhere and with necessary mitigation measures. The ERM2 2019 was prepared on behalf of the FOAG and is now available online (https://backend.blw.admin.ch/fileservice/sdweb-docs-prod-blwch-files/files/2024/11/12/cb9bce5a-926a-4a28-a2dc-5f7fca8f526e.pdf).

The tools (CP-factor-Tool and GIS-Tool) which are presented in detail in publication 3. can be programmed and further developed in open source languages. The CP-factor-tool is compared with other C-tools to justify it. The biggest difference of the C-factor within the compared tools was with 0.017 [unitless] only minimal.

2.2 Resulting key findings

In the following, the most important findings for improving (R)USLE are presented in

conceptual and methodological contributions, thematic contributions to soil research and findings for environmental and agricultural policy in Switzerland.

Conceptual and methodological contributions to (R)USLE

- The empirical (R)USLE model allows with its four factors (R*K*L*S) a simple way to generate a nationwide potential erosion risk map.
- The possibilities with the CP-factor-Tool implements a solution to calculate the cover- and management factor (C) and the protection factor (P) on small scale (field block level).
- A periodic update of input data is necessary, especially as the arable parcel layer changes slightly each year. Due to climate change, precipitation erosivity needs to be periodically updated and sowing and harvesting dates may shift. This may lead to a periodical update of the crop calendar.

Thematic (erosion-related) contributions to soil research

- Water flows derived from LS-factor based on high resolution data [2m] reflect soil erosion properties well.
- For a correction factor of the RUSLE model to overcome the tendency of overestimation a good data basis is needed at least of ten years field mapping.

Environmental and agricultural insights to Swiss policies

- With the new ERM2 2019 a new and upgraded tool for legal/regulation purposes is provided and supports sustainability-measures in agriculture and environmental management.

2.3 Conclusion

The main objectives of this thesis includes an improvement of the scientific evidence for erosion risk modelling, creation of a nationwide potential erosion risk map for Switzerland as a tool for decision support and development of software tools for scenario calculations based on adapted cover- and management and support practice factor (CP).

In the first publication, L- and LS-factors was used to simulate water runoff on the basis of the elevation model (DEM [2m]). The L-factor map allows a good identification of areas with potentially high erosion risk values. Other factors that influence water flows are water borders like (forests, roads, railways) that divide landscapes. Depending on the applied MFA's and their possible settings, water flows will be more or less channalized. As a result, more

dispersed water flows will result in shorter paths and more converging water flows will result in longer paths. Where water flows converge, higher potential erosion values result.

In publication 2 on the one hand during mapping, erosion can be overlooked or too much soil loss can be estimated. Also, during digitization processes mistakes can happen. The tendency in the field is to underestimate soil loss (Risse et al. 1993, Di Stefano et al. 2017, Saggau et al. 2019) and in contrast USLE-models tend to overestimate in some situations (Risse et al. 1993, Nearing 1998). To overcome this tendency of overestimation a broad-based correction factor has to be applied on the RUSLE-model (applied in publication 3 and 4).

Open points regarding the development of the CP-factor-tool (publication 3) are, that erosivity values may change due to climate change (Auerswald et al. 2021) which may lead to a creation of a new erosivity table for Switzerland in the valley and the hilly area. Also additional tillage methods can be considered, e.g. dykers in potato cultivation may reducing soil loss. The calculation based on cultivation parcels instead of field blocks may better incorporate crop rotations. Furthermore the implementation of buffer strips at the headland and between plots on the slope as mitigation measures may also reduce the soil loss.

The CP-Tool was developed for Switzerland including also the climatic and agricultural conditions. An adaptation of the tool will be easier for regions with similar conditions like Switzerland (climatic conditions have to be equal or at least similar to Swiss conditions). To adapt the CP-Tool for other countries with other climatic conditions more programming effort is needed.

For the applied correction factor in publication 4 not only statistical reasons have to be considered to correct a model, when tools for users are produced. An over correction can give the impression that soil loss is not a big problem. A correction factor implementation for the upgraded erosion risk map of Switzerland is not easy. Solid long term soil loss measurements during several years are needed, including representative crop rotations and high quality of input data like DEM, soil maps, landscape models for the adaptation of the modelled soil loss, which I successfully implemented in this thesis.

2.4 Outlook

Based on this research, the ERM2 2019 was updated in 2022 using new layers of Switzerland's arable land (see Federal metadata catalog). Instead of using only the mapped data from 1997-2007, a further mapping period from 2007-2017 (Prasuhn 2020) can be used to better calibrate the model. This inclusion could influence the correction factor. For the

future nationwide erosion risk map (ERM), better basic data (soil maps) for the K-factor may be available. The proportions of the field block map 2010 and 2019 have changed slightly throughout Switzerland. The coverages of the 1:5,000 and 1:25,000 maps have increased by 1.4 % and 2.1 % respectively (Bircher et al. 2019b). Also more precise data for field block map generation can be used in future, based on data from the cadastral survey instead of from the Swisstopo. Further a new calculation of the water connection map based on the new ERM2 2019 instead of the ERM2 2010 should be realized in the near future to improve the knowledge of possible material inflow in water bodies.

3. Bibliography

Alder S., Herweg K., Liniger H., Prasuhn V. (2013). Technisch-wissenschaftlicher Bericht zur Gewässeranschlusskarte der Erosionsrisikokarte der Schweiz (ERK2) im 2x2-Meter-Raster : Im Auftrag des Bundesamtes für Umwelt (BAFU) und des Bundesamtes für Landwirtschaft (BLW). Hrsg. Universität Bern und Forschungsanstalt Agroscope Reckenholz-Tänikon ART, Bern und Zürich, 1-37 S.

Auerswald, K. (1987). Sensitivität erosionsbestimmender Faktoren. – Wasser und Boden 1, 34–38.

Auerswald K., Ebertseder F., Levin K., Yuan Y., Prasuhn V., Nils Ole Plambeck, Menzel A., Kainz M. (2021). Summable C factors for contemporary soil use. Soil and Tillage Research. Volume 213, 105155.

Bircher P., Liniger H.P., Prasuhn V. (2019a). Comparing different multiple flow algorithms to calculate RUSLE factors of slope length (L) and slope steepness (S) in Switzerland. Geomorphology, Volume 346, 106850. https://doi.org/10.1016/j.geomorph.2019.106850

Bircher P., Liniger H. P. & Prasuhn V. (2019b). *Aktualisierung und Optimierung der Erosionsrisikokarte (ERK2): Die neue ERK2 (2019) für das Ackerland der Schweiz : Schlussbericht* Bern: Bundesamt für Landwirtschaft.

Bircher P., Liniger H.P., Prasuhn V., Kupferschmied P. (2021). Tools for USLE-CP-factor calculation and actual erosion risk on field block level for Switzerland. MethodsX, Volume 8, 101569. https://doi.org/10.1016/j.mex.2021.101569

Bircher P., Liniger H.P., Prasuhn V. (2022). Comparison of long-term field-measured and RUSLE-based modelled soil loss in Switzerland. Geoderma Regional. Volume 31, December 2022, e00595. https://doi.org/10.1016/j.geodrs.2022.e00595

Chen T., R.Q. Niu, P.X. Li, L.P. Zhang, B. Du (2011). Regional soil erosion risk mapping using RUSLE, GIS, and remote sensing: a case study in Miyun Watershed, North China, Environ. Earth Sci. 63 (3), 533–541.

Coulibaly S. F. M., Aubert M., Brunet N., Bureau F., Legras M., Chauvat M. (2022). Short-term dynamic responses of soil properties and soil fauna under contrasting tillage systems, Soil and Tillage Research, Volume 215.

Derpsch R., Kassam A., Reicosky D., Friedrich T., Calegari A., Basch G., Gonzalez-Sanchez E., Rheinheimer dos Santos D. (2024). Nature's laws of declining soil productivity and Conservation Agriculture, Soil Security, Volume 14.

Desmet P.J.J., Govers G., (1996). A GIS procedure for automatically calculating the USLE LS factor on topographically complex landscape units. J. Soil Water Conserv. 51 (5), 427–433.

Deumlich, D., (2012). Structure and Process - Influence of historical agriculture of linear flow paths by extreme rainfall in Brandenburg. Landscape Online 31, 1–19.

DIN 19708 (2017). Bodenbeschaffenheit - Ermittlung der Erosionsgefährdung von Böden durch Wasser mit Hilfe der ABAG, 2nd ed. Deutsches Institut für Normung e.V, Beuth, Berlin. 26 pp.

Di Stefano C., Ferro V., Pampalone V., (2017). Applying the USLE family of models at the Sparacia (South Italy) experimental site. Land Degrad. Dev. 28 (3), 994–1004.

FAO. (2019). Soil erosion: the greatest challenge to sustainable soil management. Rome. 100 pp. Licence: CC BY-NC-SA 3.0 IGO.

FAO and ITPS. (2015). Status of the World's Soil Resources (SWSR) – Main Report. Food and Agriculture Organization of the United Nations and Intergovernmental Technical Panel on Soils, Rome, Italy.

Favis-Mortlock, D. (1998). Validation of field-scale soil erosion models using common datasets. In: Boardman, J., Favis-Mortlock, D. (Eds.), Modelling Soil Erosion by Water. Springer, Berlin, Heidelberg, pp. 89–127.

Fiener, P., Dostál, T., Krása, J., Schmaltz, E., Strauss, P., Wilken, F. (2020). Operational USLE-based modelling of soil erosion in Czech Republic, Austria, and Bavaria - differences in model adaptation, parametrization, and data availability. Appl. Sci. 10 (10), 3647.

Fu, S., Cao, L., Liu, B., Wu, Z., Savabi, M.R. (2015). Effects of DEM grid size on predicting soil loss from small watersheds in China. Environ. Earth Sci. 73, 2141–2151.

Gisler S, H.P. Liniger, and V. Prasuhn. (2010). Technisch-wissenschaftlicher Bericht zur Erosionsrisikokarte der landwirtschaftlichen Nutzfläche der Schweiz im 2x2-Meter-Raster (ERK2). Bern: Centre for Development and Environment (CDE).

Gisler S., Liniger H. and Prasuhn V (2011). "Erosionsrisikokarte im 2x2 -Meter-Raster (ERK2)." Schweiz 2, no. 4: 148–55.

Koch U. & Prasuhn V. (2021). Risikokarten für den Eintrag von Pflanzenschutzmitteln in Oberflächengewässer auf Einzugsgebietsebene. Agroscope Science, 126, 1-85.

Kupferschmied P. (2018). Konzeptionierung und Operationalisierung einer aktuellen und schweizweit verwendbaren Berechnungsweise des USLE C-Faktors. Schaffung der inhaltlichen und technischen Grundlagen zur individuellen Integration des C-Faktors in die Erosionsrisikokarte der Schweiz. Geographisches Institut. Abteilung Integrative Geographie. Universität Bern. Masterarbeit.

Kupferschmied P. (2019). CP-Tool - Ein Programm zur Berechnung des Fruchtfolge- und Bewirtschaftungsfaktors (CP-Faktor) der Allgemeinen Bodenabtragsgleichung (ABAG). Anleitung zur Verwendung des CP-Tools. Agroscope.

Morgan R. P. C. (2005). Soil Erosion and Conservation. 3rd ed. Malden, MA: Blackwell Pub.

Mosimann T., Rüttimann M. (2006). Dokumentation – Berechnungsgrundlagen zum Frucht-

folgefaktor zentrales Mittelland 2005 im Modell Erosion CH (Version V2.02). Terragon, Bubendorf, 30 S.

Nazir M.J, Li G., Nazir M. M., Zulfiqar F., Siddique K. H.M., Iqbal B., Du D. (2024). Harnessing soil carbon sequestration to address climate change challenges in agriculture, Soil and Tillage Research, Volume 237.

Nearing, M.A., (1998). Why soil erosion models over-predict small soil losses and underpredict large soil losses. Catena 32 (1), 15–22.

Panagos, P., Borrelli, P., Meusburger, K., (2015a). A new European slope length and steepness factor (LS-factor) for modeling soil erosion by water. Geosciences 5, 117–126.

Panagos P., Borrelli P., Meusburger K., Alewell C., Lugato E., Montanarella L. (2015b). Estimating the soil erosion cover-management factor at the European scale, Land Use Policy 48, 38–50.

Panagos P., Borrelli P., Poesen J., Ballabio C., Lugato E., Meusburger K., Montanarella L., Alewell .C. (2015). The new assessment of soil loss by water erosion in Europe. Environmental Science & Policy. 54: 438-447. DOI: 10.1016/j.envsci.2015.08.012

Prasuhn V. (2011). Soil erosion in the Swiss midlands: Results of a 10-year field survey. Geomorphology, 126, 2011, 32-41.

Prasuhn V. (2012). On-farm effects of tillage and crops on soil erosion measured over 10 years in Switzerland. Soil Tillage Res. 120, 137–146.

Prasuhn V. (2020). Twenty years of soil erosion on-farm measurement: Annual variation, spatial distribution and the impact of conservation programmes for soil loss rates in Switzerland. Earth Surface Processes and Landforms. 1-16.

Prasuhn V. (2022). Experience with the assessment of the USLE cover-management factor for arable land compared with long-term measured soil loss in the Swiss Plateau. Soil & Tillage Research, 215, 2021, 1-12.

Prasuhn V., Liniger H.P., Gisler S., Herweg K., Candinas A. and Clément J.-P. (2013). “A High-Resolution Soil Erosion Risk Map of Switzerland as Strategic Policy Support System.” Land Use Policy 32: 281–91. doi:10.1016/j.landusepol.2012.11.006.

Renard K.G., Foster G.R., Weesies G.A., McCool D.K. and Yoder D.C. (1997). Predicting soil erosion by water. A guide to conservation planning with the Revised Universal Soil Loss Equation (RUSLE). Draft August (USA) (US Department of Agriculture). (= Agriculture Handbook. 703).

Risse L.M., Nearing M.A., Laflen J.M., Nicks A.D. (1993). Error assessment in the universal soil loss equation. Soil Sci. Soc. Am. J. 57 (3), 825–833.

Saggau P., Kuhwald M., Duttmann R. (2019). Integrating soil compaction impacts of tramlines into soil erosion modelling: a field-scale approach. Soil Syst. 3 (3), 51.

Schäuble H. (2005). AVErosion 1.0 für ArcView 3.x. Analyse der Bodenerosion nach den Modellen USLE und MUSLE87. Erweiterung für ArcView 3.x und den Spatial Analyst 1.x.

https://www.terracs.com/infosysteme/gis-software/averosion/.

Schmidt S., Alewell C., Panagos P., and Meusburger K. (2016). Regionalization of monthly rainfall erosivity patterns in Switzerland, Hydrol. Earth Syst. Sci., 20, 4359-4373, https://doi.org/10.5194/hess-20-4359-2016.

Schmidt S., Alewell C., and Meusburger K. (2018). Mapping spatio-temporal dynamics of the cover and management factor (C-factor) for grasslands in Switzerland, Remote Sensing of Environment 211, 89-104.

Schmidt S. (2018). *Soil erosion risk map for Swiss grasslands : a dynamic approach to model the spatio-temporal patterns of soil loss.* Doctoral Thesis, University of Basel, Faculty of Science. Official URL: http://edoc.unibas.ch/diss/DissB_13239

Schmidt S., Tresch S., Meusburger K. (2019). Modification of the RUSLE Slope Length and Steepness Factor (LS-Factor) for steep alpine slopes. MethodsX 6, 219-229. https://doi.org/10.1016/j.mex.2019.01.004

Schwertmann U., Vogl W., Kainz M. (1990). Soil erosion by Water. Verlag Eugen Ulmer, Stuttgart (in German).

Seibert J., and McGlynn B. L. (2007). “A New Triangular Multiple Flow Direction Algorithm for Computing Upslope Areas from Gridded Digital Elevation Models.” Water Resources Research 43, no. 4: n/a-n/a. doi:10.1029/2006WR005128.

United Nations (2016): The Sustainable Development Goals Report 2016.

Verheijen F. G. A., Jones R. J. A., Rickson R. J., Smith C. J., Bastos A. C., Nunes J. P., and Keizer J. J. (2012). Concise overview of European soil erosion research and evaluation. *Acta Agriculturae Scandinavica, Section B — Soil & Plant Science*, *62*(sup2), 185–190. https://doi.org/10.1080/09064710.2012.697573

Wischmeier W. H. & SMITH D. D. (1978). Predicting Rainfall Erosion Losses – a Guide to Conservation Planning. U.S. Dep. of Agriculture, Handbook No. 537. Washington.

Yang, X.H., (2015). Digital mapping of RUSLE slope length and steepness factor across New South Wales, Australia. Soil Research 53, 216–225.

3.1 Internet resources

Humus balance calculator (2023):
URL:
https://www.agroscope.admin.ch/agroscope/en/home/services/apps/humusbilanz-rechner.html

Soil compaction calculator (2023):
URL:
https://www.agroscope.admin.ch/agroscope/en/home/services/apps/terranimo.html

Spraycalculator (2023):
URL:

https://www.agroscope.admin.ch/agroscope/en/home/services/apps/spraycalculator.html

Official media release (2023):
URL: https://www.blw.admin.ch/blw/de/home/services/medienmitteilungen.msg-id-77771.html

Cantonal geodata (2024):

URL: https://geodienste.ch/

3.2 Data resources

Cadastral survey (2023)
URL: https://www.cadastre.ch/

Swisstopo (2023)
https://www.swisstopo.admin.ch/de/geodata/landscape/tlm3d.html

3.3 Legal resources

VBBo: Verordnung über Belastungen des Bodens (VBBo). SR 814.12.
https://www.fedlex.admin.ch/eli/cc/1998/1854_1854_1854/de.

DZV: Verordnung über die Direktzahlungen an die Landwirtschaft (DZV). SR 910.13.
URL: https://www.fedlex.admin.ch/eli/cc/2013/765/de

Part 2: Research Papers

Paper 1. Comparing different multiple flow algorithms to calculate RUSLE factors of slope length (L) and slope steepness (S) in Switzerland

Authors:
Bircher Pascal, Liniger Hanspeter and Prasuhn Volker

Originally published in: Geomorphology, 2019, 346, 106850

Boris-Link: https://boris.unibe.ch/132870/

Geomorphology 346 (2019) 106850

Contents lists available at ScienceDirect

Geomorphology

journal homepage: www.elsevier.com/locate/geomorph

Invited review

Comparing different multiple flow algorithms to calculate RUSLE factors of slope length (L) and slope steepness (S) in Switzerland

P. Bircher [a,b,*], H.P. Liniger [a,b], V. Prasuhn [c]

[a] Centre for Development and Environment (CDE), University of Bern, Mittelstrasse 43, 3012 Bern, Switzerland
[b] Institute of Geography, University of Bern, Hallerstrasse 12, 3012 Bern, Switzerland
[c] Agroscope, Division of Agroecology and Environment, Reckenholzstrasse 191, 8046 Zurich, Switzerland

ARTICLE INFO

Article history:
Received 30 April 2018
Received in revised form 20 August 2019
Accepted 21 August 2019
Available online 26 August 2019

Keywords:
Soil erosion
RUSLE
LS-factor
Multiple Flow Algorithm
DEM
GIS

ABSTRACT

The topographic LS-factor is one of the most difficult factors of the Revised Universal Soil Loss Equation (RUSLE) to define in a landscape with varying topography. For the application of the RUSLE not only at the plot but at catchment or landscape level, different multiple flow algorithms (MFA) have been developed and applied in various studies. However, these different MFAs in combination with various convergence values and applied at different resolutions of digital elevation models (DEM) have not been addressed so far. This publication focuses on filling this gap in the context of the agricultural area of Switzerland.

To evaluate different factors of slope steepness (S-factor) and slope length (L-factor), we tested four different multiple flow algorithms (MFA) (Deterministic Infinity (DINF), Multiple Flow Direction (MFD), Multiple Triangular Flow Direction (MTFD), Watershed (WAT)) and compared them with the MFA approach (Flow 95 in MUSLE87) used in the existing erosion risk map of Switzerland with a resolution of two metres. The MFAs we tested, used three different convergence settings and two digital terrain models (DEM) – one with a very fine two metre resolution (DEM2) and one with a coarser resolution of 25 m (DEM25) – enabling us to examine the influence of DEM resolution on the LS-factor. In total, we evaluated 21 L-factor variations to assess the significance for the prediction of the potential erosion risk. The calculations were applied at a local (test area Frienisberg, 88.7 ha) and at a regional scale (Lyss, 11,855 ha) in the agricultural Swiss Plateau. Both test areas were segmented into field blocks with an average size of 5 ha (14 field blocks in Frienisberg and 2305 field blocks in Lyss). A field block can contain several fields with different types of agricultural land use and is delineated by surrounding hydrological barriers. For these field blocks, the various L-factors were calculated automatically using Geographic Information Systems (GIS). Finally, the LS-factors were calculated for two selected MFAs.

The L-factors calculated with the various MFAs and the high-resolution DEM2 differed negligibly in terms of statistical values (mean values, standard deviation) and in the spatial distribution of the pixels both among each other and in comparison to the L-factor of the existing erosion risk map. As expected, using the coarser DEM25 resulted in considerably lower S-factors but surprisingly in higher L-factors, so that there was little difference in the average LS values between the DEM25 and the DEM2. However, spatial distribution of the L-factor values and the soil erosion risk was much more differentiated in the DEM2 and better reflected the topography compared with the DEM25. Erosion risk hotspots such as slope depressions with concentrated runoff and thalweg erosion could be reliably identified. Moreover, the lower-resolution DEM25 was not well suited to the chosen approach with field blocks of a mean size of 5 ha, as the intersection of polygon and raster data produced edge errors depending on the clipping method. This study showed that a high-resolution DEM was more important for the calculation of the LS-factor and potential soil erosion risk than the choice of MFA, and that the calculation of LS-factors based on field blocks offered a number of advantages mainly in determining the channel network and maximum flow length.

Contents

* Corresponding author at: Centre for Development and Environment (CDE), University of Bern, Mittelstrasse 43, 3012 Bern, Switzerland.
E-mail address: pascal.bircher@cde.unibe.ch (P. Bircher).

https://doi.org/10.1016/j.geomorph.2019.106850
0169-555X/

1. Introduction

Soil degradation including soil erosion is a well-known global, regional, and local problem highlighted by several stakeholders such as the Food and Agriculture Organization (FAO), farmers, policymakers, and social and natural scientists (Keizer et al., 2016; Borrelli et al., 2017). Soil loss is an important topic and was discussed at many conferences during the United Nations-declared International Year of Soils 2015. It was also a topic of numerous meetings of the United Nations Development Programme (UNDP, 2015) in the run-up to establishment of the UN Sustainable Development Goals.

Water erosion is often modelled for short-term periods, with physical-event-based models in small or only a few catchments (Morgan, 2009; Mitasova et al., 2013). On the other hand numerous semi- empirical, plot-field-scale models exist for assessing soil erosion risk at regional, national, continental and world-wide scales (Panagos et al., 2015b; Borrelli et al., 2017; Benavidez et al., 2018). Calculating a nationwide long-term erosion risk map requires large quantities of data that are not available from the official authorities in wished quality. An empirical-based model like the Universal Soil Loss Equation (USLE) (Wischmeier and Smith, 1978) and revised versions such as the Revised Universal Soil Loss Equation (RUSLE) (Renard et al., 1997), allow the use of data of varying accuracy. Therefore, the USLE and RUSLE are still the most frequently used erosion models despite numerous deficiencies, weaknesses, and limits (Favis-Mortlock et al., 2001; Boardman, 2006; Benavidez et al., 2018). The combination of geographical information systems (GIS) and computer processing power allows better resolution input data to be used for modelling studies and projects. Consequently, many RUSLE-based erosion risk models were recently established in several countries with databases of various resolutions (e.g. Borrelli et al., 2016, Italy, 25 m; Kotremba et al., 2016, Rheinland-Pfalz in Germany, 1 m; Hrabalíková and Janeček, 2017, Czech Republic, 5 m), as well for the entire European area (Panagos et al., 2015b, 25 m) and at a global scale (Naipal et al., 2015; Borrelli et al., 2017, 250 m). Often, the RUSLE approach is combined with remote sensing data to calculate the RUSLE-factors (Ismail and Ravichandran, 2008; Kamaludin et al., 2013) or with sediment delivery models for sediment yield (Fernandez et al., 2003; Fu et al., 2006; Bhattarai and Dutta, 2007).

Next to the C-factor, the LS-factor is the most sensitive parameter in estimating soil loss in RUSLE (Auerswald, 1987; Panagos et al., 2015a). The L and S factors are combined as the topographic LS-factor. The slope length factor (L) is more problematic to calculate than the slope steepness factor (S) and it plays a key role for the application of the RUSLE erosion model (Hickey, 2000; Winchell et al., 2008; Hoffmann et al., 2013; Oliveira et al., 2013; Liu et al., 2015; Hrabalíková and Janeček, 2017). For catchment-scale studies the one-dimensional slope length factor of individual slopes in the USLE was replaced by the upslope contributing area in newer studies to respect the topography of complex watersheds or big two- or three-dimensional areas. Different approaches and algorithms to calculate these slope length factors was described by Van Remortel et al. (2001), Garcia Rodriguez and Gimenez Suarez (2010), Hoffmann et al., 2013, Oliveira et al. (2013), and Zhang et al. (2017). These are the unit stream power method (Moore and Burch, 1986; Moore et al., 1991; Mitasova et al., 1996), raster grid cumulation (Hickey, 2000), and upslope contributing area methods (Moore and Wilson, 1992; Desmet and Govers, 1996). The method of Desmet and Govers (1996) was recently improved by several authors: Winchell et al. (2008) as well as Garcia Rodriguez and Gimenez Suarez (2012). Panagos et al. (2015a) used the unit contributing area approach based on Desmet and Govers (1996) to calculate LS-factors for Europe, and Borrelli et al. (2017) calculated it for the whole world. To avoid possible overestimation and extreme values of L-factors, often theoretical maximum values are defined. Those maximum values are often 122 m or the equivalent length in number of pixels depending on resolution because surface runoff will usually concentrate in <122 m, although longer slope-lengths are occasionally found (Fu et al., 2006; Yang, 2015; Borrelli et al., 2017). In other studies, thresholds for slope changes that indicate deposition were used (Liu et al., 2011; Zhang et al., 2013; Yang, 2015; Zhang et al., 2017). Based on the two approaches of Hickey (2000) and Van Remortel et al. (2001), new models and tools for LS-factor calculations were developed by Liu et al. (2011), Zhang et al. (2013), Yang (2015), and Zhang et al. (2017), including deposition zones, channel networks, and convergence flow areas with cut-off effects or turning points.

The upslope contributing area, also known as flow accumulation, contains the total upslope area or all upslope pixels flowing in single pixels.

The choice of a flow-routing algorithm has a big influence on the calculation of the contributing area (Wilson et al., 2008). Multiple flow direction algorithms are better accepted than single flow algorithms, because convergent and divergent flows are better represented in real landscapes (Wilson et al., 2008; Orlandini et al., 2012). Some multiple flow direction algorithms can describe overland flow dispersion (Freeman, 1991; Quinn et al., 1991; Tarboton, 1997; Seibert and McGlynn, 2007). These algorithms are not only used for LS-factor determination in soil erosion modelling, but are also important for identifying critical source areas in hydrological modelling (Thomas et al., 2016; Thomas et al., 2017). Even though there have been significant advances in recent decades in erosion modelling with RUSLE, especially thanks to geospatial technologies such as GIS (Benavidez et al., 2018; Borrelli et al., 2018), there are hardly any comparative studies on different available LS-factor calculations and their variations. Accordingly, little is known about whether and why they differ and how big the differences are.

To ensure hydrological connectivity DEM correction is an important aspect of hydrological modelling and soil erosion modelling. The correction or filling of the DEM provides hydrological connectivity and also corrects artefacts of DEM production. In advance of the LS-factor calculation and the use of a high-resolution DEM with multiple flow algorithms, most newer studies pre-process the DEM, applying DEM correction (Van Remortel et al., 2001; Liu et al., 2015; Yang, 2015). In hydrological modelling, a total connectivity without absolute sinks is necessary to model the flow pathways to the outlet of the catchment area (Thomas et al., 2017). The necessity of DEM correction also depends on the accuracy and resolution of the DEM. Lane et al. (2004) distinguish between pits, hollows, and flats. Pits are mostly single cells with minimal slope to neighbouring cells, and often they are artefacts or errors of the DEM. Hollows are multiple neighbouring pixels creating drainless sinks. Flats are planar areas without flow direction. The problem is how to distinguish between real sinks and artificial sinks (artefacts of the DEM) to best represent reality (Lane et al., 2004; Thomas et al., 2016). Different methods have been developed to fill flow sinks (Planchon and Darboux, 2002; Wang and Liu, 2006). To date, there are hardly any comparative studies and reliable statements about the benefits or problems of different DEM correction methods for LS-factor calculation.

Several authors have mentioned the fundamental importance for soil erosion risk assessment of cell size and the accuracy of DEMs on the production of different terrain parameters like slope steepness and slope length (Hickey, 2000; Thompson et al., 2001; Kienzle, 2004). Local artefacts can occur when the resolution is very high or the accuracy is low (Hengl, 2006). It is accepted that, the lower the resolution of a DEM, the greater the smoothing effects that reduce the slope steepness (Kienzle, 2004). For example, in a comparison of DEMs with 5, 10, 25, 50, and 100 m raster cell sizes, Kienzle (2004) determined an underestimation of slope steepness with bigger raster cell data, concluding that raster cell sizes >25 m are no longer able to accurately represent steep slopes. On the other hand, a very high-resolution DEM can lead to very high LS-factor values and therefore to an overestimation of soil erosion risk by RUSLE. Many studies show an overestimation of the risk of erosion based on the RUSLE approach compared to measured soil erosion (Abu Hammad et al., 2004; Rymszewicz et al., 2015). Some researchers have tried to understand the resolution effect of the digital elevation models (DEM) on the RUSLE topographic LS-factor, but most of them use a DEM resolution of 10 m or coarser: e.g. Claessens et al. (2005) [10–100 m], Wu et al. (2005) [10 m–250 m], and Mondal et al. (2017) [30–330 m]. Higher-resolution DEMs were only used by Deumlich (2012) [1–25 m], Fu et al. (2015) [2–30 m], Yang (2015) [5–100 m], and Wang et al. (2016) [2–30 m]. So far, it has not yet been systematically examined whether different DEM resolutions result in different LS-factor values and whether use of high-resolution DEMs results in higher L-, S-, and LS-factors.

Switzerland already has an online high-resolution [2 m] erosion risk map (ERM2) for agricultural land, hosted by the government (Prasuhn et al., 2013). The ERM2 is based on the MUSLE 87 approach (Moore and Burch, 1986; Moore et al., 1991) and was calculated in ArcView on a 2 m grid with an outdated plugin which is no longer supported (AVErosion, Vers 1.1, Schäuble, 2005). The MUSLE 87 approach involves the possibility of long-term erosion risk calculations with the program Flow 95, a multiple flow algorithm (MFA) like the Desmet and Govers (1996) approach. The ERM2 has proved its worth in practice as an aid to the enforcement of legal bases and as a consulting tool for farmers and agricultural advisors (Prasuhn et al., 2013). However, it needs to be upgraded, as it is based on data older than 2010 and only up-to-date maps of all RUSLE input parameters and the calculated erosion risk are credible to farmers and public authorities. The DEM of the ERM2 was created with LIDAR in 2007 and was the first version of a DEM with a 2 m resolution covering all of Switzerland up to 2000 m altitude. This first version of the DEM contains artefacts because of production errors, like cutting effects between different national map extents, and technical errors (Swisstopo 2009). It is therefore essential to find an adequate replacement for the existing approach. In addition to using the latest data, it is very important to recalculate the LS-factor – the most important factor in the potential risk of erosion. The current ERM2 has led to high soil erosion risk values compared to measured soil erosion (Prasuhn, 2011). We suspected one of the reasons for this to be that the DEM's high resolution of 2 m leads to high LS-factor values. In our study we therefore also examine different DEM resolutions, using a 2 m DEM (DEM2) and a 25 m DEM (DEM25). For computational reasons, the 21 different L-factor calculation methods cannot be tested for the whole agricultural area of Switzerland (7,686,981 ha or 19,217 million pixels including grassland and alpine area). In this study, we therefore analysed two test areas with different map scales.

Overall, the current state of the art can be summarized by stating that DEM data are available almost everywhere in the world – but differ in quality and spatial resolution. These data can easily be prepared using GIS technologies, and standard software packages offer a variety of ways to then calculate S-, L-, and LS-factors.

In this article, we present an extensive comparative analysis with which we pursued two aims. The first was to show whether different multiple flow algorithms (MFAs) and convergence options result in different modelled water flow properties influencing LS-factor calculations. To find this out, we compared four common MFAs (Deterministic Infinity (DINF), Multiple Flow Direction (MFD), Multiple Triangular Flow Direction (MTFD), Watershed (WAT)) for L-factor calculation, including varying convergence values among each other and with the MFA of the current ERM2 (Flow 95 from MUSLE87). The second aim was to examine the effect of two DEMs with different resolutions (2 m vs 25 m). We expected the use of a very high-resolution DEM (2 m) to result in higher S-, L-, and LS-factor values and therefore in a higher potential erosion risk. All in all, we analysed 21 variations at a local (Frienisberg) and a regional (Lyss) scale, in areas typical of the Swiss Plateau. The calculations for both test areas are processed in field blocks or micro-catchments of 5 ha mean size. These field blocks enabled us to distinguish between agricultural and non-agricultural areas and to adequately represent the topographic complexity and patchiness of landscapes in Switzerland. The LS-factor calculations were then executed with two chosen MFAs and both DEMs. Our results are intended to contribute to a better understanding of different L- and LS-factor calculations and to provide a basis for informed selection of suitable calculation methods so as to model soil erosion risk as realistically as possible using RUSLE.

2. Methods

2.1. Methodological overview

This section provides a brief guide to the huge amount of data and results produced in this study. We processed 20 L-factor

Table 1
Overview of the 21 approaches and basic data (in bold frame) used for comparison of statistical features; Lyss and Frienisberg are the two test areas (see Section 2.2).

Tool	Algorithm	Convergence value	Resolution of DEM		Test area		Clipping		L-factor[a]	S-factor[b]	LS-factor[c]
			2 m	25 m	Lyss	Frienisberg	soft	hard			
Saga Gis	MFD	0	x	x	x	x	x		x	x	
		1.1	x	x	x	x	x	x	x	x	x
		1.25	x	x	x	x	x		x	x	
	MTFD	0	x	x	x	x	x		x	x	
		1.1	x	x	x	x	x		x	x	
		1.25	x	x	x	x	x		x	x	
GrassGis	WAT	1	x	x	x	x	x		x	x	
		5	x	x	x	x	x	x	x	x	x
		10	x	x	x	x	x		x	x	
Saga Gis	DINF	1.1	x	x	x	x	x		x	x	
AVErosion in ArcView	MUSLE 87	–	x		x	x	x		x		

MFD: Freeman, 1991; MTFD: Seibert and McGlynn, 2007; WAT: Ehlschlaeger, 1989, Quinn et al., 1991; DINF: Tarboton, 1997; MUSLE 87: Moore and Burch, 1986, Moore et al., 1991.
[a] Calculated according to Desmet and Govers, 1996
[b] Calculated according to McCool et al., 1987
[c] Product of 1 and 2.

calculations with three convergence options plus the MUSLE 87 approach used in the current ERM2. This was done for two different test areas, which we explain in detail in Section 2.2 below. Further, we used two different DEMs and two different clipping approaches (hard and soft) (Table 1). Finally, we compared the resulting L-, S- and LS-factors. More details about the methods are provided in Sections 2.2 and 2.3.

2.2. Study area

The Frienisberg test area represents the local scale, comprising 88.7 ha or 221,673 pixels at 2 × 2 m. Frienisberg has a varied topography and is a hilly region between the northern Prealps and the Jurassic alps on the Swiss Plateau (Fig. 1). It is located about 20 km north-west of Bern, with altitudes ranging from 591 to 729 m (Table 2). The topography consists of very steep (slopes > 24.2°) and flat areas (slopes < 2.9°), with ridges, channels, peaks, and very small pits (sinks). Most soils in the test area are quite permeable Cambisols and Luvisols over ground moraine; they are mostly sandy loams which have been rated as having moderate erodibility. The predominant family farms apply mixed farming methods of growing crops and keeping livestock. Crop rotations are versatile and mostly have a high proportion of temporary grass-clover mixtures. The Frienisberg area lies in the moderate climate zone with an annual average temperature of approximately 8.5 °C and annual precipitation from 1035 to 1150 mm. Frienisberg is one of five

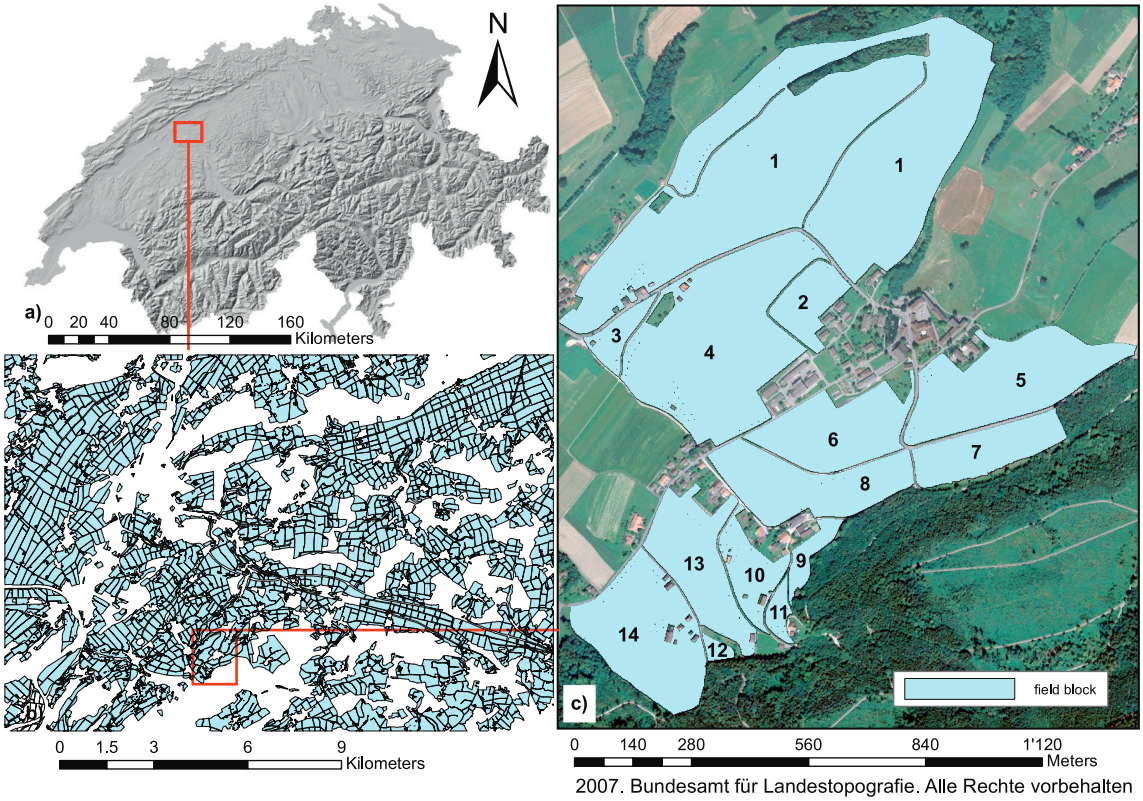

Fig. 1. Overview of study area; a) Map of Switzerland, b) 2305 field blocks of Lyss national map extent at 1:25,000, c) extent of Frienisberg with numbered field blocks (SwissALTI3D 2015, Vector 25 2008, Swisstopo, 2008).

Table 2
Comparison of statistic features of the 2 m and the 25 m DEM based on the 25 m mask for Frienisberg and Lyss; [m a. s. l. = meters above sea level]; mask (see Table 4).

Resolution of DEM	Frienisberg, masked		Lyss, masked	
	2 m	25 m	2 m	25 m
Number of cells (N)	151,280	941	20,745,979	132,829
Area [ha]	60.5	58.8	8298	8302
Minimum [m a. s. l.]	591	600.5	431.6	432.1
Maximum [m a. s. l.]	728	722.7	789.5	789.8
Mean [m a. s. l.]	660.8	660.7	521.3	521.5
Standard deviation [m a. s. l.]	26.8	26.6	69.9	69.8

long-term monitoring areas in which erosion damage has been mapped since 1987. Over a period of 10 years, the visible erosion features on 203 arable fields in the area were continuously mapped and quantified by Prasuhn (2011, 2012). Although the average soil loss was relatively low (0.75 t ha^{-1} yr^{-1})7, the maximal annual erosion in a single field was 96 t. Rill and ephemeral gully erosion accounted for 75%, while inter-rill erosion took place only in 25% of the cases (Prasuhn, 2011). Gully erosion has not been reported so far. Frienisberg is also one of 17 case studies around Europe in an EU project called RECARE (Preventing and Remediating Degradation of Soils in Europe through Land Care, 2013–2018, www.recare-project.eu), which investigated the influence of measures to combat different soil threats. Frienisberg is part of the Lyss test area. This second, larger national map extent (1:25,000) represented the regional scale in our study, covering 11,855 ha or 29,637,170 pixels of 2 × 2 m. The Lyss area consists mainly of arable land typical of the Swiss Plateau. Topographically it is more balanced than the Frienisberg area, with fewer steep and more flat slopes, as well as a few small plains. The L-factor calculation and its statistical evaluation are mainly based on the local scale (Frienisberg) (Fig. 1c); the DEM correction, slope calculation, as well as S-factor and LS-factor calculations focus on the bigger map extent of Lyss (Fig. 1b).

2.3. Basic data and calculations

2.3.1. Digital elevation model (DEM)

We used two different DEMs available for the whole area of Switzerland to study the influence of raster size and accuracy of the data. The DEM2 we used was produced with Light Detection and Ranging (LIDAR) technology. Vertical accuracy, at ±0.5 m 1 σ, is very high (Swisstopo, 2015). The DEM25 was derived from the 1:25,000 map set of Switzerland. Mean deviation is 1.5 m in the Jura region and Swiss Plateau, 2 m in the Prealps and Ticino, and 3–8 m in the Alps (Swisstopo 2005). The differences in mean value of the two DEMs in metres above sea level for both test areas (Frienisberg and Lyss) are very low (Table 2).

2.3.2. Digital elevation model (DEM) correction

Using a raw DEM generated with LIDAR results in a number of hydrological sinks and artefacts acting as absolute sinks. These absolute sinks can be avoided using a fill function, to obtain a connected DEM essential for hydrological models. This correction of the DEM is an important step to hydrologically connect the DEM and was done with the Arc Hydro Tools in ArcGis v.10.2.2, reported in Maidment (2002). Different fill heights lead to a more or less flooded area or a more or less hydrologically connected DEM. Therefore, different fill heights were tested (0.2; 0.5; 2.0; 4.0; 6.0 m; fill all) to see how big the affected area is. Fill All corresponds to a DEM completely hydrologically connected. During the application of DEM correction, a minimum slope gradient between neighbouring cells of 0.1° was enforced. This DEM correction was applied in a pre-processing to both the DEM2 and the DEM25 (Maidment, 2002). Afterwards, the slope (Zevenbergen and Thorne, 1987) and catchment area are calculated in Saga-Gis and GrassGis, and the results are included in the S-factor and L-factor calculation.

2.3.3. Field block map

The Swiss landscape is characterized by topographic complexity, patchiness, and small-scale farming (Alder et al., 2015). This makes field blocks – a reference unit used in Germany (Volk et al., 2010; Tetzlaff et al., 2013) – a good basis for calculating the L-factor. The landscape model (Vector 25) as basis data for the field block map in the ERM2 is also derived from Swisstopo (2008). Field blocks were extracted with the same approach mentioned in Prasuhn et al. (2013). The agricultural area of Switzerland is represented in the field blocks and covers grassland, meadows, pastures, crop fields, and grapes. Field blocks were delineated by surrounding hydrological barriers like roads, railways, forests, villages, rivers, lakes, and other objects that prevent a continuous water flow. A field block can thus contain several cultivation plots, feature different types of use (arable land, permanent grassland, vineyards, or different field crops), and be cultivated by different farmers. These field blocks serve as the calculation unit for the different LS-factor methods and represent hydrological micro-catchments, into which no water can flow from the outside and no water can leave. For each grid cell in a field block we calculated the

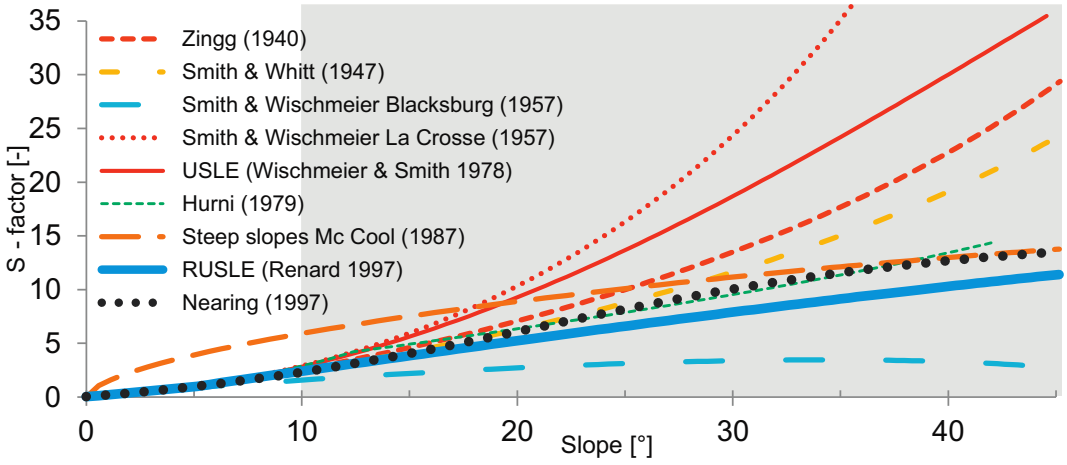

Fig. 2. Selection of different S-factor approaches calculated for a virtual slope steepness of 45° separated into steep slopes > 10° and low slopes < 10°.

L-, S-, and LS-factors. Frienisberg consists of 14 field blocks with a mean size of 6.3 ha; Lyss consists of 2305 field blocks with a mean size of 5.1 ha (Fig. 1). The field block map of Switzerland includes 180,920 field blocks ranging from 0.25 ha to 1444 ha in size, with a mean value of 5.0 ha, a standard deviation of 11.0 ha, and a median of 2.4 ha (Prasuhn et al., 2013).

2.3.4. Clipping method

A further factor influencing the waterflow calculation is the clipping method between vector (field block) and raster data with different resolutions (DEM2 vs DEM25). Using a soft clipping method in GIS systems means that the accuracy of the DEM used and its raster cells are more important than the accuracy of the cutting elements (field blocks, vector data). By contrast, with the hard clipping method, the accuracy of the vector data (field blocks) is more important than the raster cells of the DEM. For example, when soft clipping is applied with the DEM25, small roads are ignored to preserve information. But when hard clipping is applied, all small roads are cut into the DEM, regardless of data loss (Table 4, Fig. 8). The hard clipping method also provides a suitable mask based on the DEM25 for statistical analyses. For the statistical comparison of the S, L, and LS-factor values of the 2 m and 25 m elevation models, the 2 m model was always scaled down to the size of the 25 m model (masked, hard clipped). This results in considerable data loss towards the boundary of the field blocks on both DEMs due to the edge effects on the 25 m model. However, to calculate LS-factors for the whole of Switzerland with the DEM2, we used the soft clipping method without masking. With the DEM2, the clipping method is not important and the data loss is very low. In this article, the soft clipping method without masking was also used in all maps with DEM2.

2.3.5. USLE approaches and derivates

The RUSLE/MUSLE 87 (Eq. (1)) approach is based on the widely used USLE estimation (Wischmeier and Smith, 1978), and consists of six factors, where L is the slope length factor [no unit], S is the slope steepness factor [no unit], K is soil erodibility factor [$t * ha * h * ha^{-1} * MJ^{-1} * mm^{-1}$], R is the rainfall and run-off erosivity factor [$MJ * mm * ha^{-1} * h^{-1} * y^{-1}$], C [no unit] is the cover and management factor, and P [no unit] is the support practice factor. The multiplication of the factors $L * S * K * R$ results in the potential erosion risk for each grid cell, whereas the multiplication of all six factors leads to the actual soil erosion risk in tonnes per hectare and year (Wischmeier and Smith, 1978; Renard et al., 1997). The calculation in this study is limited to the potential soil erosion risk. The computations are based on a regular grid of equal-sized grid cells (2 m × 2 m or 25 m × 25 m).

$$A = L * S * K * R * C * P \quad (1)$$

The USLE/RUSLE approach was originally designed to predict long-term average annual soil loss associated with rill and inter-rill erosion on hillslopes, but not gully erosion or deposition of soil material. Furthermore the RUSLE-approach base on a standard plot with 22.1 m length and a slope of 5.1°. The use of multiple flow algorithms makes it possible to distribute virtual water on various deeper neighbouring cells, which leads to results that better reflect erosive processes on a complex topography. In addition, ephemeral gully erosion (thalweg erosion) is represented well (Prasuhn, 2011). Finally, the USLE/RUSLE approach only predicts "edge-of-field" erosion, while catchment erosion estimates are adjusted downward by a sediment delivery ratio (Boomer et al., 2008).

Table 3
Different fill heights and filled agricultural area in hectares and in % for Lyss [11,854.9 ha] and DEM2.

Fill height [m]	0.2	0.5	2.0	4.0	6.0	Fill All
Filled area [ha]	426.1	427.5	428.4	428.6	1705.3	1705.8
Filled area [%]	3.59	3.60	3.61	3.62	14.38	14.39

Table 4
Differences of soft and hard [mask] clipping methods for statistical analysis and comparison with DEM2, DEM25 and original polygon data; n = number of raster cells or polygons.

Test area	Frienisberg		Lyss	
Clipping method [resolution]	n	Area [ha]	n	Area [ha]
Soft clipped [25 m]	1400	87.5	191,993	12,000
Soft clipped [2 m]	221,673	88.7	29,637,170	11,855
Hard clipped [25 m] [mask]	941	58.8	132,832	8302
Hard clipped [2 m] [masked; based on 25 m mask]	151,280	60.5	20,745,979	8298
Area of polygons	14	88.7	2305	11,854

2.3.6. L- and S-factor approaches and combinations

There are numerous LS-factor calculation methods (Wischmeier and Smith, 1978; Moore and Burch, 1986; Moore et al., 1991; Renard et al., 1997; Böhner and Selige, 2006) with connected and separated L- and S-factor calculations. Connected LS-factor calculations (Moore and Burch, 1986; Moore et al., 1991; Böhner and Selige, 2006) use a smoothing calculation, like mean slope values for the catchment calculation or constant values for rill and inter-rill properties (Moore and Burch, 1986; Moore et al., 1991; Moore and Wilson, 1992). To consider the precise topography given by a high-resolution 2 m-DEM and also for confirmability, we applied separate S- and L-factor calculations.

2.3.7. S-factor calculation

Many S-factor equations exist in the literature, valid and measured for inclinations of up to 9.1°–11.3° (Zingg, 1940; Smith and Whitt, 1947; Smith and Wischmeier, 1957; Wischmeier and Smith, 1978; McCool et al., 1987; Nearing, 1997). Other studies extrapolated or assessed the S-factor to steeper inclinations like 28.8° (Hurni, 1979; Liu et al., 1994). To select a suitable method for our area, we tested different approaches based on virtual slope values (slopes 0°–45°) (Fig. 2). There are different properties of slope and S-factor relations among the chosen equations, especially at high slopes > 10°. Most arable land in Switzerland is on slopes < 10 degrees (see Section 3.2), where the differences of the compared approaches are not very high. Therefore, we opted for the approach of Renard et al. (1997), which is used in the RUSLE and based on McCool et al. (1987). This approach was also used by Prasuhn et al. (2013) for the current erosion risk map of Switzerland.

Slope was computed in SAGA-Gis (System for Automated Geoscientific Analyses) from the corrected DEM using the Zevenbergen and Thorne (1987) method for both DEMs. The S-factor (Eqs. (2) and (3)) was calculated with the well-known RUSLE approach in Renard et al. (1997) based on McCool et al. (1987), where S_{low} is for slopes smaller than 5.1° and S_{steep} is for slopes equal or >5.1°. θ is the slope in degrees.

$$S_{low} = 10.8 * \sin(\theta) + 0.03 \; for \; \theta < 5.1\,^{\circ} \quad (2)$$

$$S_{steep} = 16.8 * \sin(\theta) - 0.5 \; for \; \theta \geq 5.1\,^{\circ} \quad (3)$$

2.3.8. L-factor calculation

The L-factor (Eq. (4)) was calculated with the approach of Desmet and Govers (1996), where A is the upslope contributing area in square metres, d is the raster resolution in metres, m (Eq. (5)) is the slope length exponent showing the relation between rill and

inter-rill erosion, β (Eq. (6)) is the slope direction, and θ is the slope angle in degrees.

$$L_{factor} = \frac{\left(A + d^2\right)^{m+1} - A^{m+1}}{d^{m+2} * 22.13^m} \quad (4)$$

$$m = \frac{\beta}{1+\beta} \quad (5)$$

$$\beta = \left(\frac{sin(\theta)}{0.0896}\right) / \left(3 * sin(\theta)^{0.8} + 0.56\right) \quad (6)$$

Table 5
Slope [°] and S-factor [-] statistics for Frienisberg, hard clipped method (masked).

Frienisberg	Slope [2 m]	Slope [25 m]	S-factor [2 m]	S-factor [25 m]
Number of cells (N)	151,280	941	151,280	941
Area [ha]	60.5	58.8	60.5	58.8
Minimum	0	0.7	0.03	0.16
Maximum	45.8	23.1	11.5	6.1
Mean	9.11	8.88	2.18	2.11
Standard deviation	4.7	3.77	1.3	1.05

The L-factor approach was combined with four different multiple flow direction algorithms and compared with the approach of Schäuble (2005) from the current ERM2, referred to as MUSLE 87:

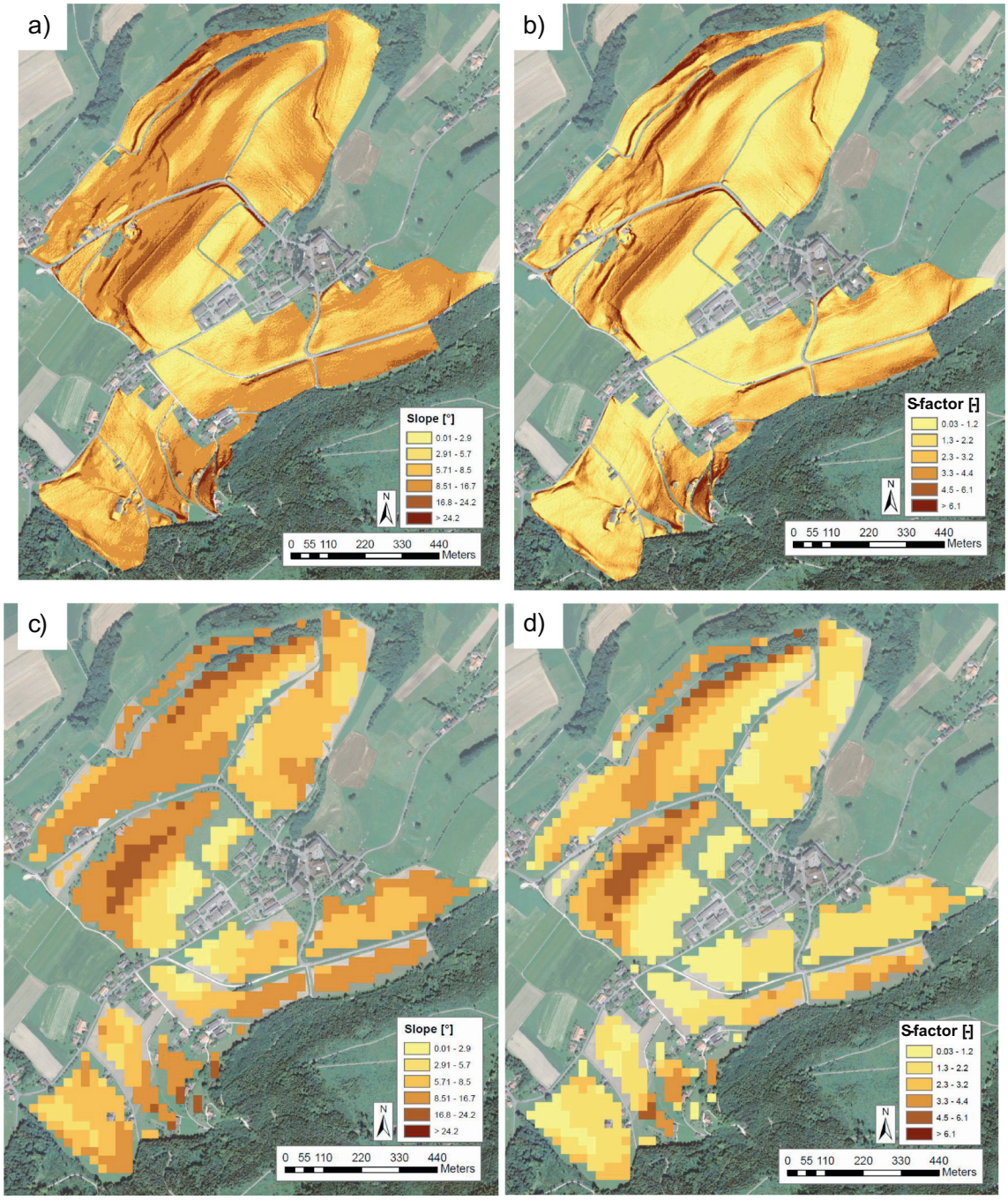

Fig. 3. Topographical properties of Frienisberg; a) Slope [°] and b) S-factor [−] calculated with the RUSLE approach based on Swisstopo DEM 2015 [2 m]; c) Slope [°] and d) S-factor [−] calculated with RUSLE approach based on Swisstopo DEM 2005 [25 m]; DEM2 soft clipped; DEM25 hard clipped.

Table 6
Slope [°] and S-factor [−] statistics for Lyss, hard clipped method (masked).

Lyss	Slope [2 m]	Slope [25 m]	S-factor [2 m]	S-factor [25 m]
Number of cells (N)	20,745,979	132,832	20,745,979	132,832
Area [ha]	8298	8302	8298	8302
Minimum	0	0	0.03	0.03
Maximum	65.2	45.5	14.88	11.48
Mean	3.63	2.92	0.83	0.63
Standard deviation	3.43	2.93	0.87	0.69

- Deterministic Infinity (DINF), SagaGis
- Multiple Flow Direction (MFD), SagaGis
- Multiple Triangular Flow Direction (MTFD), SagaGis
- Watershed (WAT), GrassGis
- MUSLE 87, AVErosion in ArcView

The DINF algorithm provides pseudo multiple flow properties because it only respects the next two deeper cells of a raster file (Tarboton, 1997). The MFD (Freeman, 1991) algorithm shares virtual water with every next deeper raster cell and the MTFD combines the DINF properties and the MFD properties and concentrates water flow in valleys, depressions, and natural sinks (Seibert and McGlynn, 2007). The WAT approach computes the water flow like an MFA and includes an option with least-cost search in the algorithm (Ehlschlaeger, 1989; Quinn et al., 1991). Other MFAs like Terraflow (Arge et al., 2003) in GrassGis, Rho (Fairfield and Leymarie, 1991), and DEMON (Costa-Cabral and Burges, 1994) algorithms in Saga-Gis were not processed due to calculation problems and the need for some physical parameters, such as amount or content of water and soil properties for event-based models.

2.3.9. LS-factor

L-and S-factors can be combined through multiplication and lead to different values depending on approaches and resolutions. Some LS-factor calculations are coupled to simplify the process of modelling in programmes like SagaGis or GrassGis but can hinder the confirmability (Moore et al., 1991; Moore and Wilson, 1992; Böhner and Selige, 2006). Most of the available LS algorithms are already implemented within GIS software, such as IDRISI, SagaGIS, GrassGis, ArcGIS, etc. SagaGis v.2.1.2 and GrassGis v.7.0.3 use different options to respect convergence properties of water flow. In SagaGis the default value is 1.1, the minimum value is 0, and the maximum is 1.25. In GrassGis the default value is 5, the minimum value is 1, and the maximum value is 10. These options were tested in each case. For both tools SagaGis and GrassGis, low convergence (0, 1) values allow the virtual water flows with higher dispersion and for high convergence values (1.25, 10) the water flows in a more concentrated manner.

3. Results

3.1. Hydrological connectivity

Considering different filling heights for a DEM correction allows the elimination of artefacts and small sinks of varying sizes. Depending on the fill height, more or less pixels/area are filled or flooded and hydrologically connected (Table 3) in Lyss. “Fill All” means a completely hydrologically connected DEM, where big sinks (e.g. depressions) are filled. Fill heights of 0.2, 0.5, 2.0, and 4.0 m lead to very similar results with only about 4% of filled area in Lyss. With about 14% of filled or

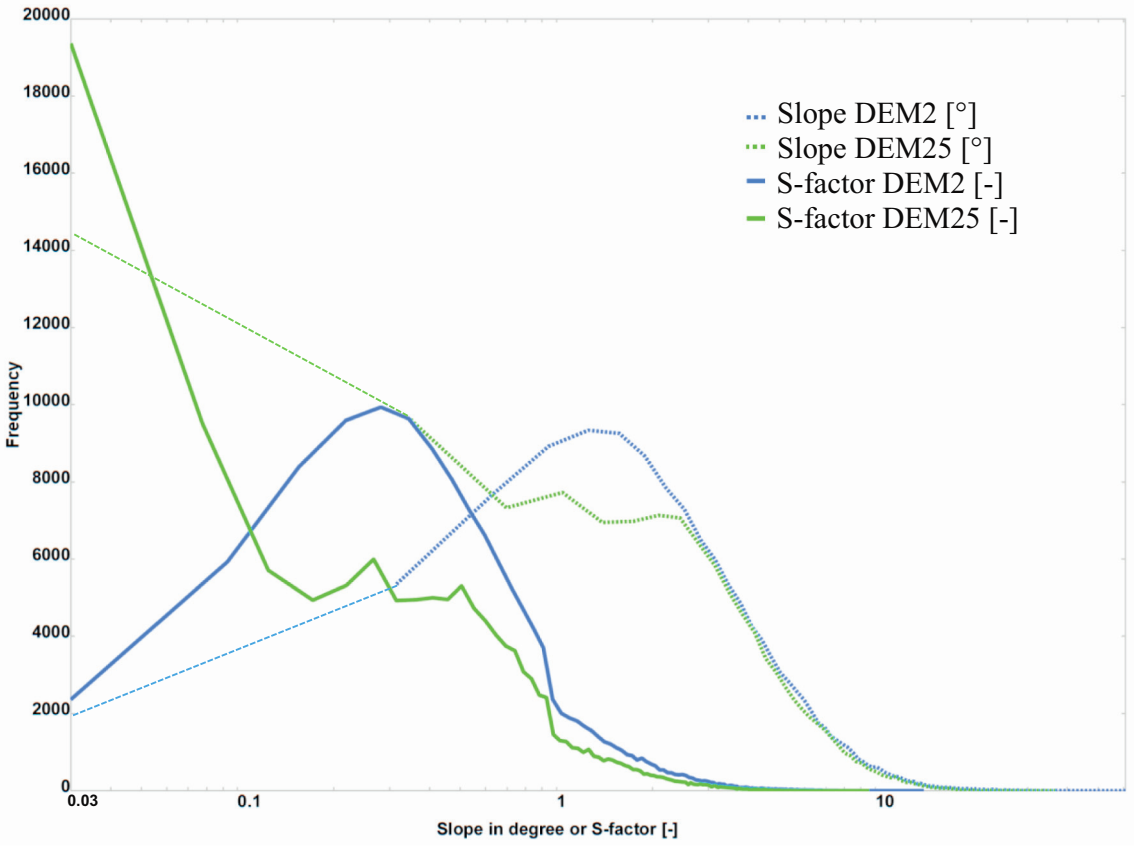

Fig. 4. Frequency analysis of slope [°] (dotted lines) and S-factor [−] (solid lines) for the 2 m DEM (blue) and the 25 m DEM (green) for Lyss; hard clipped.

flooded area in Lyss, fill heights higher than 4 m have considerably more influence (Table 3). To consider only a partly filled DEM – respecting bigger sinks as not connected – the fill height 0.5 m was applied on both DEMs and used for all following calculations.

The clipping effect of the 25 m grid with the field block map shows big differences in the number of raster cells and the area size between the soft clipping and the hard clipping method respectively, independent of region (Table 4). Using the DEM25 with the hard clipping method, 33% (Lyss) or 31% (Frienisberg) fewer pixels/less area is captured compared to the soft clipping method. Similar values of area loss resulted when soft vs hard clipping (masked) method is compared regarding the DEM2. In contrast, the area of the field block polygons and soft clipped raster cells corresponded very well to the DEM2. For the DEM25, the deviations are slightly larger, but still small (Table 4). This effect also influences slope and S-factor calculations (see Section 3.2).

3.2. Slope and S-factor [-]

Regarding slope and S-factor, both DEMs show visually almost the same properties in Frienisberg (Fig. 3). In Frienisberg, the mean of slope values is 2.5% higher for the DEM2 compared to the DEM25. With 3.2% higher mean values of S-factor of the DEM2 compared to DEM25, the difference in the slope values is slightly higher (Table 5). In Lyss, the S-factor of the DEM25 has 24% lower mean values compared to the higher-resolution DEM2 or 20% lower mean values of slope regarding the different resolutions (Table 6). Also, the maximum values and standard deviation of the S-factor regarding the DEM25 are much lower than the ones of DEM2. In contrast to Frienisberg, mean and standard deviation of Lyss show lower S-factor values. In Frienisberg the mean S-factor values of DEM2 and DEM25 have lower differences than Lyss but almost the same difference of about 20% regarding the standard deviation of S-factor (Table 5, Table 6).

In Lyss the frequency analysis of the different grid resolutions shows a high amount of very low S-factor values for the DEM25 (Fig. 4). For values higher than 10° the frequency is low for both resolutions. Only 7.1% (842 ha) of the agricultural area (11,855 ha) of Lyss have slope values higher than 10° and only 1.1% (130 ha) have slope values higher than 20° for the DEM2.

3.3. L-factor [-]

The L-factor maps show different properties of the different MFAs in Frienisberg (e.g. Fig. 5 a, d, g; low convergence values; e.g. Fig. 5 c, f, i; high convergence values). The visual differences and similarities among the chosen MFAs and convergences are small. Some show more concentrated water flow properties (Fig. 5; e, f, h and i corresponding to MTFD 1.1–1.25, WAT 5 and WAT 10) and some more divergent (Fig. 5; a, b, c, d, g, j, k corresponding to MFD 0–1.25, MTFD 0, WAT1, DINF1.1 and MUSLE 87) water flow properties. For the DEM2, the MFA and convergence values have a low influence on the mean L-factor values (Table 7). Higher convergence values result in less dispersion of water flow, while lower convergence values lead to more dispersion. Frequency analyses of the 11 L-factors show that higher convergence values have less normal distributed frequency diagrams mainly for MTFD and WAT algorithms (Fig. 6).

The comparison of the 10 L-factor mean values (see Table 7, Fig. 5, Fig. 6) calculated with the approach of Desmet and Govers (1996) and the MUSLE 87 method (a total of 11 variations), also used in the ERM2 of Switzerland by Prasuhn et al. (2013) show very low differences in the region of Frienisberg and the DEM2 (Table 7, Fig. 5, Fig. 6).

In the following, we concentrated on the MFD and on the WAT approach to compare the two tools, Saga-Gis and GrassGis. For the single field blocks in Frienisberg, the WAT algorithm shows lower mean values than MFD (Fig. 7a, number of field blocks see Fig. 1c), and higher convergence values lead to lower mean values, but, conversely, higher maximum values. The maximum values (Fig. 7b) differ more within the MFAs, and one field block shows higher maximum values for the MFD approach compared to the WAT approach (field block 12). The field blocks 2, 3, 4, 5, 7, 9, 10, and 11 show higher maximum values for the MFD 0 compared to the WAT 1 approach. The MFD approach shows that the higher the convergence values, the more concentrated the water flows are calculated, and therefore the higher the maximum values (Fig. 7b).

3.3.1. Effect of different resolution (2 m vs 25 m)

For the calculation of the L-factor based on the low-resolution DEM25, the clipping method applied is very important. The soft clipping method led to longer waterflow properties compared to the hard clipping method, which shows particularly clearly in the road pixels (Fig. 8). The visual properties of the DEM25 also show small differences within the compared maps, but mean L-factor values are higher than using the DEM2 when a soft clipping method is applied (Table 7). The mean L-factor values calculated with SagaGis algorithms (MFD, MTFD, DINF) are 1.4–1.8 times higher and those calculated with Grass-Gis algorithms (WAT) 1.1–1.3 times higher using the DEM25 compared to the DEM2 when the soft clipping method is applied (Table 7; d). When the hard clipping method is applied, the differences are not that big, but the L-factor values using the DEM25 remain higher than those using the DEM2 (Table 7).

The boxplots (Fig. 9) show that, independent of resolution, the higher the convergence values, the lower the mean and median values – which also corresponds to Table 7. There are bigger differences among the different MFA approaches (mean and median values) for the DEM25 (Fig. 9a; WAT vs MFD, MTFD and DINF) than for the DEM2 (Fig. 9b).

In Lyss, the resolution of the DEM shows the same properties of the mean L-factor values as in Frienisberg – and both locations also show higher mean values of the DEM25 compared to the DEM2 (Table 8). But the variation of L-factor values (Minimum, Maximum, Standard deviation) are higher for the DEM2 compared to the DEM25 (Table 8).

3.4. LS-factor [-]

The LS-factor was also only calculated for the algorithms MFD 1.1 and the WAT 5 (Fig. 10). We reduced the number of approaches to avoid computational complexity and to consider standard convergence values only with MFD 1.1 and WAT 5. The visual comparison of both approaches for the Frienisberg region show a similar spatial distribution pattern of the LS-factors (Fig. 10). The mean LS-factor in Frienisberg is higher using MFD 1.1 (=7.8) than using WAT 5 (=6.8) for the DEM2. It is also higher for MFD 1.1 (=8.7) than WAT 5 (6.3) for the DEM25 (Table 9). The statistical analysis of LS-factor values of Lyss confirm the tendencies of Frienisberg. The mean values of LS-factors are a little higher for MFD 1.1 than for WAT 5 for both DEMs. In the steeper area of Frienisberg, the differences of both MFAs are more distinct compared to the more balanced area of Lyss (Table 10).

For both Frienisberg and Lyss, the descriptive statistic of the LS-factor does not show the same properties as the L-factor for the different DEMs (Table 9, Table 10). The MFD algorithm shows a slightly higher mean value for the low-resolution grid DEM25 compared to the DEM2. The WAT approach shows the opposite: a higher mean value of the WAT approach with DEM2 compared to DEM25. The higher tendency of mean L-factor value comparing the DEM25 (1.87) with the DEM2 (1.71) decreases after multiplication with the S-factor for the WAT approach in Lyss (LS-factor: DEM25: 1.5; DEM2: 1.76; Table 8, Table 9, Table 10).

For Lyss, Fig. 11 shows percentages of area for slope, S-factor, L-factor, and LS-factor for defined categories calculated with MFD 1.1 for DEM2 and DEM25. Classes with values > 1.2 of S-factor include a considerably higher area of 22% for the DEM2 compared to 14% for the DEM25. Notably, very high values hardly occur in the DEM25. L-factors with very high values > 7.3 occur much more frequently in the DEM2 than

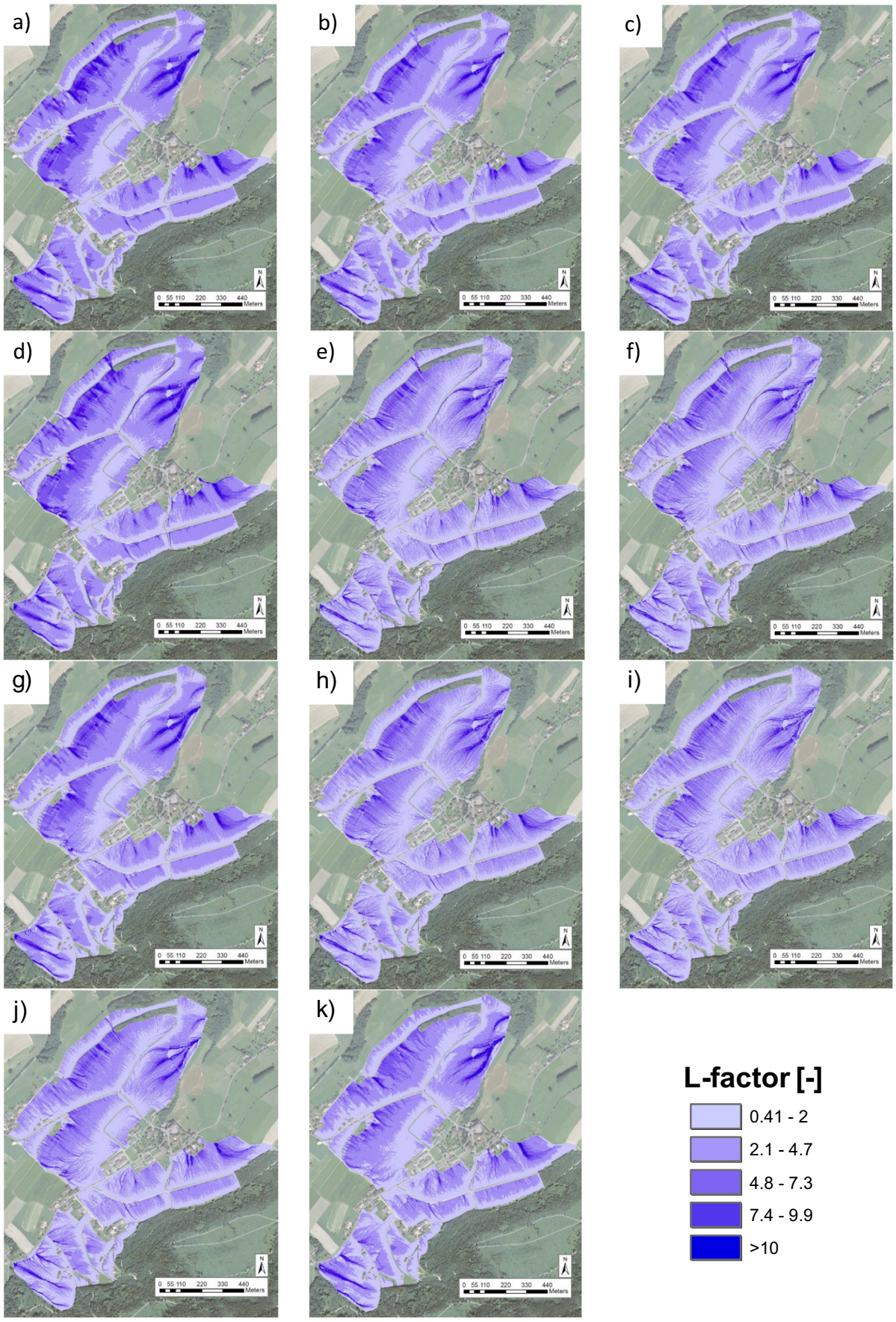

Fig. 5. L-factor in Frienisberg calculated with 2 m resolution; a) MFD Con. Value = 0, b) MFD Con. Value = 1.1, c) MFD Con. Value = 1.25, d) MTFD Con. Value = 0, e) MTFD Con. Value = 1.1, f) MTFD Con. Value = 1.25, g) WAT Con. Value = 1, h) WAT Con. Value = 5, i) WAT Con. Value = 10, j) DINF Con. Value = 1.1, k) MUSLE 87; Con. = Convergence; soft clipped.

Table 7
Compared MFAs and calculated resolution factor for the L-factor [−] for Frienisberg; Res. = Resolution; hard clipped (masked) only with MFD1.1 and WAT 5; No = method.

No	Algorithm	MFD			MTFD			WAT			DINF	MUSLE 87
	Convergence values	0	1.1	1.25	0	1.1	1.25	1	5	10	1.1	–
a)	Mean Res. [2 m] soft clipped	3.34	2.94	2.91	3.34	2.64	2.64	2.92	2.56	2.41	2.55	2.69
b)	Mean Res. [25 m] soft clipped	4.87	4.5	4.47	5.5	4.75	4.75	3.3	3.16	3.11	3.84	–
c)	Mean Res [25 m] hard clipped [mask]	–	3.8	–	–	–	–	–	2.8	–	–	–
d)	Res. factor: b/a	1.46	1.53	1.54	1.65	1.8	1.8	1.13	1.23	1.29	1.51	–

in the DEM25. But even in the lowest L-factor class (0.41–2) there is a larger area proportion in the DEM2 than in the DEM25. This partly compensates high S-factor values with low L-factor values in the DEM2, except for the highest values. Therefore, the LS-factor classes have similar values in the different resolutions except in the two highest classes (Fig. 11). In class >30 the percentage of area is three times higher for the DEM2 compared with the DEM25.

To consider the big influence of field blocks for the LS-factor calculation, we computed the LS-factor without field blocks in Lyss based on the DEMs without any flow barriers. Using the MFD algorithm with the convergence value 1.1, the mean LS-Factor values for Lyss without field blocks are 70% higher (with field blocks 1.88, without 6.36) for the DEM25 and 49.7% higher (with field blocks 1.79, without 3.56) for the DEM2. Table 11 summarizes the main results.

4. Discussion

4.1. Digital elevation model (DEM) correction and hydrological connectivity

A correction of the digital terrain model is especially necessary for high-resolution terrain models and use of multiple flow algorithms (Liu et al., 2015; Yang, 2015). The aim of partial sink filling (with 0.5 m, Table 3) was to eliminate small sinks and artefacts, but allow that larger sinks or depressions in the terrain are not necessarily connected. Flow sinks are real existing drainless sinks or plains and are not the result of vertical errors of the DEM. Thomas et al. (2016) showed that flow sinks are widespread and 16–33% of catchment areas are hydrologically disconnected from the aquatic network. In Lyss, the correction of the DEM does not have a big influence: because of the varied topography absolute sinks are large and would need high fill heights (>4 m; Table 3) to balance them. At the selected filling level of 0.5 m, only in 4% of the area, the DEM is corrected and sinks are filled such that the water flow through those areas is connected. The fill height value 0.5 m also covers the accuracy of ±0.5 m 1 σ of the DEM (SwissALTI3D 2015).

The field block map leads to differences between the DEM25 and the DEM2 due to clipping inaccuracies. Owing to the small size of the field blocks (mean value of 5 ha), there is an undesirable edge effect, especially with the DEM25. Small roads or other objects preventing a continuous water flow were sometimes not respected in the 25 m grid during the soft clipping method. This leads to higher slope lengths or slope contributing areas, and also to higher L-factor mean values using the DEM25 MFAs compared to the DEM2 MFAs (Table 7, Fig. 8). When hard clipping is applied peripheral areas are sometimes lost. In addition, flow barriers like forests and small streets are not necessarily flow barriers in every situation (Volk et al., 2010). During heavy rains those areas can act as external water sources and are therefore not considered in the field block map approach also mentioned in Prasuhn et al. (2013).

Soft clipping without mask is the standard method to receive most of the raster information and will be used for the calculation of the new erosion risk map (ERM) of Switzerland with the two-metre DEM. For this high-resolution DEM, the clipping method is not that important and data loss due to the clipping method is negligible (0% in Frienisberg and 0.01% for Lyss) (Table 4).

4.2. S-factor approaches

Comparing different S-factor approaches for slope values higher than 10° lead to big differences (Fig. 2). Very high slope values do not appear very often, so the effect of slopes higher than 10° is not very strong for Lyss (Fig. 4). The RUSLE approach shares with other widely used approaches similar S-factor values (e.g. Zingg, 1940; Hurni, 1979; Nearing, 1997; see) up to a slope steepness of 10°. Some S-factor approaches are only extrapolated and not measured on slope values higher than 11.3° (Hurni, 1979; Liu et al., 1994). Most of the slope values (98.9%) in the study area are below 20° (Lyss), where most of the nine S-factor approaches do not show big differences (Fig. 2). Hrabalíková and Janeček (2017) compared four different S-factor approaches and concluded that the values of the S-factor are within a similar range and that there is no significant difference. Thus, the choice of S-factor calculation for our purposes does not have a big influence. In the selected approach (RUSLE after Renard et al., 1997), however, there are large differences in the calculated S-factors, depending on the resolution of the DEM used. The DEM25 leads to significantly lower S-factors due to smoothing effects, both in mean values as well as in the maximum values and standard deviation (Table 5, Table 6, Fig. 11). This is in line with findings in other studies (Di Stefano et al., 2000; Kienzle, 2004). In terms of soil erosion, this means that with increasing DEM resolution, the S-factors increase and thus also soil erosion.

4.3. L-factor approaches

The MFAs do not differ very much regarding the L-factors and the mean values of the default convergence options with MFD 1.1, MTFD 1.1, WAT 5, DINF 1.1, and MUSLE 87 in Frienisberg and the DEM2 (Figs. 5, 6, 9). Between the highest of the default convergence options (MFD 1.1 = 2.94) and the lowest (DINF 1.1 = 2.55), mean L-factor values vary only about 13%. Compared with the highest and lowest convergence options of the MFA (MFD 0 = 3.34, MTFD 0 = 3.34, and WAT 10 = 2.41) the difference is 28% in Frienisberg (Table 7). For the DEM25 the default convergence options and soft clipped approach show a difference of 33% between the highest L-factor value (MTFD 1.1 = 4.75) and the lowest one (WAT 5 = 3.16). Comparing the mean L-factor values of the highest and lowest convergence options (MTFD 0 = 5.5, WAT 10 = 3.11) the difference is 43% in Frienisberg when the soft clipped approach is applied (Table 7). For both DEMs, the higher the convergence values of MFA, the lower the mean values of the L-factor. Comparing masked (hard clipped) and not masked (soft clipped) approaches in Frienisberg of the DEM25, the differences between MFD 1.1 (3.8 vs 4.5) are 16% and 11% for WAT 5 (2.8 vs 3.16) but have still higher mean L-factor values compared to the DEM2 (Table 7). In Lyss the differences of mean L-factor values are low for both DEMs, but also higher for the DEM25 than the DEM2. The L-factor of MFD 1.1 and WAT 5 showed a mean of 1.6 and 1.71 (DEM2) – i.e. 28% and 9% lower than with the DEM25 (mean values 2.24 and 1.87) (Table 8).

The use of multiple flow algorithms rather than single flow algorithms has now become an established method in most water flow or soil erosion modelling studies (Mitasova et al., 1996; Panagos et al., 2015a, 2015b; Zhang et al., 2017). Wilson et al. (2008) compared the hydrological performance of various flow-routing algorithms and

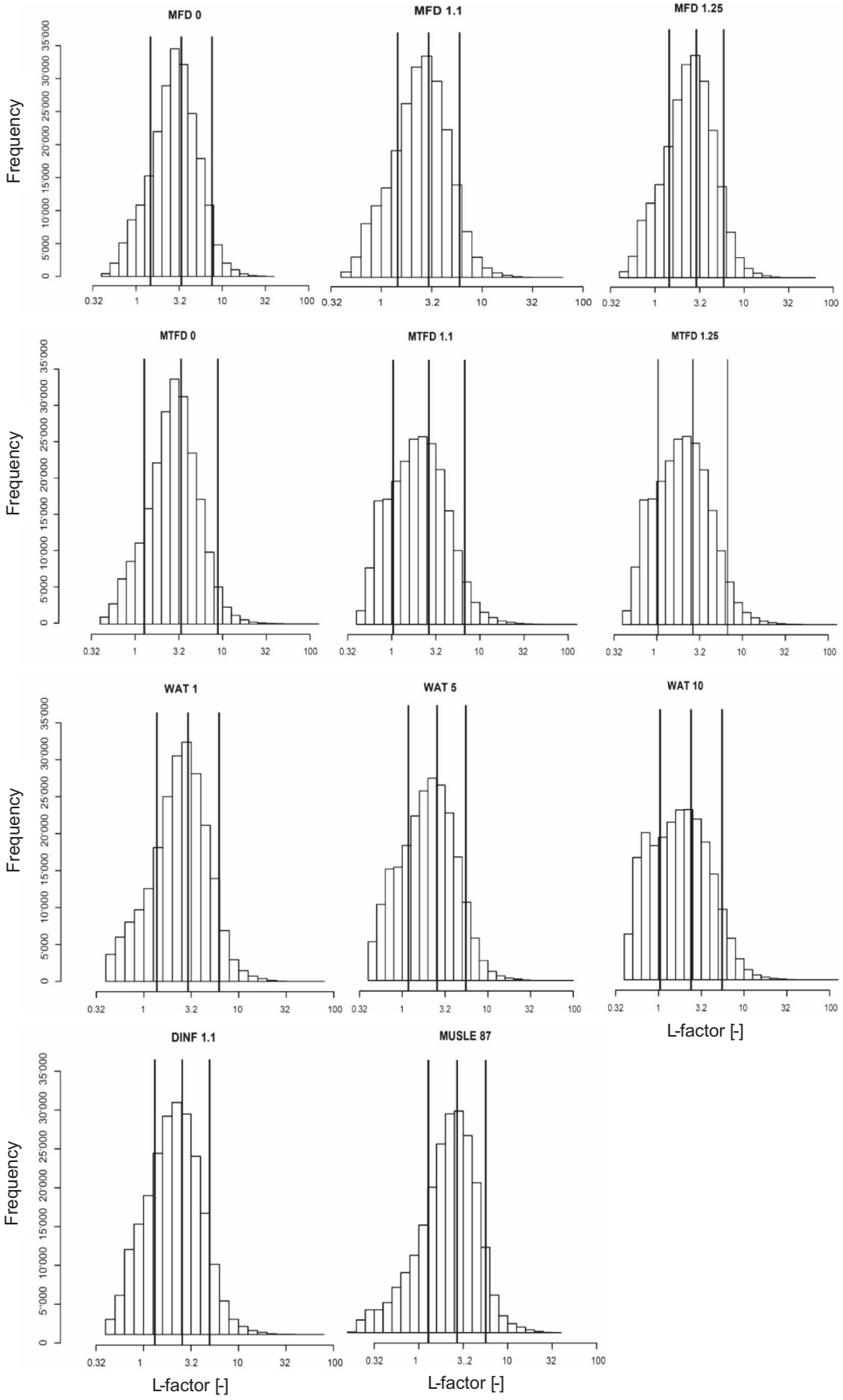

Fig. 6. Frequency (y-axis) distribution of the L-factor [−](x-axis) using MFAs with different convergence values in Frienisberg for DEM2; Lines: Mean and mean ± 1* standard deviation; soft clipped.

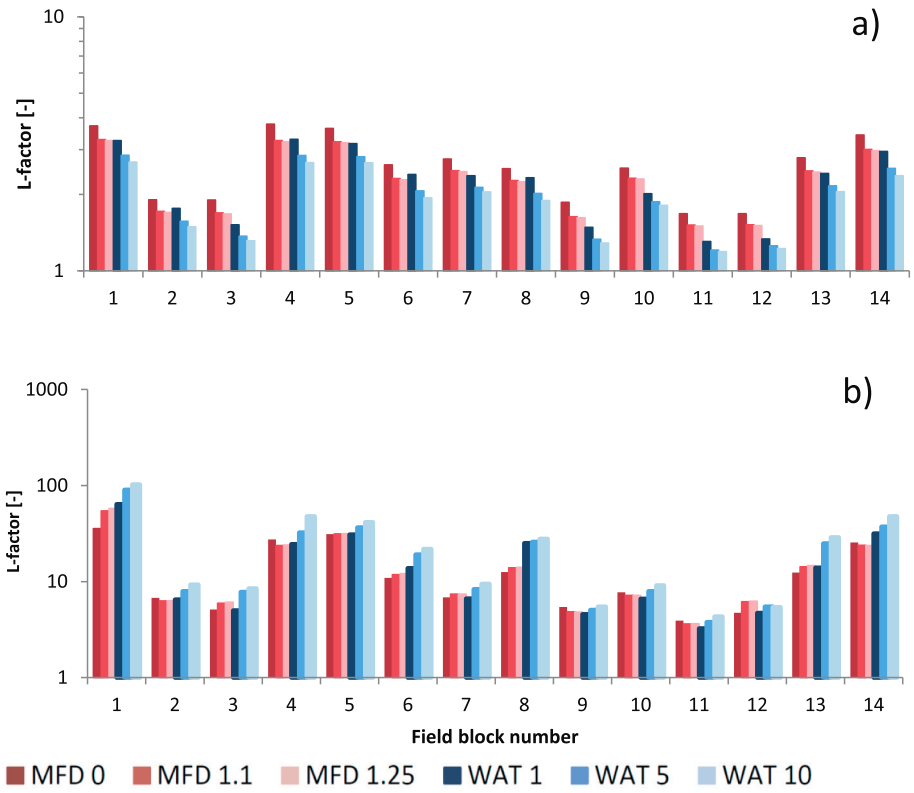

Fig. 7. Mean a) and maximum b) L-factor values for selected MFD and WAT algorithms including different convergence values on 14 selected field blocks (micro-catchments [1–14, Fig. 1c]) in Frienisberg with DEM2; soft clipped.

found that the single flow direction method produced more 'low flow' cells. Orlandini et al. (2012) showed that the multiple flow direction method performed best at very high DEM resolutions. Multiple flow direction algorithms can accommodate convergent and divergent flow and perform better than single flow direction method algorithms for real terrains. But it is not easy to evaluate the performance of the algorithms with field observations. Accordingly, there are hardly any such studies. Most of them are based on visual or qualitative assessments and recommend the algorithms used based on "goodness-of-fit" (Wilson et al., 2008). We too can only perform such a qualitative assessment in this study.

It is questionable whether the empirical relationships between the LS factor and the soil erosion risk underpinning RUSLE can be downscaled or upscaled from the size of standard USLE plots (22.1 m) to the 2 m or 25 m grid or even other grid resolutions. The adjustment of the slope length factor L on the basis of the calculation of the contributing area with MFAs may also be questioned. The observed rill and ephemeral gully erosion (thalweg erosion) is represented well but extending RUSLE beyond its empirical limitations (Prasuhn et al., 2013). The approach with MFA and high-resolution DEM of our study is actually used today as a standard method in GIS-based modelling. Whether this procedure is permissible or not is not the aim of this study.

4.4. LS-factor approaches

Comparing the LS-factors calculated with MFD 1.1 and WAT 5 using DEM2 for Frienisberg and Lyss, there are no big differences between the two algorithms (Fig. 10, Table 9, Table 10). In Lyss, the mean LS-factor is slightly higher (+ 2%) using the MFD 1.1 (1.79) than using the WAT 5 (1.76). The deviation of the values is greater (+ 9%) for WAT 5, where standard deviation was 3.50 compared to 3.20 for MFD 1.1. When we compare the two MFAs using the DEM25, the difference is higher. The mean LS-factor for the MFD 1.1 (1.88) is higher than for WAT 5 (1.50) (+ 25%). In addition, MFD 1.1 generates higher standard deviation and maximum values compared to WAT 5. In the smaller and steeper Frienisberg area, similar differences between the two MFAs result, but these are somewhat more accentuated (Table 9, Table 10).

For Frienisberg, the LS-factor of the lower-resolution DEM25 has a higher mean value than the DEM2 for the MFD approach, but a lower mean value when using the WAT approach (WAT: - 7.4%; MFD: +11.5%) and in Lyss (WAT: - 14.7%; MFD: +5%; Table 9, Table 10) Other studies (Claessens et al., 2005: 10–100 m; Wu et al., 2005: 10–250 m; Mondal et al., 2017: 30–330 m) show lower mean values using the low-resolution DEM compared to the high-resolution DEM, but do not consider DEMs with resolutions higher than 10 m. Deumlich (2012) compared different resolutions (1–25 m), modelling, on two field blocks of 69/141 ha, an average soil loss of 1.2/1.4 t ha^{-1} using DEM2 and 0.75/0.99 t ha^{-1} using DEM25. The average potential soil loss is doubled, from the highest resolution grid (1 m) to the coarsest (25 m). In a study in northern China, Wang et al. (2016) compared grid sizes of 2, 5, 10, 25, and 30 m, and used the 2 m resolution grid as a reference to calculate soil loss. They reported a decrease of 47% with a 30 m DEM, and said the DEM2 is the most accurate in describing the topography and the micro-relief. Fu et al. (2015) [2–30 m] reported that LS-factor of 10 m resolution DEM were close to the values of 2 m resolution DEM. Koo et al. (2016) obtained similar results to those in our study with lower mean values for a 5 m grid compared to a 20 m grid, but higher mean values for a 30 m grid. This corresponds to a break between 20 and 30 m and also includes the standard plot size of RUSLE estimation of 22.1 m (Wischmeier and Smith, 1978; Renard et al., 1997). Bhattarai and Dutta (2007) highlight that the better results of the 30 m resolution compared to the 90 m using the USLE methodology, is probably due to fact this resolution is closer to the 22.1 m slope length, the length used in the derivation of the USLE relationships.

In Lyss, 99.8% of calculated LS values were <30, 98.9% < 15, and 83.1% < 3 for the DEM2. For the DEM25, 99.9% of calculated LS values in Lyss were <30, 99.2% < 15, and 81% < 3 (Fig. 11). We compared LS-factors

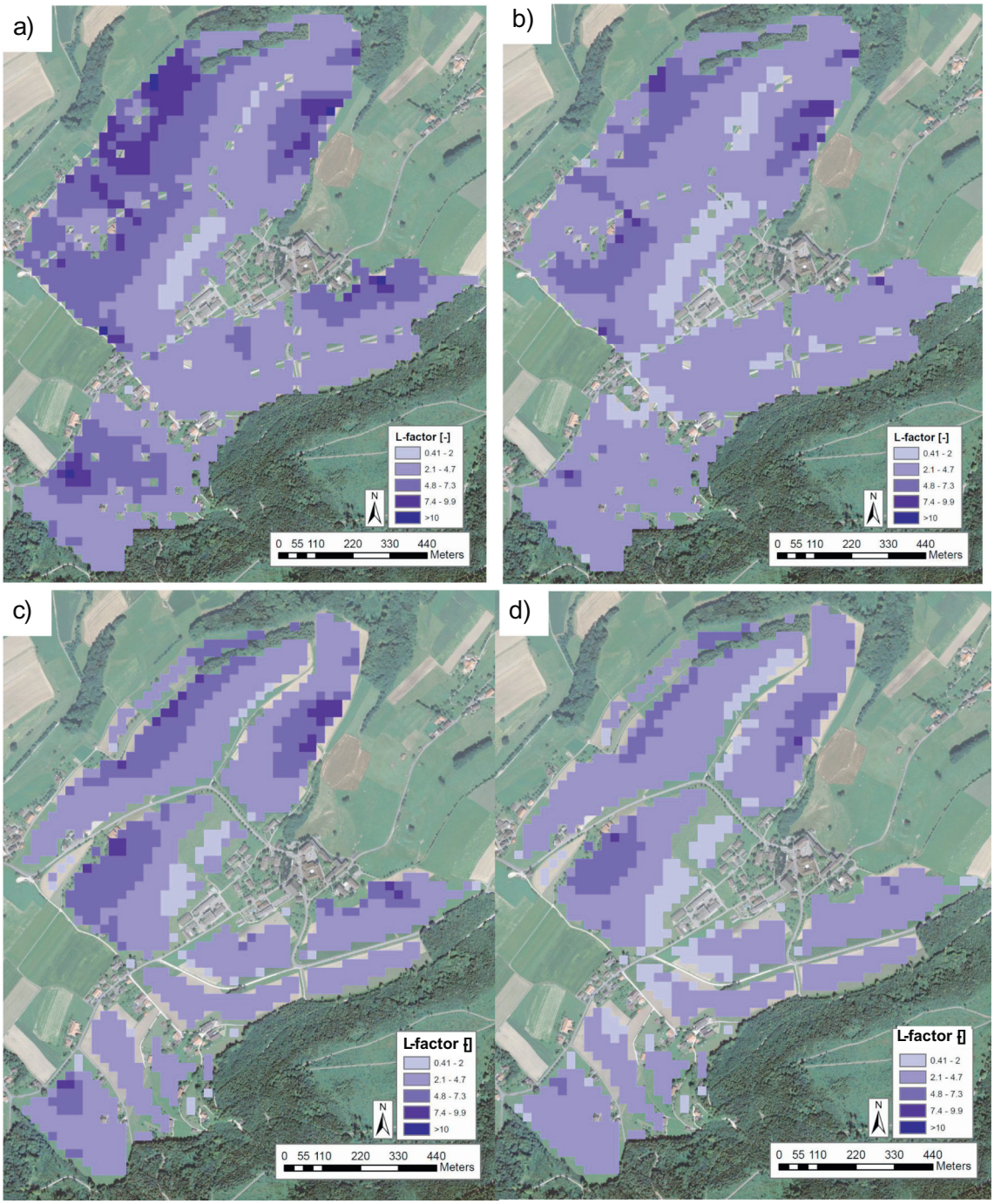

Fig. 8. L-factor in Frienisberg calculated with Desmet and Govers's (1996) approach based on Swisstopo DEM (2005) with 25 m resolution; a & c = MFD Con. Value = 1.1, b & d = WAT Con. Value = 5; Con. = Convergence; a & b = soft clipped, c & d = hard clipped (masked).

calculated with Eqs. (2)–(4) with the LS-factor values of the Tables 4.1-4.3 in the main reference RUSLE handbook of Renard et al. (1997) based on 122 m slope length. These RUSLE Tables 4.1–4.3 represent LS-factor values for uniform slopes. Table 4.1 is used for rangeland and pasture with a low interrill/rill ratio. Table 4.2 is used for cropland and pasture with a moderate interrill/rill ratio and Table 4.3 for construction sites with high ratio of interrill and rill (Renard et al., 1997). For slopes up to 3% the differences between the calculated values and the indicated values in the tables were relatively small (average deviation between 4 and 24%), depending on the used RUSLE table (4.1–4.3). For slopes between 3 and 15% our approach always resulted in slightly higher LS-values (average deviation 10–49%) compared to the RUSLE tables (4.1–4.3). For slopes > 15%, which account for <1% of the total area (Fig. 11), the deviation (average deviation between 24 and 55%) from our approach increased with increasing slope compared to the RUSLE –Tables 4.1–4.3 (Renard et al., 1997). Yang (2015) calculated for New South Wales, Australia, a similar distribution of LS-factor values as in our study. The LS-values range from 0.05 to 60 with a mean of 2.60 based on a 30 m resolution DEM. Nearly all (99%) of the calculated LS values are <30, 80% < 10, and 30% < 1.0. Very high L- and LS-factor values of single pixels are quite justified. Those pixels occur mainly in terrain depressions, where a lot of water can flow together and the upslope contributing area is very big. In those areas, very high soil loss values are manifested as rills or thalweg erosion (Prasuhn, 2011). Deumlich (2012) compared RUSLE models with measured soil losses and concluded that the DEM25 is insufficient to illustrate small-scale erosion

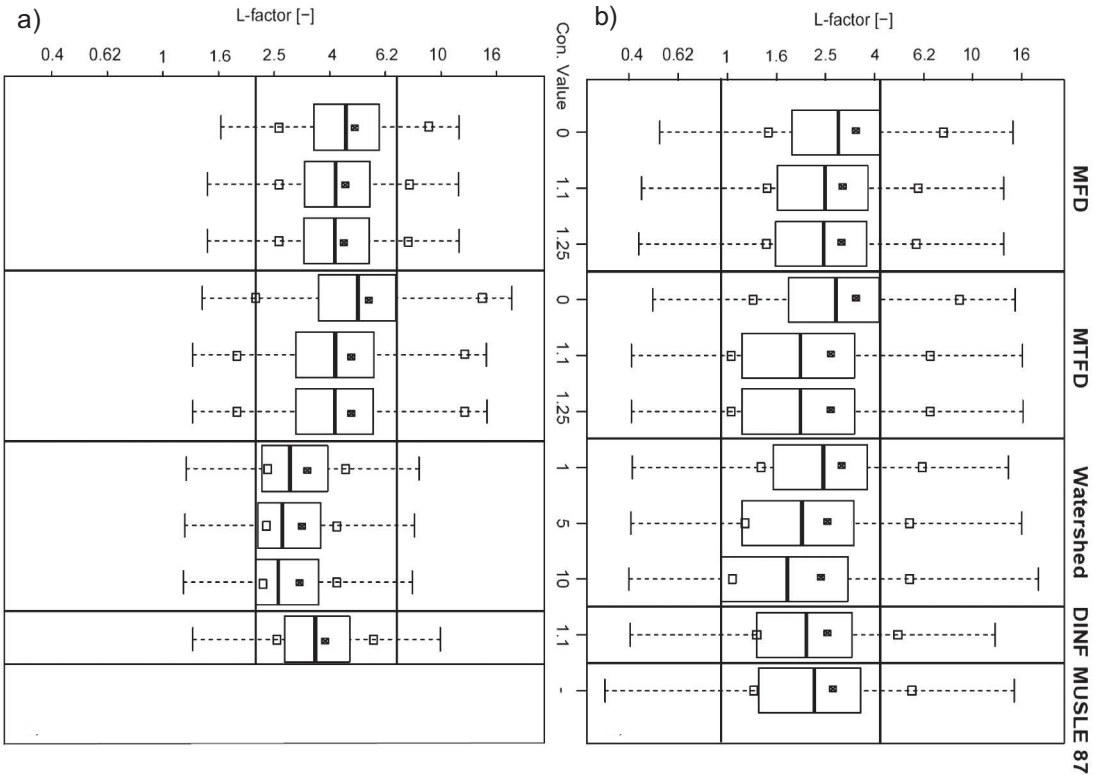

Fig. 9. L-factor boxplots of different algorithms and convergence values (con. value) for Frienisberg, Square = mean ± 1 * Standard deviation, Filled dot = Mean, outliers excluded, upper horizontal line maximum of 75% quartile, lower horizontal line minimum of 25% quartile; a) Resolution: 25 m; b) Resolution: 2 m; soft clipped on both DEMs; corresponds to a and b of Table 7.

phenomena. Even the results of DEM10 and DEM5 reflect the properties of erosion only in a simplified manner in the mentioned case. But flow paths are well represented using DEM1. Gertner et al. (2002) reported that DEMs with resolutions lower than 5 m are not suitable for the calculation of LS-factors due to large variations in upslope contributing areas. Thomas et al. (2017) reported that optimal DEM resolutions of hydrologically sensitive areas are between 1 and 2 m. Unlike the previously mentioned studies, one other study implies higher mean LS-factor values regarding the 10 m and 20 m resolution DEM compared to the 5 m resolution DEM on watersheds in Korea (Koo et al., 2016).

The chosen approach with field blocks as micro-catchments of 5 ha mean area as a basis for calculating LS-factors is only very suitable for high-resolution DEMs, such as the DEM2 used here. In coarser-resolved DEMs, clipping effects lead to large uncertainties and errors. When using DEM2, however, the chosen approach with the micro-catchment has many advantages. The problem of the maximum slope length or maximum number of pixels of the upslope contributing area, which is frequently discussed in the literature, does not exist. Several other problems are also elegantly bypassed, e.g. the need for complex models to identify breaks in slope length that involve changes in the slope turning point; the challenge of enabling variable cut-off slope angles; and the challenge of adequately considering channel networks to locate soil erosion and deposition zones (Van Remortel et al., 2001; Liu et al., 2015; Yang, 2015; Zhang et al., 2017). Maximum slope length value (e.g. 305 m; Renard et al., 1997) is already respected with the field block approach. Also, the channel network is already included and does not have to be additionally separated. Borrelli et al. (2016) used a similar approach as in our study. They used remote sensing techniques to introduce the "field boundaries/channelled flow concept" in a national-scale RUSLE application for Italy. The DEM25 was previously segmented to represent some potential man-made or natural structures, e.g. agricultural canals, roads, soil furrows, or gullies. Maugnard et al. (2013) also performed a soil erosion risk map of Wallonia (Belgium) with 10 m pixel resolution based on hydrologically isolated plots similar to the applied field block approach in this study. Our comparison of calculated LS-factors with or without field block map shows that massively higher mean LS-factors result (3.56 vs 1.79) if the whole area is considered as a homogeneous landscape without barriers. Winchell et al. (2008) compared different LS-factor calculations with and without terrain barriers and a cut at 333 m slope length and a 30 m DEM of 40 hydrologic units in the USA and confirm our observation in their analysis.

It could be pointed out that the use of various algorithms for detecting the LS-factor remains a subject of controversial discussions despite numerous new developments, GIS technologies, and better computing capacity (Mitasova et al., 2013; Oliveira et al., 2013; Hrabalíková and Janeček, 2017). Desmet and Govers (1996) stated that the LS values predicted by the GIS method are generally higher by 10–50% than those obtained by manual approach. In contrast, Hrabalíková and Janeček (2017) found that the LS values generated by the GIS method

Table 8
L-factor [-] with different resolutions and MFA approaches for Lyss; hard clipped method (masked).

L-factor [-]	MFD 1.1 [2 m]	WAT 5 [2 m]	MFD 1.1 [25 m]	WAT 5 [25 m]
Number of cells (N)	20,745,979	20,745,979	132,832	132,832
Area [ha]	8298	8298	8302	8302
Minimum	0.4	0.4	1	1
Maximum	77.5	246.4	15.0	26.5
Mean	1.60	1.71	2.24	1.87
Standard deviation	1.16	1.66	1.04	0.73

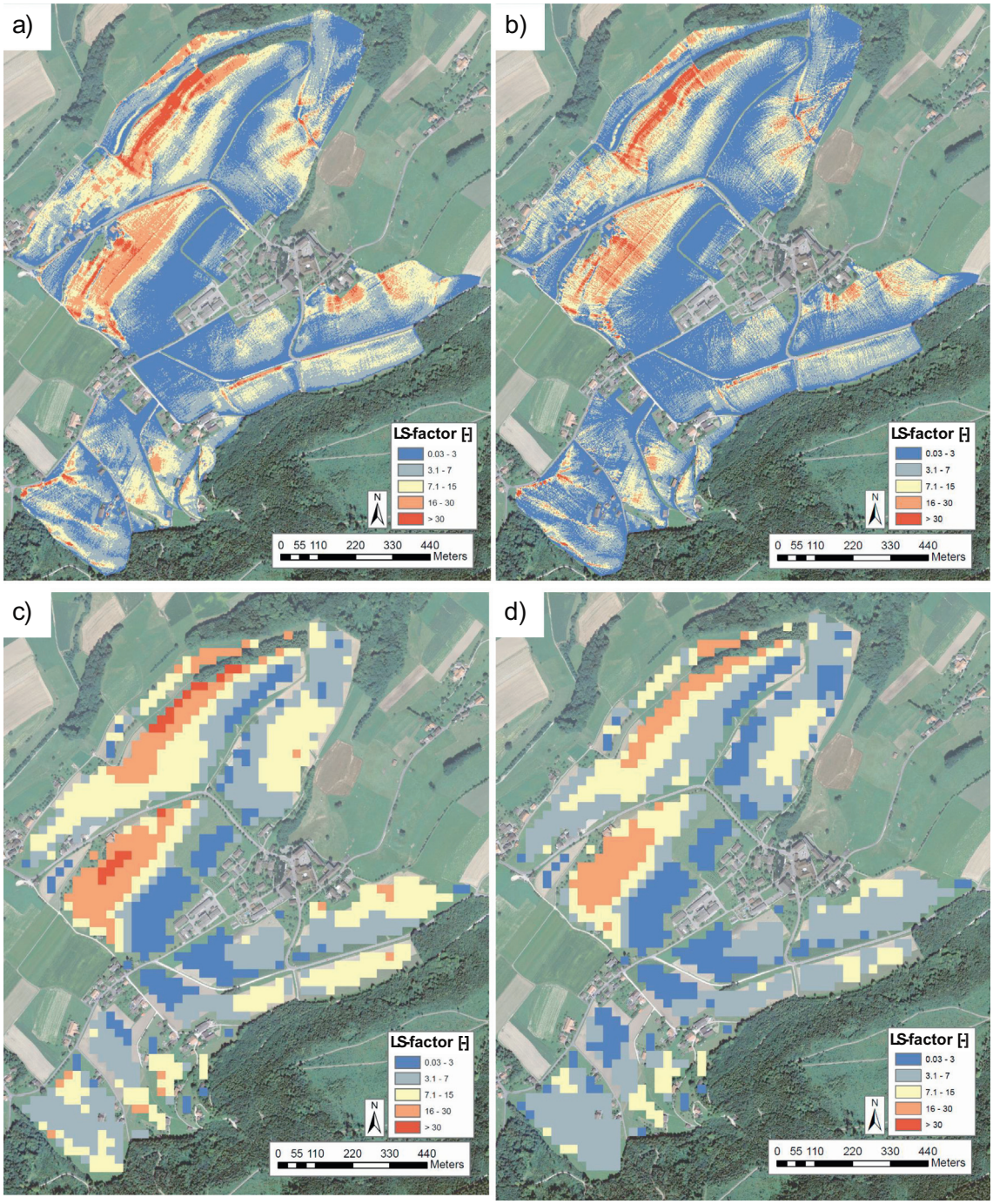

Fig. 10. LS-factor [−] multiplied based on approaches of L- and S-factor [−] a & c = MFD 1.1, b & d = WAT 5, a & b [2 m], c & d [25 m] in Frienisberg; DEM2 soft clipped; DEM25 hard clipped (masked).

Table 9
LS-factor [−] statistic of two different algorithms and resolutions calculated for Frienisberg; hard clipped method (masked).

LS-factor [-]	MFD 1.1 [2 m]	WAT 5 [2 m]	MFD 1.1 [25 m]	WAT 5 [25 m]
Number of cells (N)	151,280	151,280	941	941
Area [ha]	60.5	60.5	58.8	58.8
Minimum	0.03	0.03	0.03	0.03
Maximum	450	746	39.9	29.9
Mean	7.8	6.8	8.7	6.3
Standard deviation	8.4	8.21	6.9	5.1

Table 10
LS-factor [−] statistic of two different algorithms and resolutions calculated for Lyss; hard clipped method (masked).

LS-factor [-]	MFD 1.1 [2 m]	WAT 5 [2 m]	MFD 1.1 [25 m]	WAT 5 [25 m]
Number of cells (N)	20,745,979	20,745,979	132,832	132,832
Area [ha]	8298	8298	8302	8302
Minimum	0.03	0.03	0.03	0.03
Maximum	450	1308	68	59
Mean	1.79	1.76	1.88	1.50
Standard deviation	3.20	3.50	2.83	2.06

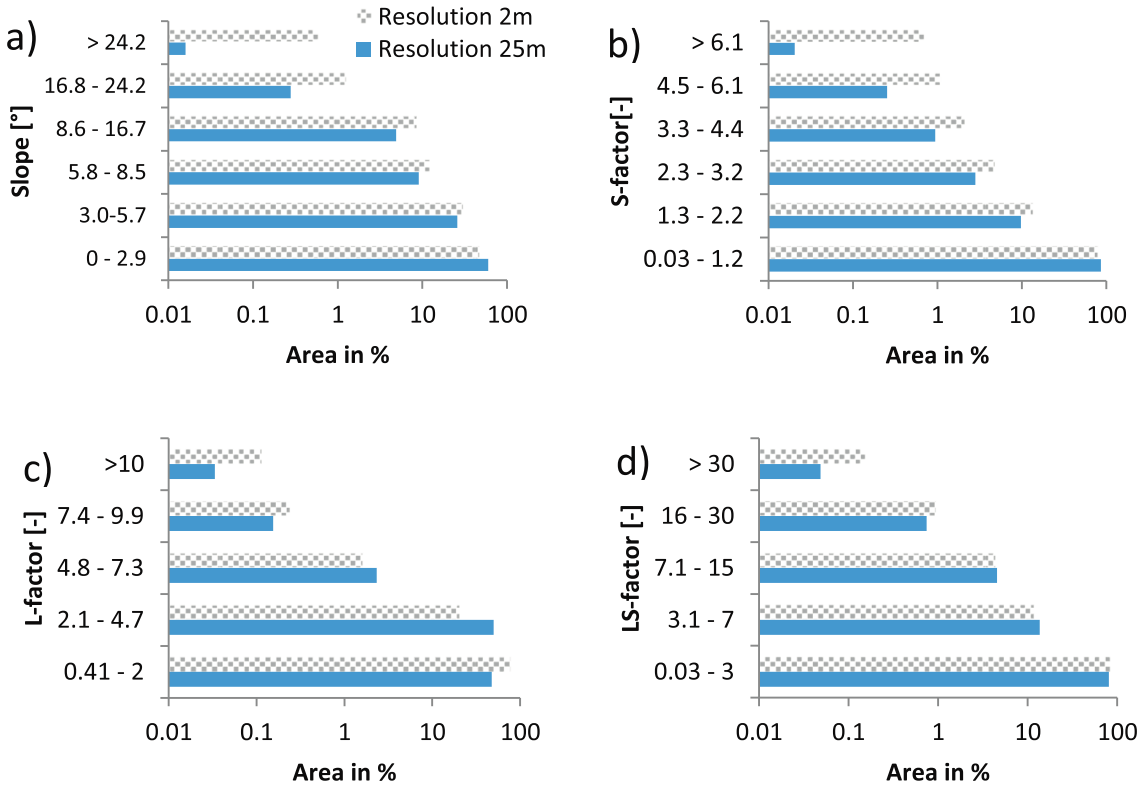

Fig. 11. Percentage of area in different categories of Slope a), S-factor b), L-factor (MFD 1.1) c), and LS-factor (MFD 1.1) d) for Lyss; hatched bar = resolution of 2 m; blue bar resolution of 25 m; hard clipped method (masked); the classes selected for the y-axes are not or only to a limited extent comparable among Slope, S-factor, L-factor, and LS-factor.

were generally 10–30% lower than those obtained by the manual method. These findings are in agreement with the conclusions of Yitayew et al. (1999) stating that the mean annual erosion was mostly under-predicted by the GIS methods. Garcia Rodriguez and Gimenez Suarez (2010) observed an overestimation in the values of the LS-factor, when it is calculated in the traditional way. Hrabalíková and Janeček (2017) conclude that the GIS-based RUSLE soil loss estimates from five of seven different approaches to calculation of LS-factor are lower than the measured average annual soil loss and two approaches over-predicted the measured soil loss.

Table 11
Overview of the main results (mean values of L- and LS-factor for the 2 m and 25 m grid) for Frienisberg (lightly shaded) and Lyss (strongly shaded).

Tool	Algorithm	Convergence value	L-factor[a] Soft clipped		L-factor[a] Hard clipped		LS-factor[b] Hard clipped	
			2 m	25 m	2 m	25 m	2 m	25 mx
Saga Gis	MFD	0	3.34	4.87	–	–	–	–
		1.1	2.94	4.5	3.24 1.60	3.8 2.24	7.8 1.79	8.7 1.88
		1.25	2.91	4.47	–	–	–	–
	MTFD	0	3.34	5.5	–	–	–	–
		1.1	2.64	4.75	–	–	–	–
		1.25	2.64	4.75	–	–	–	–
GrassGis	WAT	1	2.92	3.3	–	–	–	–
		5	2.56	3.16	2.85 1.71	2.8 1.87	6.8 1.76	6.3 1.5
		10	2.41	3.11	–	–	–	–
Saga Gis	DINF	1.1	2.55	3.84	–	–	–	–
AVErosion in ArcView	MUSLE 87	–	2.69	–	–	–	–	–

Lightly shaded: Frienisberg; strongly shaded: Lyss.
- = not calculated or not available.
MFD: Freeman, 1991; MTFD: Seibert and McGlynn, 2007; WAT: Ehlschlaeger, 1989, Quinn et al., 1991; DINF: Tarboton, 1997; MUSLE 87: Moore and Burch, 1986, Moore et al., 1991.
[a] Calculated according to Desmet and Govers, 1996.
[b] Product of L- and S-factor.

5. Conclusion and outlook

To calculate the L-factor of the RUSLE, we compared four different multiple flow direction algorithms (DINF, MFD, MTFD, WAT) with different convergence settings and the previously used MFA (MUSLE 87) of the existing erosion risk map in Switzerland. We performed this comparison with a high-resolution DEM2 and a coarser DEM25 in two different test areas in the Swiss Plateau, based on previously segmented micro-catchments of variable spatial dimension with a mean size of 5 ha. In total, we performed 21 different L-factor calculations. Selected approaches were calculated with the S-factors to obtain the LS-factors.

In terms of L-factor values, the MFAs tested in both areas using the DEM2 did not differ considerably. The L-factor values also did not differ much from those obtained in the approach used for the current erosion risk map (ERM2). As the convergence values increases, the meanL-factors decrease slightly in all MFAs. The choice of the MFA does not play a big role in the calculation of the soil erosion risk in DEM2 in our area, and there is no big difference to the approach used for the ERM2. With the DEM25, notably lower mean L-factors are calculated with WAT than with MFD, MTFD, and DINF. Surprisingly, L-factors calculated using the DEM25 are slightly higher for all MFAs than for the same MFAs when using the DEM2. Regarding the S-factors, however, smoothing effects in the coarser DEM25 lead to lower values compared to those calculated using the DEM2.

For the LS-factor calculation, only the two approaches MFD 1.1 and WAT 5 were compared for both DEMs. The MFD 1.1 and WAT 5 differ only slightly on the DEM2. Comparing the two DEMs gives an

ambivalent picture. MFD 1.1 produces lower mean LS values on the DEM2 than on the DEM25, whereas WAT 5 produces higher values for the DEM2 than the DEM25. With the 25 m model, hard clipping results in a considerable loss of data at the edges of the field blocks. This is not so important for the calculation of S and L-factors and mean values, but would lead to a significant underestimation of soil loss when calculating absolute soil loss rates. With soft clipping, the data loss on the DEM25 is lower, but the slope lengths and thus the L-factor increase. This would lead to an overestimation of the soil loss. The DEM25 is therefore unsuitable for the chosen approach with field blocks (micro-catchments averaging 5 ha).

We do not have experimental data to evaluate the results of the 21 L-factor variations. Therefore, we cannot say what is more convenient, but we can make a qualitative assessment and point out differences. The low influence of the different MFAs and the convergence options on the L- and LS-factor calculations came as a surprise, but are confirmed by our study. Furthermore, our results do not confirm the hypothesis that a higher DEM resolution leads to higher L-, S-, and LS-factor values. In a subsequent study, the various chosen LS-factors will be calculated with the other factors of the RUSLE (R, K, C, P factor) in the Frienisberg region to calculate the actual soil erosion risk for each plot and compared it with long-term measured soil loss from field data on soil erosion damage mapping of a monitoring program (Prasuhn, 2011, 2012). The LS-factor approach that best reflects the reality is then applied and will be used to validate and fine-tune the RUSLE model for the new erosion risk map of Switzerland.

Although the influence of the resolution of the DEM on mean LS-factor values is not very big, it is very important for the characterization of a land surface in terms of concavity and complexity. The spatial distribution in the DEM2 is varied and much more differentiated and better represents reality. This is crucial for the credibility of an erosion risk map to farmers, consultants, and advisors, as well as for the targeted planning of mitigation measures.

Acknowledgments

This research is part of a soil erosion risk project, funded by the Swiss Federal Office for Agriculture (FOAG). We also thank Tina Hirschbuehl[1] and Marlène Thibault[1] (CDE) for the English editing support.

References

Abu Hammad, A., Lundekvam, H., Børresen, T., 2004. Adaptation of RUSLE in the eastern part of the Mediterranean region. Environ. Manag. 34, 829–841.
Alder, S., Prasuhn, V., Liniger, H., Herweg, K., Hurni, H., Candinas, A., Gujer, H.U., 2015. A high-resolution map of direct and indirect connectivity of erosion risk areas to surface waters in Switzerland: a risk assessment tool for planning and policy-making. Land Use Policy 48, 236–249.
Arge, L., Chase, J.S., Halpin, P., Toma, L., Vitter, J.S., Urban, D., Wickremesinghe, R., 2003. Efficient flow computation on massive grid terrain datasets. GeoInformatica 7, 283–313.
Auerswald, K., 1987. Sensitivität erosionsbestimmender Faktoren. – Wasser und Boden 1, 34–38.
Benavidez, R., Jackson, B., Maxwell, D., Norton, K., 2018. A review of the (Revised) Universal Soil Loss Equation (R/USLE): with a view to increasing its global applicability and improving soil loss estimates. Hydrol. Earth Syst. Sci. Discuss. 1–34.
Bhattarai, R., Dutta, D., 2007. Estimation of soil erosion and sediment yield using GIS at catchment scale. Water Resour. Manag. 21, 1635–1647.
Boardman, J., 2006. Soil erosion science: reflections on the limitations of current approaches. Catena 68, 73–86.
Böhner, J., Selige, T., 2006. Spatial prediction of soil attributes using terrain analysis and climate regionalisation. Göttinger Geographische Abhandlungen 115, 13–28.
Boomer, K.B., Weller, D.E., Jordan, T.E., 2008. Empirical models based on the universal soil loss equation fail to predict sediment discharges from Chesapeake Bay catchments. J. Environ. Qual. 37, 79–89.
Borrelli, P., Paustian, K., Panagos, P., Jones, A., Schütt, B., Lugato, E., 2016. Effect of good agricultural and environmental conditions on erosion and soil organic carbon balance: a national case study. Land Use Policy 50, 408–421.
Borrelli, P., Robinson, D.A., Fleischer, L.R., Lugato, E., Ballabio, C., Alewell, C., Meusburger, K., Modugno, S., Schütt, B., Ferro, V., Bagarello, V., Oost, K.V., Montanarella, L., Panagos, P., 2017. An assessment of the global impact of 21st century land use change on soil erosion. Nat. Commun. 8, 1–13.
Borrelli, P., Meusburger, K., Ballabio, C., Panagos, P., Alewell, C., 2018. Object-oriented soil erosion modelling: a possible paradigm shift from potential to actual risk assessments in agricultural environments. Land Degrad. Dev. 29, 1270–1281.
Claessens, L., Heuvelink, G.B.M., Schoorl, J.M., Veldkamp, A., 2005. DEM resolution effects on shallow landslide hazard and soil redistribution modelling. Earth Surf. Process. Landf. 30, 461–477.
Costa-Cabral, M., Burges, S.J., 1994. Digital Elevation Model Networks (DEMON): a model of flow over hillslopes for computation of contributing and dispersal areas. Water Resour. Res. 30, 1681–1692.
Desmet, P.J.J., Govers, G., 1996. A GIS procedure for automatically calculating the USLE LS factor on topographically complex landscape units. J. Soil Water Conserv. 51, 427–433.
Deumlich, D., 2012. Structure and Process - Influence of historical agriculture of linear flow paths by extreme rainfall in Brandenburg. Landscape Online 31, 1–19.
Di Stefano, C., Ferro, V., Porto, P., 2000. Length slope factors for applying the Revised Universal Soil Loss Equation at basin scale in southern Italy. J. Agric. Eng. Res. 75, 349–364.
Ehlschlaeger C., 1989. Using the AT search algorithm to develop hydrologic models from digital elevation data. International Geographic Information Systems (IGIS) Symposium '89, 275–281.
Fairfield, J., Leymarie, P., 1991. Drainage networks from grid digital elevation models. Water Resour. Res. 27, 709–717.
Favis-Mortlock, D., Boardman, J., MacMillan, V., 2001. The limits of erosion modeling: why we should proceed with care. In: Harmon, R.S., Doe, W.W. (Eds.), Landscape Erosion and Evolution Modeling. Springer, Boston, pp. 477–516.
Fernandez, C., Wu, J.Q., McCool, D.K., Stoeckle, C.O., 2003. Estimating water erosion and sediment yield with GIS, RUSLE, and SEDD. J. Soil Water Conserv. 58, 128–136.
Freeman, G.T., 1991. Calculating catchment area with divergent flow based on a regular grid. Comput. Geosci. 17, 413–422.
Fu, G.B., Chen, S.L., McCool, D.K., 2006. Modeling the impacts of no-till practice on soil erosion and sediment yield with RUSLE, SEDD, and ArcView GIS. Soil Tillage Res. 85, 38–49.
Fu, S., Cao, L., Liu, B., Wu, Z., Savabi, M.R., 2015. Effects of DEM grid size on predicting soil loss from small watersheds in China. Environ. Earth Sci. 73, 2141–2151.
Garcia Rodriguez, J.L., Gimenez Suarez, M.C., 2010. Historical review of topographical factor, LS, of water erosion models. Aqua-LAC 2, 56–61.
Garcia Rodriguez, J.L., Gimenez Suarez, M.C., 2012. Methodology for estimating the topographic factor LS of RUSLE3D and USPED using GIS. Geomorphology 175 (176), 98–106.
Gertner, G., Wang, G., Fang, S., Anderson, A.B., 2002. Effect and uncertainty of digital elevation model spatial resolutions on predicting the topographical factor for soil loss estimation. J. Soil Water Conserv. 57, 164–174.
Hengl, T., 2006. Finding the right pixel size. Comput. Geosci. 32, 1283–1298.
Hickey, R., 2000. Slope angle and slope length solutions for GIS. Cartography 29, 1–8.
Hoffmann, A., da Silva, M. A., Naves Silva, M. L., Curi, N., Klinke, G., de Freitas, D. A. F., 2013. Development of Topographic Factor Modeling for Application in Soil Erosion Models, In: Hernandez Soriano, M. C. (Ed.), Soil Processes and Current Trends in Quality Assessment, pp. 111-138.
Hrabalíková, M., Janeček, M., 2017. Comparison of different approaches to LS factor calculations based on a measured soil loss under simulated rainfall. Soil and Water Research 12, 69–77.
Hurni, H., 1979. Semien-Äthiopien: Methoden zur Erfassung der Bodenerosion. Geomethodica 4, 151–182.
Ismail, J., Ravichandran, S., 2008. RUSLE2 model application for soil erosion assessment using remote sensing and GIS. Water Resour. Manag. 22, 83–102.
Kamaludin, H., Lihan, T., Ali Rahman, Z., Mustapha, M.A., Idris, W.M.R., Rahim, S.A., 2013. Integration of remote sensing, RUSLE and GIS to model potential soil loss and sediment yield (SY). Hydrol. Earth Syst. Sci. Discuss. 10, 4567–4596.
Keizer, J., Djuma, H., Prasuhn, V., 2016. Soil Erosion by Water. In: Stolte et al. (Eds.), Soil threats in Europe – Status, methods, drivers and effects on ecosystem services. A review report, deliverable 2.1 of the RECARE project. JRC Science and Policy Report, 15-24.
Kienzle, S., 2004. The effect of DEM raster resolution on first order, second order and compound terrain derivatives. Trans. GIS 8, 83–112.
Koo, J.-Y., Yoon, D.-S., Lee, D.J., Han, J.H., Jung, Y., Yang, J.E., Lim, K.J., 2016. Effect of DEM resolution in USLE LS factor. Journal of Korean Society on Water Environment 32, 89–97.
Kotremba, C., Trapp, M., Thomas, K., 2016. Hochauflösende GIS-basierte Bodenabtragsmodellierungen für ausgewählte Agrarstandorte in Rheinland-Pfalz. Bodenschutz 21, 46–56.
Lane, S.N., Brookes, C.J., Kirkby, M.J., Holden, J., 2004. A network-index-based version of TOPMODEL for use with high-resolution digital topographic data. Hydrol. Process. 18, 191–201.
Liu, B.Y., Nearing, M.A., Risse, L.M., 1994. Slope gradient effects on soil loss for steep slopes. Transactions of the ASAE 37, 1835–1840.
Liu, H., Kiesel, J., Hörmann, G., Fohrer, N., 2011. Effects of DEM horizontal resolution and methods on calculating the slope length factor in gently rolling landscapes. Catena 87, 368–375.
Liu, K., Tang, G., Jiang, L., Zhu, A.X., Yang, J., Song, X., 2015. Regional-scale calculation of the LS factor using parallel processing. Comput. Geosci. 78, 110–122.
Maidment, D.R. (Ed.), 2002. Arc Hydro: GIS for Water Resources. 3rd Ed. ESRI Press, Redlands, Calif (203).
Maugnard, A., Bielders, C.L., Bock, L., Colinet, G., Cordonnier, H., Degré, A., Demarcin, D., Dewez, A., Feltz, N., Legrain, X., Pineux, N., Mokadem, A.I., 2013. Cartographie du risqué d'érosion hydrique à l'échelle parcellaire en soutien à la politique agricole wallonne (Belgique). Étude et Gestion des Sols 20, 127–141.

McCool, D.K., Brown, L.C., Foster, G.R., Mutchler, C.K., Meyer, L.D., 1987. Revised slope steepness factor for the Universal Soil loss Equation. Transactions of the ASAE 30, 1387–1396.
Mitasova, H., Hofierka, J., Zlocha, M., Iverson, L.R., 1996. Modelling topographic potential for erosion and deposition using GIS. International Journal Geographical Information System 10, 629–641.
Mitasova, H., Barton, M., Ullah, I., Hofierka, J., Harmon, R.S., 2013. GIS-based soil erosion modeling. In: Bishop, M.P. (Ed.), Shroder J. F. Elsevier, Treatise on Geomorphology, pp. 228–258.
Mondal, A., Khare, D., Kundu, S., Mukherjee, S., Mukhopadhyay, A., Mondal, S., 2017. Uncertainty of soil erosion modelling using open source high resolution and aggregated DEMs. Geosci. Front. 8, 425–436.
Moore, I.D., Burch, G.J., 1986. Physical basis of the length-slope factor in the universal soil loss equation. Soil Sci. Soc. Am. J. 50, 1294–1298.
Moore, I.D., Wilson, J.P., 1992. Length-slope factors for the revised Universal Soil Loss Equation: simplified method of estimation. J. Soil Water Conserv. 47, 423–428.
Moore, I.D., Grayson, R.B., Ladson, A.R., 1991. Digital terrain modelling: a review of hydrological, geomorphological, and biological applications. Hydrol. Process. 5, 3–30.
Morgan, R.P.C., 2009. Soil Erosion and Conservation. Blackwell Publishing Ltd., Hoboken.
Naipal, V., Reick, C., Pongratz, J., Van Oost, K., 2015. Improving the global applicability of the RUSLE model - adjustment of the topographical and rainfall erosivity factors. Geosci. Model Dev. 8, 2893–2913.
Nearing, M.A., 1997. A single, continuous function for slope steepness influence on soil loss. Soil Sci. Soc. Am. J. 61, 917–919.
Oliveira, P.T.S., Rodrigues, D.B.B., Sobrinho, T.A., Panachuki, E., Wendland, E., 2013. Use of SRTM data to calculate the (R)USLE topographic factor. Acta Scientiarum. Technology 35, 507–513.
Orlandini, S., Moretti, G., Corticelli, M.A., Santangelo, P.E., Capra, A., Rivola, R., Albertson, J.D., 2012. Evaluation of flow direction methods against field observations of overland flow dispersion. Water Resour. Res. 48, 13.
Panagos, P., Borrelli, P., Meusburger, K., 2015a. A new European slope length and steepness factor (LS-factor) for modeling soil erosion by water. Geosciences 5, 117–126.
Panagos, P., Borrelli, P., Poesen, J., Ballabio, C., Lugato, E., Meusburger, K., Montanarella, L., Alewell, C., 2015b. The new assessment of soil loss by water erosion in Europe. Environ Sci Policy 54, 438–447.
Planchon, O., Darboux, F., 2002. A fast, simple and versatile algorithm to fill the depressions of digital elevation models. Catena 46, 159–176.
Prasuhn, V., 2011. Soil erosion in the Swiss midlands: results of a 10-year field survey. Geomorphology 126, 32–41.
Prasuhn, V., 2012. On-farm effects of tillage and crops on soil erosion measured over 10 years in Switzerland. Soil Tillage Res. 120, 137–146.
Prasuhn, V., Liniger, H., Gisler, S., Herweg, K., Candinas, A., Clément, J.-P., 2013. A high-resolution soil erosion risk map of Switzerland as strategic policy support system. Land Use Policy 32, 281–291.
Quinn, P., Beven, K., Chevallier, P., Planchon, O., 1991. The prediction of hillslope flow paths for distributed hydrological modelling using digital terrain models. Hydrol. Process. 5, 59–79.
Renard K. G., Foster G. R., Weesies G. A., McCool D. K., Yoder D. C., 1997. Predicting soil erosion by water. A guide to conservation planning with the Revised Universal Soil Loss Equation (RUSLE). Handbook. 703, US Department of Agriculture.
Rymszewicz, A., Mockler, E., O'Sullivan, J., Bruen, M., Turner, J., Conroy, E., Kelly-Quinn, M., Harrington, J., Lawler, D., 2015. Assessing the applicability of the Revised Universal Soil Loss Equation (RUSLE) to Irish Catchments. Proceedings of the International Association of Hydrological Sciences 367, 99–105.
Schäuble, H., 2005. AVErosion 1.1 für ArcView 3.x – Berechnung von Bodenerosion und –akkumulation nach den Modellen USLE und MUSLE87. URL: http://data.terracs.com/pdf/averosion-german.pdf
Seibert, J., McGlynn, B., 2007. A new triangular multiple flow direction algorithm for computing upslope areas from gridded digital elevation models. Water Resour. Res. 43, 1–8.
Smith, D.D., Whitt, D.M., 1947. Estimating soil losses from field areas of claypan soil. Soil Sci. Soc. Am. J. 12, 485–490.
Smith, D.D., Wischmeier, W.H., 1957. Factors affecting sheet and rill erosion. American Geophysical Union Transactions 38, 889–896.
Swisstopo, 2008. VECTOR25. Das digitale Landschaftsmodell der Schweiz. Bundesamt für Landestopografie swisstopo, Wabern.
Swisstopo, 2015. swissALTI3D. Ausgabebericht 2015. Bundesamt für Landestopografie swisstopo, Wabern.
Tarboton, D.G., 1997. A new method for the determination of flow directions and upslope areas in grid digital elevation models. Water Resour. Res. 33, 309–319.
Tetzlaff, B., Friedrich, K., Vorderbrügge, T., Vereecken, H., Wendland, F., 2013. Distributed modelling of mean annual soil erosion and sediment delivery rates to surface waters. Catena 102, 13–20.
Thomas, I.A., Jordan, P., Mellander, P.-E., Fenton, O., Shine, O., Ó hUallacháin, D., Creamer, R., McDonald, N.T., Dunlop, P., Murphy, P.N.C., 2016. Improving the identification of hydrologically sensitive areas using LiDAR DEMs for the delineation and mitigation of critical source areas of diffuse pollution. Sci. Total Environ. 556, 276–290.
Thomas, I.A., Jordan, P., Shine, O., Fenton, O., Mellander, P.-E., Dunlop, P., Murphy, P.N.C., 2017. Defining optimal DEM resolutions and point densities for modelling hydrologically sensitive areas in agricultural catchments dominated by microtopography. Int. J. Appl. Earth Obs. Geoinf. 54, 38–52.
Thompson, J.A., Bell, J.C., Butler, C.A., 2001. Digital elevation model resolution: effects on terrain attribute calculation and quantitative soil-landscape modeling. Geoderma 100, 67–89.
UNDP, 2015. Human Development Report 2015. Work for Human Development. United Nations Development Programme, New York 978-92-1-126398-5.
Van Remortel, R.D., Hamilton, M.E., Hickey, R.J., 2001. Estimating the LS factor for RUSLE through iterative slope length processing of digital elevation data. Cartography 30, 27–35.
Volk, M., Möller, M., Wurbs, D., 2010. A pragmatic approach for soil erosion risk assessment within policy hierarchies. Land Use Policy 27, 997–1009.
Wang, L., Liu, H., 2006. An efficient method for identifying and filling surface depressions in digital elevation models for hydrologic analysis and modelling. Int. J. Geogr. Inf. Sci. 20, 193–213.
Wang, S., Zhu, X., Zhang, W., Yu, B., Fu, S., Liu, L., 2016. Effect of different topographic data sources on soil loss estimation for a mountainous watershed in Northern China. Environ. Earth Sci. 75, 1382.
Wilson, J. P., Aggett, G., Deng, Y., Lam, C. S., 2008. Water in the landscape: a review of contemporary flow routing algorithms. In: Zhou et al. (Eds.), Advances in Digital Terrain Analysis. Springer, Berlin, 213–236.
Winchell, M.F., Jackson, S.H., Wadley, A.M., Srinivasan, R., 2008. Extension and validation of a geographic information system-based method for calculating the revised universal soil loss equation length-slope factor for erosion risk assessments in large watersheds. J. Soil Water Conserv. 63, 105–111.
Wischmeier, W. H. and Smith, D. D., 1978. Predicting Rainfall Erosion Losses – a Guide to Conservation Planning. Handbook No. 537, US Department of Agriculture.
Wu, S., Li, J., Huang, G., 2005. An evaluation of grid size uncertainty in empirical soil loss modeling with digital elevation models. Environ. Model. Assess. 10, 33–42.
Yang, X.H., 2015. Digital mapping of RUSLE slope length and steepness factor across New South Wales, Australia. Soil Research 53, 216–225.
Yitayew, M., Pokrzywka, S.J., Renard, K.G., 1999. Using GIS for facilitating erosion estimation. Appl. Eng. Agric. 15, 295–301.
Zevenbergen, L.W., Thorne, C.R., 1987. Quantitative analysis of land surface topography. Earth Surf. Process. Landf. 12, 47–56.
Zhang, H., Yang, Q., Li, R., Liu, Q., Moore, D., He, P., Ritsema, C.J., Geissen, V., 2013. Extension of a GIS procedure for calculating the RUSLE equation LS factor. Comput. Geosci. 52, 177–188.
Zhang, H., Yao, Z., Yang, Q., Li, S., Baartman, J.E.M., Gai, L., Yao, M., Yang, X., Ritsema, C.J., Geissen, V., 2017. An integrated algorithm to evaluate flow direction and flow accumulation in flat regions of hydrologically corrected DEMs. Catena 151, 174–181.
Zingg, A.W., 1940. Degree and length of land slope as it affects soil loss in runoff. Agric. Eng. 21, 59–64.

Paper 2. Comparison of long-term field-measured and RUSLE-based modelled soil loss in Switzerland

Authors:
Bircher Pascal, Liniger Hanspeter and Prasuhn Volker

Originally published in: Geoderma Regional, 2022, 31, e00595

Boris-Link: https://boris.unibe.ch/175103/

Geoderma Regional 31 (2022) e00595

Contents lists available at ScienceDirect

Geoderma Regional

journal homepage: www.elsevier.com/locate/geodrs

Comparison of long-term field-measured and RUSLE-based modelled soil loss in Switzerland

P. Bircher [a,b,*], H.P. Liniger [a], V. Prasuhn [c]

[a] Centre for Development and Environment (CDE), University of Bern, Mittelstrasse 43, 3012 Bern, Switzerland
[b] Institute of Geography (GIUB), University of Bern, Hallerstrasse 12, 3012 Bern, Switzerland
[c] Agroscope, Agroecology and Environment, Reckenholzstrasse 191, 8046 Zurich, Switzerland

ARTICLE INFO

Keywords:
Soil erosion
Field assessment
Calibration
RUSLE-based modelling
Long-term monitoring
Cambisols

ABSTRACT

Long-term field measurements to asses model-based soil erosion predictions by water are rare. We have compared field measurements based on erosion assessment surveys from a 10-year monitoring process with spatial-explicit model predictions with the Revised Universal Soil Loss Equation (RUSLE). Robust input data were available for both the mapped and the modelled parameters for 203 arable fields covering an area of 258 ha in the Swiss Midlands. The 1639 mapped erosion forms were digitized and converted to raster format with a 2 m resolution. A digital terrain model using 2 m resolution and a multiple flow direction algorithm for the calculation of the topographic factors and the support practice factor was available for modelling with the RUSLE. The other input data for the RUSLE were determined for each field. The comparison of mapped and modelled soil loss values revealed a substantially higher estimation of soil loss values from modelling by a factor of 8, with a mean mapped soil loss of 0.77 t/ha/yr vs. modelled soil loss of 6.20 t/ha/yr. However, high mapped soil losses of >4 t/ha/yr were reproduced quite reliably by the model, while the model predicted drastically higher erosion values for mapped losses of <4 t/ha/yr. Our study shows the value of long-term field data based on erosion assessment surveys for model evaluation. RUSLE-type model results should be compared with erosion assessment surveys at the field to landscape scale in order to improve the calibration of the model. Further factors related to land management like headlands, traffic lanes and potato furrows need to be included before they may be used for policy advice.

1. Introduction

Soil erosion models are nowadays used worldwide for estimation of soil erosion by water. Numerous different models are currently available (Jetten et al., 2003; Merritt et al., 2003; Aksoy and Kavvas, 2005; Pandey et al., 2016). The Universal Soil Loss Equation (USLE; Wischmeier and Smith, 1978) and its various derivates such as the Revised Universal Soil Loss Equation (RUSLE; Renard et al., 1997) are still the most common empirical models (Alewell et al., 2019). Borrelli et al. (2018) estimated that >90% of soil erosion assessments around the world are derived from USLE-based models. Since USLE estimates long-term mean soil loss and thus the risk of erosion, this model is also very popular for policy advice and measure planning, where it is used as a decision-making instrument for agricultural regulations and guidelines (e.g. Prasuhn et al. (2013) in Switzerland, and Swerts et al. (2019) in Belgium).

The USLE was originally based on an extensive dataset of about 10,000 plot years of erosion measurements under natural rainfall and under standard plot conditions with 9% slope steepness and 22.1 m slope length (Wischmeier and Smith, 1978). Boix-Fayos et al. (2006) presented a review of the advantages and limitations of the use of test plots to measure soil erosion and determine the parameter values of the USLE. For homogeneous test plots, they found an inadequate representation of natural conditions in landscapes, which are characterized by a higher heterogeneity. Boix-Fayos et al. (2006) conclude that an extrapolation of test plot data leads in most cases to an overestimation of erosion at hillslope and catchment scales. Poesen et al. (1996), Boardman (2006) and Evans et al. (2017) have confirmed this overestimation, which can be two to 10 times higher than measurements from farmers' fields. Nevertheless, mean erosion rates for different countries are derived from test plot data (Cerdan et al., 2006; Auerswald et al., 2009; Guo et al., 2015).

* Corresponding author at: Centre for Development and Environment (CDE), University of Bern, Mittelstrasse 43, 3012 Bern, Switzerland.
E-mail address: pascal.bircher@unibe.ch (P. Bircher).

https://doi.org/10.1016/j.geodrs.2022.e00595
Received 4 March 2021; Received in revised form 14 November 2022; Accepted 19 November 2022
Available online 22 November 2022
2352-0094/

Since Panagos et al. (2015) published a soil erosion map of Europe using a derivate of the RUSLE, called RUSLE 2015, which can be used as a basis for political and economic decisions, a vehement controversy has arisen in the scientific community about the use of RUSLE (Evans and Boardman, 2016a, 2016b; Fiener and Auerswald, 2016; Panagos et al., 2016a, 2016b; Fiener et al., 2020). One question is the level of quality and detail of the input data for the modelling needed to achieve a suitable result. Another is the extent to which an erosion model developed on a test plot scale can represent reality for catchment areas, landscapes or entire nations (Gobin et al., 2004; Batista et al., 2019; Boardman and Evans, 2019; Parsons, 2019). Evans et al. (2017) has stressed that the erosion risk map for Europe by Panagos et al. (2015) does not accurately reflect erosion rates and risk in Britain. Fiener et al. (2020) has also demonstrated, using catchment examples in Bavaria, the Czech Republic and Austria, that there are substantial differences in modelled mean soil loss between regionally adapted USLE models and the European soil erosion risk map by Panagos et al. (2015). Furthermore, the study has been frequently criticized in the above-mentioned literature for applying the RUSLE without any calibration or adjustment and it simplifies the calculations of some factors (C- & P-factor). Empirical USLE-type models are often used, usually with the best input data available to the authors, but mostly without any evaluation, calibration or validation.

Today, individual erosion processes are well understood and can be reproduced relatively accurately with models (Nearing et al., 2017). For process-based models, parameterization is also comparatively simple, and verification or validation can be achieved with experiments (e.g. Aksoy et al., 2020). For complex situations on the scale of catchment areas or regions, both parameterization and validation are much more difficult. Accurate erosion risk modelling presents a number of challenges, including parameterization, validation and resolution of the input data (Gobin et al., 2004; Baggaley and Potts, 2017). On one hand, there is an urgent need for sound and appropriate soil loss data to validate erosion models, and on the other hand, the acquisition of real soil loss rates is a very complex issue. Recently, several authors (Evans et al., 2017; Alewell et al., 2019; Batista et al., 2019; Parsons, 2019) have evaluated various soil erosion assessment methods (plot studies, monitoring and measuring, modelling, use of radionuclides) in order to assess their suitability, validity and scientific robustness as well as their benefits and shortcomings in terms of the reliability of the estimated soil loss rates. They have all concluded that every method has its weaknesses and uncertainties.

Many attempts to evaluate or validate the RUSLE and its predictions exist, but validation of spatial soil loss predictions is generally difficult (Gobin et al., 2004). Therefore, these models are rarely tested in the field. Soil erosion often strongly depends on randomly occurring major events (Prasuhn, 2011; Evans, 2017). Long-term studies are required, because they make it possible to minimize the bias resulting from low-frequency high magnitude effects. Evans and Boardman (2016a) stated: "*RUSLE assessments have not, as far as we know, been compared with field-based assessments*". To the best of our knowledge, only one new study with long-term measured field data, from Steinhoff-Knopp and Burkhard (2018) in Germany, is currently available. They found a significant overestimation of the soil loss by modelling and concluded that modelled erosion did not reflect real conditions very well. Evans and Boardman (2016a) also concluded: "*In Britain the two ways of assessing erosion do not relate well to each other, field-based assessment does not validate (ratify) model assessment*".

In Switzerland, there is a longstanding expertise in soil erosion research on arable land, which allows us to learn from field experiences. Long-term measurements with test plots (Schaub and Prasuhn, 1993), field measurements with sediment traps (Rüttimann et al., 1995), various field mappings (Ledermann et al., 2010; Prasuhn, 2011; Prasuhn, 2020) and several types of modelling (Mosimann and Rüttimann, 2006; Ogermann et al., 2006) have been performed. Leser et al. (2002) previously concluded, based on 25 years of soil erosion measurements, that only long-term measurements under real field conditions provide a realistic assessment of regional erosion risk.

The first simple USLE-based erosion risk map for the whole of Switzerland was produced by Schaub and Prasuhn (1998). This map has been continuously developed and improved several times (Prasuhn et al., 2007; Prasuhn et al., 2013; Bircher et al., 2019b). However, in a first attempt carried out by Ogermann et al. (2006), to compare the mapping of erosion damage in the study area and the calculation of soil erosion with three different models, higher model erosion rates were determined in the computation than in the determination by mapping.

Based on this experience and the conclusions in the literature that the RUSLE overestimates soil loss rates, we have used a long-term study on the monitoring of soil erosion in farmers' fields (Prasuhn, 2011, 2020) for this paper, in order to evaluate the reliability of RUSLE-based modelling of soil erosion. Accordingly, the aim of this study is an analysis and comparison of mapped soil loss with RUSLE-modelled soil loss. Therefore, we compared high-resolution digitized mapped soil loss data gathered over 10 years for 203 fields in Switzerland with results of erosion modelling using an extensive amount of input data adapted to Swiss conditions. In this comparison, we want to show the accuracy of fit between mapping and modelling. The results of this study are intended to be used in the future to calibrate and adapt modelled erosion rates regionally, in order to utilize the soil erosion risk map for policy advice and decision support.

2. Methods

2.1. Study site

The study site is located about 20 km north-west of Bern, in the Cantone of Bern, where five long-term assessed subareas (Frienisberg (FRI), Suberg (SUB), Lobsigen (LOB), Seedorf (SEE), Schwanden (SCH)) of soil erosion mapping provide a representative reflection of the agricultural used area in the Swiss plateau between the northern Prealps and the Jurassic Alps. The area is situated between the altitudes of 475 and 720 m a.s.l. The region is characterized by a moderate climate, with an annual average temperature of approximately 8.5 °C and annual precipitation of 1048 mm. Most soils are well drained Cambisols and Luvisols on ground moraines and tertiary molasses; they are mostly sandy loams. Farm size is relatively small, averaging 16.7 ha; the average field size is also small at 1.3 ha. Crop rotations are versatile and usually include temporary grassland of about 22% in the summer half-year and 37% in the winter half-year. The five selected study sites consist of 203 fields with crop rotation and about 258 ha, or 645,242 pixels at a resolution of 2 × 2 m.

For LS-factor calculation field blocks were formed consisting of several fields on a slope (see chapter (R)USLE modelled soil loss). This region serves as the comparison area of the field mapping and the RUSLE model (Fig. 1). A detailed description of the area has been provided by Prasuhn and Grünig (2001) and Prasuhn (2011).

2.2. Field mapped soil loss

From autumn 1997 to autumn 2007, event-related erosion damage mapping was carried out during 90 field visits (Prasuhn, 2011, 2012). A farmer living in the study area, also a member of the cantonal soil protection department, contacted the surveyor immediately after each precipitation event with visible erosion features. As soon as possible after every precipitation event, after 14 days at the latest, all fields were surveyed (= 18,270 visited fields in 10 years). If several events occurred within a few days of each other, often only the cumulative erosion could be mapped. In 78 out of 90 field observations, soil erosion was mapped on at least one field, in 12 field visits there was no visible erosion damage anywhere although there have been heavy rain events before. Of the total of 18,270 fields visited in 10 years, erosion was mapped on 873 fields or 5% of all visited fields. 89 of the 90 mappings were

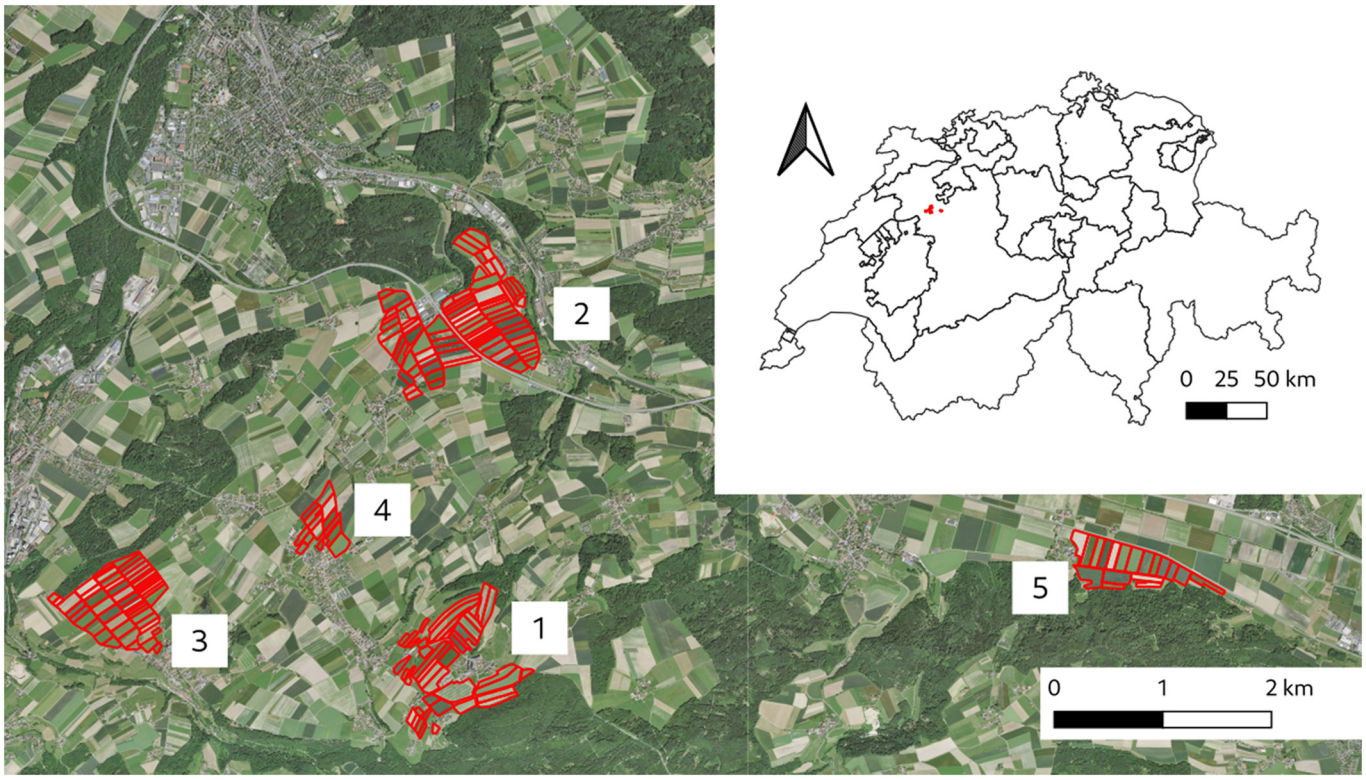

Fig. 1. Study site in the Swiss plateau: 203 fields under monitoring from 1997 to 2007 (red); 1 = Frienisberg (FRI), 2 = Suberg (SUB), 3 = Lobsigen (LOB), 4 = Seedorf (SEE), 5 = Schwanden (SCH). Insert shows the study site (red) and the boundaries of the Cantons of Switzerland. Background © Swisstopo.

performed by the same experienced mapper, so that no calibration between different mappers and over time was necessary. This mapper also carried out an accuracy analysis of the mapping method based on repeated independent mappings and statistical analysis (Rüttimann and Prasuhn, 1990). Linear erosion features (rills, ephemeral gullies), sheet-to-linear erosion and sheet erosion were recorded. With linear forms of erosion, the channel lengths and their cross-sections (depth and width) at appropriate intervals alongside the channel were measured following a uniform guideline according to Rohr et al. (1990) for Switzerland and Botschek et al. (2021) for Germany. This method has been used in various other studies (Evans, 2017; Steinhoff-Knopp and Burkhard, 2018; Saggau et al., 2019). The uncertainty of the mapping of linear erosion features amounted to plus/minus 15% for the experienced mapper and for a careful application (Rüttimann and Prasuhn, 1990). Steinhoff-Knopp and Burkhard (2018) carried out a comparison of multiple measurements from different observers and data derived using structure-from-motion methods and found an error rate of about 15% for the actual loss rates determined in Lower Saxony, Germany. Soil losses by sheet erosion were estimated visually in a semi-quantitative way, according to Ledermann et al. (2010). Considering data obtained from long-term measurements in the study area with sediment traps (40 sediment traps in 30 fields; measurements over 3 years; Mosimann et al., 1990; Rüttimann et al., 1995), three intensity values ('light' corresponds to 0.5 t/ha; 'moderate' corresponds to 1.0 t/ha; 'severe sheet erosion including small rills < 2 cm depth' corresponds to 1.7 t/ha) were formed. Maximum soil loss rates measured with sediment traps almost never exceeded 2.0 t/ha per event without showing any linear erosion features. Visual indicators observed in the field, such as soil sealing, runoff tracks, small sediment deposits, etc. were combined to determine the level of sheet erosion intensity. Steinhoff-Knopp and Burkhard (2018) have used the same method to estimate sheet erosion. However, we are aware of uncertainties concerning the values for sheet erosion.

The weight of the eroded soil was determined by multiplying the volume of the eroded soil by the bulk density of the topsoil. In the literature, these values range from 0.95 to 1.50 Mg/m^3 (see Prasuhn, 2011). In the present study, a topsoil bulk density of 1.20 Mg/m^3 was assumed for large rills (> 10 cm depth) as well as for rills in tractor lanes and furrows. However, most rills were only a few centimeters deep, and erosion occurred immediately after seed bed preparation or sowing, when the topsoil was loosely packed. Therefore, a low bulk topsoil density of 1.00 Mg/m^3 was used for shallow rills (see Ledermann et al., 2008).

Each of the 1639 erosion forms was plotted as accurately as possible on a field sketch, and the measured soil loss rates recorded in a database. The field sketches were then digitized and quantitatively transferred to a geographic information system (GIS). In order to achieve comparability with the modelled data, the mapped data were converted to a 2 m grid based on the digital elevation model (DEM) of SwissALTI3D (Swisstopo, 2015). Rill erosion features were buffered with 8 m on both sides of the linear erosion form in order to take into account the inaccuracy of the field mapping. The soil loss rates of the linear erosion features were distributed weighted with a Multiple Flow Direction (MFD) algorithm in SAGA-GIS (Freeman, 1991) in flow direction. This means that as the length of a rill increases, its soil loss increases. The total amount of soil loss of a digitized erosion feature always corresponds exactly to the amount of mapped soil loss in the database. This procedure was used in order to achieve the best possible representation of the mapped erosion forms, illustrating the spatial pattern of soil loss on a slope. To combine the spatially explicit mapped soil erosion features to high-resolution maps of soil loss all 1639 digitized erosion forms from the 10 years were finally superimposed onto a map, summed up and divided by 10. The results from the map of the field showed the long-term average soil erosion rate in a 2 m grid (for details see Prasuhn, 2020). The calculation of the soil loss rates for a single field was based on the sum of the soil loss rates of all mapped erosion forms on this field over 10 years. Related to the area of the field and the 10 years of investigation, this results in the mean soil loss in t/ha/yr. This value corresponds to the mean value of the mapped soil loss rates of all pixels of the respective field.

Accordingly, the statistical evaluation of the mapped soil loss rates always included all fields and years with and without visible erosion.

2.3. (R)USLE modelled soil loss

The RUSLE modelled soil loss is based on the USLE estimation (Wischmeier and Smith, 1978), and consists of six factors, where L is the slope length factor [no unit], S is the slope steepness factor [no unit], K is the soil erodibility factor [t*ha*h/ha/MJ/mm], R is the rainfall and runoff erosivity factor [MJ*mm/ha/h/yr], C is the cover and management factor [no unit], and P is the support practice factor [no unit]. Multiplication of these factors provides the average long-term soil erosion risk in tonnes per hectare and year [t/ha/yr] (Wischmeier and Smith, 1978; Renard et al., 1997).

$$A_{act} = L*S*K*R*C*P$$

Aact represents the modelled actual annual soil loss rate [t/ha/yr]. The soil loss rates were modelled as raster GIS layers for the 258 ha arable land of the study area at a resolution of 2 m.

The topographical factor LS was calculated using a 2 m resolution DEM from 2015. The DEM was produced with Light Detection and Ranging (LIDAR) technology with vertical accuracy, at ±0.5 m (Swisstopo, 2015). To calculate the LS-factor, Bircher et al. (2019a) tested 11 different multiple flow algorithms with different convergence settings for the study area. The variation in the LS-factor values was only small. For the present study, we decided to use the Multiple Triangular Flow Direction Algorithms (MTFD) by Seibert and McGlynn (2007) with a convergence value of 1.1. The method of Renard et al. (1997) was used for the S-factor calculation. The L-factor was calculated using the method of Desmet and Govers (1996), which replaced the slope length with the upslope contributing area. The L-factor approach was combined with the multiple flow direction algorithms (MTFD) (for details see Bircher et al., 2019a). LS was calculated as a differentiating LS for each 2 m pixel, which means that the soil loss of the upper increment was subtracted and all different increments along a slope were added. The topographical factor LS was calculated at field block level based on the 2 m DEM and are used as independent flow units. Field blocks divide areas surrounded by artificial or natural borders such as streets, forests, and villages, preventing water flow. A field block can contain several cultivation plots, feature different types of use (arable land, permanent grassland, vineyards, or different field crops), and be cultivated by different farmers. More details of the field block map of Switzerland are available in Bircher et al. (2019b) and Prasuhn et al. (2013).

Detailed soil maps with information on grain size distribution on a scale of 1:25,000, and in some cases 1:10,000, were available. For the calculation of the soil erodibility factor K, for each of the 203 fields, grain size, skeletal content and humus content were additionally determined by an experienced soil expert using a feeling finger test in the field. Laboratory analyses were performed on 21 selected fields (texture, humus content), and the K-factor was determined based on the obtained texture distribution and organic matter content using the formula by Schwertmann et al. (1990). Values for permeability class and soil structure class were estimated. (for details see Prasuhn and Grünig, 2001). A K-factor value was determined for each of the 203 fields. A differentiation within the fields was not possible. However, the fields are relatively small with an average of 1.3 ha and homogeneous with regard to soil properties.

The rainfall erosivity factor R was calculated by Schmidt et al. (2016), using datasets from federal and cantonal sources with a resolution of 1 ha grid cells for Switzerland. For the calculation, 86 rain stations distributed throughout Switzerland with 10-min rainfall amount values over 20 years were used and interpolated with covariates (DEM, altitudes of snow etc.).

Based on interviews with all farmers and observations during the field visits, the crop rotation and tillage methods (no-till and strip-till; mulch tillage that leaves >30% of crop residues on the soil surface; reduced tillage which leaves <30% of the soil surface covered with crop residues; mouldboard or disk plough with soil inversion) were determined for each field for the years 1997 to 2006 in order to calculate the cover and management factor C. The C-factors were determined using a C-factor calculation tool (Mosimann and Rüttimann, 2006), adapted to Swiss conditions. Region-specific dates for growing stages for all crops (sowing, soil cover phases, harvest), area-specific seasonal distribution of rainfall erosivity, various intermediate uses (winter fallow, stubble fallow, freezing or wintering cover crops, etc.) and various correction factors for carry-over effects were taken into account (for details see Prasuhn and Grünig, 2001; Prasuhn, 2022).

In a first step, the support practice factor P was determined in the field on the basis of observations of the tillage direction. If the tillage direction of a field was in the direction of the slope, a P-factor value of 1.0 was used for the whole field or all pixels in this field. In a second step, the effect of cross-slope cultivation was determined as a function of slope gradient and critical slope length for all other fields (Auerswald, 1992; DIN 19708, 2017; Steinhoff-Knopp and Burkhard, 2018). If tillage and cultivation was in a cross-slope direction (along the contour), the P-factor is only effective below a critical slope length (SL). The critical SL was calculated based on the field blocks and the DEM using the following formula:

$$SL_{crit} = 170 * e^{-0.13 * \text{Slope (\%)}}.$$

For all pixels of a field block exceeding the critical slope length, the P-factor value of 1.00 was used. For all pixels below the critical slope length, the P-factor value was calculated from the DEM as a function of the slope gradient based on the classification according to DIN 19708 (2017) and the formula of Schäuble (2005):

$$P = 0.4 + 0.02^{*} \text{ Slope (\%)}$$

2.4. Comparison of mapped and modelled soil loss

The comparison was made at different spatial scales:

(a) Pixel: soil loss for 2 m pixels mapped and modelled was compared ($n = 645{,}242$). It should be noted that for modelled soil loss, only the LS- and P-factor for 2 m pixels was available. The R-factor was determined at the hectare grid, and the K- and C-factors were determined per field and disaggregated to the 2 m grid.
(b) Fields: for each of the 203 fields, the mean value for the mapped and modelled soil loss and for each factor (LS, R, K, C, P) was used based on the 2 m grid. The range of the number of pixels of the 203 fields varied from 393 to 11,957.
(c) Subareas: for the five subareas, the mean value for the mapped and modelled soil loss based on the 2 m pixels was taken. The range of the number of pixels of the five subareas varied from 37,808 to 241,586.

3. Results

3.1. Compilation of the RUSLE factors

The mean LS-factor based on the 645,242 pixels was 2.23 (Table 1). The subarea FRI was the steepest and has the highest LS value with a mean of 5.10, while the subarea LOB has the lowest with 1.30. As shown in Fig. 3, the spatial variability of the LS-factor was also highest in the subarea FRI. In addition to some very steep fields, there were some slope depressions with high LS-factors. For the 203 fields, the LS-value varies between 0.40 and 16.80 (Fig. 2).

The average K-factor in the study area was 0.033 t*ha*h/ha/MJ/mm (Table 1). It was lowest in FRI and highest in LOB. The range for the 203 fields included values from 0.017 to 0.042 t*ha*h/ha/MJ/mm (Fig. 2).

The average R-factor in the study area was 985 MJ*mm/ha/h/yr and varied between 972 and 1002 MJ*mm/ha/h/yr in the five subareas and between 952 and 1029 MJ*mm/ha/h/yr in the 203 fields (Table 1,

Table 1
Mean values for the RUSLE-factors of the five subareas and the total area of the 203 fields. FRI = Frienisberg, SUB = Suberg, LOB = Lobsigen, SEE = Seedorf, SCH = Schwanden.

Mean	LS-factor [−]	K-factor [t*ha*h/ha/MJ/mm]	R-factor [MJ*mm/ha/h/yr]	C-factor [−]	P-factor [−]
FRI (n = 138,467)	5.1	0.026	1002	0.108	0.93
SUB (n = 241,586)	1.33	0.033	984	0.088	0.82
LOB (n = 136,229)	1.3	0.037	972	0.103	0.92
SEE (n = 37,808)	2.46	0.037	978	0.073	0.87
SCH (n = 91,152)	1.58	0.033	988	0.118	0.97
Mean five subareas (n = 645,242)	2.23	0.033	985	0.099	0.89

Fig. 2).

The average C-factor in the study area was 0.099 in the five subareas. The range was large for the 203 fields, with values from 0.006 to 0.247 (Table 1, Fig. 2).

The average P-factor in the study area was 0.89. For the 203 fields, the value varied between 0.46 and 1.00 (Table 1, Fig. 2).

3.2. Comparison of mapped and modelled soil loss

For the whole area, based on the analysis of the 645,242 pixel, a mean mapped soil loss of 0.77 t/ha/yr and a modelled actual soil loss of 6.20 t/ha/yr was obtained. Thus, the mean mapped soil loss was only 12% of the modelled loss, meaning modelling estimates higher soil loss by a factor of 8 (Table 2). The subarea FRI had by far the highest mean mapped soil loss (2.00 t/ha/yr), as well as the highest modelled actual (15.30 t/ha/yr) soil loss, meaning the modelled values were higher by a factor of 7.7 compared to mapped soil loss. The other four subareas – SUB, LOB, SEE, and SCH – had significantly lower mapped soil loss, which amounted to about a quarter of the mapped soil loss in FRI. In these four subareas, the modelled soil loss was also significantly higher than the mapped values, ranging from factor 5.9 (SUB) and factor 14 (SEE).

Even though the mean mapped soil loss of the 10 years in the whole area was low at 0.77 t/ha/yr, the maximum mapped annual soil loss in a single field was 96 t/yr or 58 t/ha/yr. Only a few erosion events on a few fields substantially contribute to the total extent of soil loss in the study area. Rill erosion and sheet erosion accounted for 75% and 25% of total soil loss, respectively (Prasuhn, 2011). The mapped soil loss showed a large spatial variability between different areas, between different fields, and within fields (Fig. 4). High soil erosion was mainly caused by linear erosion in slope depressions or at the field edges (headlands, tractor lanes), and thus occurred only in certain parts in a field. The modelled soil loss did not represent precisely this small-scale pattern of soil erosion. However, only the LS and P factor could be modelled at a 2 m resolution, while for the other factors R, K and C only averages of each of the 203 fields could be used, although even these factors can vary within a field.

An attempt to correlate mapped and modelled soil loss on a pixel by pixel basis (n = 645,242) did not show any significant correlation (data not shown). This is not surprising, since only the LS- and P-factor could be calculated on the basis of the 2 m pixels, while the other factors were collected at field level (K- and C-factor) or in the hectare grid (R-factor). The soil loss values were classified, based on the guideline values of soil erosion in Swiss legislation. According to the Swiss Ordinance on Soil Protection (Schweizer Bundesrat, 1998), soil erosion is tolerable if it does not exceed a mean of 2 t/ha/yr (for soil depth < 70 cm) or 4 t/ha/yr (for soil depth > 70 cm). Of the mapped soil loss, 90% of the pixels were in class 1 (0–1 t/ha/yr) (Table 3). We have used the values 2 and 4 t/ha/yr of the legal requirements as class boundaries in Table 3 and created some additional classes above and below these legal tolerance values to better show the spatial patterns of soil erosion. From class 1 to 6, the area of the mapped pixels decreased continuously, and the area for class 6 (> 16 t/ha yr) was only 2.1 ha or 0.8% of the total area. Only 3.4% of the pixels had a mapped soil loss of >4 t/ha/yr. The modelled actual soil loss showed a completely different pattern. The size of area and amount of pixels of the classes 1 to 6 decreased. 33.7% of the pixels and area had a modelled soil loss of >4 t/ha/yr and 66.3% of the pixels had a modelled soil loss of <4 t/ha/yr. In contrast to the mapped area, the modelled area contained in class 1 was only 25.1% (64.9 ha), and in class 6 9.1% (23.5 ha) (Table 3).

Despite the fact that almost 90% of the area affected by soil loss was in class 1, the mapped soil loss in these areas only represented 19.6% of the total loss, while 70.3% of the total modelled soil loss belonged to this class (Table 3). On areas with low soil loss of <4 t/ha/yr (classes 1–3) the mapped soil loss was 37.2% of the total mapped soil loss. In contrast,

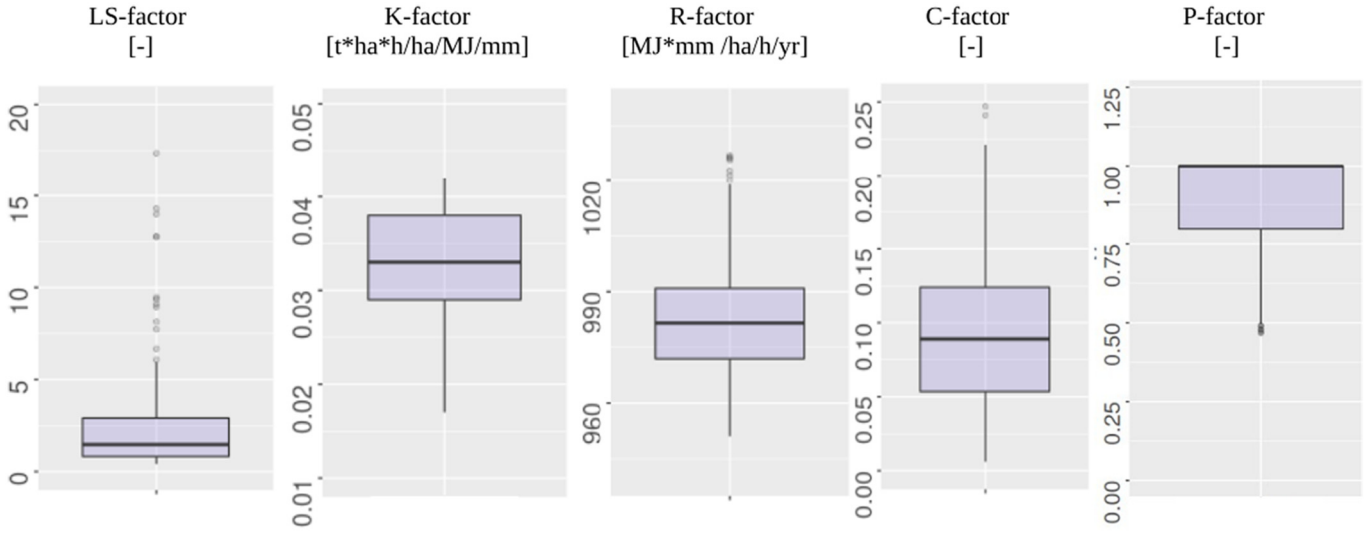

Fig. 2. Boxplots for the different factors of the RUSLE (LS, K, R, C, P) as mean values for 203 fields. Boxes indicate median and 25% and 75% quantiles, while whiskers indicate 5% and 95% quantiles (n = 203).

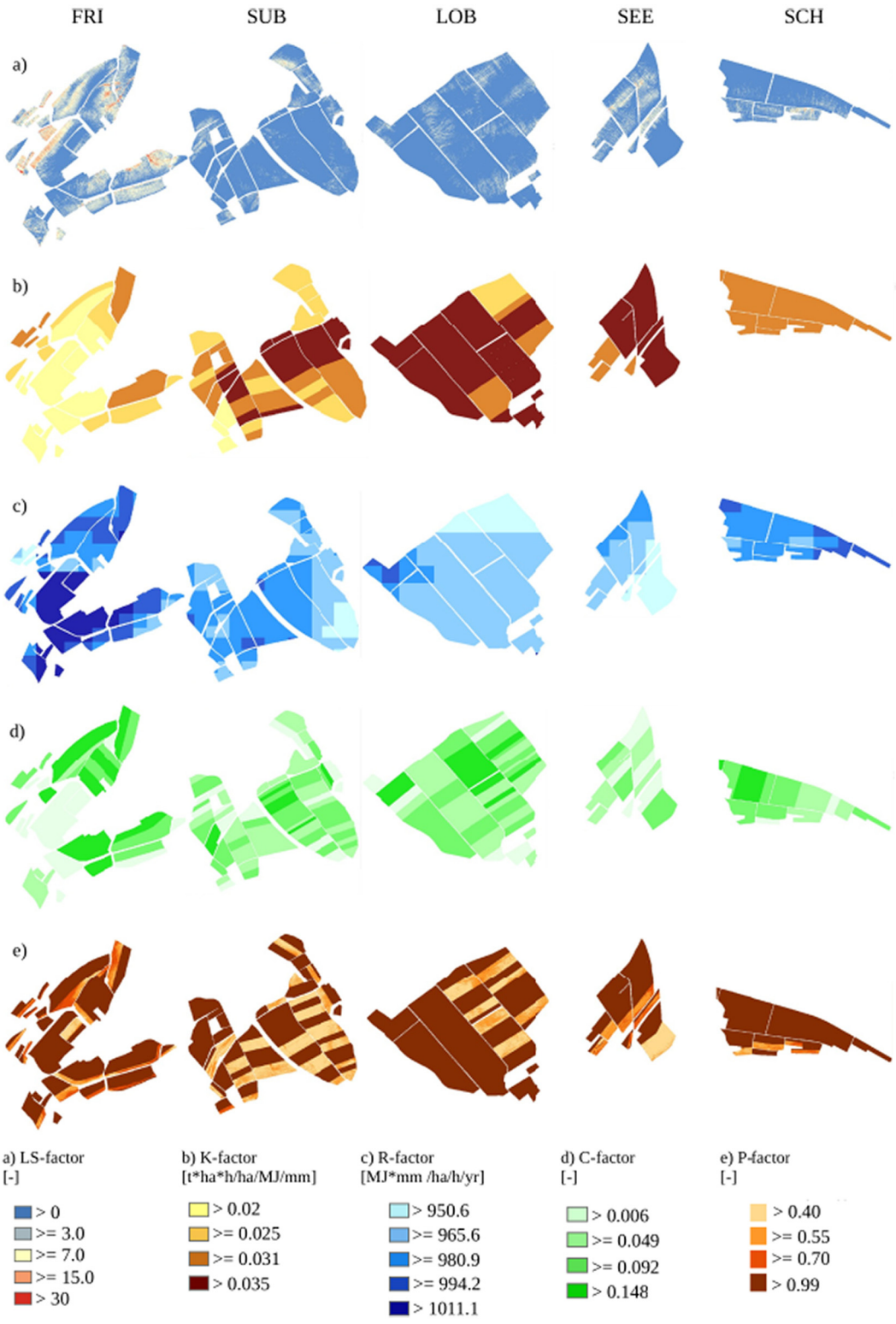

Fig. 3. Factor maps of RUSLE, based on a 2 m grid (n = 645,242 pixel): a) topographic factor (LS); b) soil erodibility factor (K); c) rainfall erosivity factor (R); d) cover management factor (C); and e) support practice factor (P), for 203 fields from left to right (FRI = Frienisberg, SUB = Suberg, LOB = Lobsigen, SEE = Seedorf, SCH = Schwanden).

88.1% of the total modelled soil loss was calculated for these areas. The mismatch between mapped and modelled soil loss was, on average, factor 18.8 for areas with low mapped soil loss. The high mapped soil loss of >4 t/ha/yr totalled 62.8% of the total mapped soil loss. In the same areas, the modelled soil loss was 11.9% of the total modelled soil loss and was thus of a similar magnitude to the mapped soil loss (mismatch factor 1.5). In total, the higher estimation of soil loss due to modelling was highest in areas with low mapped soil loss (classes 1–3) and decreased with high mapped soil loss (classes 4–6). In class 6 (> 16 t/ha/yr), the modelled soil loss rate was even slightly lower than the

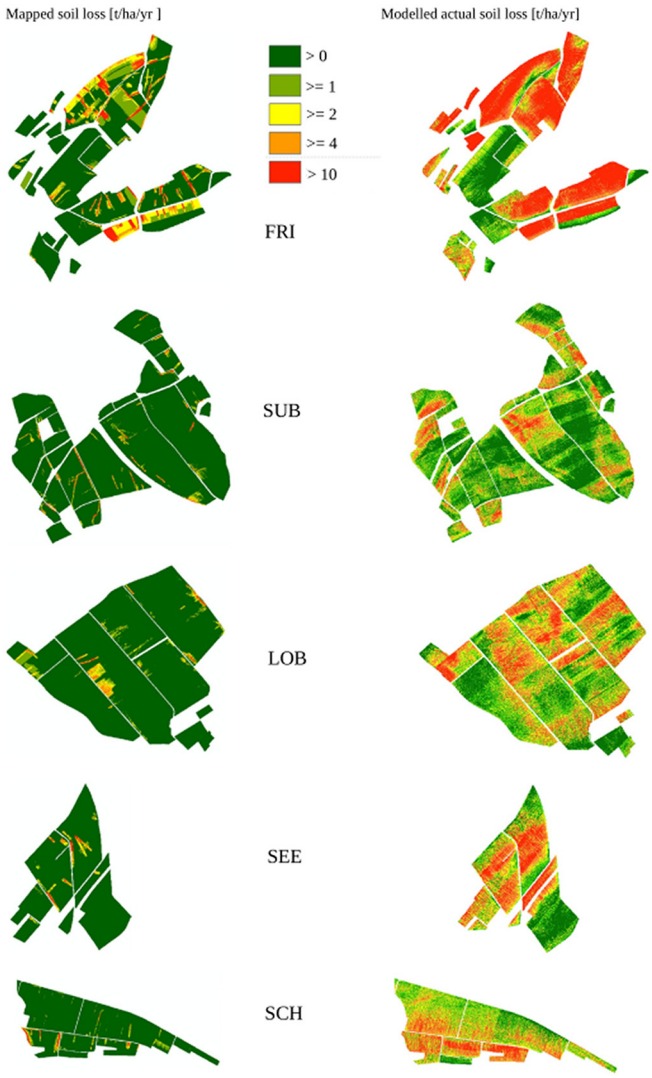

Fig. 4. Mapped soil loss over 10 years (left), modelled actual soil loss (right) for the five subareas (FRI = Frienisberg, SUB = Suberg, LOB = Lobsigen, SEE = Seedorf, SCH = Schwanden).

mapped loss rate (Table 3).

As an example, for Frienisberg (FRI), the spatial pattern in Fig. 5 shows that in areas where high mapped soil loss (> 4 t/ha/yr) occurred, high soil loss rates were modelled. On the other hand, high soil loss was modelled in many areas where only low soil loss (< 4 t/ha/yr) was mapped.

3.3. *Evaluation of the 203 fields*

The evaluation of the 203 fields with regard to mapped and modelled soil loss showed that the mean values of soil losses were significantly above the median values in all cases (Table 4). This demonstrates the large dispersion of the soil loss values and that they were not normally distributed, resp. were left-skewed distributed (Fig. 6). The modelled actual soil loss was higher by a factor of 8 than the mapped soil loss (mean values of 203 fields).

With the mapped soil loss, there were some fields with no observed erosion in 10 years and accordingly a mean soil loss of 0.00 t/ha/yr was assumed. In the model calculations with the USLE / RUSLE, some soil loss is always calculated; the modelled minimum value was 0.32 t/ha/yr.

The comparison between mapped and modelled actual soil loss gave a weak relationship ($r^2 = 0.19$) for the area related soil loss values in t/ha/yr when considering the 203 fields (Fig. 7). Five out of 203 fields with high mapped mean soil loss >4 t/ha/yr have relatively high modelled soil loss as well. In contrast, however, there are also fields with no or very low mapped soil loss that show very high modelled soil loss.

4. Discussion

The existing data sets provide the basis to compare spatially distributed mapped and spatially distributed modelled erosion. The 10-year mapping data are of high precision and quality. In 90 field surveys, area-wide mapping was carried out by the same experienced mapper. 1639 erosion forms were analysed in detail and published (Prasuhn, 2011, 2012, 2020). The field sketches were digitized at the same spatial resolution, using the 2 m grid of the digital elevation model, as the modelling. By using multiple flow algorithms for the digitization of linear erosion features, the spatial pattern of the soil loss on the slopes was implemented in the best way possible (Prasuhn, 2020).

Modelling was also carried out using high-quality and high-resolution input data. Particular attention was paid to the two especially sensitive factors of RUSLE. The C-factor of the USLE is the most sensitive model parameter, followed by the LS-factor (Borrelli et al., 2018; Covelli et al., 2020). The C-factor was calculated for each field over the 10 years on the basis of field mapping and interviews with farmers, using a tool adapted to Swiss conditions and established in Switzerland (Mosimann and Rüttimann, 2006). Region-specific growth stages of all crops, region-specific erosivity values, four different tillage methods, various cover crops, carry-over effects such as temporary ley grass and other correction factors were all taken into account. The calculated mean C-factor of 0.099 in the study area is rather low compared to international studies, due to the high proportion of temporary ley grass in the crop rotation, the use of conservation tillage practices and the cultivation of cover crops (Prasuhn, 2022). Prasuhn (2022) showed that the mean C-factors calculated with the same method over five different periods between 1987 and 2014 in the study area decreased in a similar order of magnitude as the mean mapped soil loss during these periods. The increase in conservation tillage practices was identified as the most important mitigation measure for both modelled C-factors and mapped soil loss.

For the LS-factor, various multiple flow algorithms for this area were compared and analysed in a separate study (Bircher et al., 2019a). With the accurate 2 m DEM and the selected MTFD1.1 from Seibert and McGlynn (2007), the LS- and P-factor was determined in the best way possible. Furthermore, for the R-factor, K-factor and P-factor field specific values were available.

Despite the unique data base described above, some critical points should be noted and taken into account when interpreting the results. The mapping period under consideration only lasted 10 years. Therefore, there are some fields where erosion has not been observed so far, but will occur in the future. In other fields, the average soil loss can also change over time. During the field mapping, it was considered that slight sheet erosion could have been overlooked sometimes. However, this is of little significance for the total amount of soil loss, because there were few major events that determined the total amount of soil loss (Prasuhn, 2011; Evans, 2017; Fiener et al., 2019). The mapping itself is subject to some uncertainties, but an uncertainty analysis of rill erosion is difficult, especially for complex linear erosion forms. According to various studies and our own long-term experience, an error of plus/minus 10–30% can be expected, depending on the complexity of the erosion form and the experience of the mapper (Rüttimann and Prasuhn, 1990; Herweg, 1996; van oost kristof et al., 2005; Casalí et al., 2006; Ledermann et al., 2010). Since all mapping was performed by the same experienced mapper, it is realistic to expect an error of at most plus/minus 20%. Nevertheless, we are particularly aware of uncertainties concerning the rates for sheet erosion (Ledermann et al., 2010). The conversion from mapped erosion volume (m^3) to mass (tonnes of soil) is another source of

Fig. 5. Mapped soil loss in the soil loss categories >4 t/ha/yr (top left) in the Frienisberg region and modelled soil loss for the corresponding areas (top right). Mapped soil loss in the soil loss categories <4 t/ha/year (bottom left) and modelled soil loss for the corresponding areas (bottom right).

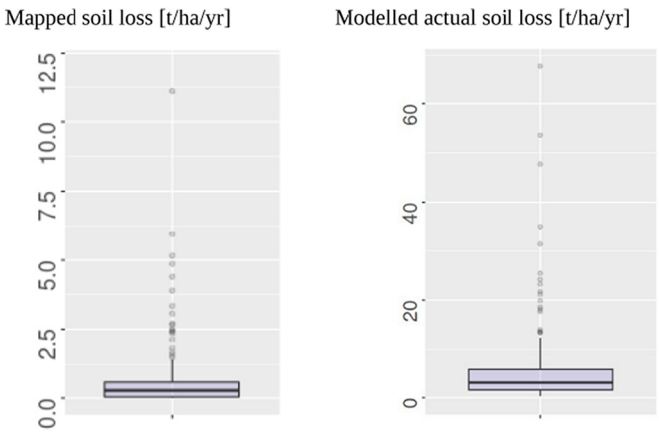

Fig. 6. Boxplot of mapped actual soil loss (left) and modelled actual soil loss (right) for the 203 fields. Boxes indicate median and 25% and 75% quantiles, while whiskers 5% and 95% quantiles (n = 203). Note the different scales for the y-axis.

uncertainty. The bulk density was assumed to be 1.0 for shallow channels and 1.2 Mg m^{-3} for deeper channels (Prasuhn, 2011). The top soil bulk density increases rapidly over time (Franzluebbers et al., 1995), but we could not take this into account as it would require extensive field measurements. Finally, there are inaccuracies in the spatial representation, which is unlikely to affect the amount of soil loss, but may affect the spatial comparability. Since no Differential Global Positioning System (dGPS) was used for mapping, the positioning accuracy of the individual erosion forms is not exact. This fact was taken into account through the buffering of the linear forms during the digitization, but it explains, nevertheless, why a pixel-wise comparison of mapped and modelled soil loss in the 2 m raster did not match.

Modelling with the RUSLE is also not perfect. "*Model predictions are intrinsically more prone to errors than measurements*" (Wainwright and Mulligan, 2013). According to our findings, the choice of LS-factor calculation does not have a great impact on the amount of soil erosion for our area with the selected DEM (Bircher et al., 2019a). However, there are some studies that have identified a decreasing soil loss with decreasing DEM resolution. Due to the high-resolution DEM used, the slope becomes more important and the S-factor is higher than with a coarser DEM (Bircher et al., 2019a). Replacing the one-dimensional LS-

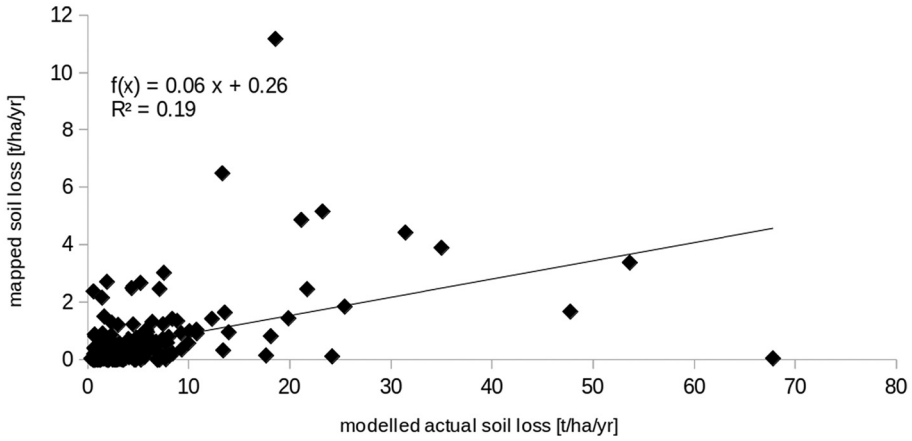

Fig. 7. Comparison of mapped and modelled actual soil loss, $n = 203$ fields.

Table 2
Mean mapped and modelled actual soil loss and derived factors for the five subareas, and mean values for the whole area. FRI = Frienisberg, SUB = Suberg, LOB = Lobsigen, SEE = Seedorf, SCH = Schwanden.

	Mapped soil loss [t/ha/yr]	Modelled actual soil loss [t/ha/yr]	Factor modelled act/mapped
FRI (n = 138,467)	2.00	15.30	7.7
SUB (n = 241,586)	0.46	2.70	5.9
LOB (n = 136,229)	0.34	4.10	12.1
SEE (n = 37,808)	0.40	5.60	14.0
SCH (n = 91,152)	0.56	4.90	8.8
Mean total area [n = 645,242 pixel]	0.77	6.20	8.0

factor calculation with a two-dimensional LS-factor calculation can lead to an overestimation of the influence of the topography because convergent and divergent flows are better represented in real landscapes. The maximum slope length is another critical parameter. By calculating the LS-factors at field block level, an upper limit is given, since field blocks in Switzerland are relatively small, with an average size of 5.22 ha. When calculating the flow paths using multiple flow algorithms, it is assumed that water and sediment from upslope areas control the soil erosion in downslope pixels. However, it is also assumed that there is a continuous, unimpeded flow of water within the slope or field block. The hydrological connectivity is controlled exclusively by topography; the influence of different vegetation cover is not considered. The L-factor thus represents a theoretically maximum contributing area (Qin et al., 2018). However, if land use varies on a slope, downslope erosion can be reduced by slowing down the runoff. In the study area and in Switzerland in general, agriculture is small-scale with small fields (mean field size = 1.3 ha), so that often several fields with different land use coexist on a slope. Qin et al. (2018) conclude: "*rational and reliable soil erosion assessment can only be acquired if the coupled effects of upslope topography and vegetation cover on downslope soil erosion are fully considered in the models*". This is not adequately addressed by the C- and P-factor since these factors are independent of the slope. In their study on the Lvergou watershed (China), the new calculation of the LS-factor resulted in a 41% lower average annual soil loss than with the conventional calculation.

However, Borrelli et al. (2018) considered the mapping of soil cover conditions and their spatio-temporal change to be a relevant factor. They developed an enhanced C-factor based on a spatially more accurate and and high temporal resolution assessment of crop dynamics in the medium-size Upper Enziwigger River Catchment in Switzerland. They reported an approximately seven times higher soil loss using traditional C-factor modelling than that predicted by their novel approach. Thus, this may solve the overestimation of factor 8 we reported in this study.

Table 4
Statistical values for the analysis of the 203 fields regarding mapped and modelled actual soil loss.

	Mean	Median	Maximum	Minimum
Mapped soil loss [t/ha/yr] ($n = 203$)	0.62	0.27	11.18	0.00
Modelled actual soil loss [t/ha/yr] (n = 203)	5.61	3.28	67.8	0.32

Table 3
Area proportions and mapped and modelled soil loss for six erosion classes based on the guideline values of soil erosion in Swiss legislation.

	Class 1 0–1 t/ha/yr	Class 2 1–2 t/ha/yr	Class 3 2–4 t/ha/yr	Class 4 4–8 t/ha/yr	Class 5 8–16 t/ha/yr	Class 6 > 16 t/ha/yr	Total
Mapped Soil loss							
Number of pixels [n]	579,253	25,999	18,312	10,236	6145	5297	645,242
Area [ha]	231.7	10.4	7.3	4.1	2.5	2.1	258.1
Percent of area mapped	***89.8***	***4.0***	***2.8***	***1.6***	***1.0***	***0.8***	***100***
Mapped soil loss [t/yr]	39.3	14.8	20.5	22.9	27.7	75.3	200.5
Percent of total soil loss mapped	***19.6***	***7.4***	***10.2***	***11.4***	***13.8***	***37.6***	***100.0***
Modelled Soil loss							
Number of pixels [n]	162,352	137,117	128,636	94,669	63,599	58,869	645,242
Area [ha]	64.9	54.8	51.5	37.8	25.4	23.5	258.1
Percent of area modelled	***25.1***	***21.3***	***19.9***	***14.7***	***9.9***	***9.1***	***100***
Modelled soil loss [t/yr]	1121.1	152.9	130.6	74.9	53.2	61.9	1594.8
Percent of total soil loss modelled	***70.3***	***9.6***	***8.2***	***4.7***	***3.3***	***3.9***	***100***
Factor: modelled / mapped soil loss	**28.5**	**10.3**	**6.4**	**3.3**	**1.9**	**0.8**	**7.9**

The USLE, resp. RUSLE models, represents long-term average soil loss through sheet and rill erosion. Gully erosion is not included, but this does not occur in the study area. However, the use of multiple flow algorithms allows a more accurate representation of concentrated runoff and the resulting rill and ephemeral gully erosion than one-dimensional approaches (Winchell et al., 2008; Prasuhn et al., 2013). In contrast, mapping has shown that erosion often has specific operational causes such as plough furrows, compacted field headlands, tractor lanes compaction (especially tramlines), and potato furrows (Prasuhn, 2011; Evans, 2017; Steinhoff-Knopp and Burkhard, 2018; Saggau et al., 2019), or is caused by extraneous water inflow from other areas. These conditions cannot be modelled using the RUSLE approach. Tractor lanes compaction and potato furrows are not explicitly spatially considered in the C-factor when modelling with RUSLE. Plough furrows and compacted headlands have not been taken into account in the C-factor calculation so far. In the headlands, the direction of tillage also changes and thus the direction of the tractor lanes. Consequently, the P-factor for the headlands would have to be calculated separately. According to our mapping, they are important in our study area. In future, they should be additionally recorded in the C-factor or a separate C- and P-factor should be developed for the headlands. However, this would require systematic measurements in the headlands in comparison to the main fields for different crops.

Accordingly, the mapped soil loss rates, which additionally captured erosion in the headlands and due to water inflow, would have to be higher than the modelled soil loss where this could not be accounted for. On the other hand, rills often occur only in certain areas of a field and not across the whole field, and do not occur every year. In contrast, with the RUSLE-model rill and sheet erosion are calculated across the whole landscape (Evans and Boardman, 2016b). Therefore, the comparison between mapped and modelled actual soil loss based on the 203 fields shows only a weak to moderate correlation. However, the field size is the ultimate area for decision making by the land users and the unit for enforcement of legal requirements.

The results of this study illustrates that the modelled actual soil loss is drastically higher than the mapped soil loss. Numerous studies have revealed that the USLE / RUSLE tends to overestimate both the severity and the extent of erosion rates. Our finding is also supported by the literature, which suggests that low erosion rates tend to be overestimated and high erosion rates are actually partly underestimated. Risse et al. (1993) found early on that "*USLE usually overestimates at sites with relatively low erosion rates and underestimates at sites with higher erosion rates […]. The accuracy in terms of the difference between measured and observed data is better at higher erosion rates.*" Rapp (1994) confirmed the results for the data set used by Risse et al. (1993), although calculated with the RUSLE. Nearing (1998) listed further examples from the literature that confirm this trend. Di Stefano et al. (2017) tested three different USLE approaches, compared measured and modelled soil loss rates and found that all three USLE approaches tended to overestimate low event soil losses (< 10 t/ha), while two of the approaches tended to underestimate high (> 10 t/ha) annual soil losses. Furthermore, Kinnell (2010) showed that when soils have a low runoff coefficient, USLE overestimates low event soil losses and underestimates high event soil losses. In a study similar to his study, Steinhoff-Knopp and Burkhard (2018) compared 1355 mapped erosion forms in 86 fields in Germany over 17 years with USLE-based modelling. The mean of the measured actual soil loss was significantly lower than the mean of the modelled actual soil loss. Evans and Brazier (2005), also found a discrepancy between predicted erosion and actual erosion for a number of localities in lowland England and Wales. Abu Hammad (2011) observed in the Central Palestinian Highlands that the RUSLE-GIS model overestimated the measured soil loss by 21%. Fernández et al. (2010) investigated post-fire soil losses predicted by the RUSLE in NW Spain and found that RUSLE model predictions overestimated actual annual soil losses without multiplying the R- and C-factors by 0.7 and 0.865, respectively. Finally, Rymszewicz et al. (2015) compared RUSLE application on a national scale against measured sediment yield values in different catchments in Ireland and reported an overestimation of modelled sediment yield values for most (8 from 12) of the selected catchments ranging from 220 to 2839% difference.

In contrast, some studies observed a good agreement between mapped and modelled erosion. Alewell et al. (2019) concluded on the basis of their literature review that "*soil loss estimation with USLE-type models are within the order of magnitude compared to measured soil loss rates*". Napoli et al. (2016) compared predicted soil loss versus field data measuring soil erosion on 566 fields over six years in Chianti (Italy). They found a good accuracy, with a predicted average soil loss of 13.8 t/ha/yr in comparison to the field measured soil loss of 14.9 t/ha/yr. Fischer et al. (2017) compared predicted event soil loss using the official prediction system in Bavaria (Germany), based on the USLE, and validated the predictions with aerial photo erosion classifications of 8100 fields. In their study, visually classified and predicted soil loss correlated very highly. Bagarello et al. (2017) tested USLE-derived models to predict the annual maxima of event soil loss. They found evidence that the USLE-based approach was very useful for estimating high soil loss rates. van oost kristof et al., 2005 conducted experiments in two catchment areas in Belgium and reported that the total sediment export, derived from erosion surveys, was substantially higher (about 30%) than the measured sediment export at the catchment outlet. Onnen et al. (2019), meanwhile, discovered an underestimation of the modelled sediment yield compared to the measured rill erosion in Denmark. However, in these last two studies, the measurement of erosion in the field and sediment exports and the comparison of the two raises additional difficulties.

Our investigations have shown that the modelled soil loss resulted in much higher rates of soil loss compared to the mapped soil loss, both in the analysis of the classified pixels (mapped 0.77 vs modelled 6.20 t/ha/yr = factor 8.0). This mismatch is significantly higher than reported by Steinhoff-Knopp and Burkhard (2018) in a comparable study (mapped 0.9 vs modelled 2.94 t/ha/yr = factor 3.3). Other geographical settings and environmental conditions between the study in Lower Saxony and our study are probably responsible for these differences. On the one hand, in Lower Saxony the field size area is larger and the loess soils are more erodible, on the other hand, rainfall erosivity is lower, slopes are less steep and crop rotations are more intensive (no temporary ley grass). Taking into account all uncertainties and errors in mapping and modelling, the huge difference in this study cannot be explained. But even supposing a maximum one-directional error in mapping of minus 30%, i.e. mapped erosion rates were 30% lower, a very conservative estimate always results in an overestimation of factor 6, which is still significantly higher than in the other studies cited.

Since models always deviate from reality, calibration and validation is important. There are no guidelines for appropriate application of models such as USLE; each user applies a different model variation based on the available data. Fiener et al. (2020) compared three different USLE applications and observed substantial differences in the modelled soil loss, with up to 75% difference in the results. Thus, there are also problems and limitations with harmonization and standardization procedures in the application of USLE. Thus, calibration and validation of erosion models remain difficult. Favis-Mortlock (1998) already stated: "*Very few models have been validated in any scientifically acceptable sense*". This is still true today. Batista et al. (2019) therefore concluded that "*calibration seems to be the main mechanism of model improvement*". Models tend to overestimate soil loss when used uncalibrated (Saggau et al., 2019) or do not lead to satisfactory model performance (Bernet et al., 2018).

A general reduction of all modelled soil loss values by factor 8 – or even conservatively by factor 6 – is not appropriate, because the overestimation is not equally distributed across all soil loss classes. High soil losses, which are the relevant losses with regard to soil protection, offsite damage or exceeding of reference values, are reproduced quite well by the model. Ledermann et al. (2010) and Prasuhn et al. (2013) have

already demonstrated through plausibility checks that certain fields with a high potential erosion risk often suffer high soil losses in reality. In particular, linear erosion in slope depressions (thalweg erosion) was relatively well captured by the model. These findings have also been confirmed by other studies (Kotremba et al., 2016; Steinhoff-Knopp and Burkhard, 2018). Thus, reducing modelled erosion in general leads to an underestimation of the soil losses in these areas. This is not desirable. On the other hand, the model predicts high erosion for uniformly stretched or convex slopes, which in reality often produce very little erosion. Furthermore, in the study by Steinhoff-Knopp and Burkhard (2018), the difference in the class "no to very low" (<0.2 t/ha/yr) was extraordinarily high for the area proportion, with 1.7% modelled and 59.8% mapped. This is disadvantageous for policy and enforcement; the credibility of the modelled erosion maps decreases, as farmers know their own fields well regarding soil erosion.

From a political point of view, a moderate overestimation of the modelled erosion rates is quite reasonable or even preferable. For raising public awareness, an overestimation is better than an underestimation, especially if only risk maps (e.g. low, moderate, high risk) are presented and absolute soil loss values are omitted. Models are often used by stakeholders to predict soil erosion, and are tools for political decision-makers to design mitigation measures and provide policy advice. In terms of soil erosion prevention, it is of course beneficial to predict soil loss rates that are slightly too high. However, too-high soil erosion rates can also lead to misguided management decisions about where and which mitigation measures should be implemented (van Oost et al., 2005). In contrast, for the implementation of legal guidelines, reliable absolute erosion rates are necessary, because this is ultimately linked to requirements for receiving direct support in form of subsidies for sustainable management or disincentives, including financial sanctions for farmers for management practices resulting in repeated high erosion events. Thus uncalibrated modelled soil loss rates are inadequate in the context of policy advice, planning and decision making (Alewell et al., 2019).

5. Conclusion

In a study in the Swiss Midlands, we compared mapped soil loss with RUSLE-based modelled soil loss values for 203 fields over 10 years. An extensive amount of input data for both mapping and modelling was available. This was crucial, as the type and spatial resolution of the input data had a significant impact on the output of the envisaged comparison. Our results show a substantial mismatch of soil loss rates between modelling and mapping. The modelled soil erosion was higher than the mapped one by a factor of 8. Even taking into account various uncertainties in soil erosion damage mapping, a more conservative evaluation results in an overestimation of approximately factor 6. Thus, our study supports numerous investigations demonstrating that USLE / RUSLE-based erosion models generally tend to overestimate both the severity and the extent of soil loss rates. However, none of the studies showed the modelled soil erosion rate to be so much higher than the mapped assessment as our study did. Yet, this substantial difference did not occur equally in all areas. Areas with relatively high mapped soil loss rates (> 4 t/ha/yr), which are above the tolerable limit, were adequately covered by the model. However, these areas are comparatively rare in the Swiss Midlands due to the widespread use of conservation tillage practices and mixed crop rotations. In particular, linear erosion by concentrated runoff in slope depressions, which was mapped several times in the same fields at the same locations, was accurately captured by the model using multiple flow algorithms and the contributing area concept. However, on many uniformly stretched or convex slopes with low mapped soil loss rates (< 4 t/ha/yr), the model predicted higher erosion rates than what was assessed and mapped in the field.

The overestimation of the modelled soil losses compared to long-term field verification is mainly driven by the LS-factor and the C-factor calculation – or a combination of both. Therefore, there is a potential or need to improve the model predictions. However, we could also demonstrate that it is difficult to improve the USLE / RUSLE in a generic way, e.g. by reducing the modelled soil loss values by factor 6, because the USLE / RUSLE does not capture some of the factors responsible for mapped soil loss (e.g. traffic lanes, compacted headlands, plough furrows) in a complex landscape. Probably process-oriented models could overcome some of the shortcomings of the USLE / RUSLE, but such models are complex and time consuming for parameterization and therefore not applicable for larger areas or whole regions or countries. Our results only pertain to the study area, which covered a wide range of topographical parameters and a typical crop rotation practised in the Swiss Midlands. The determined factors of overestimation cannot be transferred to other regions without adjustment. Any regionalization of the USLE / RUSLE must be verified. However, our findings, which are based on long-term surveys of erosion assessment within complex landscapes, confirm several plot studies showing that USLE / RUSLE-type models overestimate small soil losses and need to be calibrated.

Mapping can only be done in retrospect after erosive events have occurred, while modelling also allows for predictions or land management scenario analyses. This is the major advantage of the USLE / RUSLE and also the main practical application of the model. As long-term mapping is demanding and only feasible for selected sites, USLE / RUSLE modelling can be applied within a short period of time and with reasonable inputs. On the other hand, if the results of the USLE / RUSLE modelling were calculated and used for practical recommendation to farmers without field assessment, tolerable soil losses in our study area would be exceeded on most fields and almost all farmers would have to draw up mitigation plans and significantly change their farming practices. Yet, the field assessment showed, that the land use on most fields is adapted to the location with small field size and extended areas with temporary ley grass, cover crops and conservation tillage.

Declaration of Competing Interest

None.

Data availability

Data will be made available on request.

Acknowledgments

This research is part of a soil erosion risk project, funded by the Swiss Federal Office for Agriculture (FOAG).

References

Abu, Hammad A., 2011. Watershed erosion risk assessment and management utilizing revised universal soil loss equation-geographic information systems in the Mediterranean environments. Water Environ. J. 25 (2), 149–162.

Aksoy, H., Kavvas, M.L., 2005. A review of hillslope and watershed scale erosion and sediment transport models. Catena 64 (2–3), 247–271.

Aksoy, H., Gedikli, A., Yilmaz, M., Eris, E., Unal, N.E., Yoon, J., Kavvas, M.L., Tayfur, G., 2020. Soil erosion model tested on experimental data of a laboratory flume with a pre-existing rill. J. Hydrol. 581, 124391.

Alewell, C., Borrelli, P., Meusburger, K., Panagos, P., 2019. Using the USLE: chances, challenges and limitations of soil erosion modelling. Int. Soil Water Conserv. Res. 7 (3), 203–225.

Auerswald, K., 1992. Verfeinerte Bewertung von Erosionsschutzmaßnahmen unter deutschen Anbaubedingungen mit dem P-Faktor der allgemeinen Bodenabtragsgleichung (ABAG). Z Kulturtech Landentwicklung 33, 137–144.

Auerswald, K., Fiener, P., Dikau, R., 2009. Rates of sheet and rill erosion in Germany—a meta-analysis. Geomorphology 111 (3–4), 182–193.

Bagarello, V., Di Stefano, C., Ferro, V., Pampalone, V., 2017. Predicting maximum annual values of event soil loss by USLE-type models. Catena 155, 10–19.

Baggaley, N., Potts, J., 2017. Input factors that should be considered when running a regional soil erosion model at a catchment scale - an application in Scotland. Geoderma Reg. 11, 104–112.

Batista, P.V., Davies, J., Silva, M., Quinton, J.N., 2019. On the evaluation of soil erosion models: are we doing enough? Earth Sci. Rev. 197 https://doi.org/10.1016/j.earscirev.2019.102898.

Bernet, D.B., Zischg, A., Prasuhn, V., Weingartner, R., 2018. Modeling the extent of surface water floods in rural areas: lessons learned from the application of various uncalibrated models. Environ. Model Softw. 109, 134–151.
Bircher, P., Liniger, H.P., Prasuhn, V., 2019a. Comparing different multiple flow algorithms to calculate RUSLE factors of slope length (L) and slope steepness (S) in Switzerland. Geomorphology 346, 106850. https://doi.org/10.1016/j.geomorph.2019.106850.
Bircher, P., Liniger, H.P., Prasuhn, V., 2019b. Aktualisierung und Optimierung der Erosionsrisikokarte (ERK2): Die neue ERK2 (2019) für das Ackerland der Schweiz: Schlussbericht. Bundesamt für Landwirtschaft, Bern.
Boardman, J., 2006. Soil erosion science: reflections on the limitations of current approaches. Catena 68 (2–3), 73–86.
Boardman, J., Evans, R., 2019. The measurement, estimation and monitoring of soil erosion by runoff at the field scale: Challenges and possibilities with particular reference to Britain. Prog. Phys. Geogr. Earth and Environ. 44 (1) https://doi.org/10.1177/0309133319861833.
Boix-Fayos, C., Martínez-Mena, M., Arnau-Rosalén, E., Calvo-Cases, A., Castillo, V., Albaladejo, J., 2006. Measuring soil erosion by field plots: understanding the sources of variation. Earth Sci. Rev. 78 (3–4), 267–285.
Borrelli, P., Meusburger, K., Ballabio, C., Panagos, P., Alewell, C., 2018. Object-oriented soil erosion modelling: a possible paradigm shift from potential to actual risk assessments in agricultural environments. Land Degrad. Dev. 29 (4), 1270–1281.
Botschek, J., Billen, N., Brandhuber, R., Bug, J., Deumlich, D., Duttmann, R., Elhaus, D., Mollenhauer, K., Prasuhn, V., Röder, C., Schäfer, W., Thiermann, A., Unterseher, E., Wurbs, D., 2021. Bodenerosion durch Wasser – Kartieranleitung zur Erfassung aktueller Erosionsformen. DWA-Regelwerk, Merkblatt DWA-M 921, Deutsche Vereinigung für Wasserwirtschaft, Abwasser und Abfall, Hennef, 112 S.
Casalí, J., Loizu, J., Campo, M.A., De Santisteban, L.M., Álvarez-Mozos, J., 2006. Accuracy of methods for field assessment of rill and ephemeral gully erosion. Catena 67, 128–138.
Cerdan, O., Poesen, J., Govers, G., Saby, N., Le Bissonnais, Y., Gobin, A., Vacca, A., Quinton, J., Auerswald, K., Klik, A., Kwaad, F.J.P.M., Roxo, M.J., 2006. Sheet and rill erosion. In: Boardman, J., Poesen, J. (Eds.), Soil Erosion in Europe. Wiley, pp. 501–513. https://doi.org/10.1002/0470859202.ch38.
Covelli, C., Cimorelli, L., Pagliuca, D.N., Molino, B., Pianese, D., 2020. Assessment of erosion in river basins: a distributed model to estimate the sediment production over watersheds by a 3-dimensional LS factor in RUSLE model. Hydrology 7 (1), 13. https://doi.org/10.3390/hydrology7010013.
Desmet, P.J.J., Govers, G., 1996. A GIS procedure for automatically calculating the USLE LS factor on topographically complex landscape units. J. Soil Water Conserv. 51 (5), 427–433.
Di Stefano, C., Ferro, V., Pampalone, V., 2017. Applying the USLE family of models at the Sparacia (South Italy) experimental site. Land Degrad. Dev. 28 (3), 994–1004.
DIN 19708, 2017. Bodenbeschaffenheit - Ermittlung der Erosionsgefährdung von Böden durch Wasser mit Hilfe der ABAG, 2nd ed. Deutsches Institut für Normung e.V, Beuth, Berlin. 26 pp.
Evans, R., 2017. Factors controlling soil erosion and runoff and their impacts in the upper Wissey catchment, Norfolk, England: a ten year monitoring programme. Earth Surf. Process. Landf. 42 (14), 2266–2279.
Evans, R., Boardman, J., 2016a. The new assessment of soil loss by water erosion in Europe. Panagos P. et al., 2015. Environ. Sci. Policy 54, 438-447 - a response. Environ. Sci. Pol. 58, 11–15.
Evans, R., Boardman, J., 2016b. A reply to Panagos et al., 2016 Environ. Sci. Policy 59, 53-57. Environ. Sci. Pol. 60, 63–68.
Evans, R., Brazier, R., 2005. Evaluation of modelled spatially distributed predictions of soil erosion by water versus field-based assessments. Environ. Sci. Pol. 8, 493–501.
Evans, R., Collins, A.L., Zhang, Y., Foster, I.D., Boardman, J., Sint, H., Griffith, B.A., 2017. A comparison of conventional and 137Cs-based estimates of soil erosion rates on arable and grassland across lowland England and Wales. Earth Sci. Rev. 173, 49–64.
Favis-Mortlock, D., 1998. Validation of field-scale soil erosion models using common datasets. In: Boardman, J., Favis-Mortlock, D. (Eds.), Modelling Soil Erosion by Water. Springer, Berlin, Heidelberg, pp. 89–127.
Fernández, C., Vega, J.A., Vieira, D.C.S., 2010. Assessing soil erosion after fire and rehabilitation treatments in NW Spain: performance of RUSLE and revised Morgan–Morgan–Finney models. Land Degrad. Dev. 21 (1), 58–67.
Fiener, P., Auerswald, K., 2016. Comment on“ the new assessment of soil loss by water erosion in Europe” by Panagos et al., 2015. Environ. Sci. Policy 54, 438-447. Environ. Sci. Pol. 57, 140–142.
Fiener, P., Wilken, F., Auerswald, K., 2019. Filling the gap between plot and landscape scale - eight years of soil erosion monitoring in 14 adjacent watersheds under soil conservation at Scheyern, Southern Germany. Adv. Geosci. 48, 31–48.
Fiener, P., Dostál, T., Krása, J., Schmaltz, E., Strauss, P., Wilken, F., 2020. Operational USLE-based modelling of soil erosion in Czech Republic, Austria, and Bavaria - differences in model adaptation, parametrization, and data availability. Appl. Sci. 10 (10), 3647.
Fischer, F., Kistler, M., Brandhuber, R., Maier, H., Treisch, M., Auerswald, K., 2017. Validation of official erosion modelling based on high-resolution radar rain data by aerial photo erosion classification. Earth Surf. Process. Landf. 43 (1), 187–194.
Franzluebbers, A.J., Hons, F.M., Zuberer, D.A., 1995. Tillage-induced seasonal changes in soil physical properties affecting soil CO2 evolution under intensive cropping. Soil Tillage Res. 34, 41–60.
Freeman, T.G., 1991. Calculating catchment area with divergent flow based on a regular grid. Comput. Geosci. 17 (3), 413–422.
Gobin, A., Jones, R., Kirkby, M., Campling, P., Govers, G., Kosmas, C., Gentile, A.R., 2004. Indicators for pan-European assessment and monitoring of soil erosion by water. Environ. Sci. Pol. 7 (1), 25–38.
Guo, Q., Hao, Y., Liu, B., 2015. Rates of soil erosion in China: a study based on runoff plot data. Catena 124, 68–76. https://doi.org/10.1016/j.catena.2014.08.013.
Herweg, K., 1996. Field Manual for Assessment of Current Erosion Damage. SCRP Ethiopia, and Centre for Development and Environment. University of Berne, Berne.
Jetten, V., Govers, G., Hessel, R., 2003. Erosion models: quality of spatial predictions. Hydrol. Process. 17, 887–900. https://doi.org/10.1002/hyp.1168.
Kinnell, P.I.A., 2010. Event soil loss, runoff and the universal soil loss equation family of models: a review. J. Hydrol. 385 (1–4), 384–397.
Kotremba, C., Trapp, M., Thomas, K., 2016. Hochauflösende GIS-basierte Bodenabtragsmodellierungen für ausgewählte Agrarstandorte in Rheinland-Pfalz. Bodenschutz 21, 46–56.
Ledermann, T., Herweg G., K., Liniger P., H., Schneider, F., Hurni, H., Prasuhn, V., 2008. Erosion Damage Mapping: Assessing Current Soil Erosion Damage in Switzerland. The soils of tomorrow. Advances in Geoecology, 39. Catena, pp. 263–283.
Ledermann, T., Herweg, K., Liniger, H.P., Schneider, F., Hurni, H., Prasuhn, V., 2010. Applying erosion damage mapping to assess and quantify off-site effects of soil erosion in Switzerland. Land Degrad. Dev. 21 (4), 353–366.
Leser, H., Meier-Zielinski, S., Prasuhn, V., Seiberth, C., 2002. Soil erosion in catchment areas of Northwestern Switzerland. Methodological conclusions from a 25-year research programme. Z Geomorphol. N F 46, 35–60.
Merritt, W.S., Letcher, R.A., Jakeman, A.J., 2003. A review of erosion and sediment transport models. Environ. Model Softw. 18 (8–9), 761–799.
Mosimann, T., Rüttimann, M., 2006. Dokumentation – Berechnungsgrundlagen zum Frucht-folgefaktor zentrales Mittelland 2005 im Modell Erosion CH (Version V2.02). Terragon, Bubendorf, 30 S.
Mosimann, T., Crole-Rees, A., Maillard, A., Neyroud, J.-A., Thöni, M., Musy, A., Rohr, W., 1990. Bodenerosion im Schweizerischen Mittelland: Ausmass und Gegenmassnahmen. NFP-Bericht, Nr. 51, Liebefeld, Bern, Schweiz.
Napoli, M., Cecchi, S., Orlandini, S., Mugnai, G., Zanchi, C.A., 2016. Simulation of field-measured soil loss in Mediterranean hilly areas (chianti, Italy) with RUSLE. Catena 145, 246–256.
Nearing, M.A., 1998. Why soil erosion models over-predict small soil losses and under-predict large soil losses. Catena 32 (1), 15–22.
Nearing, M.A., Lane, L.J., Lopes, V.L., 2017. Modeling soil erosion. In: Soil Erosion Research Methods. Routledge, pp. 127–158.
Ogermann, P., Hebel, B., Prasuhn, V., Weisshaidinger, R., 2006. Erfassung von Bodenerosion in der Schweiz: vergleichende Anwendung verschiedener Methoden und Beurteilung ihrer Eignung für den Vollzug der Bodenschutzgesetzgebung. Geogr. Helv. 61 (3), 209–217.
Onnen, N., Heckrath, G., Stevens, A., Olsen, P., Greve, M.B., Pullens, J.W., Kronvang, B., Van Oost, K., 2019. Distributed water erosion modelling at fine spatial resolution across Denmark. Geomorphology 342, 150–162.
Panagos, P., Borrelli, P., Poesen, J., Ballabio, C., Lugato, E., Meusburger, K., Montanarella, L., Alewell, C., 2015. The new assessment of soil loss by water erosion in Europe. Environ. Sci. Pol. 54, 438–447.
Panagos, P., Borrelli, P., Poesen, J., Meusburger, K., Ballabio, C., Lugato, E., Montanarella, L., Alewell, C., 2016a. Reply to the comment on “the new assessment of soil loss by water erosion in Europe” by Fiener & Auerswald. Environ. Sci. Pol. 57, 143–150.
Panagos, P., Borrelli, P., Poesen, J., Meusburger, K., Ballabio, C., Lugato, E., Montanarella, L., Alewell, C., 2016b. Reply to “the new assessment of soil loss by water erosion in Europe. Panagos P. et al., 2015. Environ. Sci. Policy 54, 438-447. A response” by Evans and Boardman [environ. Sci. Policy 58, 11-15]. Environ. Sci. Pol. 59, 53–57.
Pandey, A., Himanshu, S.K., Mishra, S.K., Singh, V.P., 2016. Physically based soil erosion and sediment yield models revisited. Catena 147, 595–620.
Parsons, A.J., 2019. How reliable are our methods for estimating soil erosion by water? Sci. Total Environ. 676, 215–221.
Poesen, J.W., Boardman, J., Wilcox, B., Valentin, C., 1996. Water erosion monitoring and experimentation for global change studies. J. Soil Water Conserv. 51 (5), 386–390.
Prasuhn, V., 2011. Soil erosion in the Swiss midlands: results of a 10-year field survey. Geomorphology 126 (1–2), 32–41.
Prasuhn, V., 2012. On-farm effects of tillage and crops on soil erosion measured over 10 years in Switzerland. Soil Tillage Res. 120, 137–146.
Prasuhn, V., 2020. Twenty years of soil erosion on-farm measurement: annual variation, spatial distribution and the impact of conservation programmes for soil loss rates in Switzerland. Earth Surf. Process. Landf. 45 (7), 1539–1554. https://doi.org/10.1002/esp.4829.
Prasuhn, V., 2022. Experience with the assessment of the USLE cover-management factor for arable land compared with long-term measured soil loss in the Swiss Plateau. Soil Tillage Res. 215 https://doi.org/10.1016/j.still.2021.105199.
Prasuhn, V., Grünig, K., 2001. Evaluation der Ökomassnahmen – Phosphorbelastung der Oberflächengewässer durch Bodenerosion. Schriftenreihe der FAL Nr. 37, Zürich-Reckenholz, 152pp.
Prasuhn, V., Liniger, H.P., Hurni, H., Friedli, S., 2007. Bodenerosions-Gefährdungskarte der Schweiz. Agrarforschung 14 (3), 120–127.
Prasuhn, V., Liniger, H.P., Gisler, S., Herweg, K., Candinas, A., Clément, J.P., 2013. A high-resolution soil erosion risk map of Switzerland as strategic policy support system. Land Use Policy 32, 281–291.
Qin, W., Guo, Q., Cao, W., Yin, Z., Yan, Q., Shan, Z., Zheng, F., 2018. A new RUSLE slope length factor and its application to soil erosion assessment in a Loess Plateau watershed. Soil Tillage Res. 182, 10–24.

Rapp, J.F., 1994. Error Assessment of the Revised Universal Soil Loss Equation Using Natural Runoff Plot Data. Unpublished M.S. Thesis. University of Arizona, Tucson, Arizona, 90 pp.
Renard, K.G., Foster, G.R., Weesies, G.A., McCool, D.K., Yoder, D.C., 1997. Predicting Soil Erosion by Water, a Guide for Conservation Planning with the Revised Universal Soil Loss Equation (RUSLE). Agriculture Handbook, 703. USDA. ARS, Washington, DC.
Risse, L.M., Nearing, M.A., Laflen, J.M., Nicks, A.D., 1993. Error assessment in the universal soil loss equation. Soil Sci. Soc. Am. J. 57 (3), 825–833.
Rohr, W., Mosimann, T., Bono, R., Rüttimann, M., Prasuhn, V., 1990. Kartieranleitung zur Aufnahme von Bodenerosionsformen und -schäden auf Ackerflächen. Legende, Erläuterungen zur Kartiertechnik, Schadensdokumentation und Fehlerabschätzung. Materialien zur Physiogeographie, Heft 14, Basel, Schweiz.
Rüttimann, M., Prasuhn, V., 1990. Möglichkeiten der Fehlerabschätzung und Optimierung der Erosionsschadenskartierung. - Materialien z. Physiogeographie 14. Basel 41–49.
Rüttimann, M., Schaub, D., Prasuhn, V., Rüegg, W., 1995. Measurement of runoff and soil erosion on regularly cultivated fields in Switzerland - some critical considerations. Catena 25 (1–4), 127–139.
Rymszewicz, A., Mockler, E., O'Sullivan, J., Bruen, M., Turner, J., Conroy, E., Kelly-Quinn, M., Harrington, J., Lawler, D., 2015. Assessing the applicability of the revised universal soil loss equation (RUSLE) to Irish catchments. Proc. Intern. Assoc. Hydrol. Sci. 99–105.
Saggau, P., Kuhwald, M., Duttmann, R., 2019. Integrating soil compaction impacts of tramlines into soil erosion modelling: a field-scale approach. Soil Syst. 3 (3), 51.
Schaub, D., Prasuhn, V., 1993. The role of test plot measurements in a long-term soil erosion research project in Switzerland. In: Wicherek (Ed.), Farm Land erosion in Temperate Plains Environment and Hills. Elsevier Science Publishers B. V, pp. 111–123.
Schaub, D., Prasuhn, V., 1998. A map on soil erosion on arable land as a planning tool for sustainable land use in Switzerland. Adv. GeoEcol. 31, 161–168.
Schäuble, H., 2005. AVErosion 1.0 für ArcView 3.x. Analyse der Bodenerosion nach den Modellen USLE und MUSLE87. Erweiterung für ArcView 3.x und den Spatial Analyst 1.x. https://www.terracs.com/infosysteme/gis-software/averosion/.
Schmidt, S., Alewell, C., Panagos, P., Meusburger, K., 2016. Regionalization of monthly rainfall erosivity patterns in Switzerland. Hydrol. Earth Syst. Sci. 20 (10), 4359–4373.
Schweizer Bundesrat, 1998. Verordnung über Belastungen des Bodens (VBBo). SR 814.12. https://www.fedlex.admin.ch/eli/cc/1998/1854_1854_1854/de.
Schwertmann, U., Vogl, W., Kainz, M., 1990. Soil erosion by Water. Verlag Eugen Ulmer, Stuttgart (in German).
Seibert, J., McGlynn, B.L., 2007. A new triangular multiple flow direction algorithm for computing upslope areas from gridded digital elevation models. Water Resour. Res. 43 (4).
Steinhoff-Knopp, B., Burkhard, B., 2018. Mapping control of erosion rates: comparing model and monitoring data for croplands in northern Germany. One Ecosyst. 3, e26382 https://doi.org/10.3897/oneeco.3.e26382.
Swerts, M., Deproost, P., Oorts, K., Buyle, S., Vandekerckhove, L., 2019. 15 years of experience with the use of detailed erosion maps in soil erosion policy in Flanders, Belgium. In: Global Symposium on Soil Erosion (GSER19), 15–17 May 2019 at FAO, Working Documents, pp. 502–506.
Swisstopo, 2015. swissALTI 3D Ausgabebericht 2015. Bundesamt für Landestopografie Swisstopo, Wabern (2015).
van oost kristof, Govers, G., Cerdan, O., Thauré, D., Van Rompaey, A., Steegen, A., Nachtergaele, J., Takken, I., Poesen, J., 2005. Spatially distributed data for erosion model calibration and validation: the Ganspoel and Kinderveld datasets. Catena 61 (2–3), 105–121.
Wainwright, J., Mulligan, M., 2013. Environmental Modelling: Finding Simplicity in Complexity, Second edition. https://doi.org/10.1002/9781118351475.
Winchell, M.F., Jackson, S.H., Wadley, A.M., Srinivasan, R., 2008. Extension and validation of a geographic information system-based method for calculating the revised universal soil loss equation length-slope factor for erosion risk assessments in large water- sheds. J. Soil Water Conserv. 63, 105–111.
Wischmeier, W.H., Smith, D.D., 1978. Predicting Rainfall Erosion Losses - A Guide to Conservation Planning, Agriculture Handbook No. 537. USDA/Science and Education.

Paper 3. Tools for USLE-CP-factor calculation and actual erosion risk on field block level for Switzerland

Authors:
Bircher Pascal, Liniger Hanspeter, Kupferschmied Patrick and Prasuhn Volker

Originally published in: MethodsX, 2021, 8, 101569

Boris-Link: https://boris.unibe.ch/160762/

MethodsX 8 (2021) 101569

Contents lists available at ScienceDirect

MethodsX

journal homepage: www.elsevier.com/locate/mex

Method Article

Tools for USLE-CP-factor calculation and actual erosion risk on field block level for Switzerland

P. Bircher[a,b,*], H.P. Liniger[a,b], P. Kupferschmied[b,c], V. Prasuhn[c]

[a] Centre for Development and Environment (CDE), University of Bern, Mittelstrasse 43, 3012 Bern, Switzerland
[b] Institute of Geography (GIUB), University of Bern, Hallerstrasse 12, 3012 Bern, Switzerland
[c] Agroscope, Agroecology and Environment, Reckenholzstrasse 191, 8046 Zurich, Switzerland

A B S T R A C T

The calculation of the cover management factor (C-factor) and support practices factor (P-factor) is an important element in the Universal Soil Loss Equation (USLE). In Switzerland, a potential soil erosion risk map of arable land and a field block map that represents the basis of the agriculturally used areas in the country are available. A CP-factor tool was developed adapted to Swiss agronomic and environmental conditions, which allows to calculate CP-factors easily for various crop rotations and management practices. The calculated CP-factor values can be linked to any field block in the potential soil erosion risk map to determine the actual soil erosion risk for the field block. A plausibility check with other C-factor tools showed a sound match. This user-friendly calculation makes the CP-Tool and the actual erosion risk more accessible for authorities and GIS users. With Python and QGIS as open source resources, it is also possible to easily improve the tools. Linking the two tools provides substantial added value for education and training, advising farmers and policy, as well as scientific research, and can serve as a reference for other countries.

- USLE-CP-factor and actual erosion risk calculation on small scale field block level.
- Developed and programmed based on open source resources for further improvements.
- Both tools increase the knowledge of management practices for GIS- and non GIS users.

A R T I C L E I N F O
Method name: Calculation of USLE-CP-factor and actual erosion risk
Keywords: Soil erosion, USLE, C-factor, P-factor, CP-tool
Article history: Received 6 August 2021; Accepted 30 October 2021; Available online 6 November 2021

* Corresponding author at: Centre for Development and Environment (CDE), University of Bern, Mittelstrasse 43, 3012 Bern, Switzerland.
E-mail address: pascal.bircher@unibe.ch (P. Bircher).

https://doi.org/10.1016/j.mex.2021.101569

Specifications table

Subject Area:	Agricultural and Biological Science
More specific subject area:	Soil erosion modelling
Method name:	Calculation of USLE-CP-factor and actual erosion risk
Name and reference of original method:	Universal Soil Loss Equation (USLE) Wischmeier W.H., Smith D.D., 1978. Predicting rainfall erosion losses – A guide to conservation planning. USDA Agriculture Handbook No. 537, U.S. Department of Agriculture (Hrsg.), Washington D.C. 58 p.
Resource availability:	Links available in Supplementary S1 and S2

Introduction

The Universal Soil Loss Equation (USLE) [26] and its successor, the Revised Universal Soil Loss Equation (RUSLE) [22], are the most widely used erosion models worldwide [7]. In this erosion model, the cover and management factor (C-factor) and the support practice factor (P-factor) are the two dynamic factors that a farmer can determine for himself through his management and modify in the short term. However, the detailed assessment of the C-factor in particular is very complex and time-consuming, as many interrelated factors have to be taken into account. Therefore, standard values are often used in the literature when C-factors for specific land use types (arable land, grassland, vineyards) [9] or crop-specific C-factors (cereals, maize, sugar beet, potatoes, oilseed rape) are in use [17]. In arable farming, however, C-factors should not be determined for specific crops but instead only for entire crop rotations, because the intercropping period between the two main crops is very important for soil loss rates and carry-over effects exist between preceding and succeeding crops. Furthermore, regionally adapted and up-to-date input data should be used, as socio-economic and natural conditions differ geographically and are subject to rapid change. Changes in crop rotations, farming methods, growing periods, crop development and seasonal distribution of erosive rainfall modify the erosion potential of a given crop [3].

Recently published articles about the USLE C-factor calculation include, for example, the forested regions of southern China [15] or remote sensing approaches for tropical regions [1], and are therefore not comparable with the CP-Tool described in this paper due to climatic and crop conditions. In contrast, Brychta et al. [8] developed a similar C-factor-tool to ours for the Czech Republic in ArcGis, but they did not include the P-factor and used less detailed datasets. To our best knowledge, the only two tools that can be compared with CP-tool described in this paper are the program ErosionCH by Mosimann and Rüttimann [16] for Switzerland and the Excel application for C-factor calculation by the GIS-supported Erosion Control Management in Agriculture (EMiL) at the Chamber of Agriculture North Rhine Westfalia (NRW) in Germany [12]. The advantage of the present tool is that it contains more up-to-date basic data on crop calendars and rainfall erosivity, determines the C-factor as well as the P-factor and can be linked in the GIS with the potential erosion risk to illustrate the actual erosion risk. It allows to improve the potential risk map by calculating the actual erosion risk and to analyse hot spots of erosion and to identify impact of possible mitigation measures/scenarios to reduce erosion risks.

In this paper the application of the newly developed tools for calculating the actual erosion risk in Switzerland were explained. The first tool, the CP-Tool, allows the calculation of both the cover and management factor (C) and the support practices factor (P) from the USLE approach. With user input of the main and cover crops, soil management practices (ploughing, reduced tillage, mulch seeding, strip-till, no-till), direction of management and choice of location (low or hilly land), the CP-factor is calculated. This tool was programmed in the programming language Python. The second tool is a GIS application of calculated CP-factor, which enables the CP-Tool to be linked to the potential erosion risk map of Switzerland in order to obtain the actual erosion risk. It is designed as a QGIS model, but is also available as a Python script. By entering the previously calculated CP-factor, it allows the calculation of the actual erosion risk for a selected area, which is defined by the field block number. Both tools are available for download free of charge (see supplementary S1) and available for further development and application through the use of open source software. This paper describes the methodological framework and provides all the necessary input data.

Table 1
Used tools, programming languages and libraries. For detailed explanations/tools see download Links in supplementary S1.

Tool	language	Libraries/ Database system / other information	Operating System (OS)
C-Tool Prototype [14]	Python 3.5.x	PostGIS 2.4.4 under PostgreSQL 9.6.10 Psycopg2 2.7.3.2 pgAdmin 3 1.22.x	Developed on Ubuntu 16.04
CP-Tool [13]	Python 3.6.8	PyQt5 (5.10.1) SQLite3 (3.22.0) PyInstaller (3.4)	Developed on Ubuntu 18.04
Calculation of actual erosion risk with QGIS-model [6]	Python 3.7.x modelling Tool in QGIS 3.8	Available as Python (3.7) script and QGIS model (model3)	Developed on Fedora 30

Methods

The USLE model approach

The empirical USLE model uses six factors to calculate the actual erosion risk (A) in tonnes per hectare by multiplication (Eq.1). The factors are defined as follows. The LS-factor is the topography factor and takes into account the topographic conditions. The K-factor, the soil erodibility factor, integrates soil properties such as texture, humus content, aggregate stability and water permeability. The R-factor, the soil erosivity factor, reflects the precipitation characteristics and erosivity. In the C-factor, the land use and the type of management practices are represented. The P-factor is a protection factor that covers, for example, the tillage direction [26,22].

$$\text{USLE} - \text{approach } A = LS^{*}K^{*}R^{*}C^{*}P \quad (1)$$

The multiplication of the factors LSRK reveals the potential erosion risk, which is a rather static factor in the USLE equation. To show this potential erosion risk, a high-resolution map (2 m grid) was recently produced for Switzerland's arable land [5] and published in the official repository of Switzerland (potential erosion risk map: see supplementary S2). The potential erosion risk map of arable land of Switzerland (ERM2 2019) and the field block map of Switzerland form the basis for calculating the actual erosion risk. With the ERM2 2019, a calibrated and validated potential erosion risk map for arable land – based on long-term field assessments of soil loss rates from Prasuhn [19] - is available [4,5,6]. The LS-factor was based on a high-resolution digital elevation model of 2 metres [25] and calculated with a multiple flow direction algorithm [4]. The K-factor was derived from the soil property data of soil maps with different qualities [5]. The R-factor calculation was based on 10-min rainfall values over a 20-year period from 86 rain stations distributed throughout Switzerland and was interpolated with covariates (digital elevation model, altitudes of snow) [23]. The field blocks comprised an average size of 5 h and have been described by Bircher et al. [4] as follows: "*The agricultural area of Switzerland is represented in the field blocks and covers grassland, meadows, pastures, crop fields, and grapes. Field blocks were delineated by surrounding hydrological barriers like roads, railways, forests, villages, rivers, lakes, and other objects that prevent a continuous water flow. A field block can thus contain several cultivation plots, feature different types of use (arable land, permanent grassland, vineyards, or different field crops), and be cultivated by different farmers*."

The multiplication of the potential erosion risk with the C- and P-factors produces the actual erosion risk, which is specifically dependant on the crop and the management practices. The tools are designed to calculate the two land management dependant and variable factors, C and P, and reflect the actual erosion risk.

Used programming languages and tools

For programming the following tools and languages were used with various libraries implemented (Table 1).

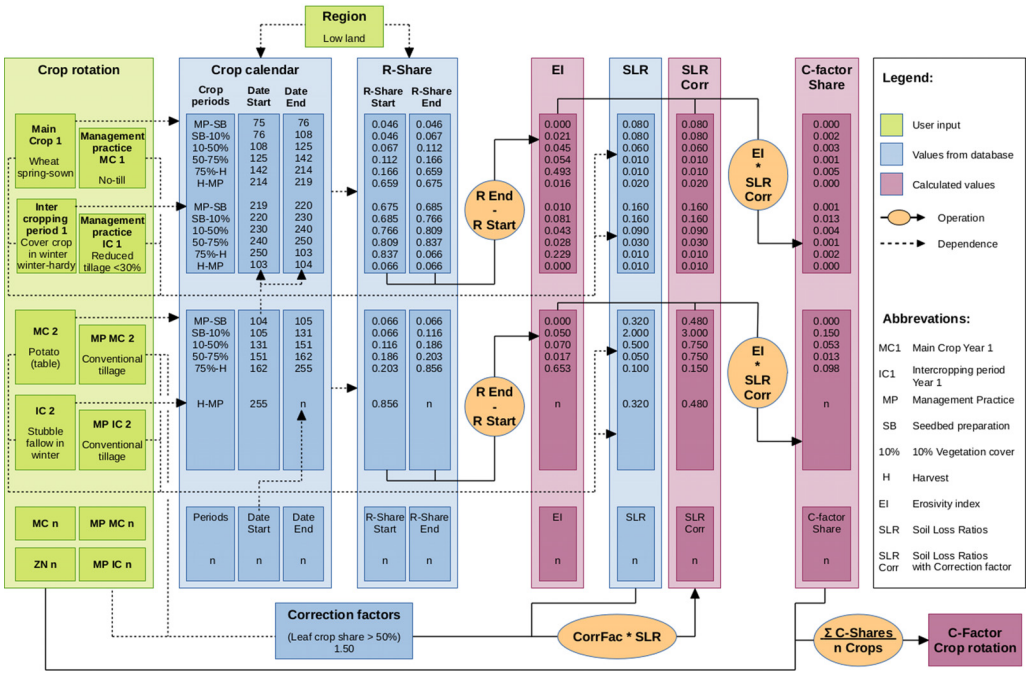

Fig. 1. Schema of calculation of the C-factor for a specific crop rotation. Crop calendar dates as Julian day calendar values. R-shares and C-shares per year are the shares within the crop stages. n acts as a place-holder for further crop sequences and their stages for following years.

- The C-Tool prototype was programmed by Kupferschmied [14] and finally released as the CP-factor tool on the Agroscope website (see supplementary S1).
- The application for calculating the CP-factor based on the new erosion risk map (ERM2 2019) by Bircher et al. [6] was released on the Agroscope website (see supplementary S1).

Study area

Switzerland's arable land is located in the low land and the hilly land. These regions are situated between the mountains of the Jura and the Alps covering a range from gentle to medium and hilly slopes. The arable land covers 408,000 ha. The main crops are winter wheat, temporary ley grass, winter barley, maize, sugar beet, oilseed rape and potatoes. There are about 50,000 farms, most of which are mixed farms with livestock and arable farming. The mean annual rainfall is 1105 mm in the low land and 1218 mm in the hilly land, the mean annual temperature is 9.3 °Celsius in the low land and 8.7 °Celsius in the hilly land. The soils were formed by glacial moraine and gravel soils, predominantly sandy-loamy to clayey-loamy cambisols and luvisols.

CP-Tool and calculation of CP-factor

The main focus of the CP-Tool is the calculation of the C-factor; this calculation is made by multiplying the factors C and P. In the CP-Tool, the user also needs to choose between the three options for management practice direction in order to define the P-factor. The calculation of the C-factor is quite complex; Fig. 1 shows a simplified concept. In the following section, this calculation approach is explained, with more detail about the individual steps of the calculation. The CP-Tool

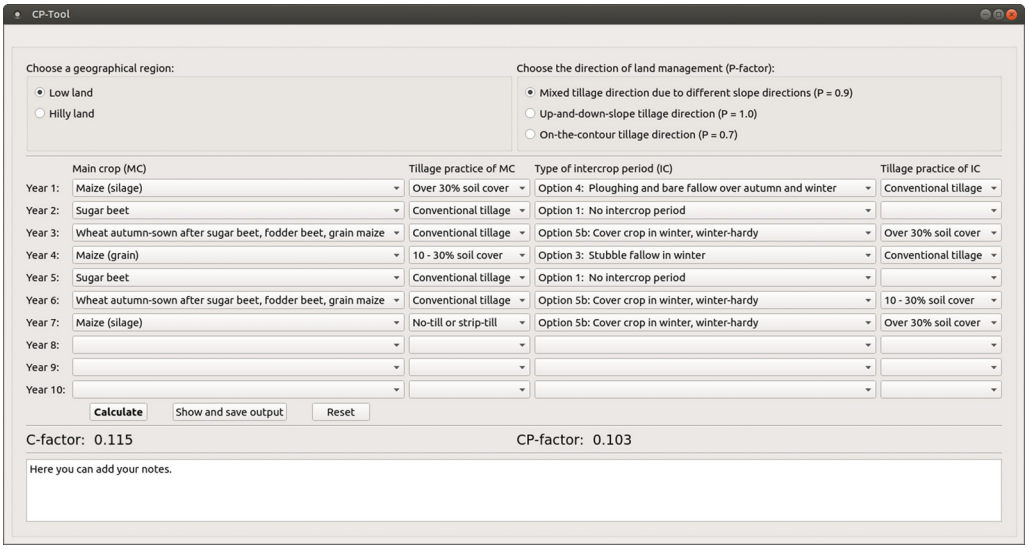

Fig. 2. User interface of the CP-factor tool. Example of a crop sequence of seven years with calculated C-factor and CP-factor values.

was written with Python 3.6.8; the user interface with PyQt5 can be run from the script or with an executable file created with PyInstaller for Windows and Linux Ubuntu (Fig. 2).

Input data and P-factor calculation

The P-factor is a non-dimensional factor between 0.1 (terracing) and 1 (up-and-down-slope tillage); for the application in Switzerland, it is restricted to the direction of soil management practices like tillage. Other structural measurements for preventing soil loss such as terrace systems are not included, because terracing is not relevant to arable farming in Switzerland.

For the P-factor, the tool allows three different options for the direction of tillage with predefined P-factor values. One option is up-and-down-slope tillage practice, which, according to the definition of Wischmeier and Smith (p. 34) [26], does not reduce soil loss and therefore accounts for a P-factor value of 1.0. Another option is a tillage practice exactly on the contour, which significantly reduces soil loss. Based on a methodological approach by Auerswald [2], which takes into account the slope gradient, the slope length and the proportion of potatoes with ridge cultivation in the crop rotation, Prasuhn and Grünig [20] found an average *P*-factor value of 0.73 for tillage practice on the contour in field research in Frienisberg, Switzerland. Based on that study, a P-factor value of 0.7 was used for this option. The third option is a tillage practice in between up-and-down-slope tillage and contour tillage, used when a field slopes in different directions. This option is the most commonly used in most cases due to the hilly relief in Switzerland. Prasuhn and Grünig [20] found some reduction in soil loss, and proposed a P-factor value of 0.9, which was used for this option. This coarse classification into three determined P-factor values entails some uncertainties. However, this assignment of the tillage direction of a plot is simple and easy to select by the farmer or an advisor. More complicated approaches with formulas that take into account the crucial factors such as slope steepness, slope length and ridge height of the tillage lanes impede a practical approach by farmers. In many other USLE-based studies, the P-factor is therefore generally omitted or set to 1.0 [9]. The present classification in three values is thus a clear improvement, even if it entails some uncertainties and inaccuracies.

Input data and C-factor calculation

The C-factor is defined as a non-dimensional number and range between zero (no crop cover) and one (best crop cover). The calculation of the C-factor is based on the method of Schwertmann et al. [24] which likewise is based on Wischmeier and Smith [26]. The methods for calculating C-factors are based on tabular approaches where the user reads the corresponding values for each variable (e.g. Erosivity Index, Soil Loss Ratios) from tables and manually calculates the C-factor. With the CP-Tool, this process is automated with a Python script. The challenge was that the logic of the tabular approach, with its many references between the variables, could not be directly converted to the technical linear logic of a simple Python script. Thus the calculation of the C-factor was revised to be programmable in Python.

To calculate the C-factor, several datasets for different variables were used (Figs. 1 and 2). Those variables were: (a) geographic region; (b) crop rotation or crop sequence, and crop calendar with crop stage periods for different regions; (c) intercropping period; (d) tillage practice of a given main crop and cover crop; (e) soil loss ratio values (SLR) for each crop, crop stage and tillage practice; (f) erosivity index (EI) for different regions; and (g) correction factors of carry-over-effects. All input data used had recently been prepared for the assessment of the agri-environmental indicator "soil erosion risk" [21].

The computed SLR values for each crop stage period were finally calculated automatically with the correction factors of the carry-over effects (see supplementary Table S14). With the corrected SLR values, the tool was able to calculate the C-factor-share of each crop stage period by multiplying the erosivity index (EI) and the corrected SLR value of the corresponding crop stage period. To calculate the C-factor of the whole crop rotation, the C-factor-shares were summed up and divided by the number of years of the crop rotation period. With this revised calculation of the C-factor, it was possible to write a Python script and automate the calculation.

Geographical region

For the geographical region, the tool offers two options: low land and hilly land. Arable land is rarely found in mountainous areas in Switzerland. The classification follows a map of the agricultural zone boundaries in Switzerland [11]. The subdivision is based on climatic condition, traffic of agricultural machinery and relief characteristics. The choice affects the crop-specific calendar dates (phenology) and the annual distribution of rainfall pattern, which are expressed in the erosivity index.

Crop rotation or crop sequence and crop stage periods

The specification of the crop rotation for each year consists of an input for the main crop and its management practice, as well as the land use of the intercropping period and its management practice. The CP-Tool allows for crop rotations of up to ten years; a minimum length of three years is needed for a reliable output. The tool offers 55 choices for main arable crops. Vegetables could not be considered. In the first step, the program creates the crop calendar according to the user input for the crop rotation. Each main crop and cover crop has individual calendar dates for the following six crop stages based on Wischmeier and Smith (1978) [26]:

- Initial tillage operation to final seedbed preparation;
- Seeding/planting to 10% soil cover;
- 10% to 50% soil cover;
- 50% to 75% soil cover;
- 75% soil cover to harvest;
- Harvest to mouldboard ploughing or sowing of the successive crop.

The crop calendar data for all main crops are given in Table S1 for low land and Table S2 for hilly land in supplementary. The crop calendar data are based on information from Swiss agri-environmental monitoring, where data on the time of sowing and harvesting of all crops is available for fields from around 300 typical farms in Switzerland over many years [21]. From these data, the other crop stage periods were derived. The resulting crop calendars were then submitted for review to various agronomic experts with a broad knowledge of crop management and finalised.

Inter-cropping period

For the time between two main crops, several options are available including no intercropping period, different kinds and lengths of fallows, cover crops and temporary grassland. In total, the tool offers nine options for the intercropping period, with corresponding SLR values:

- Sowing of the subsequent main crop within a few days;
- Stubble fallow until sowing of a winter crop;
- Stubble fallow in winter;
- Ploughing and bare fallow over autumn and winter;
- Cover crop in winter, winter-killed;
- Cover crop in winter, winter-hardy;
- Cover crop in autumn followed by fallow land in winter;
- Temporary grassland, autumn-sown;
- Temporary grassland, spring-sown.

The calendar data for cover crops for low land are listed in Table S3, and the respective autumn cover crops in Table S4. The calendar data for cover crops for hilly land are listed in Table S5, and the respective autumn cover crops in Table S6 (see supplementary).

Tillage practices of a given crop and cover crop

There are four different tillage practices, according to Mosimann and Rüttimann (2006) [16] and Prasuhn (2012) [18], that can be selected for each main crop and each cover crop to calculate SLR values:

- Conventional tillage with mouldboard plough or ploughless tillage with $<$ 10% soil cover;
- Reduced tillage with 10 to 30% soil cover;
- Mulch seeding with $>$ 30% soil cover;
- No-till or strip-till.

Soil loss ratio (SLR)

The SLR indicates the ratio of the soil loss of a given crop during a given crop stage period to the soil loss of an identical area under the standard conditions of clean-tilled continuous fallow [26]. The SLR values of the different crops for the crop stage periods and tillage practices were taken from the literature by Mosimann and Rüttimann [16]. For crops with no values available in the literature, values were determined by analogy to similar crops. No data were available, except for a few crops that are very rarely cultivated in Switzerland and thus do not have a major impact on the soil loss rate. The similarity of the plants was assessed by the type of crop (e.g. winter spelt similar to winter triticale; winter oats similar to winter barley; spring rye similar to spring wheat; fodder beet similar to sugar beet) and the corresponding tillage practice. Only for potatoes were other, significantly higher SLR values used. These higher values were based on the runoff concentration effect of the potato ridges [10] and long-term field observations by Prasuhn [19]. For each main crop and cover crop, as well as for each crop tillage practice, separate SLR values for each of the six crop stage periods were stored in an sqlite-database and automatically accessed by the script (Table S9 to S12 in supplementary).

Erosivity index (EI)

From the 10 min precipitation data for various meteorological stations in the Swiss Plateau over a period of 20 years, the mean erosivity of the rainfall over the year was determined and presented as cumulative percentage values for each day of the year for the two selected regions based on data from Schmidt et al. [23] (Table S7 for low land, Table S8 for hilly land in supplementary). For each crop stage period, the amount of erosive rainfall occurring in that specific timeframe was calculated by accessing the R-factor data in the sqlite-database. This returned the erosivity index for each crop stage period.

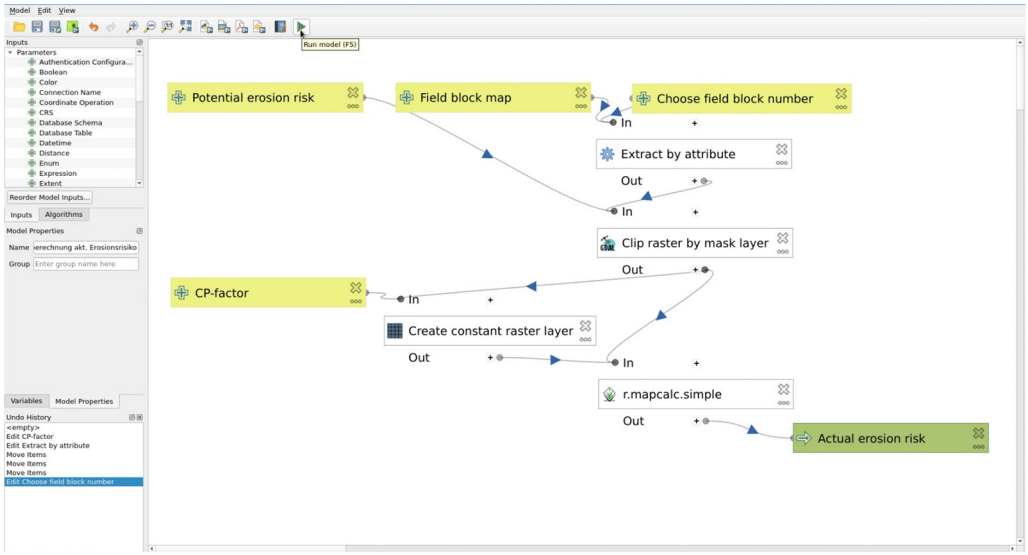

Fig. 3. QGIS-Model for calculating actual erosion risk on field block level based on field block with chosen number. r.mapcalc.simple = multiplication of constant raster layer (CP-factor) with raster (Potential erosion risk) clipped by masque layer. "In" represents essential data for the tool (e.g. Extract by attribute) to run. "Out" represents the result of the tool (e.g. Extract by attribute). Added blue arrows represent the process direction.

Carry-over effects

Depending on the crop rotation, three different carry-over effects based on the work of Wischmeier and Smith [26] and Schwertmann et al. [24] require a correction of the SLRs. These carry-over effects take into account the positive or negative effects of the preceding crop on the succeeding crops in the selected crop sequence (Tables S13 and S14 in supplementary). A high proportion of leaf crops such as sugar beet, potatoes or maize in the crop rotation leads to a stronger soil structure stress, which generally increases the risk of erosion. Cereals or oilseed rape sowing following root crops such as potatoes or late harvested sugar beets create an increased erosion risk because of the intense soil compaction during the harvest of these root crops. The residual effects of incorporated sod from temporary grassland increase aggregate stability and soil organic matter and reduce the erosion risk for the subsequent crop in the first and second year [26]. These correction factors can occur simultaneously and cumulatively.

- SLR increases if the leaf crop rate in the crop sequence is > 50%;
- SLR increases for cereals and oilseed rape after root crops;
- SLR reduces for succeeding crops in the first and second year after one or more years of temporary grassland.

Calculation of actual erosion risk with QGIS-model

To combine the calculated CP-factor with the ERM2 2019 and calculate the actual erosion risk at the field block level, a QGIS-model (see supplementary S1 for the tools and S2 for the field block map and ERM2 2019) was developed. This model is also available as Python script. A manual on using the tool is available in German [6]. Fig. 3 represents the necessary data and tools in QGIS. The ID-number of the selected field block must be chosen; this is extracted from the ERM2 2019. In the next step, a raster layer is created using the CP-factor and multiplied with the previously extracted raster layer of the ERM2 2019 (Fig. 3). When the model is running, a user interface is open (Fig. 4) where inputs like CP-factor, field block number, field block map and erosion risk map can be chosen. An output

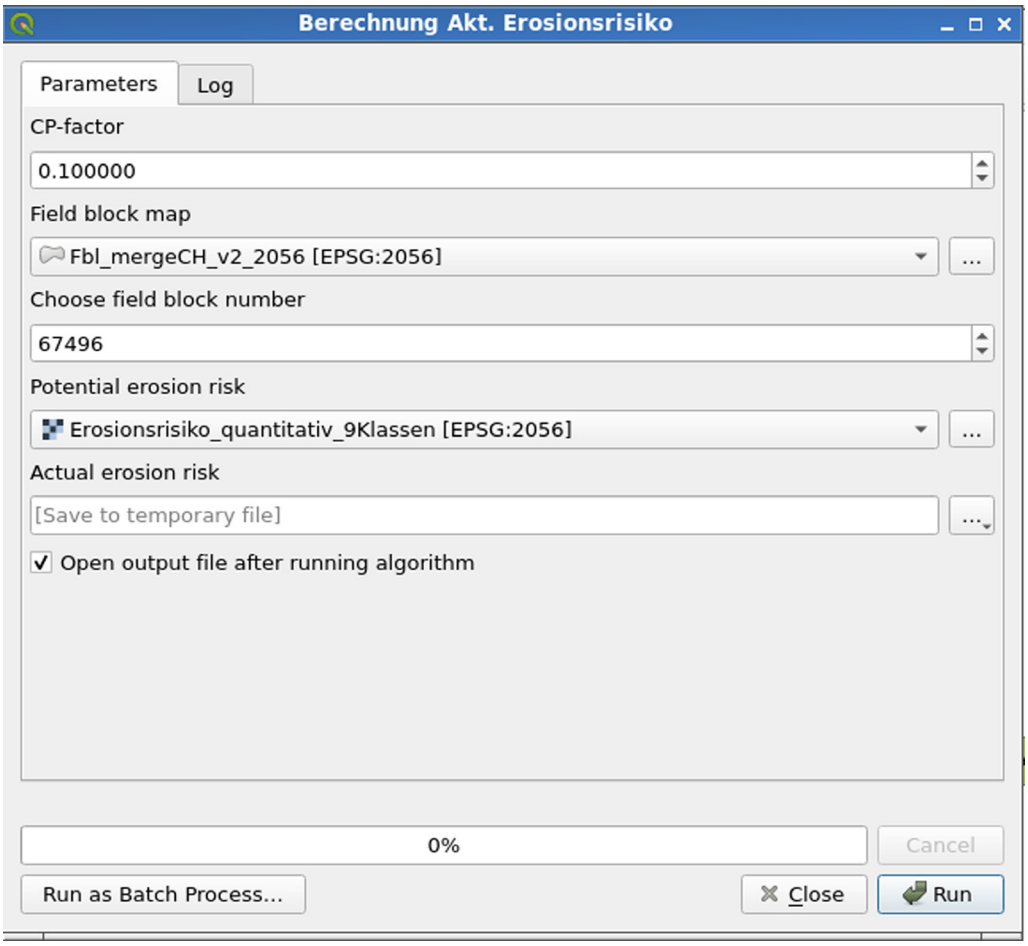

Fig. 4. User interface in QGIS. Example with standard CP-factor value 0.1 for the selected field block number 67′496.

directory also has to be chosen in order to save the result (actual erosion risk for chosen field block) (Fig. 4).

Linking of the two tools

The two tools can be linked together (Fig. 5) to calculate the actual erosion risk for a selected field block. Linking the two tools is a significant improvement, makes considerable progress in policy advice, implementation of erosion mitigation measures and training, and enhances the value of both tools tremendously.

Plausibility check of CP-Tool and example calculations

For the first step of plausibility check the developed CP-Tool, the effect of four different management practices (conventional tillage, reduced tillage, mulch tillage and no-till) on C-factor values based on the same crop sequence (Fig. 6) were calculated and compared with the results from the tools ErosionCH and EmiL. The three tools provided fairly similar C-factor values for the four tillage practices. However, EmiL was not able to distinguish between reduced tillage and

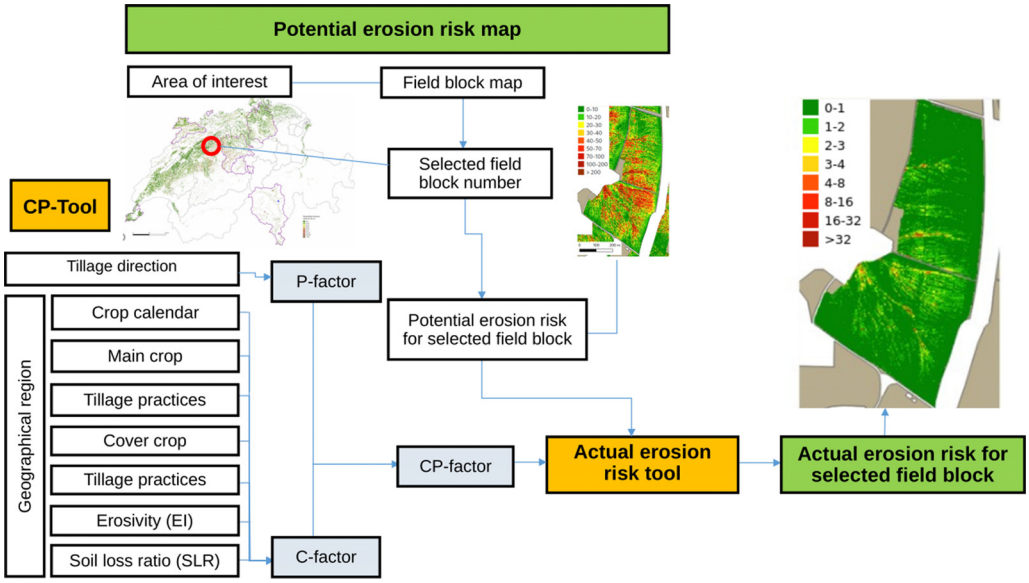

Fig. 5. Linking the CP-factor tool with the QGIS-model (Actual erosion risk tool) to calculate the actual erosion risk for a selected field block.

mulch seeding. The highest difference in calculated C-factors was 0.017 for reduced tillage between ErosionCH (0.050) and EmiL (0.033). For the other management practices with the same crop rotation, the differences were lower than 0.017 (Fig. 6). The used crop sequence is situated in supplementary S4.

For the second step, C-factor values were calculated for six typical Swiss crop sequences using the three tools (Fig. 7).The differences between the crop sequences 3–6 differed only by 0.013 in crop sequence 4 or less between the different tools. In contrast, the results for crop sequences 1 and 2 with the CP-Tool showed crop sequence 1 as 0.082 higher and crop sequence 2 as 0.061 higher than with ErosionCH, due to the much higher SLR values used for potatoes in the CP-Tool. However, the higher C-factor values in the CP-Tool for crop sequences with potatoes were calculated deliberately, as the highest soil losses in Switzerland were measured for potatoes. Using EmiL, the value of the C-factor was 0.196 for crop sequence 1, which lay between those of the CP-Tool (0.242) and ErosionCH (0.160). The used input data for the calculations of the six crop sequences are presented in supplementary S5.

Furthermore, two recent publications confirm the plausibility of the method used to calculate the C-factors. Auerswald et al. [27] have developed a calculation of summable C-factors for Germany and neighbouring countries. They conclude that the crop development used in our study is rather similar to the crop stage dates used in their study ($r^2 = 0.9755$) and that the SLRs used in our study are identical to those used in their study. Thus, the basic data we used for the calculation of the C-factor are comparable to those of Auerswald et al. [27]. Prasuhn [28] assessed the impact of mitigation measures on arable land by comparing modelled C-factor values with the tool from Mosimann and Rüttimann [16] and measured soil losses from field observations. The C-factor values were calculated in detail for 203 fields for five different periods (1987–89, 1997–99, 1997–2006, 2003–09, 2010–14) and compared with the measured soil loss rates of the same fields from the three periods 1987–89, 1997/98–2006/07, and 2007/08–2016/17. The mean annual soil loss decreased by over two-thirds from 0.74 t ha^{-1} yr^{-1} (1997/98–2006/07) to 0.20 t ha^{-1} yr^{-1} (2007/08–2016/17), while the mean C-factor values decreased by almost half from 0.094 (1997–99) to 0.050 (2010–14). The study of Prasuhn [28] demonstrated that with an in-depth calculation of C-factors over different periods, changes in average soil loss rates for a region can be satisfactorily represented.

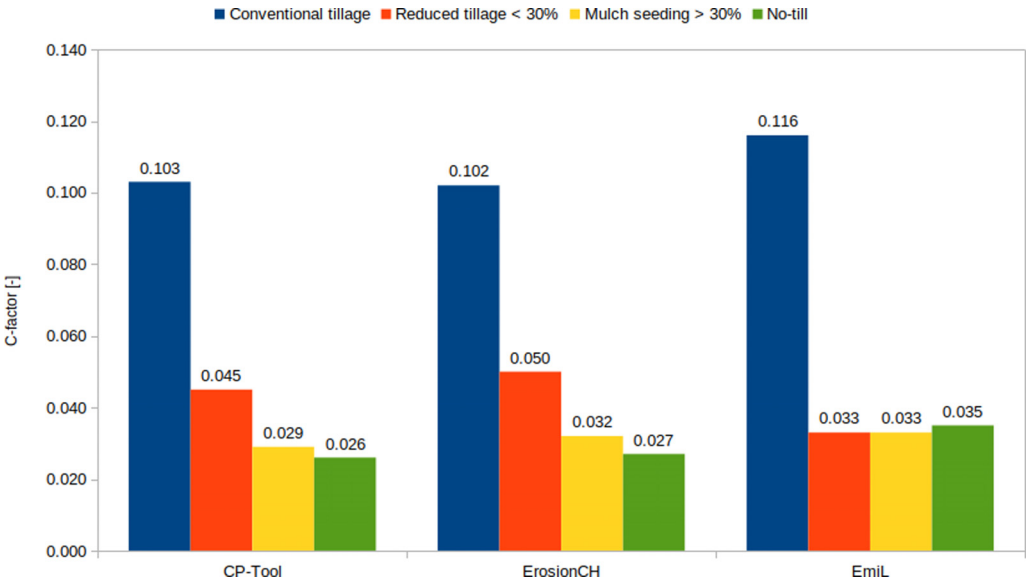

Fig. 6. Calculated C-factors according to the three different tools (CP-Tool, ErosionCH, EmiL) and four different management practices (conventional tillage, reduced tillage, mulch seeding, no-till) based on the same crop sequence. Crop sequence with 60% cereals and 40% leaf crops (see supplementary S4).

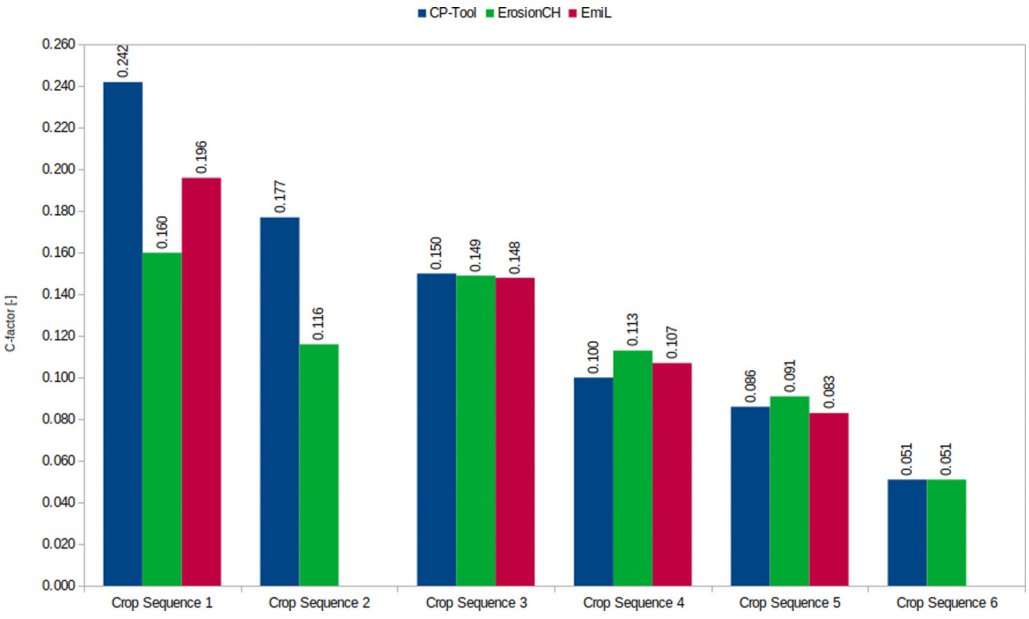

Fig. 7. Calculated C-factors according to the three different tools (CP-Tool, ErosionCH, EmiL) for six existing crop sequences, each over 10 years. EMiL does not include temporary grassland, which is why no values are available for crop sequences 2 and 6. Crop sequence 1 = crop sequence with 20% potatoes, 50% leaf crops, mouldboard ploughing; crop sequence 2 = crop sequence with 20% potatoes, 60% leaf crops, temporary grassland, partly conservation tillage; crop sequence 3 = crop sequence with 60% leaf crops, mouldboard ploughing; crop sequence 4 = crop sequence with 80% leaf crops, mostly conservation tillage; crop sequence 5 = crop sequence with 70% cereals; crop sequence 6 = crop sequence with 50% temporary grassland (see supplementary S5).

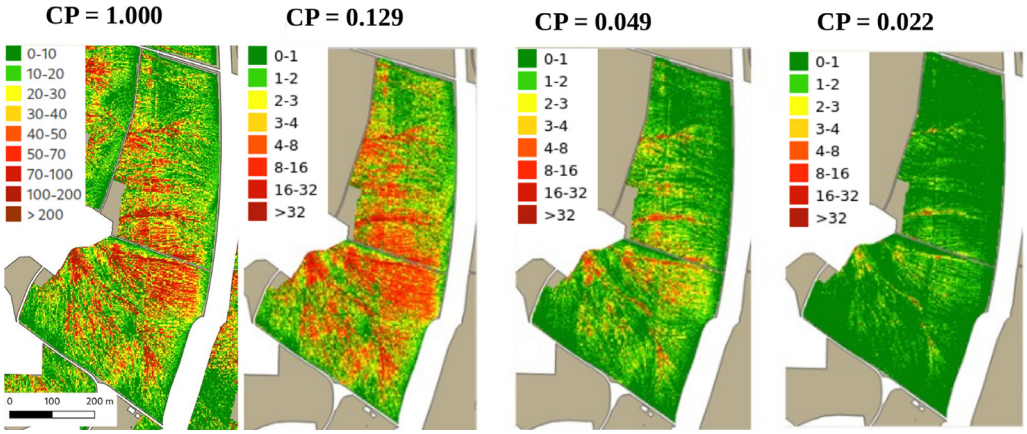

Fig. 8. Potential erosion risk from the soil erosion risk map ERM2 2019 (CP = 1.0) and example calculations with different CP-factors applied to a selected field block. Soil loss rates in t ha^{-1} $year^{-1}$. CP = 0.129 represents a crop rotation with ploughing; CP = 0.049 represents the same crop rotation with mulch seeding; CP = 0.022 represents an adapted crop rotation with no-till and temporary grassland in one year.

Nevertheless, a full validation of the USLE/RUSLE adapted for Swiss conditions could not be carried out so far. Some uncertainty in the results must therefore be expected. Thus, a verification in the field of the modelled erosion risk by an expert is recommended.

Fig. 8 illustrates the way the two tools can be used. The selected field block showed a very high potential erosion risk (CP = 1.000). Various small slope depressions generate concentrated runoff with a high erosion risk and soil loss values of > 50 t ha^{-1} $year^{-1}$. Linking the CP-factor in QGIS with the erosion risk map shows that the actual soil loss is high and frequently exceeds the tolerable soil loss of 2–4 t ha^{-1} $year^{-1}$ with reference to the Swiss legislation (yellow and red colours in Fig. 8). A standard crop rotation with mouldboard ploughing yields a CP-factor value of 0.129 as calculated with the CP-Tool. If the tillage of the whole crop rotation is changed to mulch seeding, the calculated CP-factor decreases significantly from 0.129 to 0.049. However, there are still many areas where the tolerable soil loss is exceeded. Only when tillage is changed to no-till and an additional year of temporary grassland integrated into the crop rotation is calculated soil loss reduced to a level where the risk of erosion is almost low. This example clearly demonstrates how the two tools can be used for planning best management practices; they can be used for the implementation of agricultural policy measures or for extension and training.

Conclusion

The new tools allows to calculate the CP-factor and combine the results with the potential erosion risk map in order to derive the actual erosion risk at field block level. This provides substantial added value and makes a significant improvement to policy advice, implementation of erosion mitigation measures and training. An attempt has been made to make these tools more user-friendly than existing methods and more easily accessible for GIS users and authorities. Furthermore, the program codes are also available on request as Python scripts, which allows and simplifies improvement and further development by programmers. The CP-factor-Tool is programmed under Swiss conditions. Application in other areas of the world (i.e. in other climate zones) is not advisable, since the tool integrates precipitation characteristics and crop development and management practices from Switzerland. However, the tool can provide a basis for adaptation to other agro-ecological and climatic conditions and further land management practices in other countries.

Both tools are available to farmers and extension services, and have been submitted to all cantonal agricultural agencies for testing and reviewing. Feedback will be gathered in the next years and

the tools will be adapted and improved if necessary. Furthermore, the modelled average soil loss predicted with the tools will be compared with the long-term measured soil loss rates in the test region Frienisberg on 203 arable fields [19].

Declaration of Competing Interest

The authors have whether financial nor other conflicts of interest to disclose.

Supplementary materials

Supplementary material associated with this article can be found, in the online version, at doi:10.1016/j.mex.2021.101569.

References

[1] A. Almagro, T.C. Thomé, C.B. Colman, R.B. Pereira, J.M. Junior, D.B.B. Rodrigues, P.T.S. Oliveira, Improving cover and management factor (C-factor) estimation using remote sensing approaches for tropical regions, Int. Soil Water Conserv. Res. 7 (4) (2019) 325–334.

[2]] K. Auerswald, Verfeinerte Bewertung von Erosionsschutzmaßnahmen unter deutschen Anbaubedingungen mit dem P-Faktor der Allgemeinen Bodenabtragsgleichung (ABAG), Z. Kulturtechnik Landentwicklung 33 (1992) 137–144.

[3] K. Auerswald, A. Menzel, Change in erosion potential of crops due to climate change, Agric. For. Meteorol. 300 (2021) 108338.

[4] P. Bircher, H.P. Liniger, V. Prasuhn, Comparing different multiple flow algorithms to calculate RUSLE factors of slope length (L) and slope steepness (S) in Switzerland, Geomorphology (2019) 346, doi:10.1016/j.geomorph.2019.106850.

[5] Bircher P., Liniger H.P., Prasuhn V., 2019b. Aktualisierung und Optimierung der Erosionsrisikokarte (ERK2). Die neue ERK2 (2019) für das Ackerland der Schweiz. Schlussbericht 2019. Agroscope, Zürich and University of Bern, Bern, 61 p. Available at: https://www.blw.admin.ch/dam/blw/de/dokumente/Nachhaltige%20Produktion/Umwelt/Boden/Erosionsrisikokarte%202019.pdf.download.pdf/Erosionsrisikokarte%202019.pdf.

[6] Bircher P., Liniger H.P., Prasuhn V., 2020. Berechnung des aktuellen Erosionsrisikos für das Ackerland einzelner Feldblöcke. Anwendung des CP-Faktors auf die neue potentielle Erosionsrisikokarte ERK2 (2019). Anleitung. Agroscope, Zürich and University of Bern, Bern, 17 p. Available at: https://www.agroscope.admin.ch/dam/agroscope/de/dokumente/themen/umwelt-ressourcen/boden-gewaesser-naehrstoffe/erosion/tool-aktriskanleitung.pdf.download.pdf/tool_aktriskAnleitung.pdf.

[7] P. Borrelli, C. Alewell, P. Alvarez, J.A.A. Anache, J. Baartman, C. Ballabio, N. Bezak, M. Biddoccu, A. Cerdà, D. Chalise, S. Chen. https://doi.org/10.31223/X5GS3T.

[8] J. Brychta, M. Janeček, A. Walmsley, Crop-management factor calculation using weights of spatial-temporal distribution of rainfall erosivity, Soil Water Res. 13 (2018) 150–160.

[9] T. Chen, R.Q. Niu, P.X. Li, L.P. Zhang, B. Du, Regional soil erosion risk mapping using RUSLE, GIS, and remote sensing: a case study in Miyun Watershed, North China, Environ. Earth Sci. 63 (3) (2011) 533–541.

[10] T.L. Chow, H.W. Rees, Effects of potato hilling on water runoff and soil erosion under simulated rainfall, Can. J. Soil Sci. 74 (4) (1994) 453–460.

[11] FOAG, 2020. Weisungen und Erläuterungen zur Verordnung über den landwirtschaftlichen Produktionskataster und die Ausscheidung von Zonen (Landwirtschaftliche Zonen-Verordnung; SR 912.1). Federal Office of Agriculture (FOAG). Available at: https://s.geo.admin.ch/6ee4f215a7

[12] D.A. Hiller, in: Bodenerosion durch Wasser – Ursachen, Bedeutung und Umgang in der Landwirtschaftlichen Praxis von NRW, Landwirtschaftskammer Nordrhein-Westfalen, Münster, 2007, pp. 1–37. https://www.landwirtschaftskammer.de/landwirtschaft/ackerbau/pdf/broschuere-bodenerosion.pdf.

[13] P. Kupferschmied, CP-Tool – Ein Programm zur Berechnung des Fruchtfolge- und Bewirtschaftungsfaktors (CP-Faktor) der Allgemeinen Bodenabtragsgleichung (ABAG). Anleitung zur Verwendung des CP-Tools, 20, Agroscope, Zürich and University of Bern, Bern, 2019.

[14] P. Kupferschmied, Konzeptionierung und Operationalisierung einer aktuellen und schweizweit verwendbaren Berechnungsweise des USLE C-Faktors. Schaffung der inhaltlichen und technischen Grundlagen zur individuellen Integration des C-Faktors in die Erosionsrisikokarte der Schweiz. Geographisches Institut. Abteilung Integrative Geographie, Universität Bern. Masterarbeit, 2018 Available athttps://www.agroscope.admin.ch/dam/agroscope/de/dokumente/themen/umwelt-ressourcen/boden-gewaesser-naehrstoffe/erosion/kupferschmied-2018-masterarbeit.pdf.download.pdf/Kupferschmied_2018_Masterarbeit.pdf .

[15] C. Li, L. Lin, Z. Hao, C.J. Post, Z. Chen, J. Liu, K. Yu, Developing a USLE cover and management factor (*C*) for forested regions of southern China, Front. Earth Sci. 14 (2020) 660–672.

[16] Mosimann T., Rüttimann M., 2006. Dokumentation – Berechnungsgrundlagen zum Fruchtfolgefaktor zentrales Mittelland 2005 im Modell Erosion CH (Version V2.02). Terragon, Bubendorf. 30 p.

[17] P. Panagos, P. Borrelli, K. Meusburger, C. Alewell, E. Lugato, L. Montanarella, Estimating the soil erosion cover-management factor at the European scale, Land Use Policy 48 (2015) 38–50.

[18] V. Prasuhn, On-farm effects of tillage and crops on soil erosion measured over 10 years in Switzerland, Soil Till. Res. 120 (2012) 137–146.

[19] V. Prasuhn, Twenty years of soil erosion on-farm measurement: annual variation, spatial distribution and the impact of conservation programmes for soil loss rates in Switzerland, Earth Surf. Process. Landf. 45 (2020) 1539–1554.

[20] V. Prasuhn, K. Grünig, Evaluation der Ökomassnahmen – Phosphorbelastung der Oberflächengewässer durch Bodenerosion, Schriftenreihe der FAL 37 (2001) 1–152 Zürich.
[21] V. Prasuhn, S. Blaser, Der Agrarumweltindikator «Erosionsrisiko», Bulletin BGS 39 (2018) 11–18.
[22] K.G. Renard, G.R. Foster, G.A. Weesies, D.K. McCool, D.C. Yoder, Predicting Soil Erosion by Water. A Guide to Conservation Planning with the Revised Universal Soil Loss Equation (RUSLE). Handbook, 703, US Department of Agriculture, 1997.
[23] S. Schmidt, C. Alewell, P. Panagos, K. Meusburger, Regionalization of monthly rainfall erosivity patterns in Switzerland, Hydrol. Earth Syst. Sci. 20 (2016) 4359–4373.
[24] U. Schwertmann, W. Vogl, M. Kainz, in: Bodenerosion durch Wasser – Vorhersage des Abtrags und Bewertung von Gegenmaßnahmen, Ulmer Verlag, Stuttgart, 1990, pp. 1–64.
[25] SwissALTI3D: swisstopo: edition 2015. Available at: https://www.swisstopo.admin.ch/en/geodata/height/alti3d.html
[26] W.H. Wischmeier, D.D. Smith, in: Predicting Rainfall Erosion Losses – A guide to Conservation planning. USDA Agriculture Handbook No. 537, U.S. Department of Agriculture, Washington D.C, 1978, pp. 1–58.
[27] K. Auerswald, F. Ebertseder, K. Levin, Y. Yuan, V. Prasuhn, N.O. Plambeck, A. Menzel, M. Kainz, Summable C factors for contemporary soil use, Soil Tillage Res. 213 (2021), doi:10.1016/j.still.2021.105155.
[28] V. Prasuhn, Experience with the assessment of the USLE cover-management factor for arable land compared with long-term measured soil loss in the Swiss Plateau, Soil Tillage Res. 215 (2022), doi:10.1016/j.still.2021.105199.

Paper 4. Upgrade and optimization of the erosion risk map (ERM2). The new ERM2 (2019) for the arable land of Switzerland. Final report. 2019

Aktualisierung und Optimierung der Erosionsrisikokarte (ERK2) Die neue ERK2 (2019) für das Ackerland der Schweiz. Schlussbericht. 2019

Authors:
Bircher Pascal, Liniger Hanspeter and Prasuhn Volker

Originally published on the Homepage of Federal Office for Agriculture (FOAG). 2019.

URL: https://www.blw.admin.ch/blw/de/home/nachhaltige-produktion/umwelt/boden.html

Boris-Link: https://boris.unibe.ch/132878/

Schweizerische Eidgenossenschaft
Confédération suisse
Confederazione Svizzera
Confederaziun svizra

Eidgenössisches Departement für
Wirtschaft, Bildung und Forschung WBF
Agroscope

UNIVERSITÄT
BERN

CDE
CENTRE FOR DEVELOPMENT
AND ENVIRONMENT

Aktualisierung und Optimierung der Erosionsrisikokarte (ERK2)
Die neue ERK2 (2019) für das Ackerland der Schweiz

Schlussbericht

2019

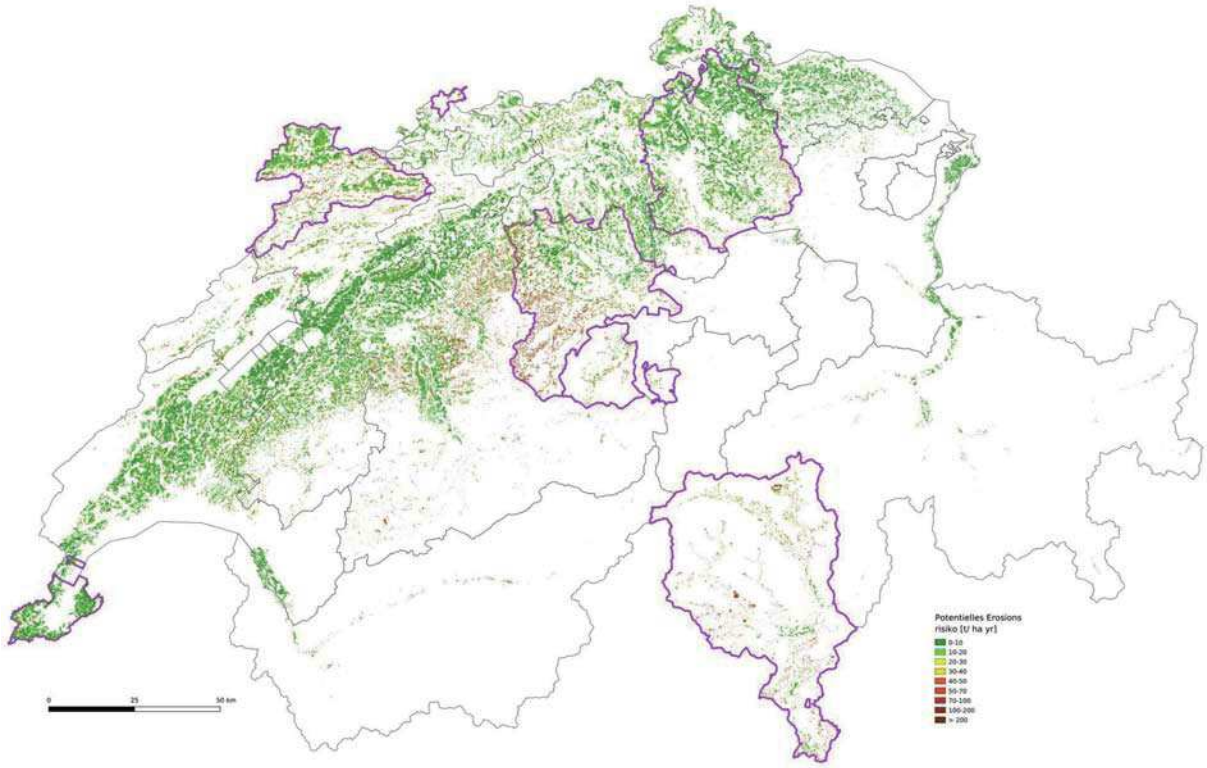

Pascal Bircher (CDE / Geographisches Institut, Universität Bern)
Hanspeter Liniger (CDE, Universität Bern)
Volker Prasuhn (Agroscope)

Auftraggeber: Bundesamt für Landwirtschaft (BLW)

Inhaltsverzeichnis

Zusammenfassung

Die neue Erosionsrisikokarte (ERK2 2019) der Schweiz basiert weiterhin auf der Revised Universal Soil Loss Equation (RUSLE), allerdings mit einem neuen Berechnungsalgorithmus und anderer Software. Die RUSLE ist ein empirisches Erosionsmodell und zeigt das mittlere langjährige Erosionsrisiko in Tonnen pro Hektare und Jahr. Sie erlaubt mit ihrem modularen Aufbau von sechs Faktoren Daten unterschiedlicher Qualität zu verbinden. Die ERK2 2019 verwendet hierzu vier der sechs erwähnten Faktoren, um das potentielle Erosionsrisiko ohne Bedeckungs- und Bearbeitungsfaktor sowie erosionsmindernde Massnahmen (C- und P-Faktor) darzustellen. Neu gegenüber der alten Erosionsrisikokarte (ERK2) sind folgende Punkte: A) Die neue Feldblockkarte basiert nun auf den neuen Daten des topographischen Landschaftsmodells (TLM3D; 2015; Version 1.3) von Swisstopo. B) Zur Berechnung des L-Faktors (Hanglänge bzw. Grösse des Einzugsgebietes) wurden verschiedene Multiple Flow Algorithmen auf der Grundlage des Höhenmodells SwissALTI3D im 2x2m-Raster ausführlich getestet und bewertet. Der Ansatz MTFD von Seibert & Glynn (2007) mit der Konvergenzeinstellung 1.1 wurde schliesslich ausgewählt. C) Die Berechnung des S-Faktors (Hangneigung) blieb weitgehend unverändert. D) Der neue LS-Faktor unterscheidet sich statistisch nicht markant von der bisherigen ERK2, basiert nun aber auf der Open Source Software SagaGis. E) Der K-Faktor (Bodenerodibilität) wurde methodisch gleich wie bei der bisherigen ERK2 umgesetzt, beinhaltet aber zusätzliche detaillierte kantonale Bodendaten. F) Die neue R-Faktor-Karte (Erosivität der Niederschläge) erreicht deutlich höhere Durchschnittswerte als der R-Faktor der bisherigen ERK2. Dies ist auf eine andere Methodik und eine bessere Datenlage zurückzuführen.

Das berechnete potentielle Erosionsrisiko wurde in der Region Frienisberg mit C- und P-Faktoren zum aktuellen Erosionsrisiko verrechnet und mit den 10-jährigen Erosionsschadenskartierungen in der Region Frienisberg verglichen. Das Erosionsmodell führte zu einer massiven Überschätzung des Bodenabtrages in der Grössenordnung von Faktor 5. Deshalb wurde das potentielle Erosionsrisiko entsprechend korrigiert und neu klassiert. Die neue, korrigierte ERK2 2019 unterscheidet sich daher deutlich von der alten ERK2 2010. Die neue ERK2 2019 kann durch diese Korrektur mit C- und P-Faktoren zum aktuellen Bodenabtrag verrechnet und zu den gesetzlichen Richtwerten für tolerierbaren Bodenabtrag in Bezug gesetzt werden.

Die Unterscheidung von Acker- und Dauergrünland – und damit eine ERK2 nur für das Ackerland (inklusive Kunstwiese) – konnte bisher nur für 19 Kantone, für die die entsprechenden parzellenscharfen digitalen Daten vorhanden waren, umgesetzt werden. Entsprechend liegt neu eine Karte des potentiellen Erosionsrisikos des Ackerlandes für diese 19 Kantone vor. Rund 75 % der Ackerfläche der Schweiz konnte dadurch parzellenscharf erfasst werden. Der längjährige mittlere potentielle Bodenabtrag dieser Flächen beträgt rund 17 t ha^{-1} a^{-1}. Für die restlichen sieben Kantone beruht die Unterscheidung von Ackerland und Dauergrünland unter anderem auf Satellitendaten (Fcover 300m, MODIS). Die Datenqualität ist hier deutlich schlechter. Zusätzlich zur Erosionsrisikokarte wird neu eine Karte der Fliesswege für Oberflächenabfluss auf der landwirtschaftlich genutzten Fläche basierend auf dem L-Faktor zur Verfügung gestellt.

Ein C-Faktor-Tool, welches die Bewirtschaftung (Fruchtfolge und Bodenbearbeitung) berücksichtigt, wurde neu entwickelt. Es ist als Alpha-Version auf einem virtuellen Rechner verfügbar. Eine Web-Applikation, die das neue C-Faktor-Tool mit der neuen ERK2 2019 verknüpfen soll, ist noch in Entwicklung.

Résumé

La nouvelle carte de risques d'érosion (CRE2 2019) de la Suisse se fonde toujours sur la Revised Universal Soil Loss Equation (RUSLE), mais avec un nouvel algorithme de calcul et un autre logiciel. La RUSLE est un modèle d'érosion empirique montrant le risque d'érosion moyen à long terme en t ha^{-1} a^{-1}. Elle permet de relier des données de différente qualité grâce à sa conception modulaire en six facteurs. La CRE2 2019 utilise à cette fin quatre des six facteurs mentionnés afin de représenter le risque potentiel d'érosion en excluant les facteurs de la couverture et du mode de travail du sol, ainsi que les mesures de réduction de l'érosion (facteurs C et P). Les nouveautés par rapport à l'ancienne carte de risques d'érosion (CRE2) sont les suivantes :
A) La nouvelle carte des blocs de parcelles se base désormais sur les nouvelles données du modèle topographique de paysage (TLM3D ; 2015 ; version 1.3) de Swisstopo.
B) Divers algorithmes Multiple Flow ont été testés et évalués en profondeur sur la base du modèle numérique de terrain SwissALTI3D dans une grille de 2x2 m, en vue du calcul du facteur L (déclivité et longueur des pentes). L'approche MTFD de Seibert & Glynn (2007) avec le réglage de convergence 1.1 a été finalement choisie.
C) Le calcul du facteur S (déclivité) reste largement inchangé.
D) Le nouveau facteur LS ne se distingue pas de manière marquante au plan statistique de l'actuelle CRE2, mais se fonde sur le logiciel Open Source SagaGis.
E) Le facteur K (potentiel d'érosion du sol) a été appliqué de manière semblable à la CRE2 actuelle au plan de la méthode, mais il comprend des données cantonales détaillées supplémentaires sur le sol.
F) La nouvelle carte du facteur R (agressivité des précipitations) atteint des valeurs moyennes nettement plus élevées que le facteur R de l'actuelle CRE2. Cela s'explique par un changement de méthode et par une amélioration des données disponibles.

Le risque d'érosion potentiel calculé dans la région du Frienisberg a été multiplié par les facteurs C et P. Il en est résulté le risque d'érosion actuel, qui a été comparé à la cartographie décennale des dommages causés par l'érosion dans la région du Frienisberg. Le modèle d'érosion a conduit à une surestimation massive de l'érosion des sols de l'ordre du facteur 5 et par conséquent, le risque potentiel d'érosion a été corrigé et reclassifié. La nouvelle ERK2 2019 corrigée diffère donc sensiblement de l'ancienne ERK2 2010. La correction avec les facteurs C et P permet de calculer l'érosion actuelle du sol avec la nouvelle ERK2 2019. Ceci peut être comparé avec les valeurs indicatives légales pour l'érosion tolérable des sols.

La distinction entre les terres assolées et les prairies permanentes – et donc une CRE2 uniquement pour les terres assolées (y compris les prairies temporaires) – n'a pu être effectuée jusqu'ici que pour 19 cantons pour lesquels les données numériques correspondantes concernant chaque parcelle étaient disponibles. Une carte du potentiel de risque d'érosion des terres assolées est donc maintenant disponible pour ces 19 cantons. Environ 75% des terres assolées de Suisse ont ainsi été saisies à la parcelle près. La perte potentielle moyenne de sol à long terme pour ces surfaces est d'environ 17 t ha^{-1} a^{-1}. Pour les sept autres cantons, la différenciation entre les terres assolées et les prairies permanentes repose entre autres sur des données satellites (Fcover 300m, MODIS). La qualité des données est nettement moins bonne dans ce cas. En plus de la carte des risques d'érosion, une carte des lignes d'écoulement pour le ruissellement sur les surfaces agricoles est mise à disposition sur la base du facteur L.

Un nouvel outil Facteur C prenant en compte l'exploitation (assolement et travail du sol) a été développé. Il s'agit d'une version alpha disponible sur une machine virtuelle. Une application web servant à connecter l'outil facteur C avec la nouvelle CRE2 2019 est en cours de développement.

Riassunto

La nuova carta del rischio d'erosione (CRE2 2019) della Svizzera continua a basarsi sulla Revised Universal Soil Equation (RUSLE), tuttavia con un nuovo algoritmo di calcolo e altri software. La RUSLA è un modello d'erosione empirico e mostra il rischio d'erosione medio a lungo termine in t $ha^{-1}a^{-1}$. Grazie alla sua struttura modulare di sei fattori permette di collegare dati di qualità diversa. La CRE2 2019 utilizza a tal proposito quattro dei sei fattori menzionati per rappresentare il rischio d'erosione potenziale senza fattore di copertura e di lavorazione nonché le misure di riduzione dell'erosione (fattore C e P). Le novità rispetto alla vecchia carta del rischio d'erosione (CRE2) sono:
A) La nuova carta dei blocchi di particelle si basa ora sui nuovi dati del modello topografico del paesaggio (TLM3D; 2015; versione 1.3) di Swisstopo.
B) Per il calcolo del fattore L (lunghezza del pendio e dimensione del comprensorio) sono stati testati e valutati approfonditamente vari algoritmi Multiple Flow in base al modello altitudinale SwissALTI3D nel reticolo a celle 2x2 metri. Infine è stato selezionato l'approccio MTFD di Seibert & Glynn (2007) con l'impostazione di convergenza 1.1.
C) Il calcolo del fattore S (declività) è rimasto sostanzialmente invariato.
D) A livello statistico il nuovo fattore LS non è molto diverso rispetto alla CRE2 finora in uso, ma si basa sul software open source SagaGis.
E) Il fattore K (erodibilità del suolo) è stato ottenuto dal profilo metodico analogamente alla CRE2 finora in uso, pur contenendo supplementari dati sul suolo cantonali dettagliati.
F) La nuova carta fattore R (erosività delle precipitazioni) raggiunge valori medi nettamente più elevati rispetto al fattore R della CRE2 finora in uso. Ciò è riconducibile a un metodo diverso e a una migliore base di dati.

Il potenziale rischio d'erosione calcolato è stato combinato per la regione di Frienisberg con i fattori C e P per il rischio d'erosione attuale e confrontato con le mappe decennali dei danni da erosione nella regione di Frienisberg. Il modello di erosione ha portato ad una massiccia sovrastima dell'erosione del suolo nell'ordine di un fattore 5. Pertanto, il potenziale rischio d'erosione è stato corretto e riclassificato di conseguenza. La nuova CRE2 2019 corretta differisce quindi in modo significativo dalla vecchia CRE2 2010. Grazie a questa correzione, la nuova CRE2 2019 può essere combinata con i fattori C e P, ottenendo così la perdita di suolo attuale. Questa può a sua volta essere posta in relazione con i valori guida legali per la perdita di suolo tollerabile.

Finora la differenziazione tra la superficie coltiva e quella permanentemente inerbita, e quindi una CRE2 soltanto per la superficie coltiva (incl. prato artificiale), ha potuto essere realizzata soltanto per 19 Cantoni per i quali erano disponibili i relativi dati digitali a livello particellare. Di conseguenza vi è una nuova carta del potenziale rischio d'erosione della superficie coltiva per questi 19 Cantoni. Circa l'75 per cento della superficie coltiva svizzera ha potuto essere rilevata in tal modo a livello particellare. La potenziale perdita di suolo media a lungo termine di queste superfici ammonta a 17 t ha^{-1} a^{-1} circa. Per i restanti 7 Cantoni la differenziazione tra superficie coltiva e superficie permanentemente inerbita si basa, tra l'altro, su dati satellitari Fcover 300m, MODIS), il che pregiudica considerevolmente la qualità dei dati. Oltre alla carta del rischio d'erosione è ora messa a disposizione una nuova carta delle vie d'infiltrazione per i deflussi superficiali sulla superficie agricola utilizzata a scopo agricolo in base al fattore L.

È stato sviluppato un nuovo strumento per il fattore C, che considera la gestione (avvicendamento delle colture, lavorazione del suolo), ed è disponibile quale versione alfa su una macchina virtuale. È

ancora in fase di sviluppo un'applicazione web che connetta questo strumento con la nuova CRE2 2019.

1. Einleitung

1.1 Ausgangslage und Auftrag

Vom Centre for Development and Environment (CDE) der Universität Bern und Agroscope wurde im Jahr 2010 im Auftrag des Bundesamtes für Landwirtschaft (BLW) eine Erosionsrisikokarte der Schweiz im 2x2m-Raster (ERK2) erstellt (Gisler et al. 2010; Gisler et al. 2011; Prasuhn et al. 2013) und auf dem Geoportal öffentlich zugänglich gemacht (https://map.geo.admin.ch). Die ERK2 erfasst das potentielle Erosionsrisiko, d.h. das aufgrund der Standortfaktoren Niederschlag, Boden und Relief bedingte Erosionsrisiko für die landwirtschaftlich genutzte Fläche der Schweiz bis zur Bergzone 2. Die ERK2 dient zur Sensibilisierung der Landwirtinnen und Landwirte sowie den Behörden als Hilfsmittel für den Vollzug. Sie wird in der Vollzugshilfe Umweltschutz in der Landwirtschaft, Modul Boden, explizit als Hilfsmittel erwähnt (BLW & BAFU 2013). Der bisherige Einsatz der ERK2 hat gezeigt, dass sie ein brauchbares Instrument sowohl für die Praxis als auch für die Behörden ist. Ein häufig geäussertes Manko der ERK2 ist es aber, dass sie nicht nur die Ackerflächen, sondern auch die Dauergrünlandflächen umfasst. Weiterhin wurde häufig der Wunsch geäussert, nicht nur das potentielle Erosionsrisiko zu erfassen, sondern auch das aktuelle Erosionsrisiko unter Einbezug von Landnutzung und Bodenbearbeitung (Hänni 2017). Da es zwischenzeitlich auch zahlreiche neue Datengrundlagen gibt und das Modell, auf dem die ERK2 beruht, auf aktueller GIS-Umgebung nicht mehr läuft, wurde vom BLW der Auftrag erteilt, eine neue, aktualisierte und verbesserte ERK2 zu erstellen.

1.2 Ziel der neuen Erosionsrisikokarte

Ab 2018 soll eine neue und stark verbesserte ERK2 für den Vollzug im Umwelt- und im Landwirtschaftsrecht zur Verfügung stehen, welche für die darauf folgenden 5-10 Jahre ihre Gültigkeit hat. Dazu werden zunächst die zahlreichen, in der letzten Zeit erneuerten Grundlagendaten verwendet. Zudem werden die für die Erstellung der Karte notwendigen EDV-Tools durch neue Instrumente abgelöst. Mit diesen Anpassungen kann die ERK2 für den Vollzug gesetzlicher Grundlagen im Bereich Erosion im Umweltschutzgesetz bzw. der Verordnung über Belastungen des Bodens (VBBo) auch in 10 Jahren sinnvoll genutzt und ab 2018 auch allenfalls im Landwirtschaftsgesetz bzw. der Direktzahlungsverordnung (DZV) berücksichtigt werden.

Die Entwicklung im Bereich digitaler Daten verläuft rasant. In absehbarer Zukunft wird das der ERK2 zugrunde liegende Erosionsmodell AVErosion nicht mehr verwendet werden können. Seit dem Start zur Erarbeitung der ERK2 im Jahr 2008 wurden viele weitere Grundlagendaten aktualisiert oder stehen neu zur Verfügung. Vor allem war es bislang nicht möglich, Landnutzung und Bodenbearbeitung – wichtige Faktoren im Bodenschutz – flächenhaft in das Modell zu integrieren. Somit geht die momentane Erosionsrisikokarte praktisch von einer „Schweiz ohne Pflanzenbedeckung“ mit unrealistisch hohen – rein theoretischen – Erosionswerten aus. Mit der Ausscheidung der Dauergrünflächen und der Modellierbarkeit der Fruchtfolgen von Ackerland besteht nun erstmals die Chance, eine noch realitätsnähere Karte zu produzieren. Zudem sollen neu digitale Parzellenpläne in die ERK2 (2019) aufgenommen werden. Damit werden die Voraussetzungen geschaffen, dass die ERK2 (2019) für den Vollzug der DZV als Hilfsmittel genutzt werden kann. Daher ist eine vollständige Überarbeitung der ERK2 nötig.

Im Auftrag des Bundesamtes für Umwelt (BAFU) wird vom geowissenschaftlichen Institut der Universität Basel parallel zu diesem Projekt eine Erosionsrisikokarte für das Dauergrünland (inklusive Söm-

merungsgebiet) erstellt. Dazu wurde teilweise ein anderes methodisches Vorgehen gewählt (siehe dazu Schmidt et al. 2018; Schmidt et al. in prep)

1.3 Inhalt des vorliegenden Berichtes

Im vorliegenden Bericht werden die Grundlagen zur Erstellung der neuen ERK2 (2019) kurz erläutert und die verschiedenen neuen Karten der einzelnen Faktoren und des potentiellen Erosionsrisikos präsentiert. Detaillierte Ausführungen zum methodischen Vorgehen erfolgen in wissenschaftlichen Publikationen im Rahmen der Dissertation von Pascal Bircher (Bircher et al. 2019a; 2019b). Da die erforderlichen Grundlagen für die Separierung des Ackerlandes bis Ende 2018 – wider Erwarten – nicht flächendeckend zur Verfügung standen, kann hier nur für 19 Kantone das Ergebnis aufgezeigt werden. Alle Berechnungen zum potentiellen Erosionsrisiko erfolgten zunächst für die gesamte landwirtschaftlich genutzte Fläche der Schweiz auf Basis von Feldblöcken. Die Separierung des Ackerlandes erfolgte erst anschliessend.

Im zweiten Teil des Berichtes (Kap. 4) erfolgt eine Überprüfung des verwendeten Erosionsmodells anhand langjähriger Feldkartierungen zur Bodenerosion in der Region Frienisberg. Basierend auf diesem Vergleich erfolgt eine Korrektur des Erosionsmodells (Kap. 5). Die auf dem Geoportal des Bundes verfügbare neue ERK2 (2019) des Ackerlandes entspricht dieser korrigierten Version.

2. Methodik

2.1 Verwendetes Erosionsmodell

Es wurden verschiedene Erosionsmodelle für die Erstellung der neuen ERK2 (2019) in Erwägung gezogen. Physikalisch-deterministische Erosionsmodelle wie Erosion 3D (Schmidt 1991, Schmidt et al. 1999) scheiden aus, da eine Parametrisierung eines solchen Modelles für die ganze Schweiz nicht möglich ist und auch enorme Rechenkapazitäten notwendig wären. Die „Unit Stream Power - based Erosion Deposition“ (USPED) (Mitasova et al. 1996, Mitas and Mitasova 1998) wurde als Alternative getestet, da sie Erosion und Deposition abbildet. Sie führte aber zu unbefriedigenden Resultaten. Erosion und Deposition lagen häufig unmittelbar in benachbarten Zellen. Eine mögliche Ursache dafür war vermutlich die hohe Auflösung des von uns verwendeten Höhenmodells (2mx2m).

Die Entscheidung fiel auf die „Revised Universal Soil Loss Equation“ (RUSLE) (Renard et al. 1997), die auch Modellgrundlage der bisherigen ERK2 war. Die RUSLE bzw. ihre Vorgängerversion USLE ist das bewährteste und weitläufig bekannteste Erosionsmodell zur Risikoabschätzung. Ausserdem entspricht die RUSLE internationalen Standards und kann somit einfach mit Erosionskarten anderer Regionen und Ländern abgeglichen werden. Daneben bietet die RUSLE durch ihren modularen Aufbau die höchste Transparenz für den Vollzug, da sie sich einfach in einzelne, nachvollziehbare Faktoren zerlegen lässt und sich damit einfach verändern, verbessern und erneuern lässt. Das „Joint Research Centre“ (JRC) (Panagos et al. 2012, European Soil Data Centre ESDAC) und die Uni Basel haben die Diskussion zur Auswahl des Modells RUSLE bereits ausführlich geführt und auch publiziert (Panagos et al. 2015 a,b,c).

Das RUSLE-Modell erlaubt die Berechnung des mittleren langjährigen Erosionsrisikos (A) in t ha^{-1} a^{-1} über sechs Faktoren

$$A=R*K*LS*C*P$$

- Der Erosivitätsfaktor (R) erfasst die Erosivität des Niederschlags in [MJ mm ha^{-1} h^{-1} a^{-1} oder N h^{-1} a^{-1}].
- Der K-Faktor (Erodibilitätsfaktor) [t ha h ha^{-1} MJ^{-1} mm^{-1} oder t h N^{-1} ha^{-1}] berücksichtigt die Bodeneigenschaften Körnung und organisches Material.
- Der LS-Faktor [-] ist der Hanglängen (L) und Hangneigungsfaktor (S) und wird basierend auf dem Höhenmodell (SwissALTI3D; 2015) modelliert.
- Der C-Faktor [-] ist der Bedeckungs- und Bearbeitungsfaktor und enthält Informationen bezüglich Feldfruchtwechsel und Bearbeitungsmethoden wie Pflug, Mulch-, und Direktsaat.
- Der P-Faktor [-] entspricht dem Faktor, welcher erosionsschützende Massnahmen berücksichtigt, wie hangparallele oder hangquere Bearbeitung sowie Terrassierung (z.B.: Reben und Hecken).

Das potentielle Erosionsrisiko [t ha^{-1} a^{-1}] unterscheidet sich vom aktuellen Erosionsrisiko [t ha^{-1} a^{-1}] dadurch, dass der C- und P-Faktor fehlen. Deshalb ist das potentielle Erosionsrisiko erheblich höher (Faktor 10-100; abhängig von der Feldfrucht und Bearbeitungsmethode) als das aktuelle Erosionsrisiko (A) (Wischmeier & Smith 1978, Renard et al. 1997).

2.2 Neue Feldblockkarte

Feldblöcke bilden die Grundlage für die Erosionsberechnung. Einerseits stellen sie die räumliche Berechnungseinheit für die Relieffaktoren dar, da sie als hydrologisch abgeschlossen betrachtet werden. Andererseits wurde die landwirtschaftlich genutzte Fläche der Schweiz pro Feldblock ermittelt. Im Feldblockplan sind Ackerflächen, Reben und andere Dauerkulturen, Wiesen, Weiden und alpwirtschaftlich genutzte Graslandflächen enthalten. Verglichen mit der amtlichen Vermessung der Schweiz entspricht die Feldblockkarte mit grosser Übereinstimmung (92 %) dem Attribut 8, 9 und 10 (Tabelle 1) der amtlichen Vermessung der Schweiz (Quelle: Amtliche Vermessung Bern).

Tabelle 1: Attribute und deren Beschreibungen basierend auf den Daten der amtlichen Vermessung.

Attribut	Beschreibung nach amtlicher Vermessung
8	Acker, Wiese, Weide
9	Intensivkultur (Reben)
10	Übrige Intensivkultur

Die bisherige Feldblockkarte der ERK2 (Gisler et al. 2010) basiert auf den Vector 25-Daten von 2008 (Genauigkeit: 3 - 8 m) und wurde aus den 1:25‘000 Kartenblättern digitalisiert (Swisstopo). Die neue Datengrundlage, das topographische Landschaftsmodel (TLM3D Version 1.3; 2015), weist eine höhere Qualität (Genauigkeit: 1 - 3 m) auf, ist aktueller und hat eine höhere Deckungsgleichheit mit der amtlichen Vermessung. Die Daten der amtlichen Vermessung konnten aufgrund der unvollständigen kantonalen Datenlage nicht berücksichtigt werden. Die Anzahl der Feldblöcke ist um etwa 14‘000 höher als im alten Feldblockplan (Tabelle 2), wenn die die gleiche Maske wie bei der ERK2 verwendet

wurde. Der Durchschnitt und der Median der Feldblockgrösse sind nicht erheblich höher. Die Minimalfläche wurde auf 0.25 ha festgelegt, um Verschneidungsartefakte zu entfernen. Die neue Feldblockkarte unter Einschluss der Bergzonen 3 und 4 sowie des Sömmerungsgebietes hat eine deutlich höhere Anzahl an Feldblöcken und umfasst eine grössere Fläche (Tabelle 2, Abbildung 1).

Tabelle 2: Statistischer Überblick der alten und neuen Feldblockkarten der Schweiz.

Feldblockkarte	ERK2, Gisler et al. (2010); (bis Bergzone 2)	ERK2 (2019); gleiche Maske wie 2010	ERK2 (2019) mit Dauergrünland und Sömmerungsgebiet
Anzahl	176‘159	190‘276	328‘477
Fläche in ha	886‘835	993‘109	2‘018‘510
Fläche in km^2	8‘868	9‘931	20‘185
Min in ha *	0.25	0.25	0.25
Max in ha	545	381	5‘674
Durchschnitt in ha	5.03	5.22	6.15
Standardabweichung in ha	8.06	8.24	34.69
Median in ha	2.48	2.56	1.69

Die Unterschiede zwischen alter und neuer Feldblockkarte sind nicht sehr gross (siehe Abbildung 1: Anzahl, Durchschnitts- und Medianwerte im Diagramm), jedoch ist nun auch das Dauergrünland im Sömmerungsgebiet erfasst worden. Die Feldblöcke in Gisler et al. (2010) wurden nur bis und mit Bergzone II erzeugt. Die Werte der beiden Feldblockkarten sind ziemlich ähnlich, wobei in der neuen Karte alle Werte in der Tal- bis Bergzone I immer etwas höher sind. Einzig in der Bergzone II ist die Anzahl an Feldblöcken von Gisler et al. (2010) höher. Im Sömmerungsgebiet gibt es eine hohe Anzahl an Feldblöcken, vergleichbar mit der Talzone. Der Medianwert im Sömmerungsgebiet zeigt, dass vereinzelte dieser Feldblöcke eine grosse Ausdehnung aufweisen, was auf die Produktionsmethode zurückzuführen ist und grosse Alpweiden einschliesst (Abbildung 1).

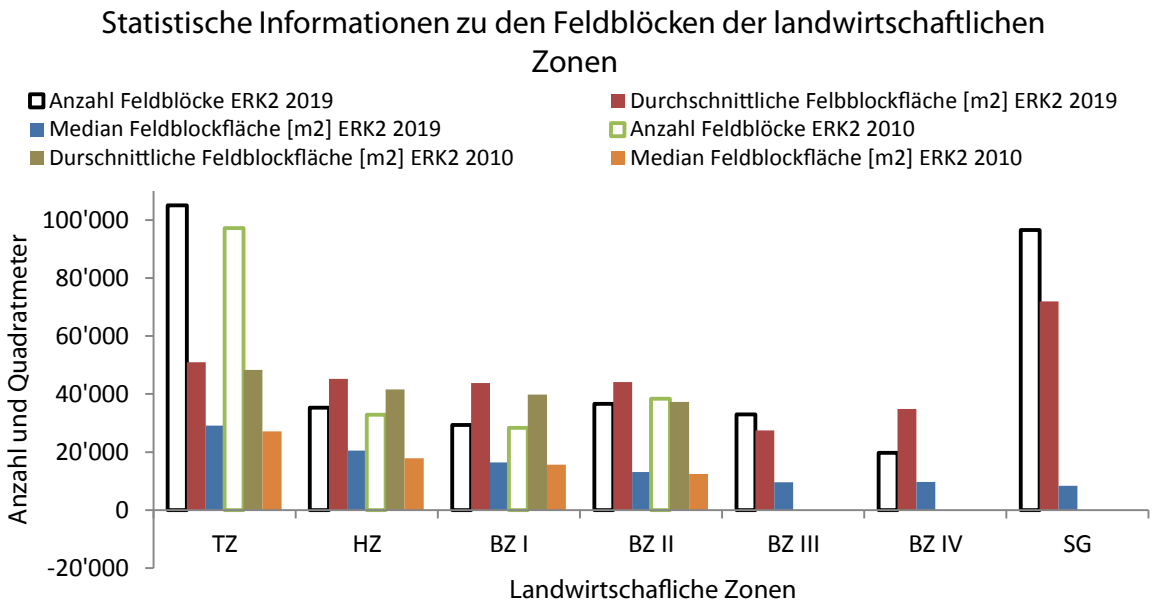

Abbildung 1: Statische Werte der neuen und alten Feldblockkarten im Vergleich über die verschiedenen Landwirtschaftlichen Zonen (TZ = Talzone, HZ = Hügelzone, BZ = Bergzone, SG = Sömmerungsgebiet).

2.3 Vorgehen

Die Berechnung mit dem neuen Erosionsmodell bzw. die Ermittlung der einzelnen Faktoren erfolgte i.d.R. auf drei räumlichen Ebenen. Zuerst wurden die Berechnungen auf Feldblock- bzw. Parzellenebene in der Region Frienisberg (265 ha) durchgeführt, vor allem für die Berechnung der L- und S-Faktoren. Für dieses Gebiet ist zum einen die Datenlage am besten und es existiert viel Felderfahrung und Expertenwissen, zum anderen erlauben kurze Rechenzeiten für solch ein kleines Gebiet zahlreiche Variantenberechnungen. Dieses Gebiet wurde auch für Plausibilitätstest und die Kalibrierung und Validierung (s. Kap. 4) des Modelles verwendet.

Im zweiten Schritt wurden ausgewählte Berechnungsvarianten auf dem Kartenblatt 1146 Lyss der Landeskarte der Schweiz 1:25‘000 (LK 1146 Lyss) durchgeführt. Abhängig von der Datengrundlage unterscheidet sich die Grösse der landwirtschaftlich genutzten Fläche im Kartenblatt 1146. Mit dem neuen topographischen Landschaftsmodell TLM3D (2015) ergibt sich eine Fläche von 11‘597 ha gegenüber der Feldblockkarte der ERK2 2010 mit einer Fläche von 11‘854ha. Die LK 1146 Lyss ist typisch für die Ackerbauregion des Schweizerischen Mittellandes, und alle Berechnungen sind mit vertretbarem Rechenaufwand durchführbar. Auf Grundlage der Ergebnisse dieses Kartenblattes wurde die definitive Entscheidung für die zu verwendende Variante getroffen.

Im letzten Schritt wurden die Berechnungen für die ganze Schweiz bzw. die in der Feldblockkarte abgebildeten Flächen durchgeführt. Aufgrund der hohen Auflösung des Höhenmodells und damit verbundenen Rechenaufwand mussten die Berechnungen auf 1:100‘000 Kartenblätter durchgeführt werden. Entsprechend mussten 25 Kartenblätter gerechnet und wieder zusammengesetzt werden.

Um den Einfluss der Auflösung des verwendeten digitalen Geländemodells auf die Resultate der Erosionsmodellierung abzuschätzen, wurden die Berechnungen der Topographiefaktoren (L- und S-Faktor) mit dem Höhenmodell SwissALTI3D im 2x2m-Raster (Ausgabe 2015) und dem DHM25 im 25x25m Raster durchgeführt und verglichen. Die Ergebnisse dieses Vergleichs sind nicht Bestandteil dieses Berichtes. Siehe dazu Bircher et al. (2019a).

Zur Überprüfung der neuen ERK2 (2019) wurde neben der Berechnung des potentiellen Erosionsrisikos (Faktor R, K und LS) auch das aktuelle Erosionsrisiko (Faktoren C und P zusätzlich) für die Region Frienisberg berechnet. Die Resultate dazu und die daraus abgeleiteten Korrekturfaktoren des Erosionsmodells finden sich im zweiten Teil dieses Berichtes in den Kapiteln 4 und 5. Details dazu siehe auch Bircher et al. (2019b).

3. Resultate unkorrigiertes Erosionsmodell

3.1 Topographiefaktoren (*LS*) [-]

Zunächst wurde eine Korrektur des digitalen Geländemodells SwissALTI3D durchgeführt, um kleine abflusslose Senken und Artefakte zu eliminieren und so die hydrologische Konnektivität zu gewährleisten. Verschiedene Füllhöhen wurden mittels Arc Hydro Tools in ArcGis v.10.2.2 getestet, schliesslich wurde eine Füllhöhe von 0,5m verwendet. Dadurch werden kleine Senken hydrologisch verbunden, grosse abflusslose Senken und Talebenen bleiben aber erhalten (Details siehe Bircher et al. 2019a).

Der Topographiefaktor (LS) zusammengesetzt aus Fliessweg L (Länge) und der Hangneigung S (englisch slope) wurde in der alten ERK2 in ArcView mit AV Erosion 1.1 (Schäuble 2005) berechnet. Dieses Plugin ist in der neuen ArcGis-Umgebung nicht mehr ausführbar, folglich musste eine Alternative gefunden werden. Die Auswahl von GIS-Systemen ist heute gross (Arc-Gis, SagaGis, GrassGis etc.). Unter den quelloffenen Programmen wurden fünf verschiedene Multiple Flow Algorithmen (MFA) ausgewählt und mit unterschiedlichen Einstellungen (Konvergenzwerten) verglichen (Tabelle 3, Abbildung 3 und Abbildung 4) (Details hierzu siehe Bircher et al. 2019a und b). Multiple Flow Algorithmen erlauben die Fliesswege-Modellierung auf komplexem Terrain. Anders als bei Single Flow Algorithmen (Abbildung 2a) berücksichtigen Multiple Flow Algorithmen nicht nur die tiefste Rasterzelle von acht Nachbarzellen, sondern geben das virtuelle Wasser in unterschiedlichen Portionen an alle tieferliegenden Zellen ab, dargestellt mit unterschiedlichen Grauwerten (Abbildung 2b,c,d).

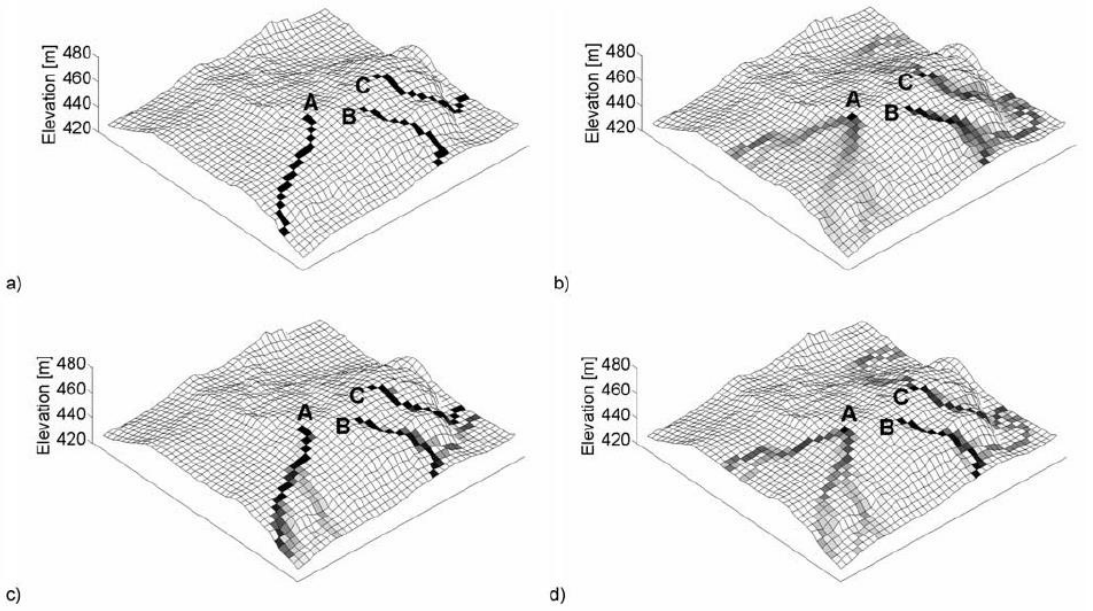

Abbildung 2: Verhalten ausgewählter Algorithmen der Fliesswegberechnungen im Terrain (a=Single Flow Algorithmus, b= Multiple Flow Algorithmus MFD, c = DINF, d = MTFD) aus Seibert & McGlynn (2007).

Tabelle 3: Die im Projekt verwendeten fünf Multiple Flow Algorithmen (MFA) zur Fliesswegberechnung mit Abkürzungen, Referenzen und dazugehörendem GIS-Programm (MUSLE 87 = ERK2, Gisler et al. (2010)).

No.	Approach	Abr.	Program/ Tool	Reference
a)	Deterministic Infinity	DINF	Saga-Gis	Tarboton (1997)
b)	Multiple Flow Direction	MFD	Saga-Gis	Freeman (1991)
c)	Multiple Triangular Flow Direction	MTFD	Saga-Gis	Seibert & McGlynn (2007)
d)	Watershed	WAT	GrassGis	Quinn et al. (1991)
e)	MUSLE 87	-	AvErosion in Arc View	Hensel (1991)

Der Entscheid für den optimalen Fliesswegalgorithmus zur Berechnung des L-Faktors (Tabelle 3, Abbildung 3) wurde auf Basis dreier statistischer Analysen und Expertengesprächen gefällt.

1. Es wurden die Abträge aller 203 Parzellen der Region Frienisberg anhand der kartierten Erosionsereignisse 1997-2007 den verschiedenen Modellergebnissen gegenübergestellt (Abbildung 4) (siehe Kap 4.1).
2. Es wurden die verschiedenen Modellergebnisse mit den aufsummierten Abträgen der fünf Gebiete (Frienisberg, Schwanden, Seedorf, Suberg und Lobsigen) verglichen (siehe Kap 4.1).

3. Die kartierten Bodenabträge > 4t ha^{-1} wurden in zwei Abtragsklassen (4-10 t ha^{-1}, >10 t ha^{-1}) eingeteilt, um pixelbasiert qualitativ und quantitativ die Modellgüte zu eruieren (siehe Kap 4.2).

Die Unterschiede zwischen den verschiedenen Modellen sind nicht sehr gross, sowohl beim statistischen Vergleich (Abbildung 3, Tabelle 4) als auch beim visuellen Vergleich (Abbildung 4) der Berechnungen in der Region Frienisberg (Details siehe Bircher et al. 2019a, b). Die detaillierte Kalibrierung und Validierung des Modells mit den 10-jährigen Feldabschätzungen (1997-2007) von Prasuhn (2010; 2011; 2012) befinden sich im Kapitel 4 und 5. **Ausgewählt für die Berechnung der neuen ERK2 (2019) wurde der Algorithmus MTFD von Seibert & Glynn (2007) mit der Konvergenzeinstellung 1.1.** Abbildung 5 zeigt den angewendeten L-Faktor für die Schweiz.

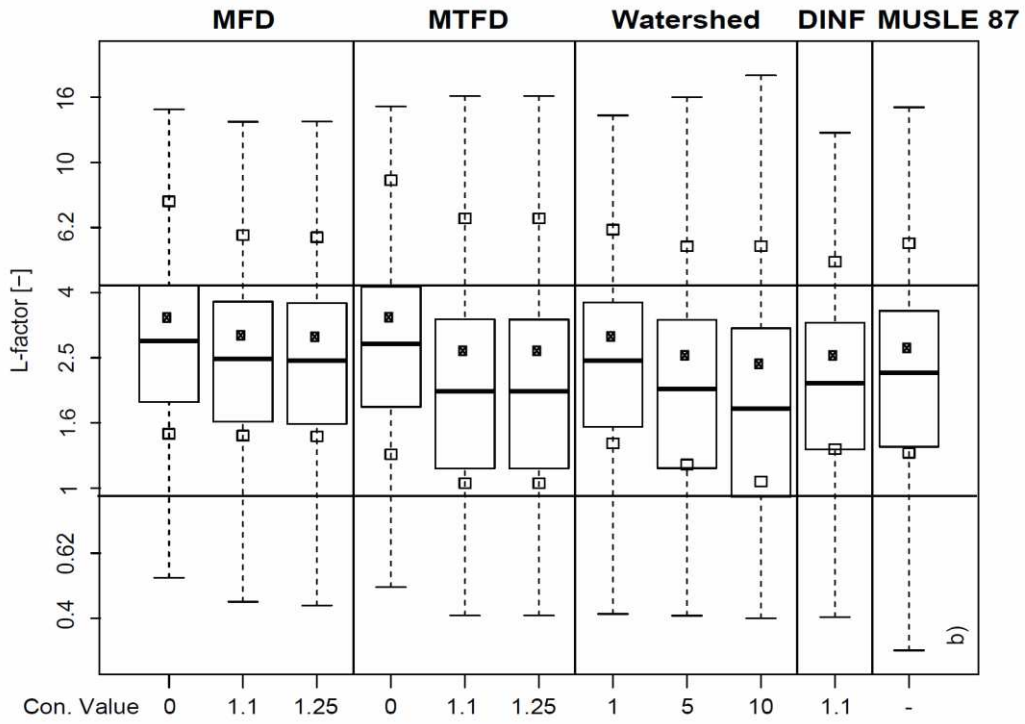

Abbildung 3: Berechnete Fliessweg L-Faktoren [-] für die verglichenen Algorithmen im Teilgebiet Frienisberg; gefüllte Quadrate= Mittelwert; helle Quadrate= Mittelwert ± Standard Abweichung; Con. Value= Konvergenzwert; Abkürzungen der Modelle siehe Tab. 3 (Quelle: Bircher et al. (2019a)).

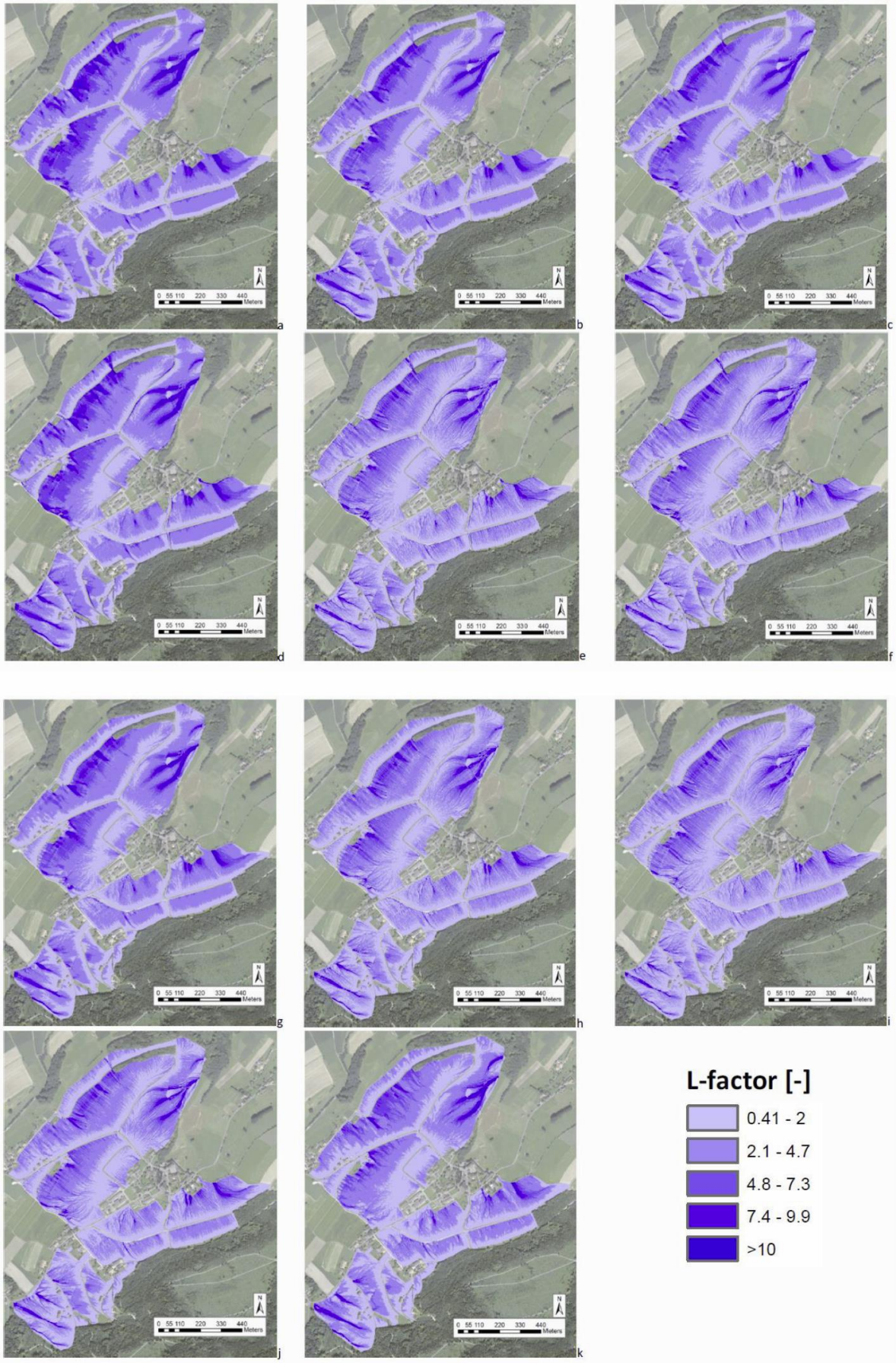

Abbildung 4: Fliessweg L-Faktor-Berechnungen mit unterschiedlichen Multiple Flow Algorithmen und steigenden Konvergenzwerten von links nach rechts im Teilgebiet Frienisberg; Reihenfolge gleich wie bei Abbildung 3; a-b = MFD, d-f = MTFD, g-i = WAT, j= DINF, k= MUSLE87; Abkürzungen der Modelle siehe Tab. 3, (Quelle: Bircher et al. 2019 a).

Die Unterschiede des L-Faktors aufgrund der unterschiedlichen Feldblockkarten (ERK2 2010 vs 2019) sind ebenfalls sehr gering. Trotz geringer Unterschiede bei der Anzahl an Feldblöcken (11 % Unterschied) und deren summierter Flächen (2 % Unterschied) ergeben sich für den Mittelwert des L-Faktors kaum Unterschiede; die Streuung ist bei der neuen Berechnung aber grösser (Tabelle 4).

Tabelle 4: Ergebnisse der Fliessweg L-Faktor-Berechnungen nach Gisler et al. (2010) und ERK2 (2019) für den Ausschnitt LK 1146 Lyss.

	Mit Feldblockkarte von 2010		Mit neuer Feldblockkarte von 2019
L-Faktor [-]	ERK2 (Gisler et al. (2010)	ERK2 (2019)	ERK2 (2019)
Anzahl Feldblöcke	2'305	2'305	2'587
Fläche [ha]	11'854	11'854	11'597
Minimum	0.16	0.4	0.39
Maximum	72.5	103.0	97.8
Mittelwert	1.38	1.39	1.39
Standardabweichung	1.14	1.28	1.28

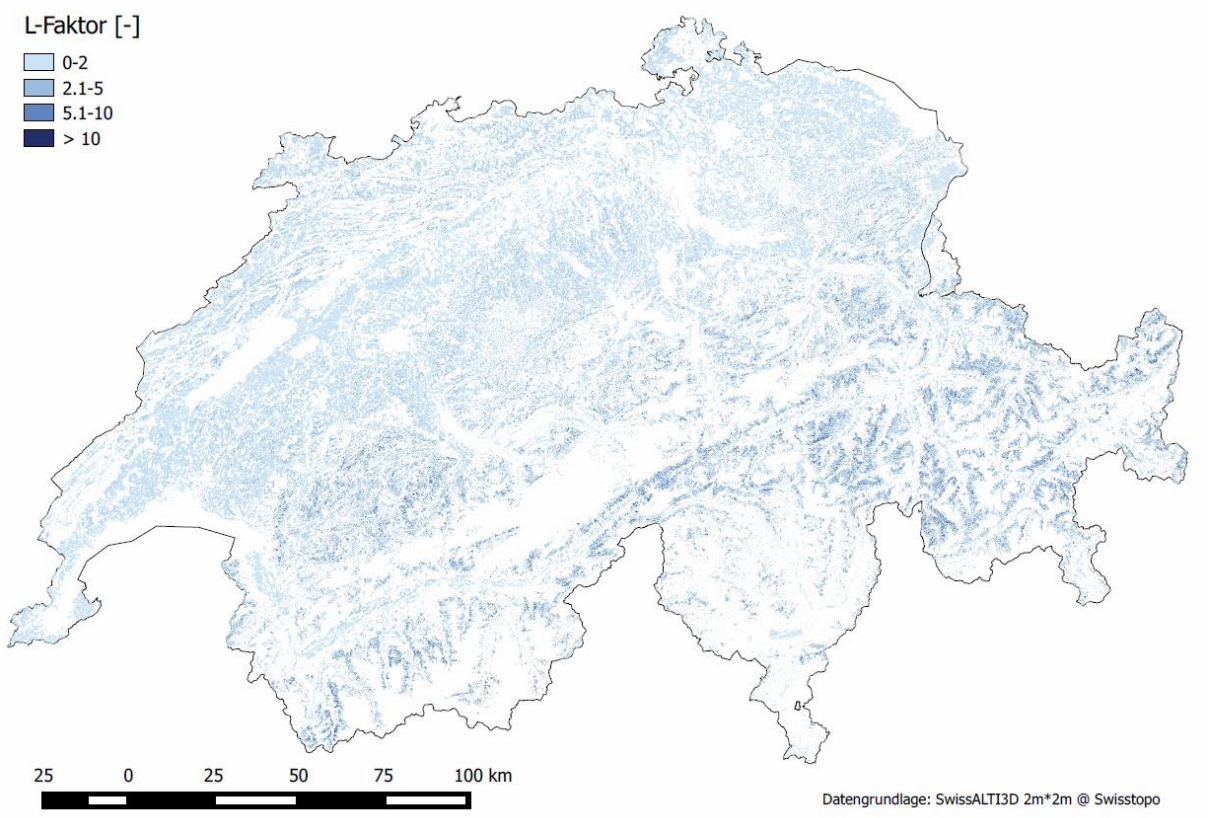

Abbildung 5: Fliessweg L-Faktor-Karte [-] der LN der Schweiz und dem Fürstentum Liechtenstein, berechnet mit MTFD 1.1 und 0.5 m gefülltem DEM (inklusive Dauergrünlandflächen mit Sömmerungsgebiet) (grössere Karte siehe Anhang).

Abbildung 6 zeigt einen Ausschnitt der L-Faktor Karte im Kanton Luzern. Der L-Faktor bildet das hydrologische Einzugsgebiet basierend auf dem 2m*2m Höhenmodell ab und zeigt wo sich Fliesswege akkumulieren und konzentrieren. Dadurch werden die Fliesswege für Oberflächenabfluss und lineare Erosion sowie mögliche Übertrittstellen (Off-site Schäden) gut erkennbar (dunkelblau in Abbildung 6). In der Praxis hat sich gezeigt, dass die L-Faktorkarte neben der potentiellen Erosionsrisikokarte hilfreich ist. Entsprechend wird auf dem Geoportal in Zukunft auch diese Karte online zur Verfügung zu stehen.

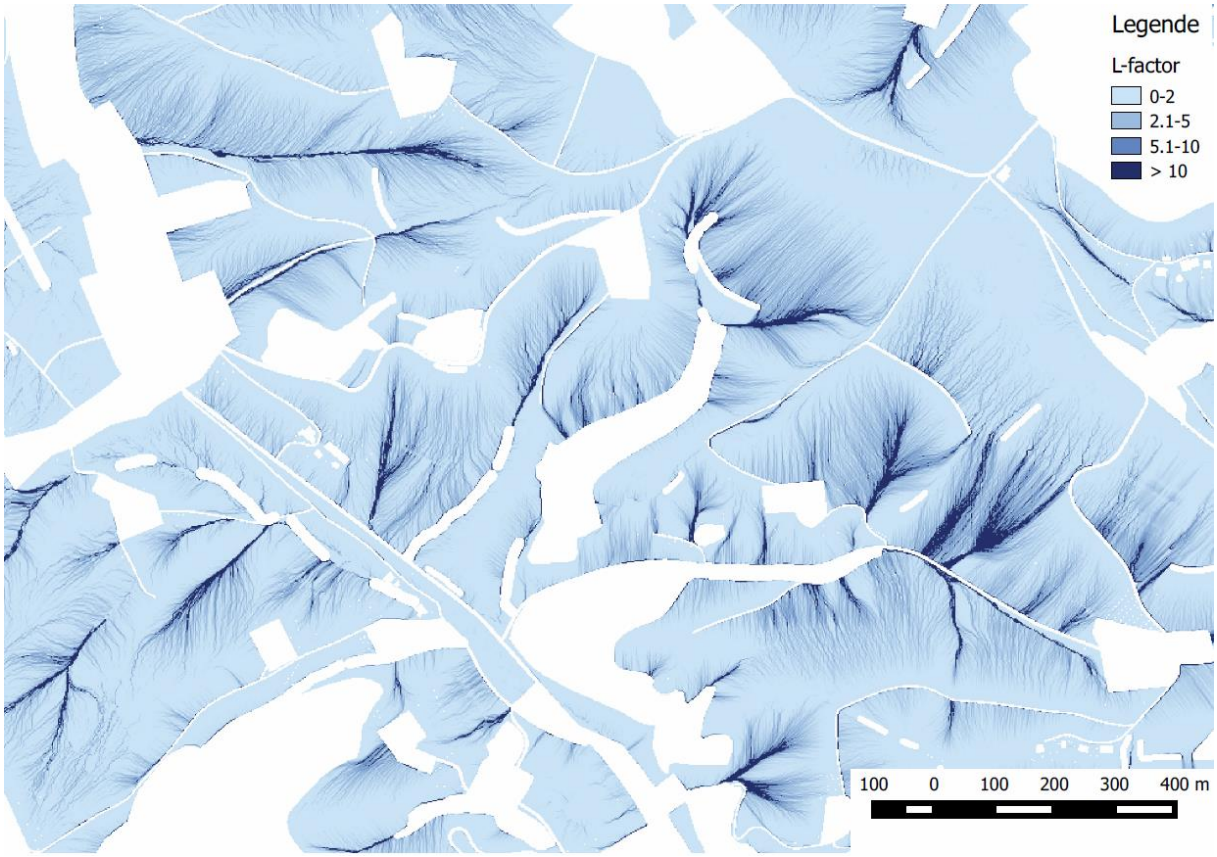

Abbildung 6: Ausschnitt der Fliessweg L-Faktor-Karte [-] der LN der Schweiz im Kanton Luzern, berechnet mit MTFD 1.1 und 0.5 m gefülltem DEM.

Der Hangneigung S-Faktor (Abbildung 7) wurde für die LN der gesamten Schweiz (inklusive Dauergrünland) mit dem gleichen Ansatz wie bei Gisler et al. (2010) berechnet und weist entsprechend keine grossen Unterschiede zur bisherigen ERK2 auf (Tabelle 5). Die S-Faktor-Berechnung basiert auf den Gleichungen von McCool et al. (1987), wobei die Neigung nach Zevenbergen & Thorne (1987) berechnet wurde. Die Dauergrünlandflächen wurden für die Berechnung des S- und L-Faktors mitberücksichtigt, da die Fliesswege für Oberflächenabfluss auch über Dauergrünlandflächen stattfinden. Die Dauergrünlandflächen werden später noch extrahiert (siehe Kapitel 3.5 Dauergrünland-Ackerland-Unterscheidung). Die Unterschiede des S-Faktors beim Mittelwert aufgrund der unterschiedlichen Feldblockkarten (ERK2 2010 vs 2019) sind mit +4 % ebenfalls gering (Tabelle 5).

Tabelle 5: Ergebnisse der Hangneigung S-Faktor-Berechnungen nach Gisler et al. (2010) und ERK2 (2019) für den Ausschnitt LK 1146 Lyss.

	Mit Feldblockkarte von 2010		Mit neuer Feldblockkarte von 2019
S-Faktor [-]	ERK2 (Gisler et al. (2010)	ERK2 (2019)	ERK2 (2019)
Anzahl Feldblöcke	2‘305	2‘305	2‘587
Fläche [ha]	11‘854	11‘854	11‘597
Minimum	0.03	0.03	0.03
Maximum	14.86	16.10	15.6
Mittelwert	0.87	0.93	0.91
Standardabweichung	0.99	1.04	0.99

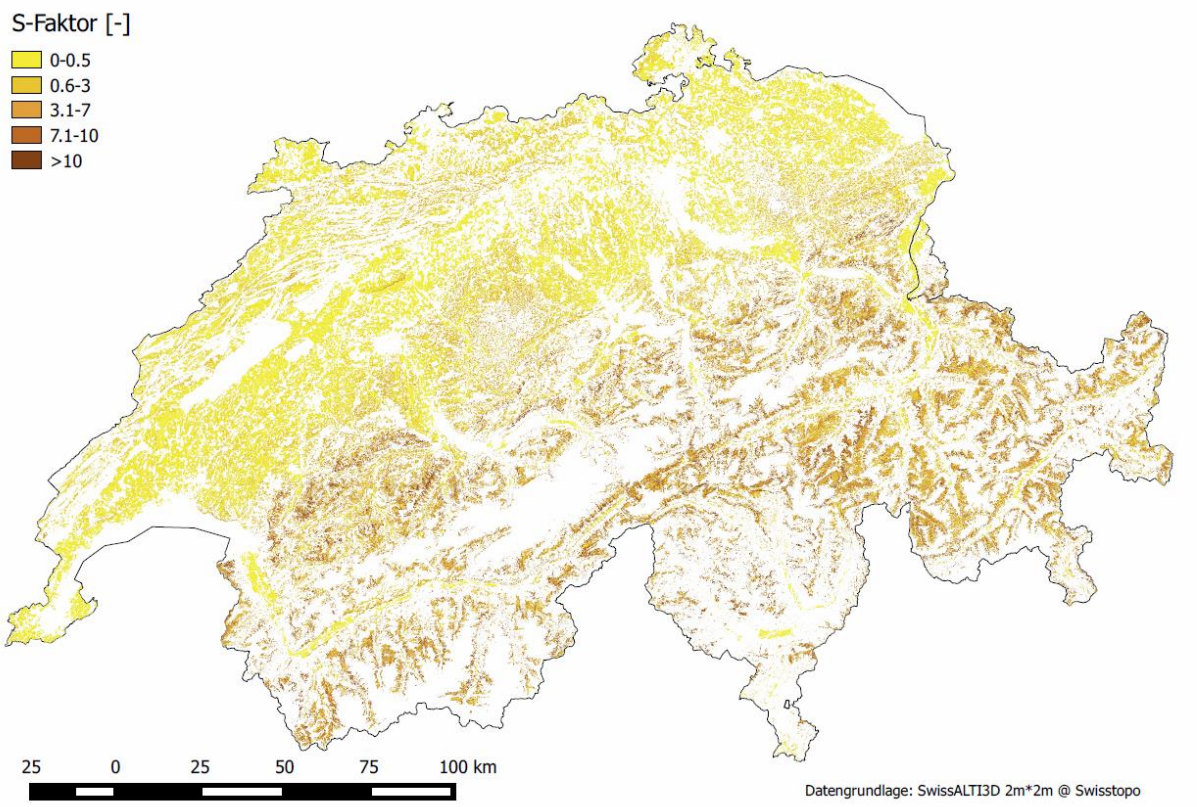

Abbildung 7: Hangneigung S-Faktor-Karte [-] der LN der Schweiz und dem Fürstentum Liechtenstein, inklusive Dauergrünlandflächen mit Sömmerungsgebiet (grössere Karte siehe Anhang).

3.2 Erodibilitätsfaktor (K) [t h N^{-1} ha^{-1}]

Der Erodibilitätsfaktor (K) wurde aus Bodenkarten unterschiedlicher Massstäbe berechnet. Die Massstäbe reichen von 1:1‘000 bis 1:200‘000, wobei Letzterer die gesamtschweizerische Bodeneignungskarte (BEK200) darstellt, die bereits seit 1980 existiert. Wo neue Daten vorhanden waren, wurden kantonale Bodenkarten für die Berechnung hinzugezogen. In den Kantonen Bern, Freiburg, Solothurn, Graubünden, Wallis und Luzern sind seit 2010 neue Daten hinzugekommen. Insgesamt sind mit den erwähnten Kantonen detaillierte Bodendaten mit einer Fläche von 59‘935 ha hinzugekommen. Die Anteile am Feldblockplan 2010 und 2019 haben sich gesamtschweizerisch etwas verändert Die Anteile der Karten 1:5‘000 und 1:25‘000 haben sich um 1.4 % bzw. um 2.1 % erhöht (Tabelle 6, Abbildung 8). Die unterschiedliche Gesamtfläche ist darauf zurückzuführen, dass mit neuen Grundlagendaten gearbeitet wurde (TLM3D 2015; Swisstopo).

Tabelle 6: Anteile Bodendaten verschiedener Qualität für den alten (Gisler et al.2010) und neuen Erodibilitätsfaktor (K) (2019).

Massstab	ERK2 (Gisler et al. 2010)	ERK2 (2019)
Gesamtfläche [km^2]	9’058	9’931
Bis 1:5‘000 [%]	11.7	13.1
Bis 1:10‘000[%]	4.3	4.2
Bis 1:25'000 [%]	1.9	4.0
Bis 1:50'000 [%]	6.1	5.6
Bis 1:200‘000 [%]	75.9	73.0

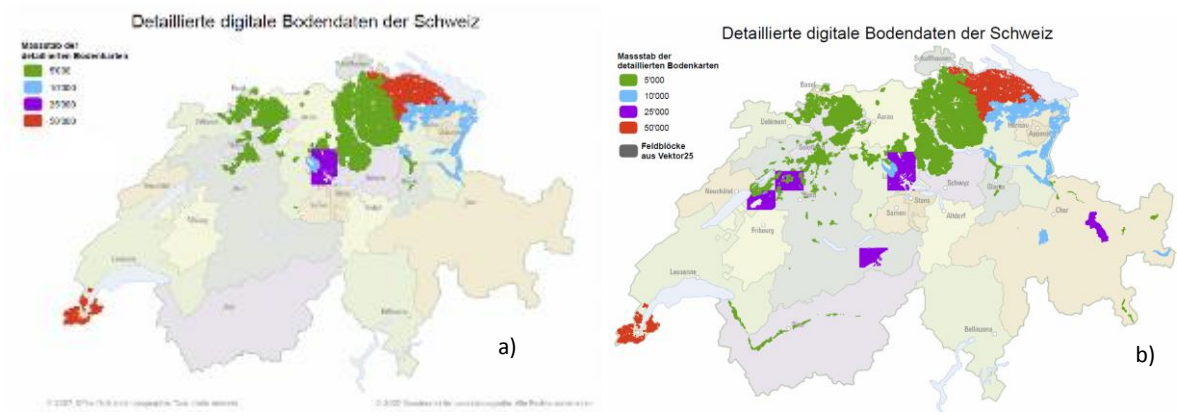

Abbildung 8: a) Datenlage Erodibilitätsfaktor (K) 2010 (Gisler et al.2010); b) Datenlage für Erodibilitätsfaktor (K) 2019.

Gesamtschweizerisch ergeben sich folgende Werte für den K-Faktor. Das Minimum liegt bei **0.02,** das Maximum bei **0.70** der Durchschnitt bei **0.22** und die Standardabweichung bei **0.088** [t h N^{-1} ha^{-1}], was nahezu identische Werte wie bei der ERK2 (Gisler et al. 2010) sind. Für das Kartenblatt LK 1146 Lyss ändert sich bezüglich verschiedener Massstäbe der Durchschnitt im K-Faktor (Tabelle 7). Die Spannweite ist beim Massstab 1:5'000 am höchsten, was durch die bessere Datenlage und Varianz zu begründen ist. Die Interpolation der Daten ist auf ein kleineres Gebiet beschränkt, was sich in einer besseren Qualität der Daten widerspiegelt.

Tabelle 7: Deskriptive Statistik für den Erodibilitätsfaktor (K) für das Kartenblatt LK 1146 Lyss, basierend auf unterschiedlicher Datenlage; mit Feldblockkarte 2010 als Grundlage.

K-Faktor[t h N^{-1} ha^{-1}]	1:5'000	1:25'000	1:200'000
Minimum	0.03	0.05	0.15
Maximum	0.52	0.50	0.45
Range	0.50	0.45	0.30
Mittelwert	0.24	0.26	0.35
Standardabweichung	0.058	0.028	0.036

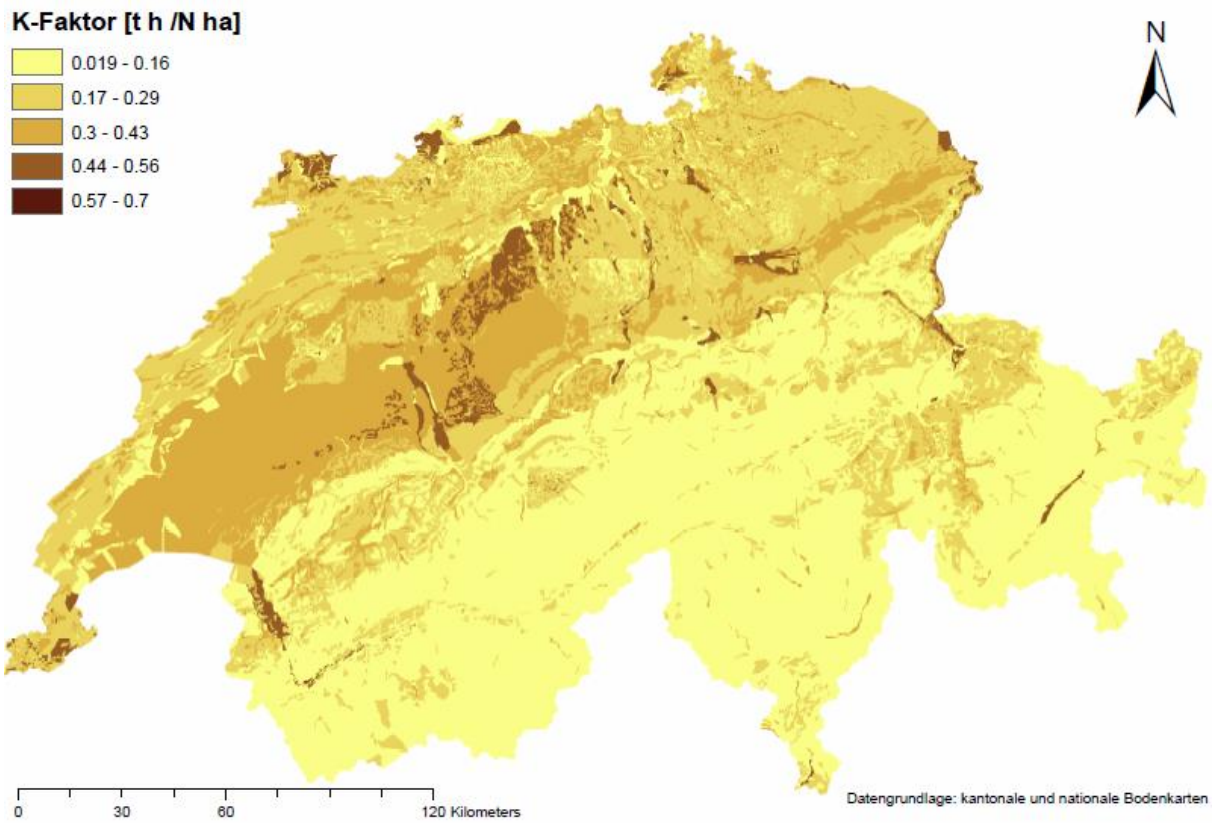

Abbildung 9: Erodibilität K-Faktor-Karte [t h N^{-1} ha^{-1}] der gesamten Schweiz (grössere Karte siehe Anhang).

Die Datengrundlage für die LK 1146 Lyss ist im Vergleich zur restlichen Schweiz gut. Immerhin annähernd 20 % der Fläche sind im Massstab 1:5‘000 oder besser vorhanden. Und nur 9.6 % der Fläche haben eine Datenlage niedriger Qualität mit 1:200‘000 (Tabelle 8). Der Dauergrünlandanteil in der LK 1146 Lyss erreicht 25 %. Der Flächenüberschuss von 12.4 % erklärt sich damit, dass die Massstäbe 1:1‘000 bis 1:5‘000 den Massstab 1:25‘000 teilweise überlagern und deshalb eine Doppelzählung vorkommt.

Tabelle 8: Anteil der verschiedenen Massstäbe von Bodenkarten am Kartenblatt LK 1146 Lyss in Hektar und Prozent der Gesamtfläche ohne Berücksichtigung der Feldblockkarte.

MASSSTAB	Fläche [ha]	Prozent [%]
1:1'000	35.7	0.2
1:2'000	7.1	0.03
1:5'000	4‘027.7	19.2
1:25'000	17‘549.2	83.5
1:200'000	2‘024.3	9.6
Summe	23‘643.9	112.4
Gesamtgebiet von LK 1146	21‘028.8	

3.3 Erosivitätsfaktor (R) [N h^{-1}]

Bei der ERK2 (Gisler et al. 2010) wurde die Hektarrasterkarte von Friedli (2006) verwendet, welche auf Daten aus dem hydrologischen Atlas der Schweiz basierte und einen Durchschnittswert des R-Faktors von 92.1 N h^{-1} hatte. Nogler (2012) berechnete für den R-Faktor einen Mittelwert von 153 N h^{-1} und Meusburger (2012) 133 N h^{-1}. Der neu berechnete und in der ERK2 (2019) verwendete Mit-

telwert des R-Faktors liegt bei 114.6 N h^{-1} (Schmidt et al. 2016) (Tabelle 9). Der Niederschlagsfaktor wurde von (Schmidt et al. 2016) auf Grundlage verschiedener eidgenössischer und kantonaler Meteodaten (86 Stationen; Meteoschweiz & Kantone BE, LU, SG) mit Kovariaten (Schneehöhen, CombiPrecip, DEM u.a.) interpoliert. Die Karte zeigt hohe Werte in den nördlichen Voralpen und im Süden der Schweiz (Tessin), was auf die Niederschlagscharakteristik der Schweiz zurückzuführen ist (Sommergewitter im Süden; Herbstgewitter in den nördlichen Voralpen). Der R-Faktor (Abbildung 10) wurde für die ERK2 (2019) mit einer bikubischen Methode neu interpoliert, da die Ausdehnung und Auflösung nicht mit den Faktoren LS und K übereinstimmten.

Tabelle 9: Statistik des Erosivitätsfaktors (R) der Schweiz (Schmidt et al. 2016).

R-Faktor [N h^{-1} a^{-1}]	Gesamte Schweiz
Minimum	12.1
Maximum	1042.4
Mittelwert	114.6
Standardabweichung	76.3

Im Kartenblatt LK 1146 Lyss erreicht der R-Faktor einen 13 % höheren Durchschnittswert als in der ERK2, was sich auch auf das potentielle Erosionsrisiko auswirkt (Tabelle 10).

Tabelle 10: Statistik des Erosivitätsfaktors (R) der Schweiz (Schmidt et al. 2016) im Kartenblatt LK 1146; mit Feldblockkarte 2010 als Grundlage.

R-Faktor [N h^{-1} a^{-1}]	ERK2, Gisler et al. (2010)	ERK2 (2019) Schmidt et al. (2016)
Minimum	79.7	88.7
Maximum	95.4	115.5
Mittelwert	87.5	100.8
Standardabweichung	2.46	3.6

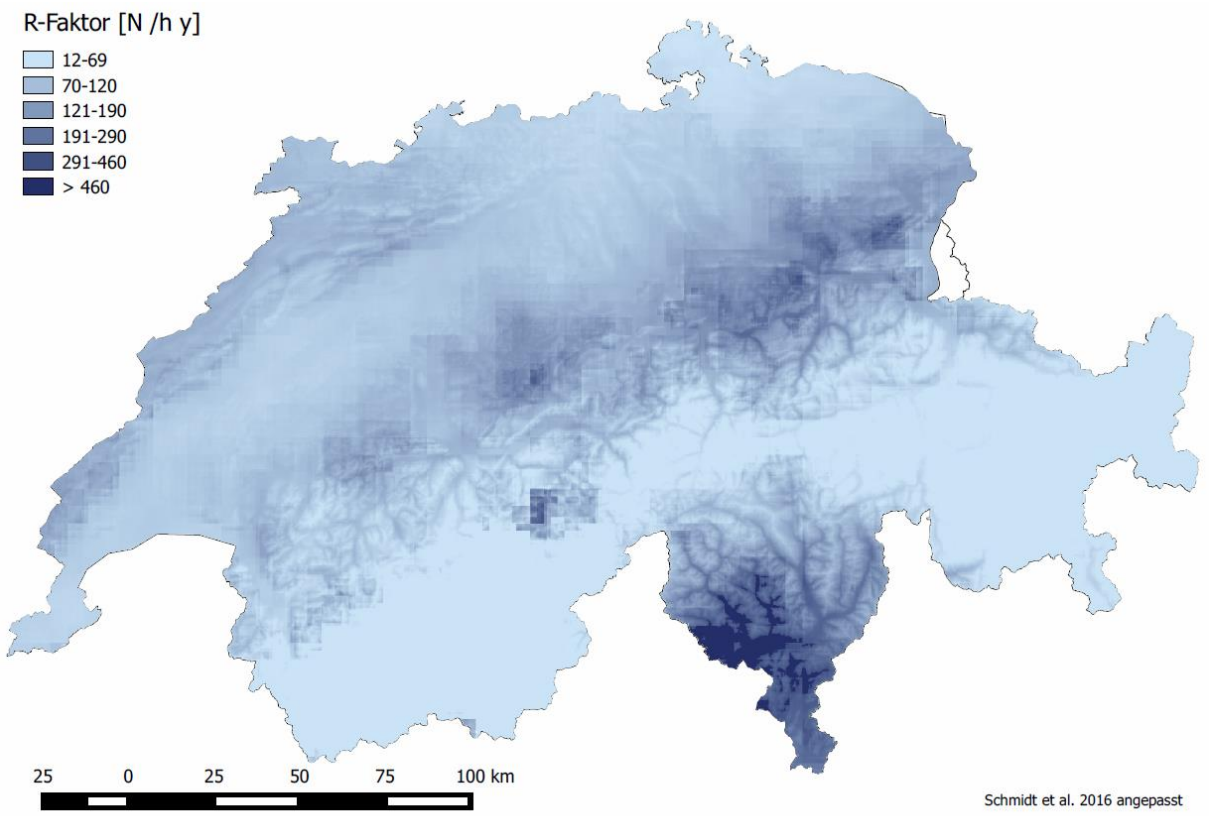

Abbildung 10: Erosivität R-Faktor-Karte der gesamten Schweiz [N h^{-1} a^{-1}] (Schmidt et al. 2016) (grössere Karte siehe Anhang).

3.4 Potentielles Erosionsrisiko, unkorrigiert (LS*K*R) [t/ha a]

Der statistische Vergleich des potentiellen Erosionsrisikos im Kartenblatt LK 1146 Lyss zeigt keine grossen Unterschiede beim Mittelwert zwischen der alten Erosionsrisikokarte (ERK2; Gisler et al. 2010) und der neuen ERK2 (2019) (Tabelle 11). Dies war aufgrund der Ähnlichkeit der Ergebnisse der verschiedenen Algorithmen zu erwarten (Abbildung 4). Eine leichte Abnahme von 5 % ergibt sich für den Mittelwert des Bodenabtrages. Der Maximalwert und die Standardabweichung unterscheiden sich jedoch erheblich (Tabelle 11), da der neue Fliesswegalgorithmus die Abflüsse stärker konzentriert im Vergleich zur ERK2. Die Unterschiede des potentiellen Erosionsrisikos aufgrund der unterschiedlichen Feldblockkarten (ERK2 2010 vs 2019) wirken sich mit einem 7 % niedrigeren Durchschnittswert für das Kartenblatt LK 1146 Lyss nicht erheblich aus (Tabelle 11).

Tabelle 11: Deskriptive Statistik potentielles Erosionsrisiko (unkorrigiert) für Kartenblatt LK 1146 Lyss.

	Mit Feldblockkarte von 2010		Mit neuer Feldblockkarte von 2019
Pot. Erosionsrisiko	ERK2, Gisler et al. (2010)	ERK2 (2019)	ERK2 (2019)
Anzahl Feldblöcke	2‘305	2‘305	2‘587
Fläche [ha]	11‘854	11‘854	11‘597
Minimum [t ha^{-1} a^{-1}]	0.15	0.16	0.16
Maximum [t ha^{-1} a^{-1}]	4‘123	23’177	24‘357
Mittelwert [t ha^{-1} a^{-1}]	45.4	43.0	42.4
Standardabweichung [t ha^{-1} a^{-1}]	80.8	99.0	96.3

Die Berechnung des potentiellen Erosionsrisikos wurde für die gesamte landwirtschaftlich genutzte Fläche der Schweiz mit der vorgestellten Methode durchgeführt (Abbildung 11). Diese Karte bildet auch die Grundlage für die Neuberechnung der Gewässeranschlusskarte (GAK2) (Joss und Prasuhn 2019). In den Bergzonen und im Sömmerungsgebiet sind diese Resultate mit Unsicherheiten behaftet, da die verwendete Methode im alpinen Gebiet mit sehr grossen Hangneigungen und Hanglängen nicht validiert ist. Für diese Gebiete ist der Ansatz von Schmidt et al. (in prep.) geeigneter und wird aucht für das Dauergrünland verwendet. Es ergeben sich somit zwei Erosionsrisikokarten; eine für das Ackerland (Abbildung 12) und eine für das Dauergrünland (BAFU-Projekt).

Abbildung 11: Karte des potentiellen Erosionsrisikos (unkorrigiert) der LN der Schweiz [t ha^{-1} a^{-1}] der neuen ERK2 (2019), inklusive Dauergrünlandflächen mit Sömmerungsgebiet; gleiche Klassen wie bei ERK2 2010 (grössere Karte siehe Anhang).

3.5 Unterscheidung von Ackerland und Dauergrünland

Die Unterscheidung von Acker- und Dauergrünland wurde mit parzellenscharfen, digitalen kantonalen Daten umgesetzt, wobei einige Kantone leider erst Ende 2019 oder 2020 diese Daten zur Verfügung stellen können. Komplette Daten haben bisher 19 von 26 Kantonen geliefert. Der Kanton Zürich hat Daten geliefert, welche aber noch nicht vollständig sind und deswegen unberücksichtigt blieben. Eine Zusammenstellung der Daten der Kantone liefert Tabelle 22 in Kapitel 5.2. Ebenfalls ersichtlich sind dort die Flächenangaben zur Landwirtschaftlichen Nutzfläche und zum Ackerland nach der Arealstatistik 2016 und aus der Betriebsstrukturerhebung (2015). Um das Ackerland (inklusive Kunstwiese) zu erhalten, wurden drei verschiedene Methoden angewendet. Diese unterschiedlichen Vorgehensweisen waren notwendig, da je nach Kanton die Datenlage unterschiedlich war. Wir wollten damit die genaueste Übereinstimmung des jeweiligen Ackerlandlayers erreichen. Auf verschiedene methodische Probleme und Fehler bei der Erstellung der Ackerlandkarte mit den verschiedenen Methoden wird in Kapitel 5.3 mit Fallbeispielen noch detaillierter eingegangen.

Methode 1 (Kantone AG, AI, AR, BL, GL, GR, NE, NW, SG, SH, SZ, TG, UR, VD, VS, ZG): Im kantonalen Parzellen-Datensatz existierte die Kategorie „Ackerfläche (inklusive Kunstwiesen)“. Diese Flächen wurden mit der Feldblockkarte (LN) verschnitten.

Methode 2 (Kantone BE, FR, SO): Im kantonalen Parzellen-Datensatz lag keine Kategorie „Ackerfläche“ vor. Deshalb wurden die vorliegenden Kategorien „Dauergrünlandflächen, Dauerkulturen, Kulturen in ganzjährig geschütztem Anbau sowie andere, der Landwirtschaftsfläche zugeordnete Flächen wie Hecken, Gehölze, ökologische Ausgleichsflächen, Ruderalflächen, Hochstammfeldobstbäume“ aus den kantonalen Datensätzen von der Feldblockkarte (LN) entfernt, um das Ackerland zu erhalten.

Methode 3 (Kantone BS, GE, JU, LU, OW, TI, ZH): Für die sieben Kantone, welche keine kantonalen Parzellendaten zur Verfügung gestellt haben, wurde basierend auf Daten von Schmidt et al. (2018) zum Dauergrünland (Swissimage FCIR, FCover 300m und MODIS) das Dauergrünland mit der landwirtschaftlichen Nutzfläche (LN) der Feldblockkarte verschnitten. Details zur Dauergrünlandkarte finden sich in Schmidt et al. (2018) (violett umrandet in Abbildung 12).

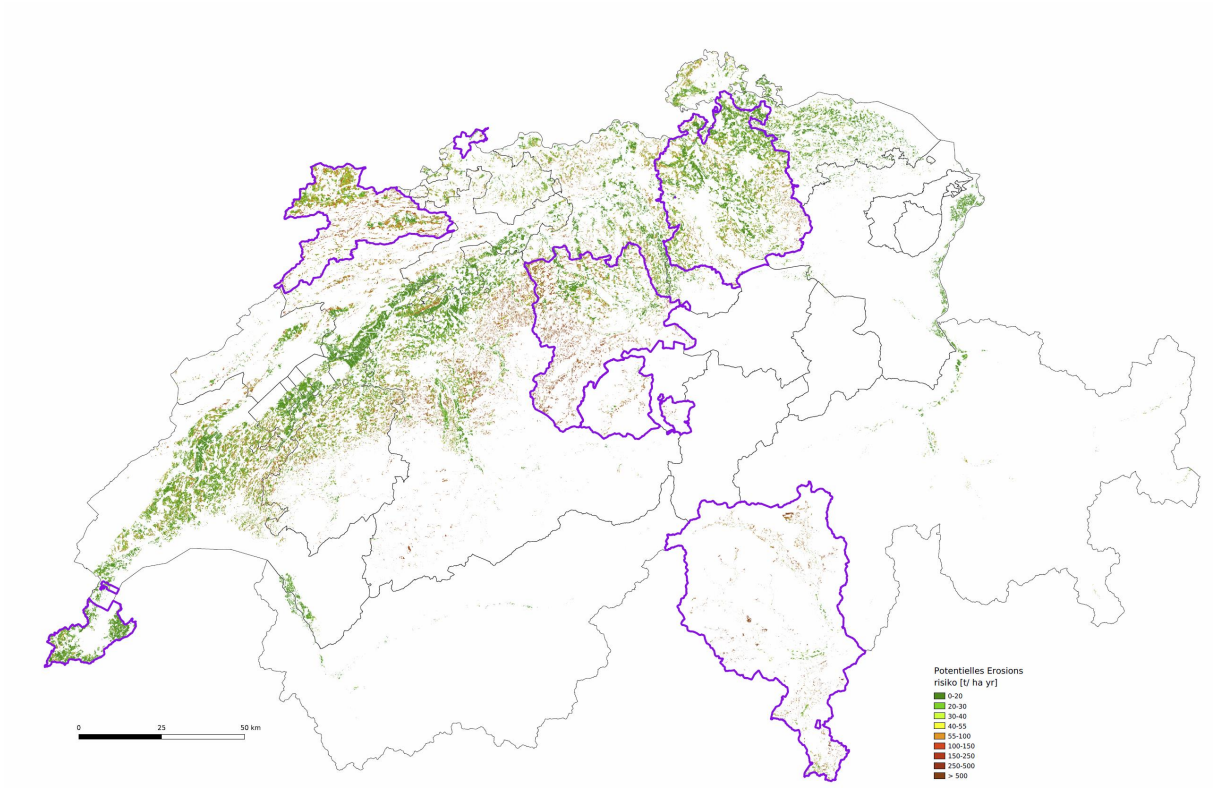

Abbildung 12: Potentielles Erosionsrisiko (unkorrigiert) für das Ackerland der Schweiz [t ha^{-1} a^{-1}] und verwendete kantonale Daten der Schweiz; violett umrandet; restliche 7 Kantone ohne parzellenscharfe Ackerlanddaten, stattdessen mit Satellitenbildern abgeschätzt.

Für den Kanton Bern wurde das Dauergrünland und das Sömmerungsgebiet (BLW 2016) beispielhaft mit Daten aus dem GELAN (LANDKULT 2016) bereits entfernt (Tabelle 12, Abbildung 13). Im Kanton Bern beträgt die berechnete Dauergrünlandfläche fast 65 % an der LN, entsprechend geht die berücksichtigte Fläche um fast 65 % zurück, wenn man nur das Ackerland betrachtet, da im Kanton Bern grosse Anteile in alpinen, voralpinen und Jura-Regionen liegen (Abbildung 13). Der mittlere potentielle Bodenabtrag (unkorrigiert) geht markant um 56 % zurück, da die Dauergrünlandflächen

häufig in Steillagen liegen und ein überdurchschnittliches potentielles Erosionsrisiko haben. Er hat mit 144 t ha^{-1} aber immer noch einen vergleichsweise hohen Wert. Der aufsummierte Bodenabtrag (unkorrigiert) geht wegen der geringeren Fläche und dem niedrigerem mittleren Bodenabtrag entsprechend mit 85 % noch stärker zurück (Tabelle 12).

Tabelle 12: Potentielles Erosionsrisiko (unkorrigiert) im Kanton Bern mit und ohne Dauergrünland und Sömmerungsgebiet: statistische Grundlagen basierend auf der Feldblockkarte 2019.

Kanton Bern	Feldblockkarte mit Dauergrünland	Feldblockkarte ohne Dauergrünland und Sömmerungsgebiet
Fläche [ha]	255‘123	89‘200
Mittelwert [t ha^{-1} a^{-1}]	324.9	144
Standardabweichung [t ha^{-1} a^{-1}]	810.4	369.8
Summe [t]	82‘889‘333	12‘812‘303

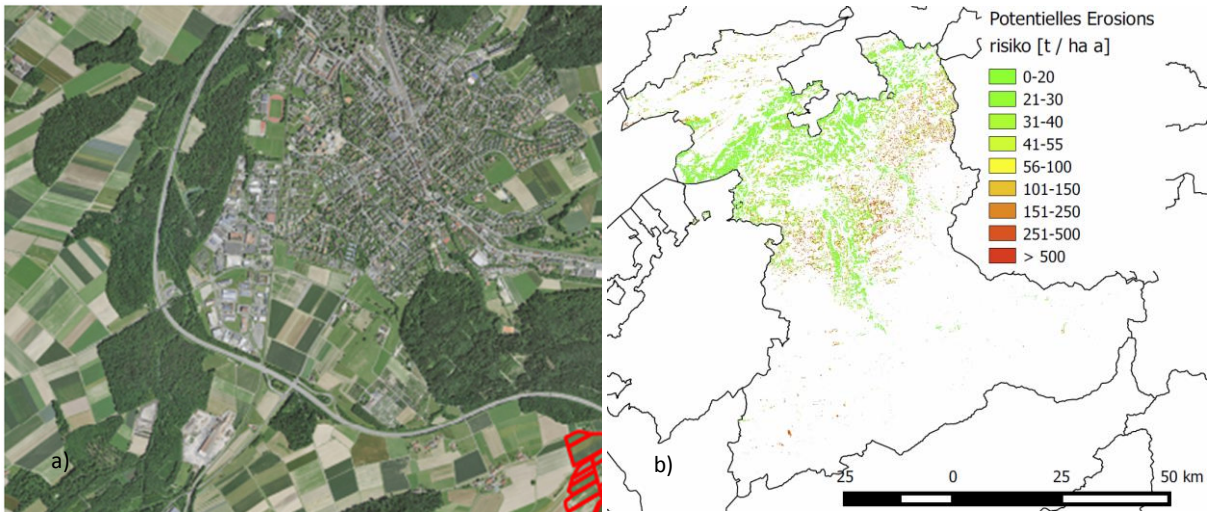

Abbildung 13: Potentielles Erosionsrisiko (unkorrigiert) a) mit Dauergrünland und Sömmerungsgebiet b) ohne Dauergrünland und Sömmerungsgebiet für den Kanton Bern.

Ähnliches lässt sich im Kartenblatt Lyss beobachten; allerdings nicht so ausgeprägt, da wir uns hier ausschliesslich im Mittelland befinden. Im ackerbaulich geprägten Kartenblatt LK 1146 Lyss beträgt der Dauergrünlandanteil nur rund 25 %. Der mittlere potentielle Bodenabtrag (unkorrigiert) geht um 23 % zurück, da die Dauergrünlandflächen auch hier häufig in steileren Lagen liegen und ein überdurchschnittliches potentielles Erosionsrisiko haben. Der aufsummierte Bodenabtrag (unkorrigiert) geht durch den Ausschluss des Dauergrünlandes um ca. 43 % zurück (Tabelle 13).

Tabelle 13: Potentielles Erosionsrisiko (unkorrigiert) der LK 1146 Lyss mit und ohne Dauergrünland und Sömmerungsgebiet: statistische Grundlagen basierend auf der Feldblockkarte 2019.

Blatt Lyss	Feldblockkarte mit Dauergrünland	Feldblockkarte ohne Dauergrünland und Sömmerungsgebiet
Fläche [ha]	11‘597	8‘645
Mittelwert [t ha^{-1} a^{-1}]	42.4	32.6
Standardabweichung [t ha^{-1} a^{-1}]	96.3	67.6
Summe [t]	491‘652	281‘459

Vergleicht man das berechnete potentielle Erosionsrisiko auf Ackerflächen des Blattes LK 1146 Lyss der alten ERK2 mit den Berechnungen der neuen ERK2 (2019), ergibt sich folgendes Bild: Die Fläche des Ackerlandes unterscheidet sich um ca. 270 ha bzw. 3 %, wenn die gleiche Maske für die Ackerflä-

che wie bei der ERK2 (2019) verwendet wurde (Tabelle 14). Dies ist auf die unterschiedlichen Datengrundlagen zurückzuführen (Vector 25 vs TLM3D). Ein Vergleich auf der Ebene Ackerfläche ist folglich nur eingeschränkt möglich. Ähnlich wie beim potentiellen Erosionsrisiko mit Dauergrünland (Tabelle 11) ist der mittlere Bodenabtrag (unkorrigiert) bei der Berechnung mit der ERK2 (2019) ebenfalls etwas geringer (Abnahme um 11 %). Trotz grösserer Ackerflächen bei der ERK2 (2019) ergibt sich wegen des geringeren mittleren Bodenabtrages ein um 8 % geringerer aufsummierte Gesamtabtrag (Tabelle 14). Die Ursache für diese Abnahme liegt in dem deutlich geringeren K-Faktor aufgrund neuer Bodeninformationen für die LK 1146 Lyss. Die Auswirkungen der Dauergrünlandentfernung sind zusätzlich im Gebiet Frienisberg dargestellt (Abbildung 14).

Tabelle 14: Statistische Grundlagen des Kartenblatts LK 1146 Lyss bezüglich potentiellem Erosionsrisiko (unkorrigiert) auf Ackerland; unterschiedliche Feldblockkarten als Grundlage.

KB 1146 Lyss	ERK2, Gisler et al. (2010)	ERK2 2019
Fläche [ha]	8'371	8'645
Mittelwert [t ha^{-1} a^{-1}]	36.7	32.6
Standardabweichung [t ha^{-1} a^{-1}]	61.3	67.6
Summe [t]	307'455	281'459

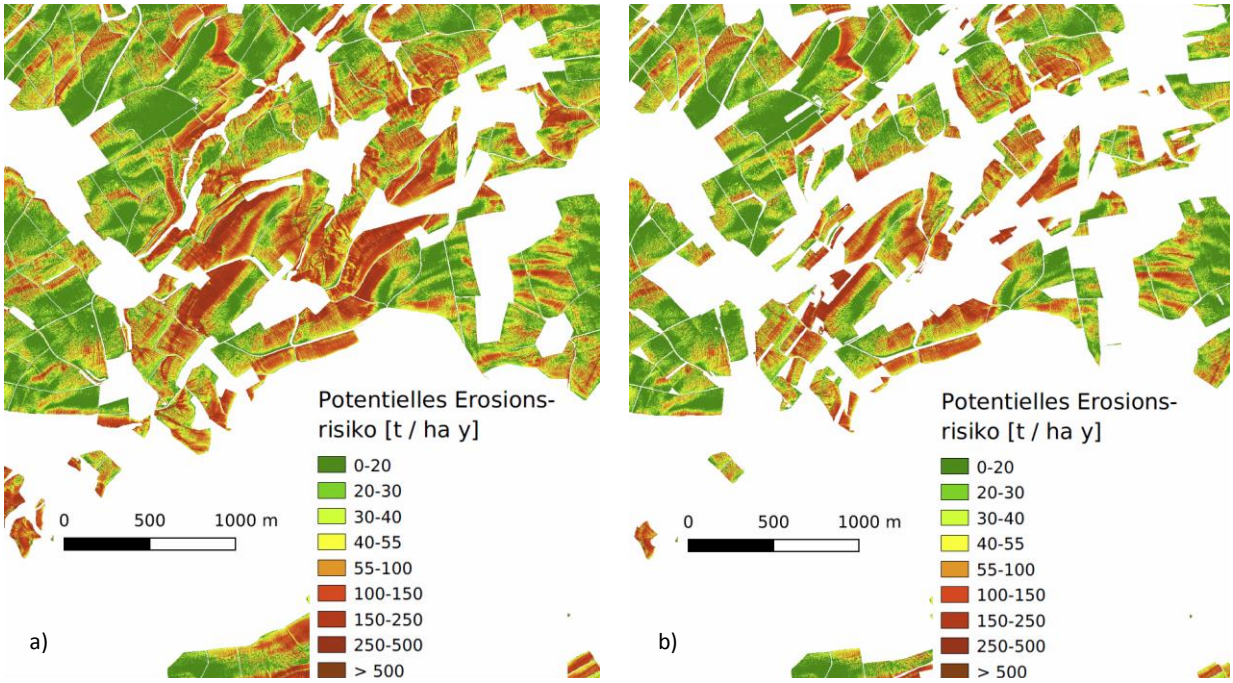

Abbildung 14: Potentielles Erosionsrisiko (unkorrigiert): a) mit Dauergrünland und Sömmerungsgebiet b) ohne Dauergrünland und Sömmerungsgebiet für das Gebiet um Frienisberg.

3.6 Zusammenfassende Beurteilung der neuen Grundlagen bzw. Faktoren

- **Feldblockkarte:** Die neue Feldblockkarte führt zu genaueren und aktuelleren Feldblöcken. Der Einfluss auf das berechnete Erosionsrisiko ist schweizweit gering. Im Einzelfall kann die veränderte Feldblockgrösse zu höherem oder niedrigerem Erosionsrisiko führen. Bezüglich Kartenblatt LK 1146 Lyss sinkt das potentielle Erosionsrisiko um rund 1 % aufgrund der unterschiedlichen Feldblockkarten (ERK 2010 vs 2019).

- **Fliessweg L-Faktor:** Ausgewählt für die Berechnung der neuen ERK2 (2019) wurde der Algorithmus MTFD von Seibert & Glynn (2007) mit der Konvergenzeinstellung 1.1. Der mit einer neuen Methode und neuen Datengrundlagen berechnete L-Faktor unterscheidet sich nicht relevant vom bisherigen L-Faktor. Auf der LK 1146 Lyss ist der neu berechnete L-Faktor im Mittel um knapp 1 % höher, d.h. das Erosionsrisiko für das Ackerland der Schweiz wird auch ca. 1 % höher eingestuft. Auf einzelnen Parzellen kann es aber zu grösseren Abweichungen kommen.
- **Hangneigung S-Faktor:** Die Berechnungsweise des S-Faktors hat sich nicht geändert. Das neue digitale Geländemodell und die neue Feldblockkarte können vereinzelt zu geringen Abweichungen führen. Auf der LK 1146 Lyss ist der neu berechnete S-Faktor sehr ähnlich. Der S-Faktor weist im LK 1146 Lyss einen 4 % höheren Mittelwert als in der alten ERK2 auf. Folglich erhöht sich das Erosionsrisiko im Vergleich zur alten ERK2 leicht.
- **Erodibilität K-Faktor:** Die Berechnungsweise des K-Faktors hat sich nicht geändert. In den Regionen, in denen neue Bodenkarten zur Verfügung standen (Teile der Kantone BE, FR, LU, SO, GR, VS), liegen räumlich und qualitativ bessere Daten vor, die zu positiven oder negativen Abweichungen beim Bodenabtrag führen können. Auf der LK 1146 Lyss ist der neu berechnete K-Faktor aufgrund detaillierter neuer Bodendaten im Mittel um rund 24 % geringer.
- **Erosivität R-Faktor**: Die neu erstellte R-Faktorkarte der Schweiz führt zu generell höheren R-Faktoren. Dadurch erhöht sich der berechnete mittlere Bodenabtrag um ca. 20 % im Mittel für die Schweiz. Für das Kartenblatt LK 1146 Lyss ist eine Erhöhung um 13 % gegenüber der alten ERK2 berechnet worden.
- **Potentielles Erosionsrisiko**: Das potentielle Erosionsrisiko (unkorrigiert) der LN ist auf der LK 1146 Lyss im Mittel um knapp 5 % niedriger als in der bisherigen ERK2. Das potentielle Erosionsrisiko (unkorrigiert) der Ackerflächen ist im Mittel um 11 % geringer. Der deutlich niedrigere K-Faktor (neue Bodenkarte) wird durch einen deutlich höheren R-Faktor und leicht erhöhten LS-Faktor nicht komplett kompensiert. Auf einzelnen Parzellen kann es zu grösseren Abweichungen kommen. Insgesamt ist in der Schweiz aber im Mittel mit einer Erhöhung des potentiellen Erosionsrisikos von ca. 17 % zu rechnen, da nur vereinzelt neue Bodenkarten vorliegen. Die im Mittel deutlich höheren R-Faktoren und leicht höheren LS-Faktoren der neuen Berechnungsweise führen zu diesem Anstieg.
- **Separierung Ackerland**: Durch das Ausschneiden des Dauergrünlandes sinkt das berechnete mittlere potentielle Erosionsrisiko. Im Kanton Bern mit sehr hohem Dauergrünlandanteil ist dies massiv. Legt man das Kartenblatt LK 1146 Lyss als Ackerbauregion zugrunde, beträgt der Dauergrünlandanteil 25 %, was ein Absinken des mittleren Bodenabtrages (unkorrigiert) von 23 % und des aufsummierten Bodenabtrages (unkorrigiert) um 43 % zur Folge hat.
- Für 19 Kantone mit knapp 75 % der Ackerfläche der Schweiz konnte die Ackerfläche parzellenscharf separiert werden. Das potentielle Erosionsrisiko (unkorrigiert) auf diesen Ackerflächen beträgt im Mittel 87 t ha^{-1} a^{-1}.

4. Kalibrierung und Validierung des Erosionsmodells

Die wissenschaftlichen Grundlagen des verwendeten Erosionsmodells und dessen Kalibrierung und Validierung werden in wissenschaftlichen Publikationen ausführlich beschrieben (Bircher et al. 2019a, b). Im Folgenden werden nur die wichtigsten Erkenntnisse zusammenfassend widergegeben.

4.1 Quantitative Statistik

Für die Kalibrierung und Validierung des Erosionsmodells standen die von Prasuhn (2010, 2011, 2012) kartierten Bodenabträge der Periode 1997 bis 2007 für 203 Parzellen der Region Frienisberg zur Verfügung. Sie stellen den langjährigen mittleren Bodenabtrag dar und können mit den verschiedenen Modellberechnungen der RUSLE verglichen werden, wenn entsprechende Bedeckungs- und Schutzfaktoren (C und P) im Modell eingesetzt werden. Parzellenscharfe C- und P-Faktoren für diese Periode standen von Prasuhn (unveröffentlicht) zur Verfügung. Die analogen Kartierungen wurden von Schelbert (2016) digitalisiert und in ein 2x2m-Raster transformiert, um auch eine räumliche Vergleichbarkeit zu ermöglichen.

Im ersten Schritt der Kalibrierung und Validierung wurden die mittleren modellierten Abtragswerte mit den mittleren kartierten Abtragswerten aller 203 Parzellen verglichen. Die Modelle wurden zur besseren Vergleichbarkeit mit log10 transformiert und die kartierten Daten einer kubischen Transformation (Normalisierung) unterzogen. Den niedrigsten Standardfehler bezüglich der Abtragswerte aller 203 Parzellen weist der Algorithmus Watershed 10 auf, den grössten Standardfehler hat MTFD 0. Zu beachten ist jedoch, dass kartierte Erosionsursachen wie externer Wasserzufluss und Fahrspuren vom Erosionsmodell nicht berücksichtigt werden. Es wurden also die Parzellen entfernt, welche die oben erwähnten Erosionsursachen aufweisen. Auch die Parzellen, die keine Erosion innerhalb der 10-jährigen Messstudie hatten, wurden entfernt, da davon auszugehen ist, dass diese irgendwann einmal Bodenabtrag haben werden. Im Erosionsmodell ist eine Erosion von Null auf Ackerflächen nicht möglich. So wurde die bestmögliche Übereinstimmung von Modell und kartiertem Abtrag gewährleistet. Nun wurden die Modelle und Messungen erneut transformiert und nach dem höchsten und niedrigsten Standardfehler untersucht (Tabelle 15). Den niedrigsten Standardfehler weist der Ansatz nach MUSLE 87 bei Gisler et al. (2010) auf. Den zweitniedrigsten Standardfehler zeigt der MTFD 1.1-Algorithmus und den grössten Standardfehler hat der Watershed-Algorithmus mit Konvergenzwert 1. Da die Standardfehler jedoch sehr ähnlich sind, reicht diese Auswertung für einen Entscheid des passenden Algorithmus nicht aus. Eine Tendenz Richtung MTFD lässt sich aber erkennen, da der MUSLE87 Ansatz veraltet und nicht mehr verfügbar ist (Tabelle 15).

Tabelle 15: Standardfehler der gefitteten Modelle gegenüber den mittleren Abtragswerten der 203 Parzellen nach Entfernung von Erosionsursachen wie Fahrspuren, externer Wasserzufluss und Parzellen ohne Erosion (0 t ha^{-1} a^{-1}).

Algorithmus	MFD			MTFD			Watershed			DINF	MUSLE87
Konvergenzwert	0	1.1	1.25	0	1.1	1.25	1	5	10	1.1	-
Standardfehler	0.5876	0.5874	0.5874	0.5873	0.5871	0.5871	0.5905	0.5895	0.589	0.5874	0.5851

Im zweiten Schritt wurde eine weitere Kalibrierung und Validierung anhand der aufsummierten Bodenabträge der fünf Gebiete Frienisberg, Suberg, Seedorf, Schwanden und Lobsigen durchgeführt und ebenfalls mit dem Standardfehler überprüft. Zur Kalibrierung wurden die kartierten Abtragswer-

te um 10 % erhöht, da es möglich ist, dass die Bodenabträge bei der Kartierung leicht unterschätzt wurden, weil z.B. kleine Erosionsereignisse übersehen wurden (Prasuhn Expertenwissen). Den niedrigsten Standardfehler erreichte der MTFD 1.1-Algorithmus. Jedoch ergab die Validierung einen um 38 t a^{-1} niedrigeren Summenwert des Bodenabtrages als die aufsummierten Bodenabträge aus den 10-jährigen Kartierungen (1997-2007). Die anderen Modelle haben jedoch noch höhere Abweichungen (Tabelle 16; Abbildung 15).

Tabelle 16: Kalibrierung und Validierung der Modelle mit 10 jährigen Erosionsabschätzungen auf Basis der aufsummierten kartierten Abtragswerte + 10 % (1997-2007). Beispiele mit hohem (Watershed1), mittlerem (DINF 1.1) und niedrigem (MTFD1.1; grau hinterlegt) RMSE (Standardfehler); FR=Frienisberg LO=Lobsigen SCH=Schwanden SE=Seedorf SU=Suberg.

		Originale Mittelwerte der Modelle [t a^{-1}]			Kalibrierte Modelle [t a^{-1}] $y=ax^b$			Validierte Modelle [t a^{-1}] Angewendete Fits		
Gebiet	Summierte kartierte Abtragswerte 1997-2007 in t/ yr+ 10%	MTFD 1.1	Watershed1	DINF 1.1	MTFD1.1 Eq.1: a=0.0623 b= 1.14053	Watershed 1 Eq.2: a=0.01135 b=1.39185	DINF 1.1 Eq.3: a= 0.04224 b=1.20824	MTFD 1.1	Watershed1	DINF 1.1
FR	67.7	461.8	512.9	450.5	68.11	67.14	67.9	48.84	24.4	39.7
LO	18.1	189.7	270.4	200.1	24.66	27.54	25.5	16.52	8.5	13.6
SCH	8.0	81.0	102.9	84.7	9.34	7.17	9.02	7.10	3.08	5.7
SE	5.0	71.6	79.7	71.40	8.13	5.02	7.34	6.05	2.3	4.7
SU	33.2	181.09	247.4	187.42	23.37	24.3	23.5	15.10	6.9	11.8
Summe	132.0	985.1	1213.2	994.1	133.6	131.2	133.3	93.6	45.2	75.5

Die Validierung zeigt bei den drei Gebieten mit durchschnittlichen Abtragswerten niedriger als 20 t a^{-1} eine gute Übereinstimmung, jedoch zeigt sich eine Unterschätzung bei den beiden Gebieten mit hohen durchschnittlichen Abtragswerten > 20 t a^{-1}. D.h., dass von der Validierung Gebiete (3 & 5) mit hohen durchschnittlichen Abtragswerten (>20 t a^{-1}) unterschätzt werden und Gebiete (1, 2 & 4) mit niedrigen oder mittleren Werten (5-20 t a^{-1}) relativ gut abgeschätzt werden (Abbildung 15).

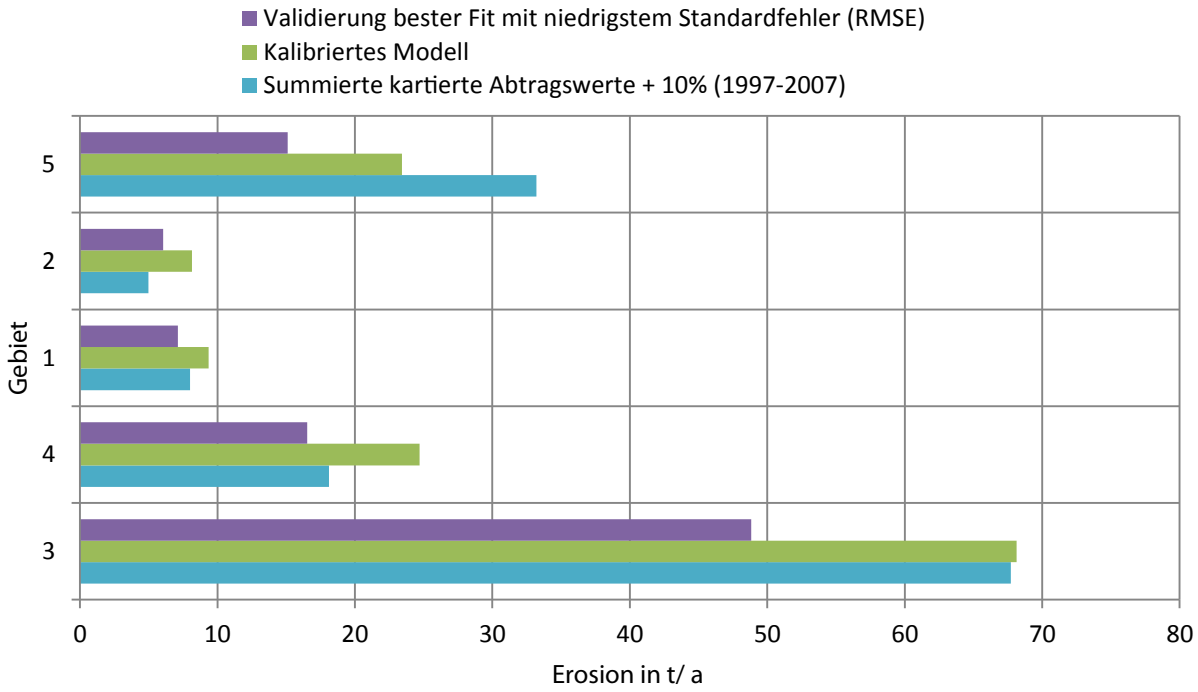

Abbildung 15: Darstellung der aufsummierten Abträge +10 % (1997-2007) gegenüber dem kalibrierten Modell und der angewendeten Validierung für MTFD 1.1; 1=Schwanden, 2=Seedorf,3=Frienisberg, 4=Lobsigen, 5=Subergentnommen aus Tabelle 16.

4.2 Pseudo -Qualitative Analyse

Ein direkter pixel-basierter Vergleich zwischen aufsummierten, digitalisierten kartierten Bodenabträgen über 10 Jahre und den mit verschiedenen Modellen berechneten Bodenabträgen war nicht zielführend. Die aufgezeigte und auch aus der Literatur bekannte Überschätzung der modellierten Abtragswerte sowie die Lageungenauigkeit der kartierten Bodenabträge lässt kaum exakte Übereinstimmungen der Abtragswerte einzelner Pixel erwarten. Entsprechend ergab sich auch kein Zusammenhang bei einem pixelbasierten Vergleich im Gebiet Frienisberg. Daher wurden die kartierten Abtragswerte klassiert und die Klassen verglichen. Da es von prioritärem Interesse ist, die Flächen mit hohen kartierten Bodenabträgen mit dem Modell bestmöglich abzubilden, haben wir uns bei diesem Vergleich auf Bereiche mit mittlerer bis hoher Erosion konzentriert. Zwei Bodenabtragsklassen wurden basierend auf den aufsummierten digitalisierten Kartierdaten von 1997-2007 gebildet (Schelbert 2016). Klasse 1 entspricht den aufsummierten Bodenabträgen zwischen 4 t ha^{-1} a^{-1} bis 10 t ha^{-1} a^{-1}, Klasse 2 stellen aufsummierten Bodenabträge über 10 t ha^{-1} a^{-1} dar. Dies wurde über das ganze Gebiet (Frienisberg, Suberg, Lobsigen, Seedorf und Schwanden) durchgeführt. (siehe Beispiel: Frienisberg; Abbildung 16).

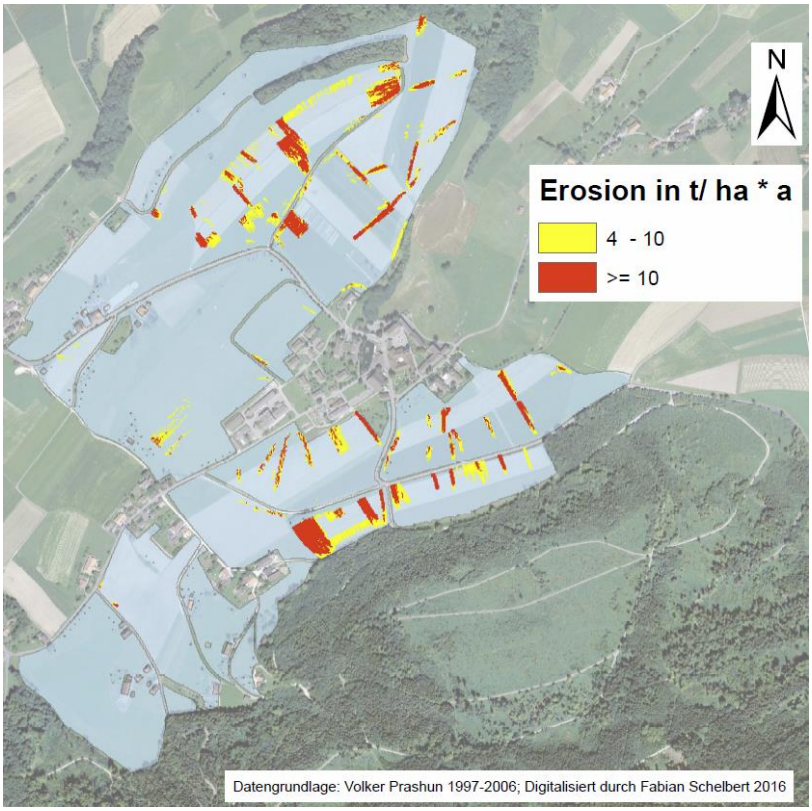

Abbildung 16: Aufsummierter Bodenabtrag nach Klassen in t/ha*a für den Zeitraum 1997-2007, digitalisiert von Schelbert (2016); hinterlegt mit Feldblockplan in Frienisberg.

Eine wichtige Rolle spielt in der pseudo-qualitativen Analyse die Streuung (Dispersion) der Fliesswege, die über die verschiedenen Konvergenzeinstellungen der Modelle gewählt werden kann. Insgesamt zeigt sich eine relativ gute Übereinstimmung zwischen 60-70 % - je nach Modell und Konvergenzeinstellung - bei der höheren Abtragsklasse 2. Bei der niedrigeren Abtragsklasse 1 ist die Übereinstimmung mit 20-25 % gering, d.h. im Modell werden diese Pixel häufig mit höherem oder geringerem Bodenabtrag abgebildet (Tabelle 17). Da die RUSLE-Modelle und deren Derivate ohne Kalibrierung und Validierung Bodenabträge überschätzen, ist ein Korrekturfaktor angezeigt, welcher zu einer höheren Übereinstimmung bei beiden Klassen führen könnte (Klik & Zartl 2001, Rymszewicz et al. 2015, Hammad et al. 2004). Details zum Korrekturfaktor werden in Bircher et al. (2019b) ausführlich diskutiert. Bei höherer Streuung (MFD & MTFD 0; Watershed 1) ist die Übereinstimmung besser als bei niedriger Streuung bezüglich Klasse 2 (>10 t ha^{-1} a^{-1}). Bezüglich Klasse 1 (4 t ha^{-1} a^{-1} – 10 t ha^{-1} a^{-1}) würde sich eher der Watershed-Algorithmus mit Konvergenzwert 10 eigenen, die Unterschiede zwischen den Modellen und Konvergenzen sind hier aber recht klein. Da das Ziel der Erosionsrisikokarte eher auf der möglichst guten Abbildung der grösseren Abträge (> 10 t ha^{-1} a^{-1}) liegt, zeigt der MTFD-Algorithmus mit dem Konvergenzwert 0 die besten Werte (Tabelle 17).

Tabelle 17: Qualitative Analyse von kartierten Ereignissen pixelbasiert und Vergleich der Modelle im gesamten Gebiet (Frienisberg, Suberg, Seedorf, Lobsigen und Schwanden); hellblau hinterlegt niedrigste Übereinstimmung; grün hinterlegt höchste Übereinstimmung.

Klasse	Gesamt-zahl Pixel	MFD			MTFD			Watershed			DINF	MUSLE 87
	Konvergenz	0	1.1	1.25	0	1.1	1.25	1	5	10	1.1	-
4 t - <= 10 t	12‘796	2626	2793	2810	2514	3056	3058	2822	3062	3159	3134	2871
Anteil in %	100	20.5	21.8	22.0	19.6	23.9	23.9	22.0	23.9	24.7	24.5	22.4
>10 t	9340	6334	6228	6210	6450	5850	5845	6323	5963	5599	5824	5750
Anteil in %	100	67.8	66.7	66.5	69.1	62.6	62.6	67.7	63.8	59.9	62.4	61.6

4.3 Synthese der verschiedenen statistischen Verfahren

Aufgrund der verschiedenen statistischen Auswertungen lässt sich der optimale Algorithmus eruieren. Die ausgewählten vier neuen Multiple Flow Algorithmen (mit verschiedenen Konvergenzeinstellungen) unterscheiden sich nicht gravierend untereinander und vom bisher verwendeten Algorithmus MUSLE87. Der **MTFD-Algorithmus** kristallisiert sich aber als Favorit bei den pseudo-qualitativen Analysen und den Auswertungen nach den fünf Gebieten heraus. Bei geringer Streuung sinkt die pseudo-qualitative Übereinstimmung (MTFD 1.25) allerdings. Um die Streuung und Konvergenz ausgeglichen zu berücksichtigen, haben wir den **Konvergenzwert 1.1** verwendet, welcher die beiden Extreme 0 und 1.25 berücksichtigt.

Der Vergleich von kartierten Bodenabtragsdaten und modellierten Abtragswerten unter Einbezug von parzellenscharfen K-, C- und P-Faktoren (= aktuelles Erosionsrisiko) zeigt eine massive Überschätzung der modellierten Abtragswerte gegenüber den kartierten Abträgen. Ein entsprechender Korrekturfaktor wurde entwickelt (Kap. 5). Eine präzise Kalibrierung und Validierung und deren Diskussion finden sich in Bircher et al. (2019b).

5. Korrektur der Erosionsrisikokarte und Ergebnisse der neuen ERK2 (2019) des Ackerlandes

5.1 Korrektur der Erosionsrisikokarte

Beim Vergleich der mit dem gewählten Algorithmus MTFD 1.1 (Seibert & Glynn (2007) berechneten aktuellen Bodenabträge mit den 10-jährigen kartierten Bodenabträgen in der Region Frienisberg ergab sich im Mittel eine massive Überschätzung der Bodenabträge durch das Erosionsmodell. Diese Überschätzung war jedoch nicht überall gleich gross. Dort, wo hohe Bodenabträge kartiert wurden, sagte das Modell auch ähnlich hohe Bodenabträge vorher und stimmte relativ gut. Dort, wo sehr geringe oder keine Bodenabträge kartiert wurden, sagte das Modell aber oftmals auch hohe Bodenabträge vorher. In den Bereichen, wo für Fliesswege hohe L-Faktoren vorkommen (Geländemulden, grosse Hanglängen, grosse hydrologische Wassereinzugsgebiete) und viel Rillenerosion oder flächenhaft-lineare Erosion kartiert wurde, stimmten Modell und Kartierung relativ gut überein, während in Bereichen mit hohen S-Faktoren (steile, gestreckte Hangpartien) das Modell hohe flächenhafte Erosion vorhersagt, die aber im Feld so nicht kartiert wurde. Aufgrund dieser Beobachtung haben wir verschiedene Varianten mit unterschiedlicher Gewichtung der LS-Faktoren getestet. Eine leichte Erhöhung des L-Faktors (Faktor 1,1) bei gleichzeitiger entsprechender Verringerung des S-Faktors (Faktor 0,9) führte zu einer besseren räumlichen Verteilung der modellierten Bodenabträge (Abbildung 18-22, Tabelle 18; Details dazu siehe Bircher et al. 2019b).

Visuell ergeben sich auf den ersten Blick zwischen alter ERK2 2010, neuer unkorrigierter ERK2 2019 und neuer LS-Faktor-korrigierter ERK2 2019 kaum Unterschiede (Abbildung 17). Bei einer detaillierten Analyse und statistischen Auswertung zeigen sich aber Unterschiede (Tabelle 18). Die Maximalwerte liegen bei der unkorrigierten ERK2 2019 und der LS-Faktor-korrigierten ERK2 2019 erheblich höher als bei der ERK2 2010. Die Mittelwerte hingegen und Standardabweichungen sowie Minimumwerte zeigen keine grossen Unterschiede, was die Ähnlichkeit der Ansätze unterstreicht.

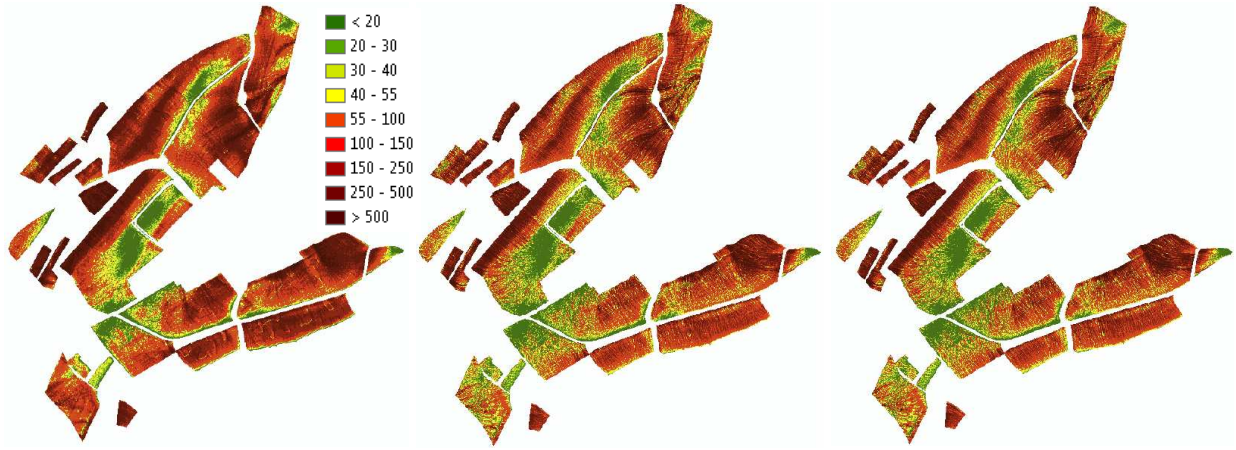

Abbildung 17: Vergleich der Karten des potentiellen Erosionsrisikos der alten ERK2 2010 (links) mit der unkorrigierten neuen ERK2 2019 (mitte) und der neuen ERK2 2019 mit korrigiertem LS-Faktor (Gewichtung L-Faktor 1,1 und S-Faktor 0,9) (rechts) für das Teilgebiet Frienisberg.

Tabelle 18: Potentielles Erosionsrisiko in t ha^{-1} a^{-1} der verschiedenen Ansätze für das Teilgebiet Frienisberg (s. Abb. 17).

	ERK2 2010 unkorrigiert	ERK2 2019 unkorrigiert standard Ansatz	ERK2 2019 Ansatz mit LS-Korrektur
Minimum	0.99	0.54	0.61
Mittelwert	166.3	134.8	117.7
Maximum	2202	5108	5285
Standardabweichung	146.5	157.5	149.2

In einem zweiten Schritt musste aber trotzdem noch eine generelle Modellkorrektur durchgeführt werden, da die so berechneten Bodenabträge deutlich zu hoch waren (Tabelle 19). Ein Vergleich der modellierten und gemessenen Werte für verschiedene Erosionsklassen zeigt dass die Überschätzung in den unteren und mittleren Klassen den einen Faktor von 4 bis 6 erreicht in den oberen Klassen Faktor 9 oder sogar 13 erreichen kann. Als Korrekturfaktor wurde der Wert 5 gewählt. D.h., alle modellierten Bodenabtragswerte wurde durch 5 dividiert. In Anbetracht der Unsicherheiten bei der Modellierung und der Kartierung und im Sinne der Prävention wurde diese eher konservative Korrektur gewählt. Mit dem Faktor 5 wurde sichergestellt, dass der mittlere modellierte Bodenabtrag weiterhin klar über dem kartierten mittleren Bodenabtrag liegt (Tabelle 19). Durch diese Korrektur kann die Berechnung des aktuellen Erosionsrisikos ohne weitere Korrektur direkt aus dem potentiellen Erosionsrisiko gemacht werden.

Tabelle 19: Einteilung in potentielle Erosionsklassen zur Kontrolle von Korrekturansätzen bezüglich der Gebiete (Frienisberg, Lobsigen, Seedorf, Suberg und Schwanden).

	Einheit	Klasse 1	Klasse 2	Klasse 3	Klasse 4	Klasse 5	Klasse 6	Summe
Erosionsklassen	t/ha	0-20	20-40	40-80	80-160	160-320	> 320	-
Anzahl Pixel	N	231'191	133'567	116'847	90'181	44'452	15'203	631'441
Fläche in ha	ha	92.5	53.4	46.7	36.1	17.8	6.1	252.6
Unkorrigiertes potentielles Erosionsrisiko der summierten Pixel pro Klasse	t	1082.9	1527.3	2678.8	4055.4	3878.3	2967.5	16190.3
Unkorrigiertes aktuelles Erosionsrisiko der summierten Pixel pro Klasse	t	98.1	136.0	231.3	356.3	359.1	281.4	1462.1
Kartierte Erosion	$t\ a^{-1}$	24.9	26.0	37.8	48.4	38.6	21.1	196.8
Korrekturfaktor berechnet	-	4	5	6	7	9	13	7
Aktuelles Risiko mit verwendetem Ansatz	$T\ a^{-1}$	17.3	23.5	40.5	62.6	63.6	52.3	259.7

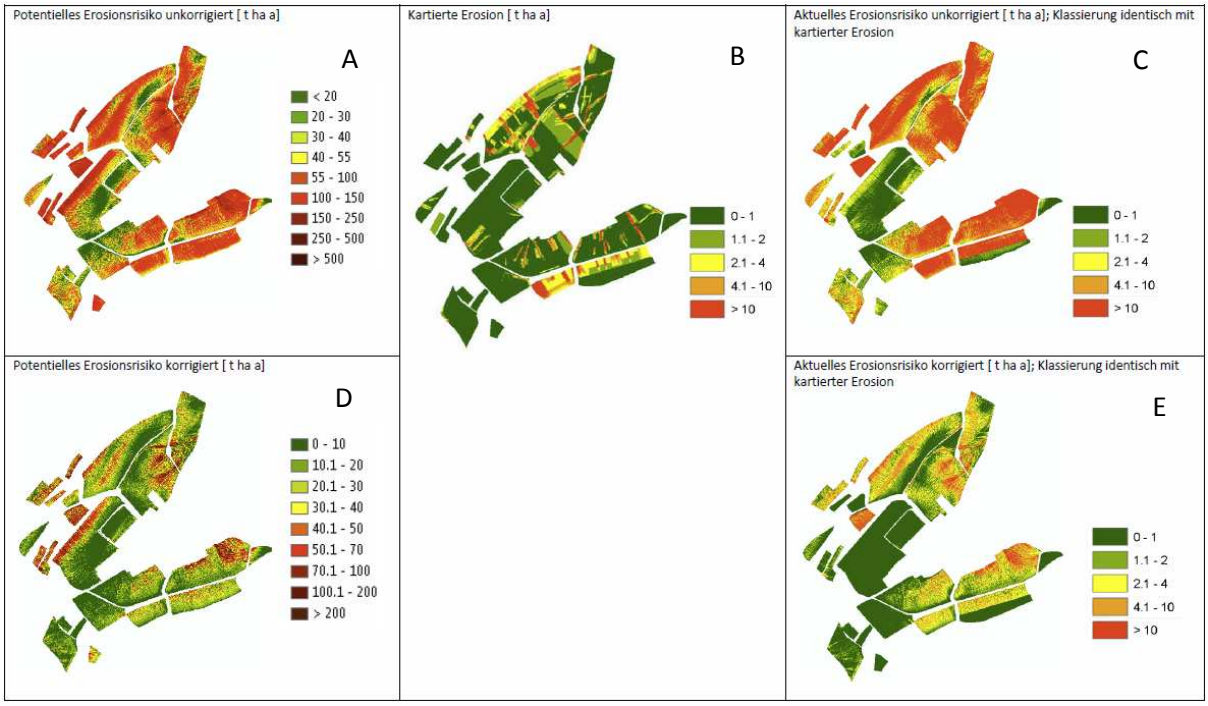

Abbildung 18: Vergleich von unkorrigierten und korrigierten Erosionsrisiko mit dem kartierten Erosionsrisiko für das Gebiet Frienisberg. A: unkorrigiertes potentielles Erosionsrisiko mit alter Klassierung, B: mittlerer kartierter Bodenabtrag über 10 Jahre, C: unkorrigiertes aktuelles Erosionsrisiko mit parzellenscharfen C- und P-Faktoren, D: korrigiertes potentielles Erosionsrisiko (LS-Faktorgewichtung 1.1 zu 0.9 und Division durch Faktor 5) mit neuer Klassierung, E: aktuelles korrigiertes Erosionsrisiko.

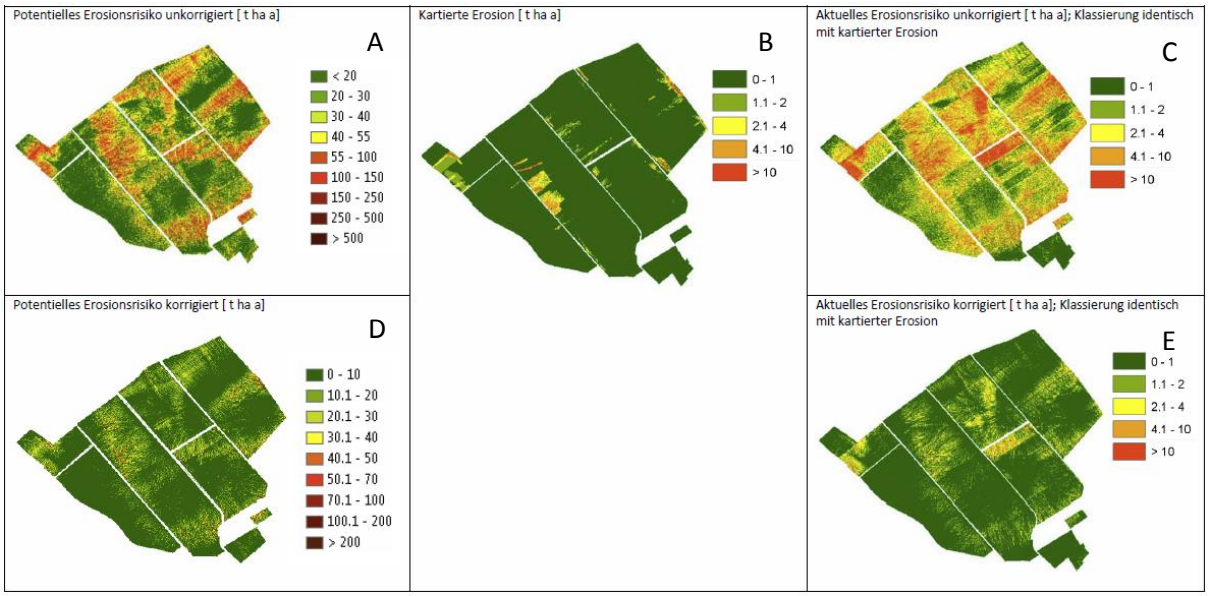

Abbildung 19: Vergleich von unkorrigierten und korrigierten Erosionsrisiko mit dem kartierten Erosionsrisiko für das Gebiet Lobsigen. A: unkorrigiertes potentielles Erosionsrisiko mit alter Klassierung, B: mittlerer kartierter Bodenabtrag über 10 Jahre, C: unkorrigiertes aktuelles Erosionsrisiko mit parzellenscharfen C- und P-Faktoren, D: korrigiertes potentielles Erosionsrisiko (LS-Faktorgewichtung 1.1 zu 0.9 und Division durch Faktor 5) mit neuer Klassierung, E: aktuelles korrigiertes Erosionsrisiko.

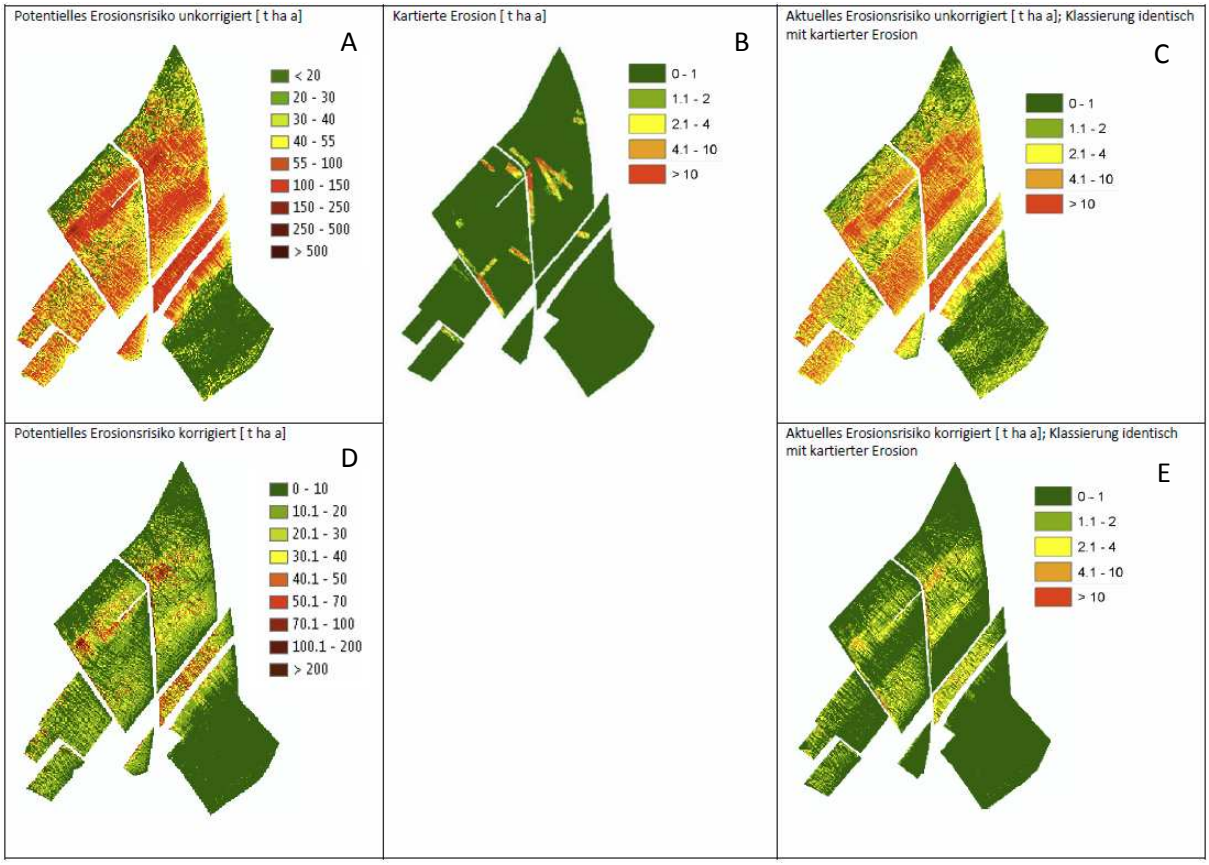

Abbildung 20: Vergleich von unkorrigierten und korrigierten Erosionsrisiko mit dem kartierten Erosionsrisiko für das Gebiet Seedorf. A: unkorrigiertes potentielles Erosionsrisiko mit alter Klassierung, B: mittlerer kartierter Bodenabtrag über 10 Jahre, C: unkorrigiertes aktuelles Erosionsrisiko mit parzellenscharfen C- und P-Faktoren, D: korrigiertes potentielles Erosionsrisiko (LS-Faktorgewichtung 1.1 zu 0.9 und Division durch Faktor 5) mit neuer Klassierung, E: aktuelles korrigiertes Erosionsrisiko.

Abbildung 21: Vergleich von unkorrigierten und korrigierten Erosionsrisiko mit dem kartierten Erosionsrisiko für das Gebiet Suberg. A: unkorrigiertes potentielles Erosionsrisiko mit alter Klassierung, B: mittlerer kartierter Bodenabtrag über 10 Jahre, C: unkorrigiertes aktuelles Erosionsrisiko mit parzellenscharfen C- und P-Faktoren, D: korrigiertes potentielles Erosionsrisiko (LS-Faktorgewichtung 1.1 zu 0.9 und Division durch Faktor 5) mit neuer Klassierung, E: aktuelles korrigiertes Erosionsrisiko.

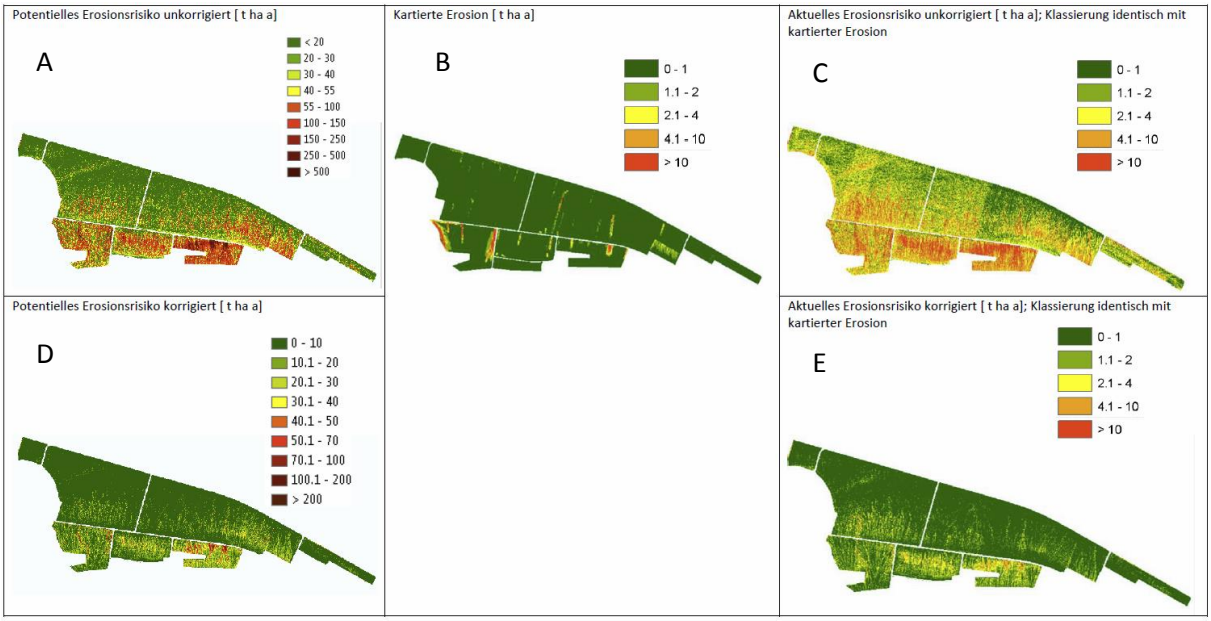

Abbildung 22: Vergleich von unkorrigierten und korrigierten Erosionsrisiko mit dem kartierten Erosionsrisiko für das Gebiet Schwanden. A: unkorrigiertes potentielles Erosionsrisiko mit alter Klassierung, B: mittlerer kartierter Bodenabtrag über 10 Jahre, C: unkorrigiertes aktuelles Erosionsrisiko mit parzellenscharfen C- und P-Faktoren, D: korrigiertes potentielles Erosionsrisiko (LS-Faktorgewichtung 1.1 zu 0.9 und Division durch Faktor 5) mit neuer Klassierung, E: aktuelles korrigiertes Erosionsrisiko.

Tabelle 20: Statistische Werte für potentielles und aktuelles Erosionsrisiko (unkorrigiert / korrigiert) und kartierter Erosion) aller fünf Gebiete (Frienisberg, Lobsigen, Seedorf, Suberg und Schwanden) aus Abb 18-22 in t / ha a.

	Pot. Erosionsrisiko unkorrigiert	**Kartierte Erosion**	**Aktuelles Erosionsrisiko unkorrigiert**
Minimum	0.90	0.00	0.01
Mittelwert	56.70	0.77	5.10
Maximum	7‘165	532	1‘174
Standardabweichung	93.2	4.3	10.9
	Pot. Erosionsrisiko korrigiert		**Aktuelles Erosionsrisiko korrigiert**
Minimum	0.18		0.002
Mittelwert	11.34		1.02
Maximum	1‘433		235
Standardabweichung	18.6		2.2

Aus den Abbildungen 18-22 und Tabelle 20 wird ersichtlich, dass das aktuelle Erosionsrisiko bei der unkorrigierten Modellversion massiv über den mittleren kartierten Bodenabträge liegt. Nach der Modellkorrektur ergibt sich dagegen eine relativ gute Übereinstimmung zwischen modellierten und kartiertem Bodenabtrag. Die meisten Areale mit hoher kartierter Erosion zeigen auch in der modellierten Version ein hohes Erosionsrisiko. Viele Flächen mit geringem kartierten Bodenabtrag zeigen nun auch im Modell ein geringes Erosionsrisiko. Auf einzelnen Parzellen oder Arealen kann es aber weiterhin zu Abweichungen kommen. Die Realität ist sehr komplex und kann mit dem relativ einfachen Erosionsmodell in einigen Fällen nur bedingt oder nicht richtig abgebildet werden.

Die Korrektur des Erosionsmodells bedingt auch, dass die Klassierung des potentiellen Erosionsrisikos (Klasseneinteilung und Farbgebung) ebenfalls neu gestaltet werden musste. Hier wurde ein möglichst pragmatisches Vorgehen gewählt und ein einfacher und zugleich transparenter Ansatz gewählt. Der mittlere C-Faktor der am häufigsten vorkommenden Ackerkultur in der Schweiz (Winterweizen) liegt bei rund 0,11. Der mittlere C-Faktor von typischen Kulturabfolgen der Schweiz liegt nach Prasuhn & Blaser (2018) in etwa bei 0,12. Berücksichtigt man noch den P-Faktor, ergibt sich ein CP-Wert von ungefähr 0,10. Das bedeutet, dass das aktuelle Erosionsrisiko im Mittel der Ackerflächen der Schweiz um einen Faktor 10 kleiner als das potentielle Erosionsrisiko ist. Legt man für das aktuelle Erosionsrisiko die Richtwerte der Verordnung über Belastungen des Bodens (VBBo) in Höhe von 2 bzw. 4 t/ha und Jahr zugrunde sowie den Wert von 2 t/ha für relevante Erosion eines Einzelereignisses gemäss Direktzahlungsverordnung (DZV), ergeben sich für das potentielle Erosionsrisiko entsprechend Schwellenwerte von 20 bzw. 40 t/ha und Jahr. Bei einem potentiellen Bodenabtrag von <20 t/ha und Jahr besteht also bei einer durchschnittlichen Bewirtschaftung ein geringes Erosionsrisiko (Farbe grün). Bei einem potentiellen Bodenabtrag von >40 t/ha und Jahr existiert entsprechend bei einer durchschnittlichen Bewirtschaftung ein hohes Erosionsrisiko (Farbe rot), da bei einer durchschnittlichen Bewirtschaftung der VBBo-Richtwert von 4 t/ha und Jahr überschritten würde. Dem Bereich zwischen 20 und 40 t/ha und Jahr wird ein mittleres Risiko (Farbe gelb) zugewiesen (Abbildung 23).

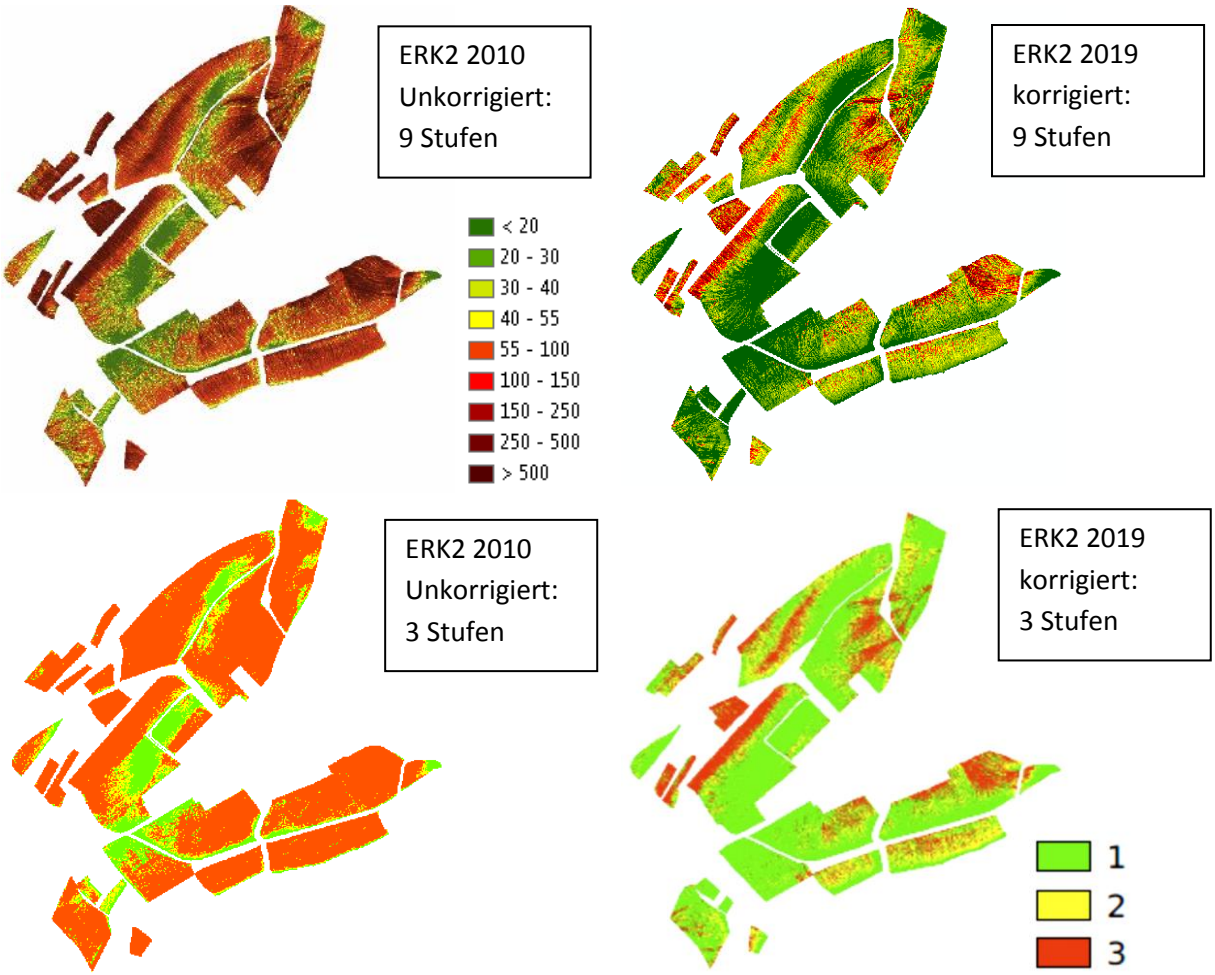

Abbildung 23: Links Erosionsklassen nach altem unkorrigiertem Ansatz (ERK2 2010); Rechts ERK2 2019 mit neuer korrigierter Klasseneinteilung (Oben 9 Klassen [t ha^{-1} a^{-1}]; Unten 3 Klassen mit 1 = geringes potentielles Erosionsrisiko, 2 = mässiges potentielles Erosionsrisiko, 3 = hohes potentielles Erosionsrisiko).

Für die praktische Anwendung (Beratung, Sensibilisierung) und den Vollzug gesetzlicher Grundlagen ergeben sich mit der neuen ERK2 2019 aber auch neue Herausforderungen bezüglich der Interpretation der Karten. Insgesamt erscheinen deutlich weniger Flächen in der Klasse «rot». Dies einerseits, weil steile Graslandflächen weggefallen sind, andererseits aber auch durch die Korrektur des berechneten potentiellen Erosionsrisikos und die neue Klassierung. Dies war zum einen gewollt, da ein häufig geäusserter Kritikpunkt der alten ERK2 der zu hohe Flächenanteil roter Flächen war und eine massive Überschätzung der Erosionswerte. Ein Feldblock, der in der alten ERK2 überwiegend rot gefärbt war und damit ein sehr hohes potentielles Erosionsrisiko angezeigt hat, erscheint in der neuen ERK2 2019 nur noch in einigen Bereichen rot eingefärbt (Abbildung 24). In diesen Bereichen besteht aber ein hohes Risiko für lineare Erosion mit sehr hohen Bodenabträgen (siehe Erosionskartierung), so dass in diesem Feldblock dringend angepasste Bewirtschaftungsmassnahmen notwendig sind. Die neue ERK2 2019 zeigt räumlich differenzierter und realitätsnaher die gefährdeten Bereiche eines Feldblocks an. In allen gelben und roten Bereichen sind Massnahmen, die über eine durchschnittliche Bewirtschaftung (C-Faktor = 0,10) hinausgehen, zur Erhaltung der Bodenfruchtbarkeit notwendig. Da sich die meisten agronomischen Massnahmen nicht auf die besonders stark erosionsgefährdeten Bereiche (z.B. Mulde) beschränken lassen, sind meistens Massnahmen auf dem gesamten Feldblock bzw. der ganzen Parzellen durchzuführen, auf denen gelbe und/oder rote Bereiche auftreten. Hier ist also ein gewisses Umdenken notwendig.

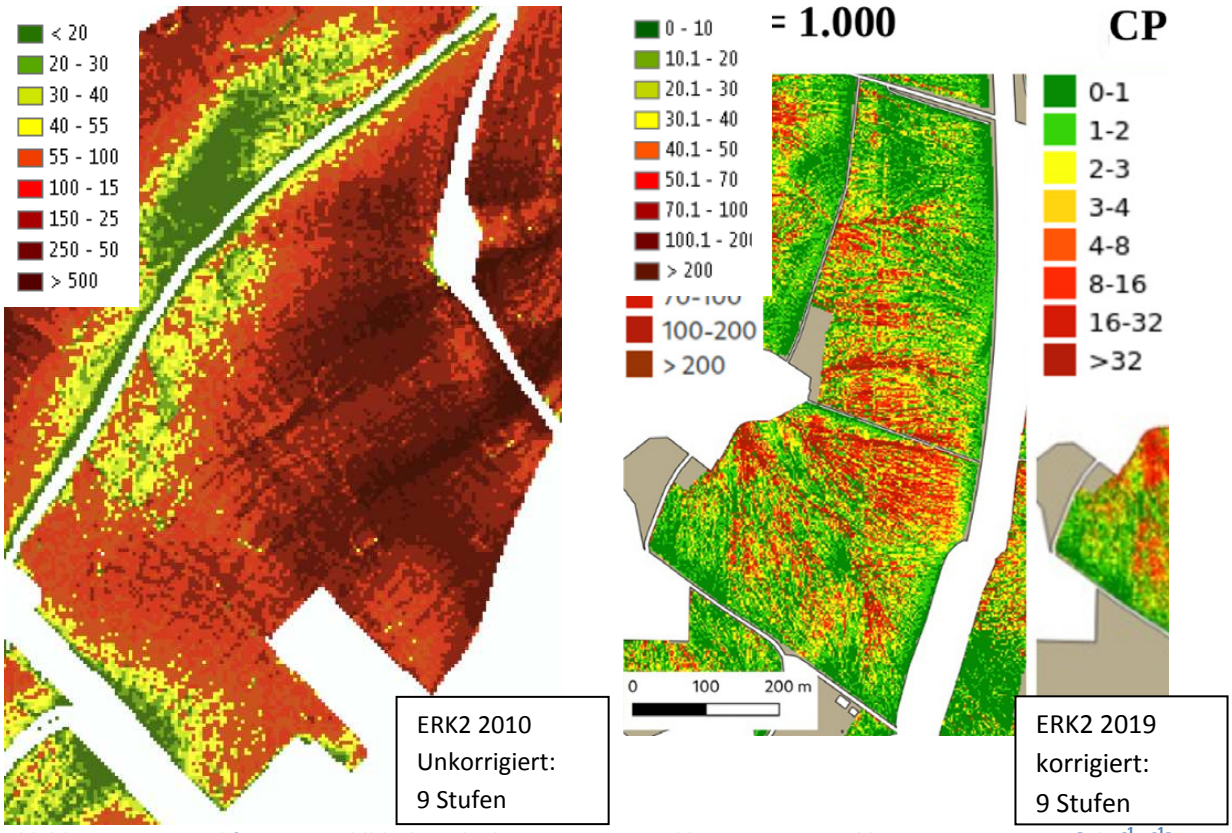

Abbildung 24: Beispiel für einen Feldblock nach alter ERK2 2010 und korrigierter, neu klassierter ERK2 2019 [t ha^{-1} a^{-1}].

5.2 Die neue, korrigierte Erosionsrisikokarte des Ackerlandes der Schweiz

Abbildung 25 zeigt die neue, korrigierte ERK2 2019 in der einfachen, dreistufigen Klassierung (Ampelsystem), Abbildung 26 die gleiche Karte in der 9-stufigen Klassierung. In beiden Karten sind die 7 Kantone, in denen keine vollständigen kantonalen Daten zur Ackerlandnutzung vorlagen und die mit der relativ ungenauen Methode 3 (Kapitel 3.5) ermittelt wurden, violett umrandet. Verschiedene Detailausschnitte der 9-stufigen Karte finden sich in Kapitel 5.3.

Der Flächenanteil des Ackerlandes welches in der grünen Klasse liegt, ist mit 79% relativ hoch. Die gelbe Klasse und rote Klasse nehmen mit jeweils 10% bzw. 11% eine kleinere, aber trotzdem relevante Fläche ein (Tabelle 21).

Tabelle 21: Flächenanteil der jeweiligen Erosionsklasse in Hektar und Prozent für die 19 Kantone mit präzisen Daten.

Erosionsrisikoklasse	Klassennummer	Klassengrösse in t ha^{-1} a^{-1}	Fläche in ha	Prozentual
Geringe Gefährdung	1	0-20	242‘963	79
Mässige Gefährdung	2	20-40	31‘156	10
Hohe Gefährdung	3	>40	32‘139	11

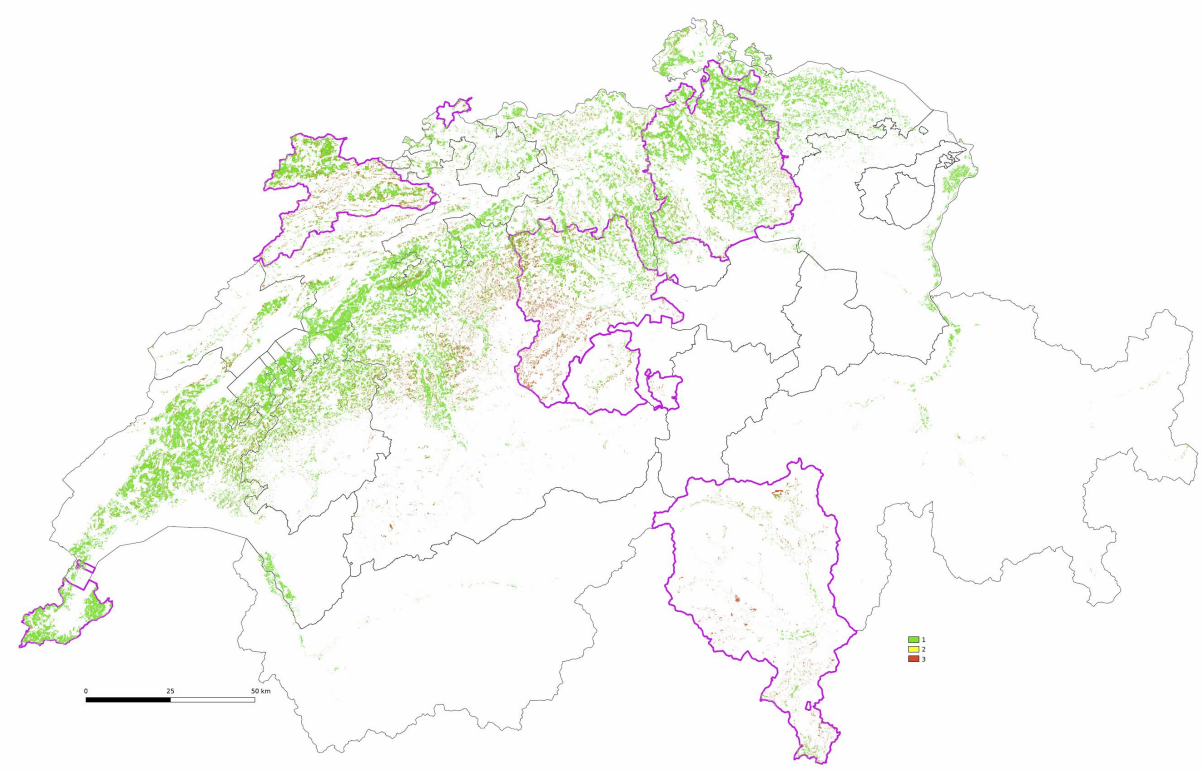

Abbildung 25: Neue Potentielle Erosionsrisikokarte ERK2 2019 des Schweizer Ackerlandes, korrigiert, mit 3-Klassenlegende für grün = geringes potentielles Erosionsrisiko, gelb = mässiges potentielles Erosionsrisiko und rot = hohes potentielles Erosionsrisiko (grössere Karte siehe Anhang).

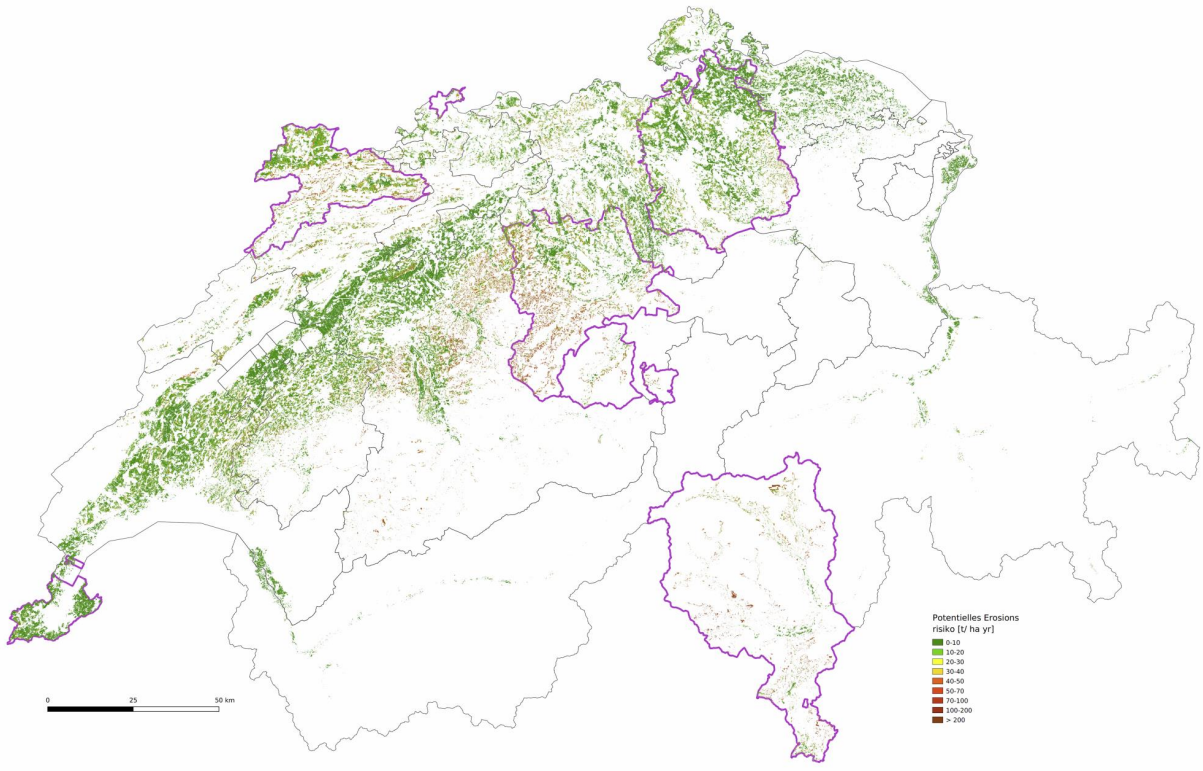

Abbildung 26: Neue Potentielle Erosionsrisikokarte ERK2 2019 des Schweizer Ackerlandes korrigiert mit 9 Klassenlegende (grössere Karte siehe Anhang).

Tabelle 22: Vergleich der Landwirtschaftlichen Nutzfläche (LN) und Ackerfläche inklusive potentiellem Erosionsrisiko (Summe und Durchschnitt der 19 Kantone) gemäss neuer ERK2 2019 mit Arealstatistik und Betriebsstrukturerhebung, Stand März 2019.

Kanton	LN ERK2 2019	LN[1]	LN[2]	Ackerland ERK2 2019	Ackerland		Verwendete Methode	Potentielles Erosionsrisiko der Ackerlandfläche	
					Daten [1]	Daten[2]		Summe [t]	Durchschnitt [in t ha^{-1} a^{-1}]
AG	59'500	61'858	60'817	33'656	37'850	36'338	1	481'552	14
AI	6'981	6'530	7'184	11	0	5	1	444	39
AR	12'297	11'778	11'865	7	7	47	1	305	44
BE	183'052	170'934	191'662	89'200	78'754	81'642	2	2'562'207	29
BL	21'333	20'073	21'621	8025	8'344	9'250	1	110'764	14
BS	443	445	428	-	245	185	3	-	-
FR	76'855	75'633	75'679	39'363	40'123	35'247	2	702'196	18
GE	11'624	11'161	11'139	-	7'738	7'431	3	-	-
GL	6'829	6'058	6'894	102	228	95	1	469	5
GR	59'621	40'673	55'866	3'682	3'715	4'015	1	27'777	8
JU	38'117	32'726	40'207	-	15'131	17'538	3	-	-
LU	71'744	71'685	76'488	-	25'730	27'701	3	-	-
NE	30'861	24'352	31'764	7'006	6'373	7'537	1	137'377	20
NW	5'667	5'280	6'002	30	41	31	1	161	5
OW	7'323	7'007	7'801	-	117	38	3	-	-
SG	67'721	67'930	71'555	7'163	8'808	8'019	1	27'782	4
SH	12'767	13'058	15'602	8'238	9'166	11'011	1	83'486	10
SO	33'211	30'226	31'528	17'875	16'090	14'757	2	300'715	17
SZ	20'932	21'597	24'381	407	848	551	1	3'930	10
TG	5'1038	51498	49'466	22'419	26'244	23'080	1	112'110	5
TI	17'789	11003	14'266	-	2'258	1'625	3	-	-
UR	6'499	5'237	6'747	7	48	10	1	19	3
VD	112'440	107'698	108'764	64'372	73'713	68'818	1	772'328	12
VS	43'209	31'234	37'723	2'245	4'454	3'432	1	5'872	3
ZG	9'796	10'255	10'631	2'451	2'817	2'567	1	27'602	11
ZH	70'011	71'875	73'645	-	38'226	37'429	3	-	-
Schweiz (gesamt)	**1'037'662**	**967'804**	**1'049'725**	**-**	**407'068**	**398'399**	-	-	-
Schweiz (18 Kantone)	**799'276**	**741'829**	**804'130**	**306'259**	**317'623**	**306'451**	**-**	**5'357'096**	**17**

LN inklusive Alpweiden und Alpwiesen: 1'481'659 ha gemäss Arealstatistik 2004-2009

[1] aus Arealstatistik 2016 Daten:2004-2009

[2] aus Betriebsstrukturerhebung 2015

- keine Daten vorhanden oder verfügbar

5.3 Methodische Probleme und Ungenauigkeiten bei der Erstellung der Ackerlandkarte

Fehler im TLM

Bei der Erstellung der Feldblockkarte wurde das TLM3D von Swisstopo 2015 verwendet. Dieses hat an einigen wenigen Stellen Fehler, die in neueren Versionen des TLM inzwischen behoben werden konnten, in der ERK2 2019 aber noch enthalten sind. Abbildung 27 zeigt einen Ausschnitt aus der Region Solothurn/Limpachtal. Eine grössere Waldfläche wurde hier als LN ausgeschieden. Da im Kanton Solothurn kein digitaler Datensatz zum Ackerland vorlag, wurde nach Methode 2 das Dauergrünland vom TLM-Datensatz extrahiert und die restliche Fläche als Ackerland bezeichnet. Entsprechend wurde auch ein Erosionsrisiko für diese Waldfläche berechnet, mit zum Teil sehr hohen Abtragswerten in Steillagen. Bei der Schlusskontrolle der neuen ERK2 2019 ist uns nur dieser Fall zwischen den Kantonen Bern und Solothurn (Blatt Lyss) aufgefallen (Abbildung 27).

Abbildung 27: Nicht erfasster Wald im TLM3D-Datensatz (Blatt Lyss) an der Grenze (violette Linie) südlich Bern, nördlich Solothurn.

Im Kanton Aargau gibt es einige wenige Bereiche, in denen die Feldblöcke nicht komplett und korrekt erfasst wurden. Dies ist wahrscheinlich auf die Genauigkeit des TLM3D‘s zurückzuführen, die von GIS-Systemen womöglich fehlerhaft berechnet wurden. Leider wurde dies bei der Plausibilisierung der Feldblockkarte nicht erkannt. Im Kanton Aargau ergeben sich somit Bereiche mit nicht komplett erfasster LN (Abbildung 28).

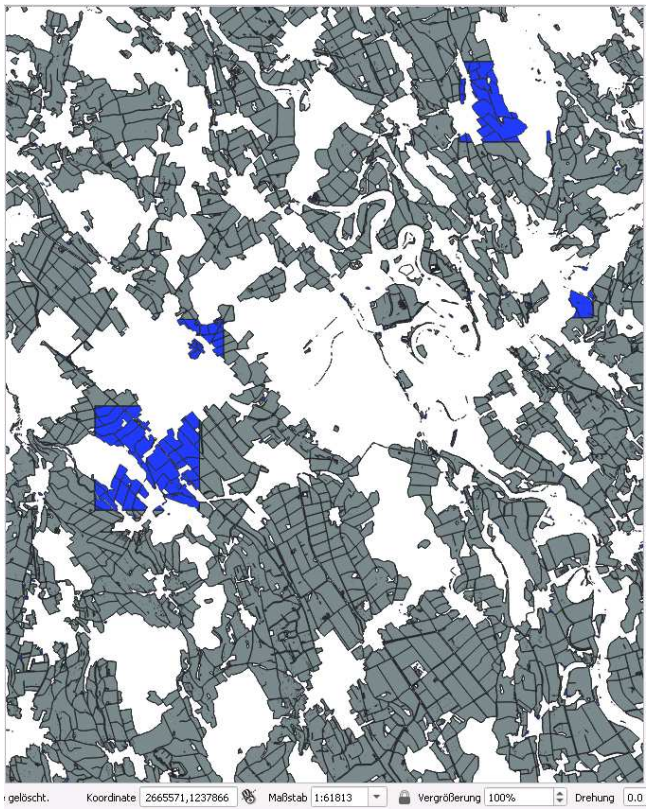

Abbildung 28: Nicht erfasste Feldblöcke der LN im Kanton AG in blau.

Unvollständiger kantonaler Datensatz beim Ackerland (Methode 1)

Methode 1 (siehe Kapitel 3.5) liefert die besten Resultate bei der Ausscheidung des Ackerlandes. Sofern die kantonalen Datensätze vollständig sind, wird die reale Ackerfläche abgebildet. Es entstehen keine Probleme bei Verschneidungen mit der LN der Feldblockkarte. Auf Luftbildern sind aber offensichtlich einige Flächen erkennbar, die mit grösster Wahrscheinlichkeit Ackerflächen sind, aber nicht als solche ausgeschieden wurden. Hierbei könnte es sich um Ackerflächen handeln, die nicht irgendwelchen Direktzahlungen unterstehen. Die kantonalen Stellen erfassen nur Flächen, die Direktzahlungen erhalten. Weiterhin können solche Flächen auch im Besitz ausserkantonaler Betriebe sein. Jeder Kanton erfasst nur die Flächen von den Betrieben, die im jeweiligen Kanton Direktzahlungen erhalten. Leider liegen exakte Daten zur Ackerfläche nur für 16 Kantone mit rund 159‘820 ha (= knapp 39 % der Ackerfläche der Schweiz) vor. Ein Beispiel für Methode 1 zeigt Abbildung 29. Auf dem Luftbild im Zentrum sind einige Flächen erkennbar, die nicht erfasst wurden. Dies könnten Ackerflächen sein, die einem anderen Kanton (z. B. FR) zugeordnet sind. Ausserkantonale Flächen wurden aufgrund der hohen Rechendauer nicht zusätzlich extrahiert. Es liegen aber mit dem verwendeten Datenstand nicht viele Ackerflächen in ausserkantonalen Bereichen.

Abbildung 29: Potentielles Erosionsrisiko für Ackerland ERK2 2019 (korrigiert) [t ha^{-1} a^{-1}] mit parzellenscharfen Daten (Methode 1) im Kanton VD (links). Rechts der gleiche Ausschnitt mit den zur Verfügung gestellten kantonalen Daten (grüne Flächen = Dauergrünland, braune Flächen = Ackerland); violette Linie Kantonsgrenze zu FR.

Die Daten des Kantons Wallis weisen noch einige Schwächen auf, was anhand Abbildung 30 zu erkennen ist. Es gibt eigenartige verschachtelte Polygone, welche teilweise von Ackerland umgebenes Grasland darstellen. Ebenfalls stimmen die Dimensionen nicht, was das hinterlegte Luftbild bestätigt. Das Problem wurde dem Kanton schon vom BLW mitgeteilt, es liegen zur Zeit aber keine besseren Daten vor.

a) b)

Abbildung 30: Kantonale Daten des Kantons VS a) grün= Grasland, violett= Ackerland und orange= Ackerland Kanton VD; b) kantonale Daten VS (rot) mit Swissimage hinterlegt.

Verschneidungsprobleme (Methode 2)

Methode 2 (siehe Kapitel 3.5) führt zu diversen Verschneidungsproblemen mit der LN der Feldblockkarte. Die aus dem TLM3D abgeleitete LN der Feldblockkarte ist häufig nicht deckungsgleich mit der LN aus den kantonalen Parzellen-Datensätzen. Dadurch entstehen diverse „Restflächen“, die in der ERK2 2019 als Ackerfläche abgebildet sind, aber andere Nutzungen beinhalten. Beispiele für solche Verschneidungsprobleme sind diverse kleine Flächen entlang von Strassen, Siedlungen, Wäldern etc. (Beispiel siehe Abbildung 31).

Alle Flächen, die in der Feldblockkarte als landwirtschaftliche Nutzungsfläche (LN), in den kantonalen Daten aber nicht als LN klassiert wurden, bleiben als Ackerflächen in der ERK2 2019 bei Methode 2 vorhanden. Beispiele hierfür sind Golfplätze, Kiesgruben, Schrebergartenareal oder nicht erfasstes Dauergrünland (Beispiele siehe Abbildung 32, Abbildung 33, Abbildung 34). Teilweise sind diese Daten im TLM3D aufgeführt, wurden aber aufgrund des langandauernden Extraktionsprozesses nicht von der LN entfernt.

Somit ist die abgebildete Ackerfläche in der ERK2 2019 in den Kantonen nach Methode 2 etwas zu gross und umfasst auch Flächen mit anderer Nutzung. Diese Flächen sind aber in der Regel einfach zu identifizieren. Sie sind relativ klein und haben für Ackerflächen untypische Formen. Durch Hinterlegung eines Luftbildes sind diese Flächen ebenfalls einfach zu identifizieren.

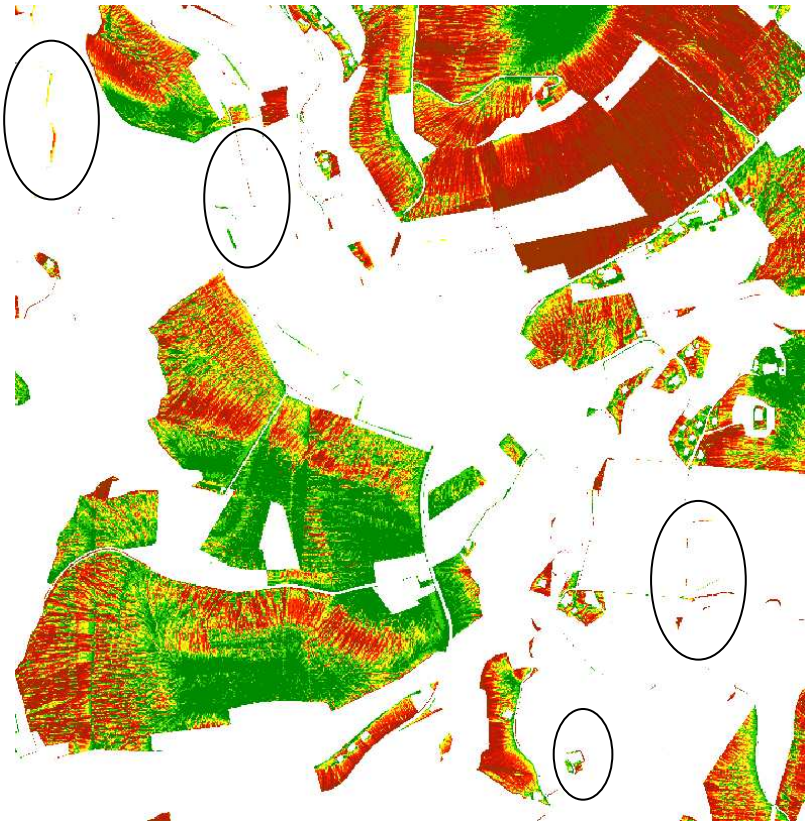

Abbildung 31: Potentielles Erosionsrisiko [t ha^{-1} a^{-1}] korrigiert mit parzellenscharfen Daten (Methode 2) jedoch mit Verschneidungsartefakten (hervorgehoben mit schwarzer Umrandung) im Kanton Bern.

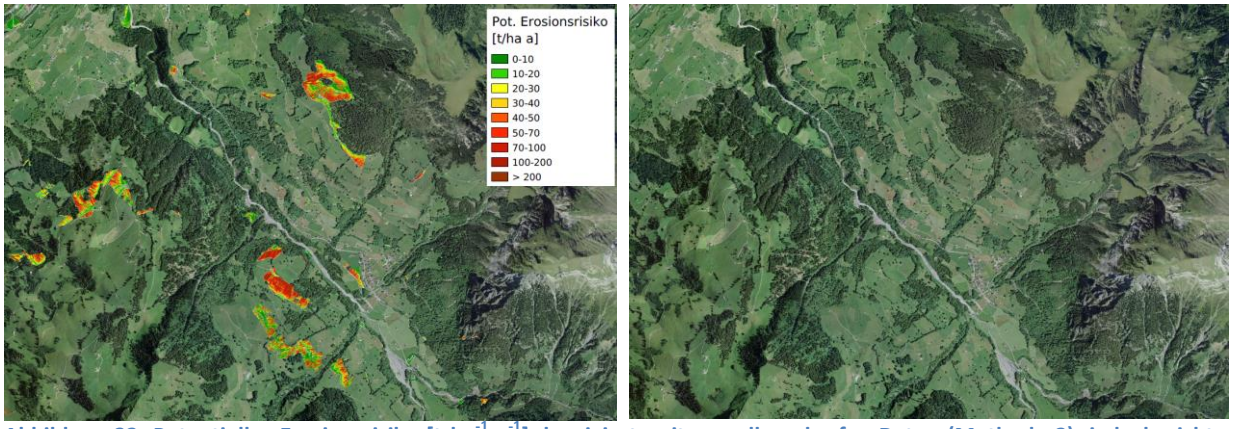

Abbildung 32: Potentielles Erosionsrisiko [t ha^{-1} a^{-1}], korrigiert, mit parzellenscharfen Daten (Methode 2), jedoch nicht komplett erfasstem Dauergrünland im Kanton Bern.

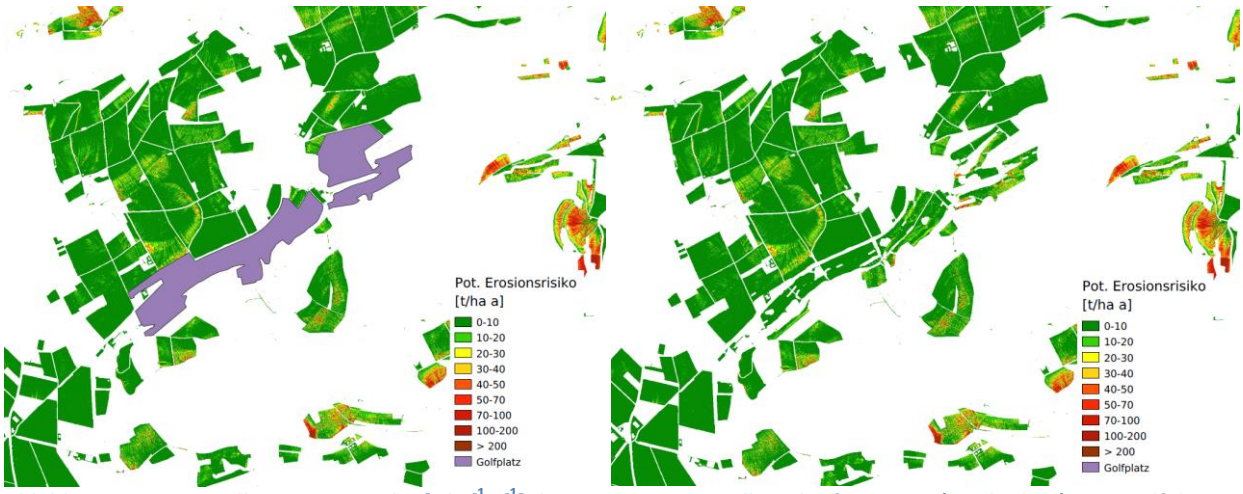

Abbildung 33: Potentielles Erosionsrisiko [t ha^{-1} a^{-1}], korrigiert, mit parzellenscharfen Daten (Methode 2). Der Golfplatz (violett) in Solothurn wurde in der Feldblockkarte als LN erfasst, bei den kantonalen Parzellendaten aber nicht. Entsprechend bleibt er als «Restfläche» und wird als Ackerfläche klassiert mit einem Erosionsrisiko abgebildet.

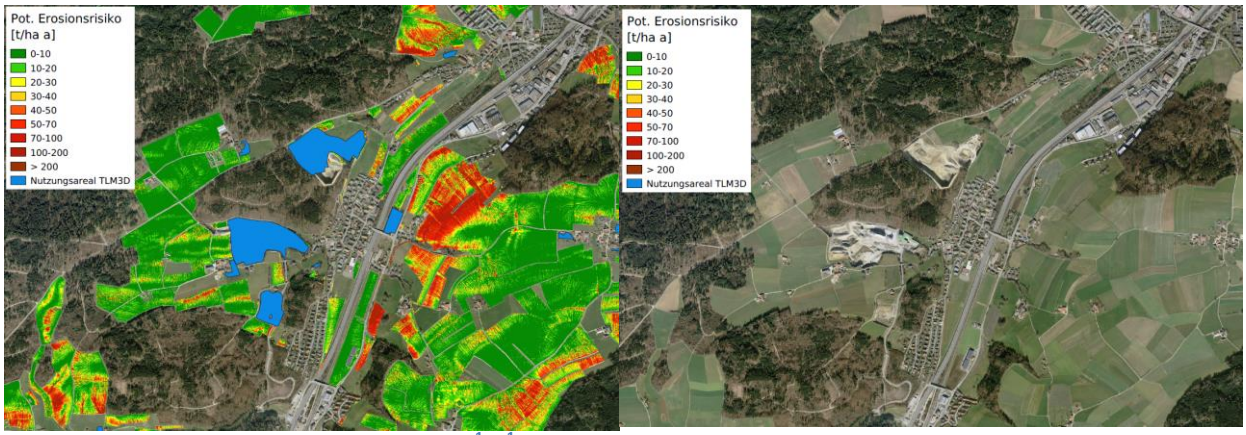

Abbildung 34: Potentielles Erosionsrisiko [t ha^{-1} a^{-1}], korrigiert, mit parzellenscharfen Daten (Methode 2). Die Kiesgrube (blau) im Kanton Bern wurde in der Feldblockkarte als LN erfasst, bei den kantonalen Parzellendaten aber nicht. Entsprechend bleibt sie als «Restfläche» und wird als Ackerfläche klassiert mit einem Erosionsrisiko abgebildet.

Keine kantonalen Parzellendaten vorhanden (Methode 3)

Die dritte Methode (siehe Kapitel 3.5) der Dauergrünlandentfernung führt in den sieben verbliebenen Kantonen aufgrund der verwendeten Daten (Auflösung 300m) zu einer deutlich weniger präzisen und lückenhaften Ackerlandkarte. Bis die parzellenscharfen kantonalen Daten vorliegen (voraussichtlich 2020), ist diese provisorische Lösung aber der einzig praktikable Weg, das Ackerland zu erzeugen. Wie sich die unterschiedlichen Methoden auswirken, erkennt man an einem Ausschnitt zwischen Bern und Luzern. Es ergeben sich mehr Artefakte und grössere Lücken auf der Luzerner Seite (vergl. Abbildung 35, Abbildung 36, rechts und links). Einerseits werden auch viele Dauergrünlandflächen mit zum Teil hohem potentiellem Erosionsrisiko abgebildet, andererseits wurde verschiedene Ackerflächen ausgeschnitten, für die nun kein potentielles Erosionsrisiko mehr abgebildet wird. Wegen der grösseren Ungenauigkeiten und Unsicherheiten der Berechnung der Ackerflächen in diesen sieben Kantonen erfolgt auch keine statistische Auswertung der Daten für diese Kantone (siehe Tabelle 22). Sobald kantonale Daten vorliegen, sollten in diesen Kantonen Aktualisierungen vorgenommen werden.

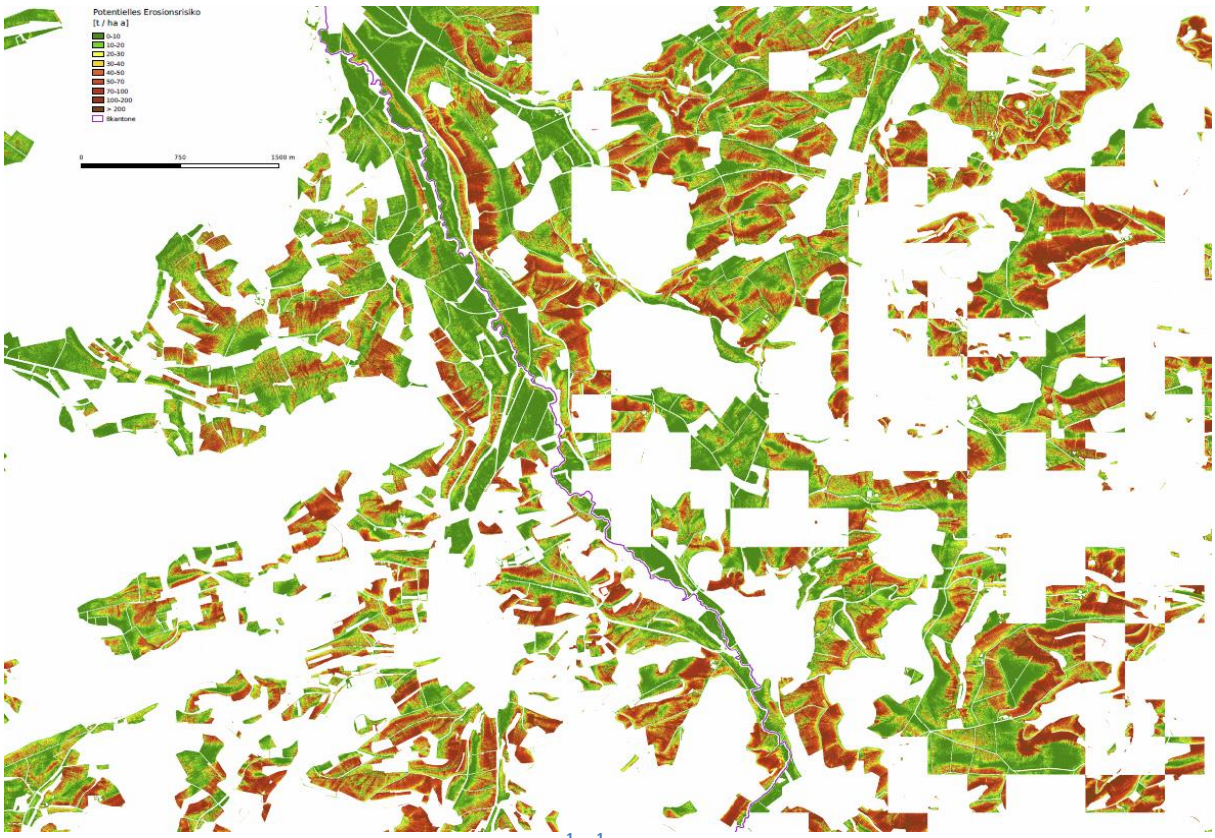

Abbildung 35: Potentielles Erosionsrisiko korrigiert [t ha^{-1} a^{-1}]; Links der violetten Kantonsgrenze Bern mit parzellenscharfen Daten (Methode 2) rechts davon Luzern nach Abzug des abgeschätzten Dauergrünlandes basierend auf Schmidt et al. (2019) (Methode 3).

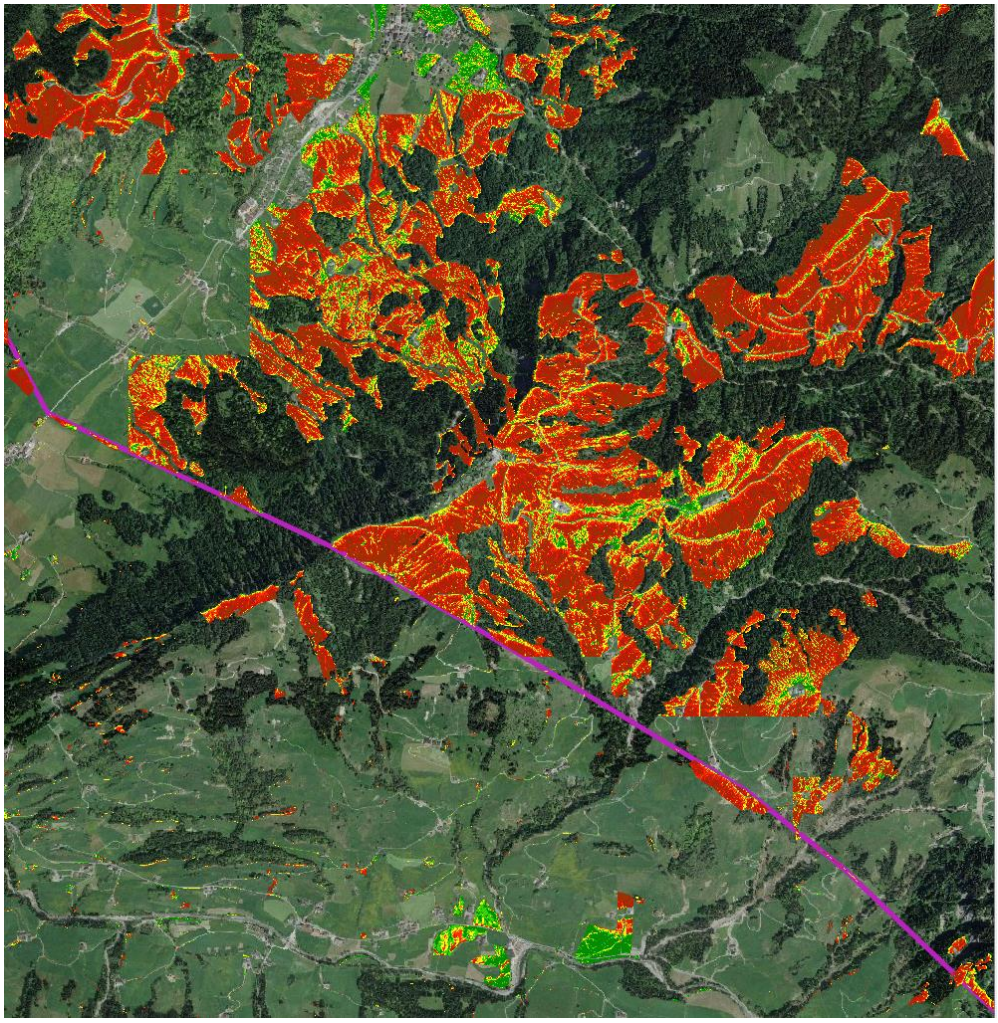

Abbildung 36: Potentielles Erosionsrisiko korrigiert [t ha^{-1} a^{-1}] mit parzellenscharfen Daten; Methode 2 mit nicht komplett erfasstem Dauergrünland südlich der violetten Kantonsgrenze; nördlich Methode 3 zwischen den Kantonen Bern und Luzern.

6. Web-Applikation zur Berechnung des aktuellen Erosionsrisikos

Es war im Projektrahmen nicht möglich, eine voll funktionierende Web-Applikation umzusetzen. Jedoch bietet der Prototyp erste Einsichten in den Aufwand und die Machbarkeit einer solchen Applikation. Der vorliegende Prototyp besteht aus zwei Teilen (Applikationen). Der eine Teil besteht aus einer Web-Oberfläche, von welcher Feldblockdaten heruntergeladen werden können und mittels Eingabe eines berechneten C-Faktors das aktuelle Erosionsrisiko berechnet werden kann (Version Alpha 0.2). Des Weiteren ist im Prototyp erst das Kartenblatt 1146 Lyss enthalten.

Mit dem zweiten Teil der Applikation kann man den C-Faktor berechnen. Details zu beispielhaften C-Faktoren und eine qualitative Überprüfung befinden sich in der Masterarbeit von Patrick Kupferschmied (Kupferschmied 2018). Eine Eingabeoberfläche ist bisher noch nicht entwickelt worden, ist aber aktuell in Planung und soll Mitte 2019 verfügbar sein.

Weitere Details zu den Applikationen können der Offline-Version entnommen werden. Momentan ist die Applikation von einer virtuellen Maschine ausführbar (VDI-file). Die Applikation zum Runterladen von Dateien und zur Berechnung des C-Faktors (als Python-Script) sind vorhanden. Weitere Details kann man beim Start der virtuellen Maschine entnehmen.

7. Schlussfolgerung und Ausblick

Die neue Erosionsrisikokarte ERK2 (2019) ist aktueller und genauer. „Kinderkrankheiten“ der ersten ERK2 (z.B. Probleme an Kachelgrenzen), wie sie Gisler et al. (2010) beschreiben, konnten behoben werden. Die ERK2 (2019) läuft auf aktueller GIS-Umgebung und kann daher anderen Nutzern zugänglich gemacht werden. Die vorgenommenen Korrekturen - basierend auf langjährigen Feldkartierungen in der Region Frienisberg - führen zu einer realistischeren Abbildung des potentiellen Erosionsrisikos. Die neue, korrigierte ERK2 (2019) erlaubt dadurch und mit der zukünftigen Web-Applikation, das aktuelle Erosionsrisiko zu berechnen. Die Erstellung der ERK2 (2019) ausschliesslich für das Ackerland konnte noch nicht komplett realisiert werden. Die Separierung von Acker- und Dauergrünland ist bisher noch nicht in allen Kantonen möglich, da die Datenverfügbarkeit erst Ende 2019 oder 2020 gesamtschweizerisch gewährleistet ist. Für 19 Kantone konnte die Ackerlandkarte parzellenscharf umgesetzt werden. Sobald für die restlichen 7 Kantone parzellenscharfe Daten vorliegen, sollte eine Aktualisierung der ERK2 2019 für diese Kantone durchgeführt werden.

Mit diesem Bericht wird das Projekt mit dem Titel: „Entwicklung eines C-Faktortools für die Massnahmenplanung als Ergänzung zur neuen Erosionsrisikokarte (ERK2)“, abgeschlossen. Eine umfassende Beschreibung des C-Faktortools findet sich in Kupferschmied (2018). Die Alphaversion der Web-Applikation zur Berechnung des aktuellen Erosionsrisikos ist momentan in Entwicklung, das Tool steht als virtuelle Maschine zur Verfügung (Kupferschmied 2018). Eine Eingabemaske zur Berechnung des C-Faktors wird derzeit entwickelt.

Referenzen

BAFU und BLW (2013): Bodenschutz in der Landwirtschaft. Ein Modul der Vollzugshilfe Umweltschutz in der Landwirtschaft. Bundesamt für Umwelt und Bundesamt für Landwirtschaft, Bern. Umwelt-Vollzug Nr. 1313: 59 S.

Bircher P., Liniger H., Prasuhn, V. (2019a): Comparing different multiple flow algorithms to calculate RUSLE factors of slope lenght (L) and slope steepness (S) in Switzerland. Geomorphology, Submitted 30.04.2018.

Bircher P., Liniger H., Prasuhn, V. (2019b): Comparison of RUSLE-modelled and field -measured long-term soil loss in Switzerland. (in preparation).

Desmet, P. J. J., and G. Govers (1996). "A GIS procedure for automatically calculating the USLE LS factor on topographically complex landscape units" Journal of Soil and Water Conservation 51(5): 427 -433.

Foster, G.R., L.D. Meyer, and C.A. Onstad. (1977). A runoff erosivity factor and variable slope length exponents for soil loss estimates. Trans. ASAE 20:683-687.

Friedli, S. (2006): Digitale Bodenerosionsgefährdungskarte der Schweiz im Hektarraster – Unter besonderer Berücksichtigung des Ackerlandes; Masterarbeit der Philosophisch-naturwissenschaftlichen Fakultät der Universität Bern.

Gisler S, H.P. Liniger, and V. Prasuhn. (2010) Technisch-wissenschaftlicher Bericht zur Erosionsrisikokarte der landwirtschaftlichen Nutzfläche der Schweiz im 2x2-Meter-Raster (ERK2). Bern: Centre for Development and Environment (CDE).

Gisler, S., Liniger H. and Prasuhn V (2011). "Erosionsrisikokarte im 2x2 -Meter-Raster (ERK2)." Agrarforschung Schweiz 2, no. 4: 148–55.

Hammad, A. Abu, H. Lundekvam, and T. Børresen (2004) "Adaptation of RUSLE in the Eastern Part of the Mediterranean Region." Environmental Management 34, no. 6: 829–41. https://doi.org/10.1007/s00267-003-0296-7.

Hänni N. (2017): Studie zur Nutzung der Schweizerischen Erosionsrisikokarte in der Praxis. Abteilung Integrative Geographie, Geographisches Institut Universität Bern. Bachelorarbeit

Joss. L. und Prasuhn, V. (2019): Technisch-wissenschaftlicher Bericht zur Erneuerung der Gewässeranschlusskarte (GAK2). Agroscope. Zürich.

Klik A. and A.S. Zartl. (2001) "Comparison of Soil Erosion Simulations Using WEPP and RUSLE with Field Measurements." American Society of Agricultural and Biological Engineers. https://doi.org/10.13031/2013.3278.

Kupferschmied, P. (2018): Konzeptionierung und Operationalisierung einer aktuellen und schweizweit verwendbaren Berechnungsweise des USLE C-Faktors. Schaffung der inhaltlichen und technischen Grundlagen zur individuellen Integration des C-Faktors in die Erosionsrisikokarte der Schweiz. Geographisches Institut. Abteilung Integrative Geographie. Universität Bern. Masterarbeit.

McCool, D.K., G.R Foster, C.K. Mutchler, and L.D. Meyer. (1989). Revised slope length factor for the Universal Soil Loss Equation. Trans. ASAE 32:1571-1576.

McCool, D.K., L.C. Brown, G.R Foster, et al. (1987). Revised slope steepness factor for the Universal Soil Loss Equation. Trans. ASAE 30:1387-1396.

Meusburger, K., A. Steel, P. Panagos, L. Montanarella, and C. Alewell (2012) "Spatial and Temporal Variability of Rainfall Erosivity Factor for Switzerland." Hydrology and Earth System Sciences 16, no. 1: 167 – 77. doi:10.5194/hess-16-167-2012.

Mitas, L., and Mitasova, H. (1998) Distributed soil erosion simulation for effective erosion prevention. Water Resources Research 34(3), 505-516

MITASOVA H, HOFIERKA J., ZLOCHA M., IVERSON L.R. (1996) Modeling topographic potential for erosion and deposition using GIS. International Journal of GIS v. 10, no. 5, p.629-641

MOSIMANN, TH. & RÜTTIMANN, M. (1999). Bodenerosion selber abschätzen - Ein Schlüssel für Betriebsleiter und Berater; Ackerbaugebiete des zentralen Mittellandes. Hrsg.: Finanzdepartement Aargau; Abteilung Landwirtschaft, Abteilung Umwelt und Landwirtschaft des Kantons Bern, Militär-, Polizei- und Umweltdepartement des Kantons Luzern; Amt für Umweltschutz, Volkswirtschaftsdepartement des Kantons Luzern; Landwirtschaftsamt, Amt für Umweltschutz und Amt für Landwirtschaft des Kantons Solothurn.

MOSIMANN, TH. & RÜTTIMANN, M. (2002). Erosion CH V2.02 : Bodenerosion selber abschätzen – Ein Schlüssel für Betriebsleiter und Berater. Terragon Ecoexperts AG. Bubendorf

Nogler, S. (2012): Erosivität der Niederschläge im schweizerischen Mittelland; Masterarbeit der Philosophisch-naturwissenschaftlichen Fakultät der Universität Bern

Panagos P., Van Liedekerke M., Jones A., Montanarella L. (2012) “European Soil Data Centre: Response to European policy support and public data requirements”; Land Use Policy, 29 (2), pp. 329-338. doi:10.1016/j.landusepol.2011.07.003

Panagos, Panos, Pasquale Borrelli, and Katrin Meusburger. (2015) “A New European Slope Length and Steepness Factor (LS-Factor) for Modeling Soil Erosion by Water.” Geosciences 5, no. 2: 117–26. https://doi.org/10.3390/geosciences5020117. [a]

Panagos, P., Borrelli, P., Poesen, J., Ballabio, C., Lugato, E., Meusburger, K., Montanarella, L., Alewell, .C. (2015). The new assessment of soil loss by water erosion in Europe. *Environmental Science & Policy*. **54**: 438-447. DOI: 10.1016/j.envsci.2015.08.012 [b]

Panagos, P., Borrelli, P., Robinson, D.A. (2015) Common Agricultural Policy: Tackling soil loss across Europe. Nature 526, 195, doi:10.1038/526195d [c]

Prasuhn V. (2010) Zeitliche Variabilität von Bodenerosion - Analyse von 10 Jahren Erosionsschadenskartierungen im Schweizer Mittelland. Die Bodenkultur. 61, (2), 47-57.

Prasuhn, V. (2011) “Soil Erosion in the Swiss Midlands: Results of a 10-Year Field Survey.” Geomorphology 126, no. 1–2: 32–41. https://doi.org/10.1016/j.geomorph.2010.10.023.

Prasuhn V (2012). On-farm effects of tillage and crops on soil erosion measured over 10 years in Switzerland. Soil & Tillage Research. 120, 137-146.

Prasuhn, V., Blaser, S. (2018). Der Agrarumweltindikator «Erosionsrisiko». Bulletin BGS 39, 11-18.

Prasuhn, V., H.P. Liniger, S. Gisler, K. Herweg, A. Candinas, and J.-P. Clément. (2013) “A High-Resolution Soil Erosion Risk Map of Switzerland as Strategic Policy Support System.” Land Use Policy 32: 281–91. doi:10.1016/j.landusepol.2012.11.006.

Renard K.G., Foster G.R., Weesies G.A., McCool D.K. and Yoder D.C. (1997): Predicting soil erosion by water. A guide to conservation planning with the Revised Universal Soil Loss Equation (RUSLE). Draft August (USA) (US Department of Agriculture). (= Agriculture Handbook. 703).

Rymszewicz, A., E. Mockler, J. O’Sullivan, M. Bruen, J. Turner, E. Conroy, M. Kelly-Quinn, J. Harrington, and D. Lawler. (2015) “Assessing the Applicability of the Revised Universal Soil Loss Equation (RUSLE) to Irish Catchments.” Proceedings of the International Association of Hydrological Sciences 367: 99–105. https://doi.org/10.5194/piahs-367-99-2015.

Schäuble, H. (2005) “Erosionsprognosen Mit GIS Und EDV-Ein Vergleich Verschiedener Bewertungskonzepte Am Beispiel Einer Gäulandschaft”. http://w210.ub.uni-tuebingen.de/volltexte/2005/1904/.

Schelbert F. (2016). Entwicklung einer GIS-basierten Methode zur Digitalisierung von Erosionsschadenkartierungen im Gebiet Frienisberg (BE). Geographisches Institut, Centre for Development and Environment (CDE). Universität Bern. Masterarbeit.

Schmidt, J. (1991): A mathematical Model to Simulate Rainfall Erosion. Catena Supplement 19, pp. 101-109.

Schmidt, J, M.v Werner, and A Michael. (1999) “Application of the EROSION 3D Model to the CATSOP Watershed, The Netherlands.” CATENA 37, no. 3–4: 449–56. https://doi.org/10.1016/S0341-8162(99)00032-6.

Schmidt, S., Alewell, C., Panagos, P., and Meusburger, K. (2016): Regionalization of monthly rainfall erosivity patterns in Switzerland, Hydrol. Earth Syst. Sci., 20, 4359-4373, https://doi.org/10.5194/hess-20-4359-2016.

Schmidt, S., Tresch, S., Meusburger, K.: Modification of the RUSLE Slope Length and Steepness Factor (LS-Factor) for steep alpine slopes. MethodsX, in prep.

Schmidt, S., Alewell, C., and Meusburger, K. (2018): Mapping spatio-temporal dynamics of the cover and management factor (C-factor) fpr gasslands in Switzerland, Remote Sensing of Environment 211, 89-104.

Seibert, J., and B. L. McGlynn. (2007) “A New Triangular Multiple Flow Direction Algorithm for Computing Upslope Areas from Gridded Digital Elevation Models.” Water Resources Research 43, no. 4: n/a-n/a. doi:10.1029/2006WR005128.

Smith, D. D. and W. H. Wischmeier, W. H. (1957). Factors affecting sheet and rill erosion. American Geophysical Union Transactions 38:889-896.

Wischmeier W. H. & SMITH D. D. (1978): Predicting Rainfall Erosion Losses – a Guide to Conservation Planning. U.S. Dep. of Agriculture, Handbook No. 537. Washington.

Zevenbergen, L. W., and C. R. Thorne. (1987) “Quantitative Analysis of Land Surface Topography.” Earth Surface Processes and Landforms 12, no. 1: 47–56. doi:10.1002/esp.3290120107.

Datengrundlagen:

Amtliche Vermessung Bern Metadaten und Produkteinformation (2014):
AVR: Reduzierte Daten der amtlichen Vermessung, basierend auf DM.01-AV-BE:
URL: http://files.be.ch/bve/agi/geoportal/geo/lpi/AVR_2011_03_LANG_DE.PDF

BLW (2016): Landwirtschaftliche Zonengrenzen: Minimale Geodatenmodelle Landwirtschaftliche Bewirtschaftung
URL: https://www.blw.admin.ch/blw/de/home/politik/datenmanagement/geografisches-informationssystem-gis.html

European Soil Data Centre (ESDAC), esdac.jrc.ec.europa.eu, European Commission, Joint Research Centre

LANDKULT (2016): Landwirtschaftliche Kulturen des Kantons Bern © Amt für Landwirtschaft und Natur des Kantons Bern, Abteilung Direktzahlungen

Swisstopo (2015): SwissALTI3D
URL: http://www.swisstopo.admin.ch

Swisstopo (2015): SwissTLM3D
URL: http://www.swisstopo.admin.ch

Anhang

Auf den nachfolgenden Seiten befinden sich die sechs wichtigsten Karten zur besseren visuellen Darstellung in grösserer Form.

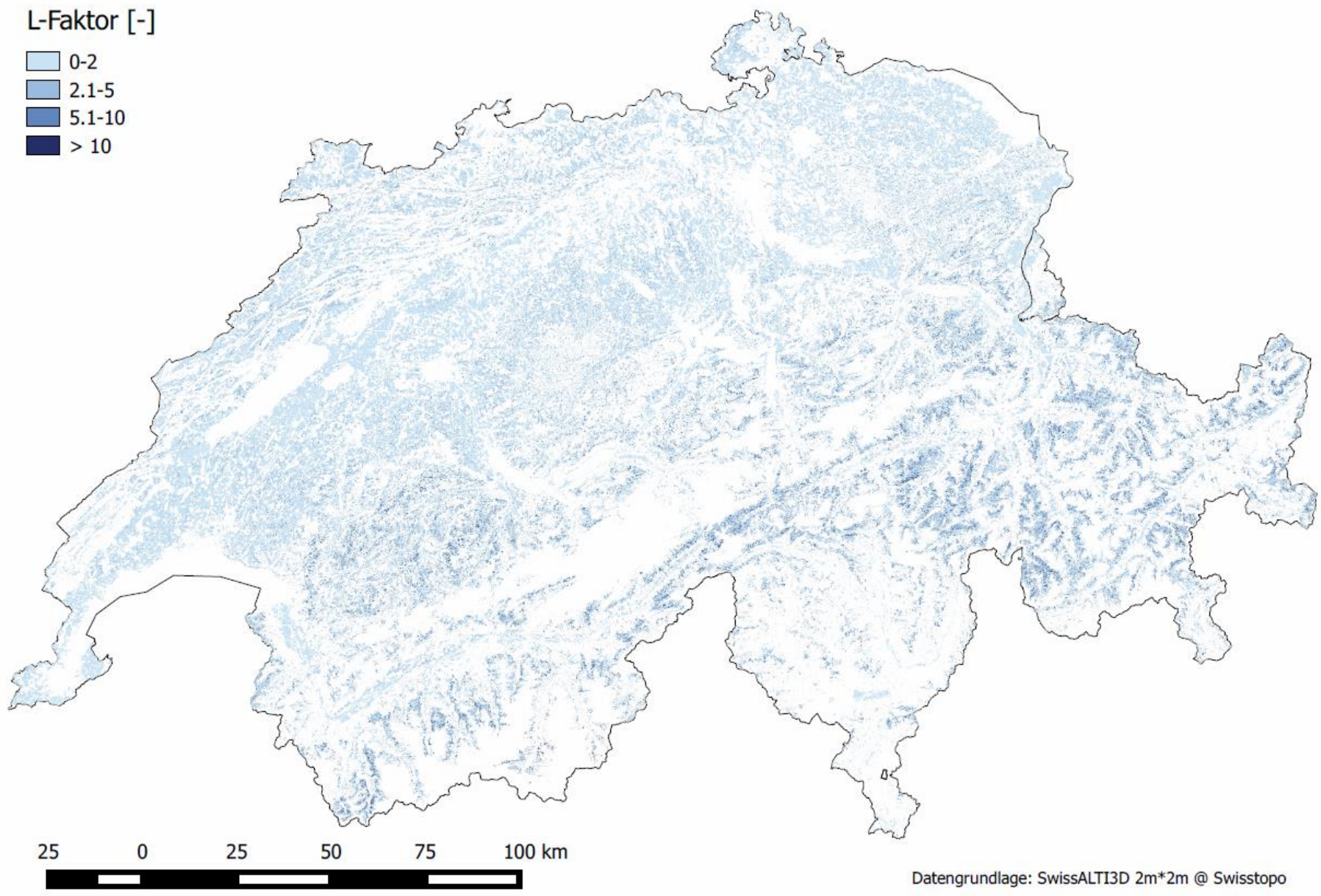

Abbildung : Fliessweg L-Faktor-Karte [-] der LN der Schweiz und dem Fürstentum Liechtenstein, berechnet mit MTFD 1.1 und 0.5 m gefülltem DEM (inklusive Dauergrünlandflächen mit Sömmerungsgebiet)

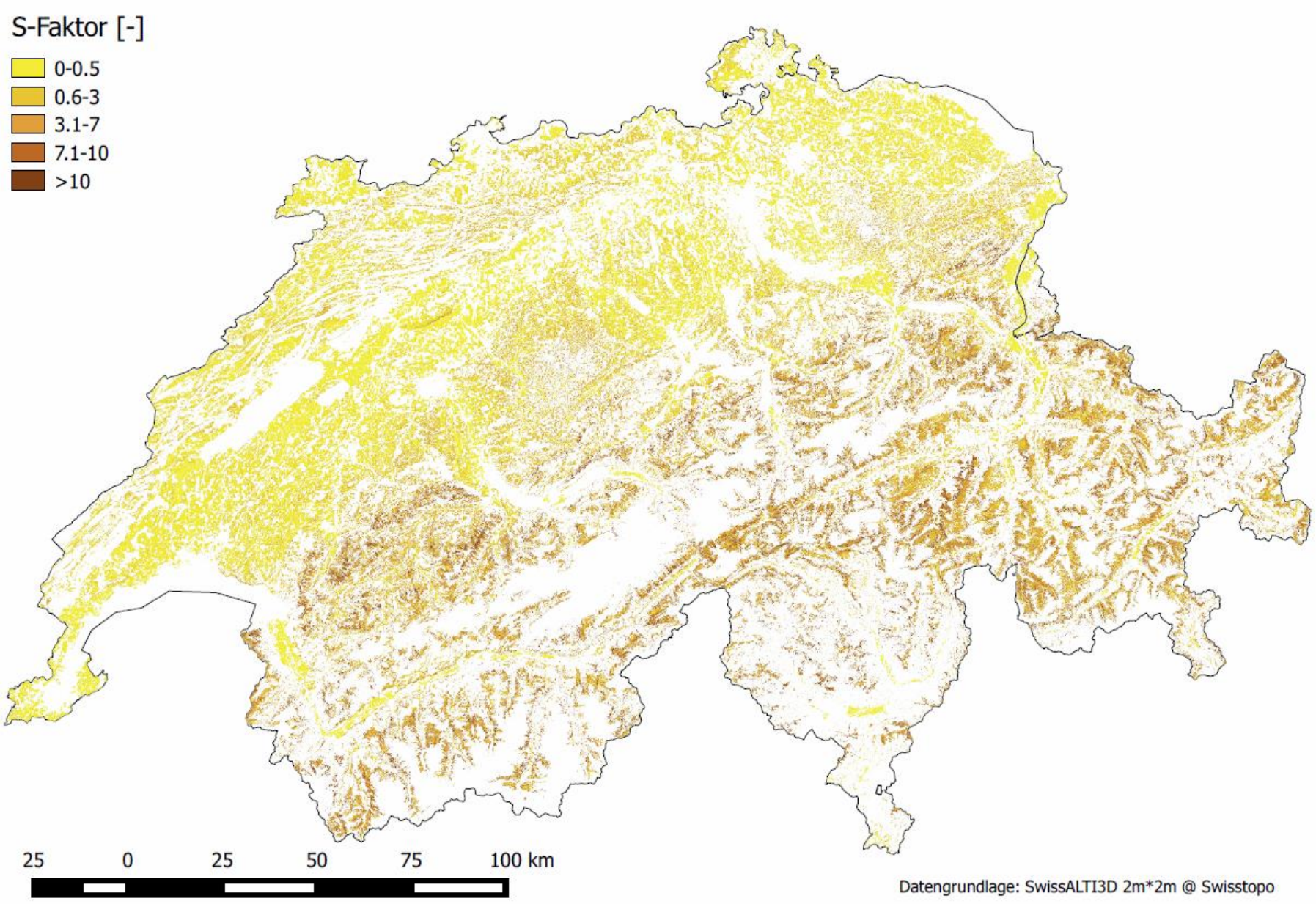

Abbildung Hangneigung S-Faktor-Karte [-] der LN der Schweiz und dem Fürstentum Liechtenstein, inklusive Dauergrünlandflächen mit Sömmerungsgebiet.

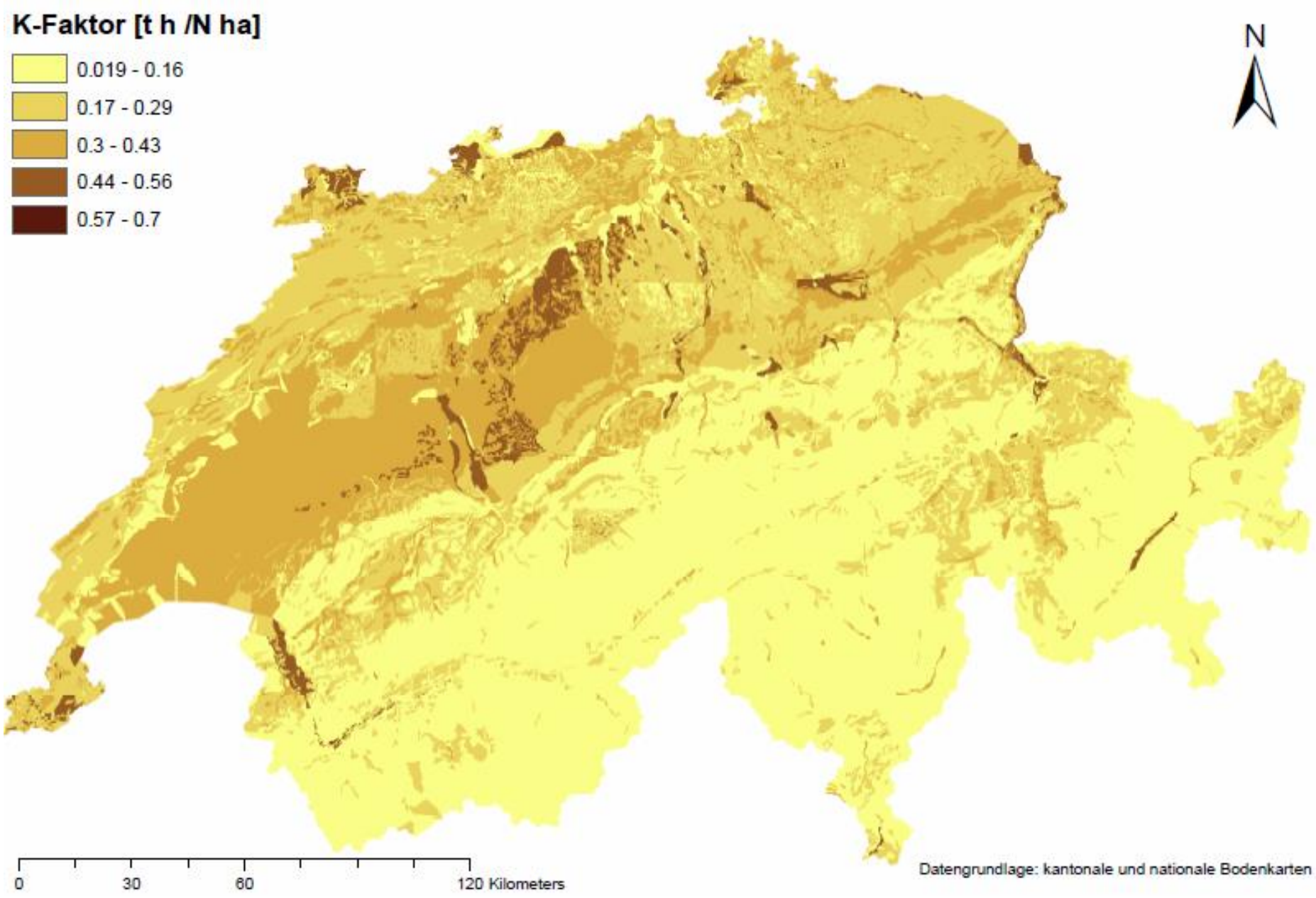

Abbildung Erodibilität K-Faktor-Karte [t h N^{-1} ha^{-1}] der gesamten Schweiz.

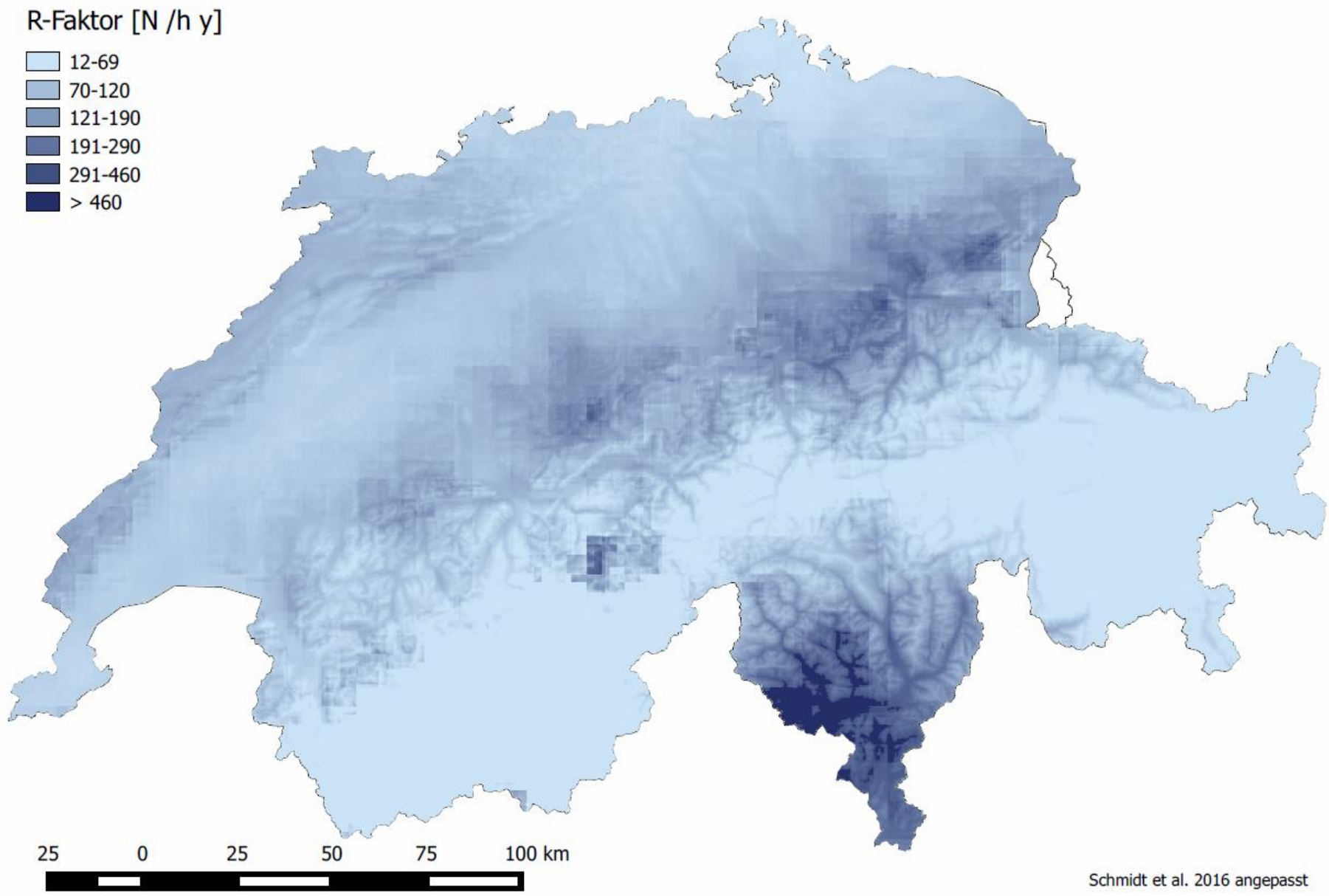

Abbildung Erosivität R-Faktor-Karte der gesamten Schweiz [N h^{-1} a^{-1}] (Schmidt et al. 2016)

Abbildung Karte des potentiellen Erosionsrisikos (unkorrigiert) der LN der Schweiz [t ha^{-1} a^{-1}] der neuen ERK2 (2019), inklusive Dauergrünlandflächen mit Sömmerungsgebiet; gleiche Klassen wie bei ERK2 2010.

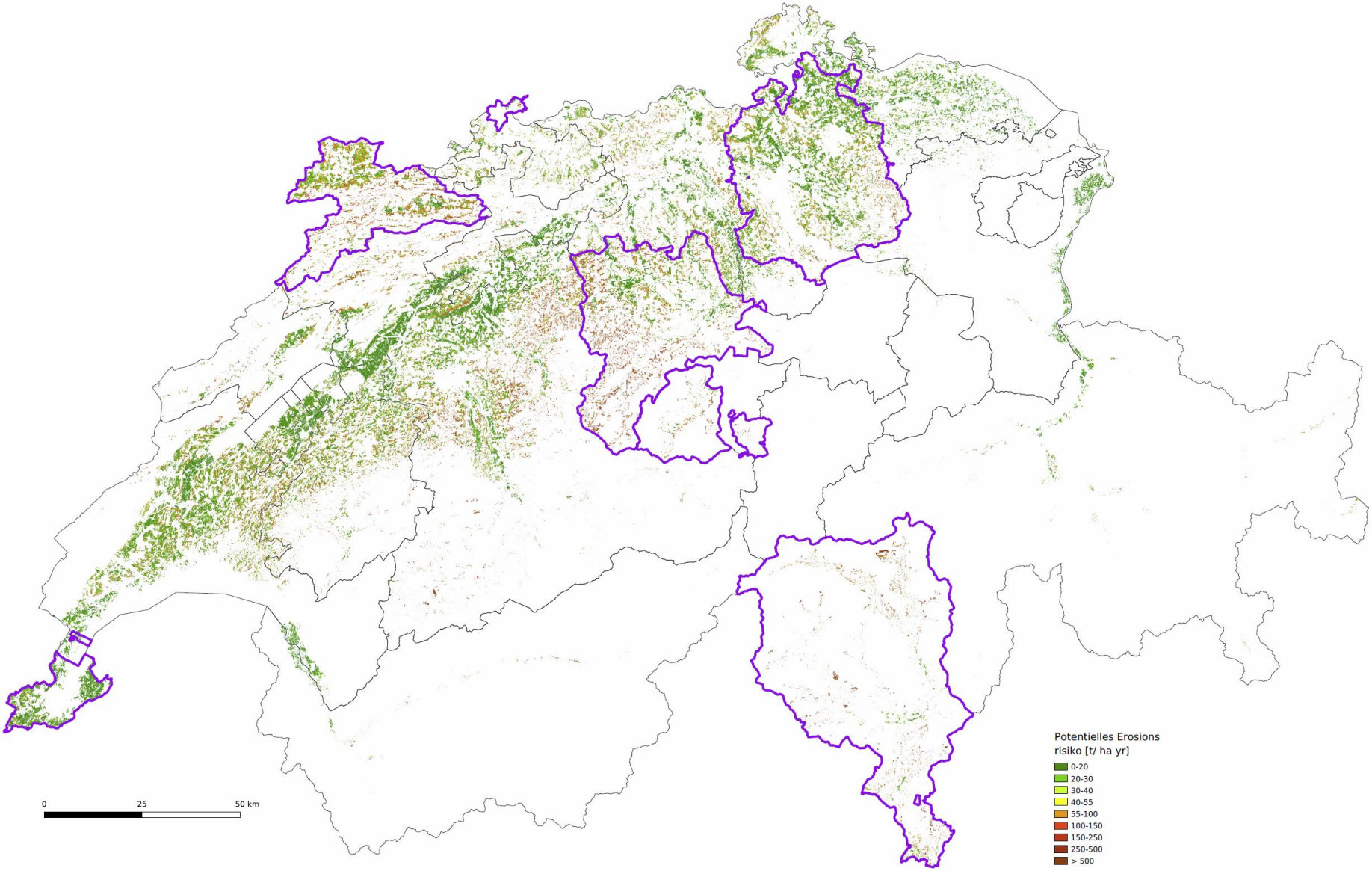

Abbildung Potentielles Erosionsrisiko (unkorrigiert) für das Ackerland der Schweiz [t ha^{-1} a^{-1}] und verwendete kantonale Daten der Schweiz; violett umrandet; restliche 7 Kantone ohne parzellenscharfe Ackerlanddaten, stattdessen mit Satellitenbildern abgeschätzt.

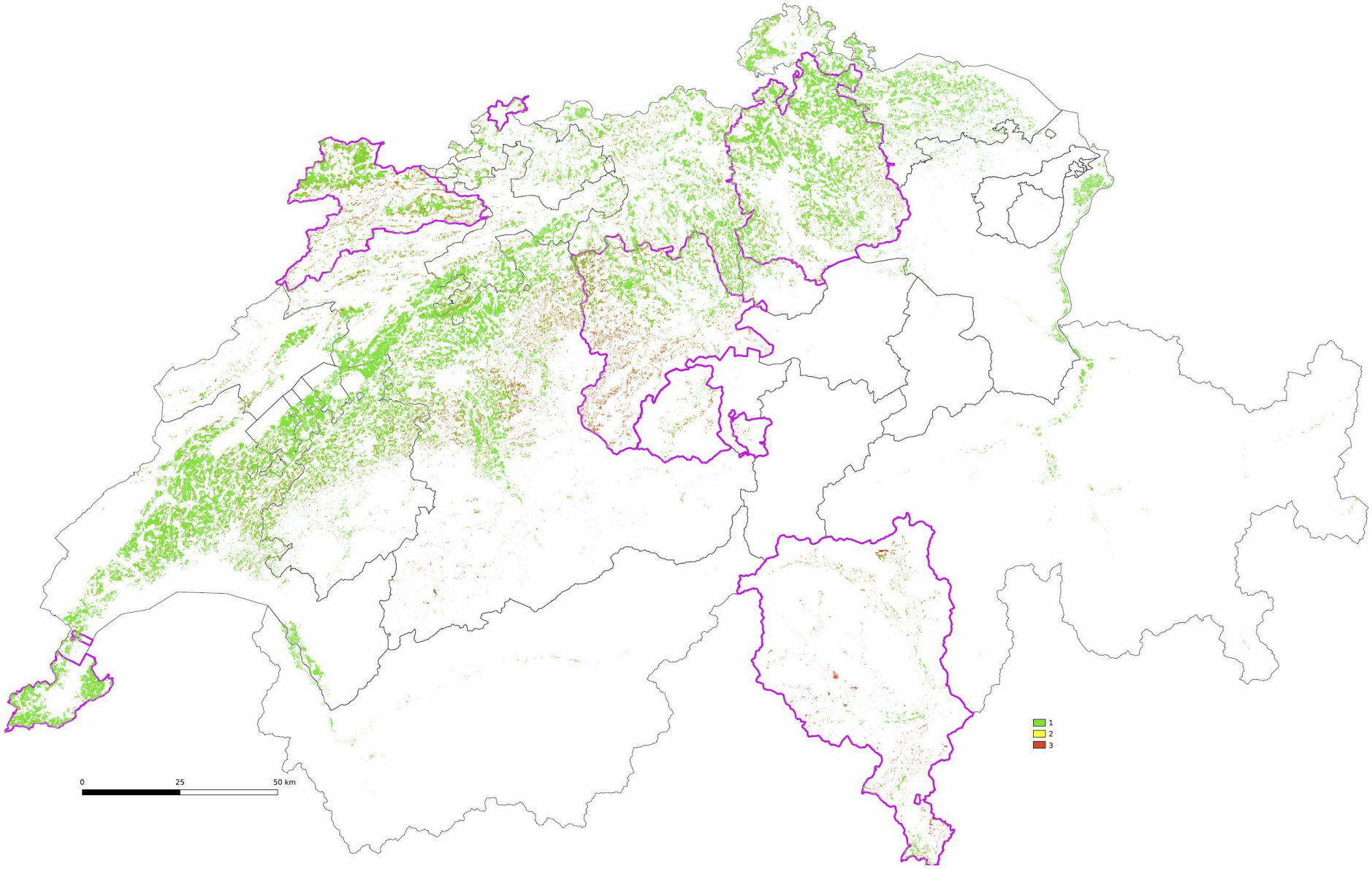

Abbildung Neue Potentielle Erosionsrisikokarte ERK2 2019 des Schweizer Ackerlandes, korrigiert, mit 3-Klassenlegende für grün = geringes potentielles Erosionsrisiko, gelb = mässiges potentielles Erosionsrisiko und rot = hohes potentielles Erosionsrisiko.

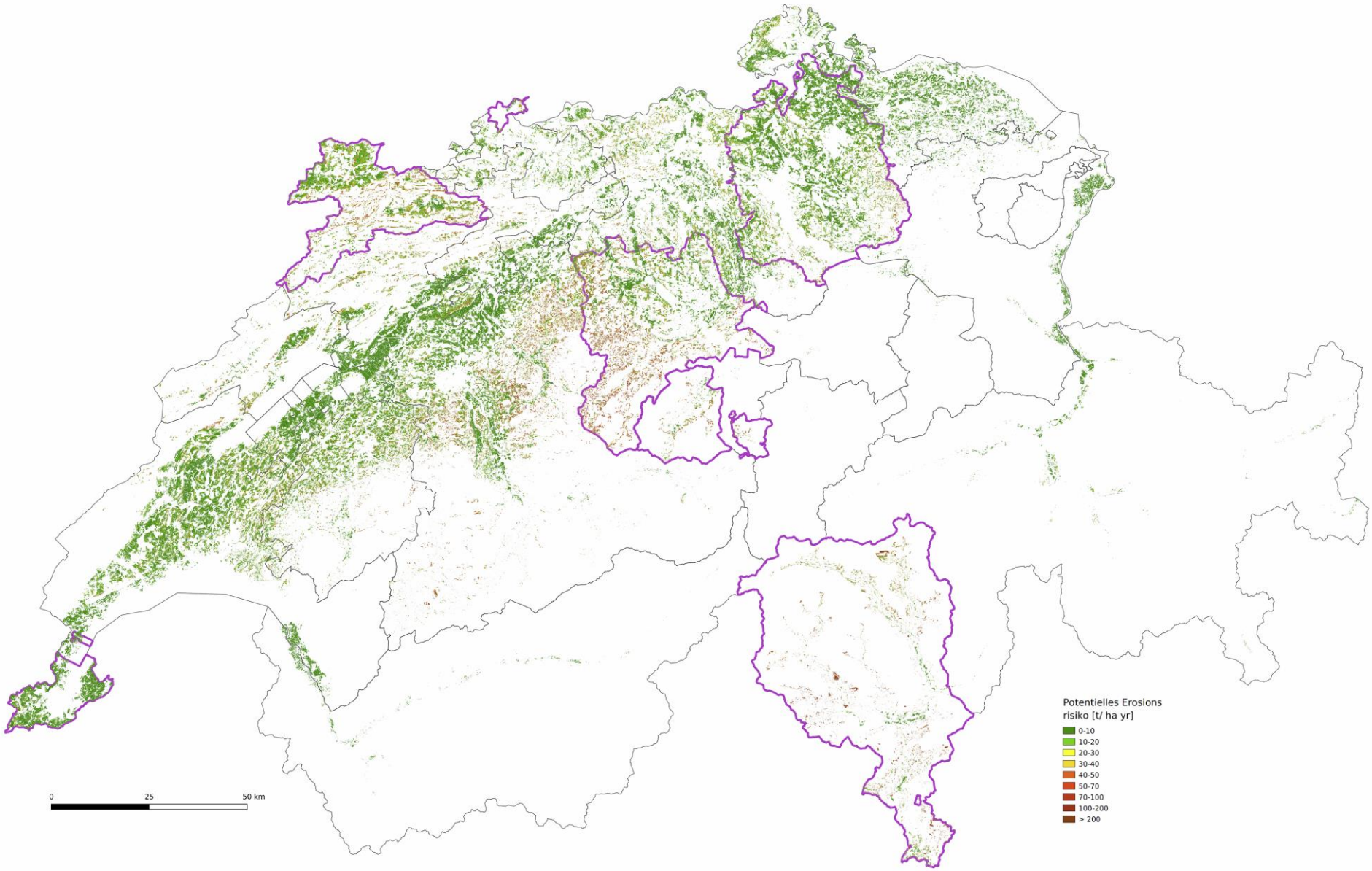

Abbildung Neue Potentielle Erosionsrisikokarte ERK2 2019 des Schweizer Ackerlandes korrigiert mit 9 Klassenlegende.

Part 3: Annexes

Erklärung gemäss Art. 18 PromR Phil.-nat. 2019.

Erklärung

gemäss Art. 18 PromR Phil.-nat. 2019

Name/Vorname:

Matrikelnummer:

Studiengang:

Bachelor ☐ Master ☐ Dissertation ☐

Titel der Arbeit:

LeiterIn der Arbeit:

Ich erkläre hiermit, dass ich diese Arbeit selbständig verfasst und keine anderen als die angegebenen Quel-len benutzt habe. Alle Stellen, die wörtlich oder sinn-gemäss aus Quellen entnommen wurden, habe ich als solche gekennzeichnet. Mir ist bekannt, dass andern-falls der Senat gemäss Artikel 36 Absatz 1 Buchstabe r des Gesetzes über die Universität vom 5. September 1996 und Artikel 69 des Universitätssta-tuts vom 7. Juni 2011 zum Entzug des Doktortitels be-rechtigt ist.
Für die Zwecke der Begutachtung und der Überprüfung der Einhaltung der Selbständigkeitserklärung bzw. der Reglemente betreffend Plagiate erteile ich der Univer-sität Bern das Recht, die dazu erforderlichen Perso-nendaten zu bearbeiten und Nutzungshandlungen vor-zunehmen, insbesondere die Doktorarbeit zu vervielfäl-tigen und dauerhaft in einer Datenbank zu speichern sowie diese zur Überprüfung von Arbeiten Dritter zu verwenden oder hierzu zur Verfügung zu stellen.

Ort/Datum

Unterschrift 

Curriculum Vitae